UNIVERSITY OF CALIFORNIA, SAN DIEGO

Stress, Mixed Messages, and Hormone Signaling:
Regulation of Translation and the Unfolded Protein Response in Pituitary Gonadotropes

A dissertation submitted in partial satisfaction of the
Requirements for the degree Doctor of Philosophy

in

Biomedical Sciences

by

Minh-Ha T. Do

Committee in charge:

Professor Mark Lawson, Chair
Professor Don Cleveland
Professor Pamela Mellon
Professor Daniel O'Connor
Professor Nick Webster

2008

The Dissertation of Minh-Ha T. Do is approved, and it is acceptable in quality and form for publication on microfilm:

_____

_____

_____

_____

_____
Chair

University of California, San Diego

2008

TABLE OF CONTENTS

LIST OF FIGURES

LIST OF TABLES

ACKNOWLEDGEMENTS

I would like to thank:

My advisor, Professor Mark A. Lawson, for his never-ending encouragement, for ensuring I had and took opportunities to advance my training, and for providing a lab environment that was easy to come in to everyday for the past 5 years.

Professor Pamela Mellon, for providing a fresh mind in critiquing my work and keeping on top of my progress. I would also like to thank the members of the Mellon lab for bearing with me during lab meetings and always being available for advice. Thank you in particular to Dr. Djurdjica Coss, for answering all my questions, large and small.

The rest of the members of my dissertation committee, Professor Nick Webster, Professor Don Cleveland, and Professor Daniel O'Connor, for asking me the difficult questions and thus providing me with the ideas and guidance I needed to complete this body of work. Dr. Cleveland, thank you for trying to ensure that I was sufficiently toughened up.

The Biomedical Sciences program has provided an invaluable opportunity to learn and train through the expertise of the faculty, support of the staff, and a body of classmates and friends who have supported me in so many ways. I would especially like to thank Theresa Operaña for being so generous with her time, support, thoughts and care.

My colleagues, Sharon Santos, Dr. Amy Navratil, Dr. Kathryn Nguyen, and Janine Low. I am so grateful to have been able to pick their minds, laugh with them, and have their voices of reason to hear.

My friends back home, I cannot express enough how all the potlucks, adventures, and emails have supported me. The drive to LA is worth it every time.

And finally:

Thank you to Jonathan Tang, who patiently waited for me all these years, drove down to San Diego all this time, gave up so many weekends, and who listened, understood, and supported me in every way he could and knew how. At last!

To my sisters, who have turned into women I am so proud of and have motivated me by setting such a high standard of achievement. And last, but furthest from least, thank you to my parents. Only recently have I begun to truly realize and appreciate what all their hard work and sacrifice has provided me and our family. I hope each day fulfills another part of the dream they had in mind and heart when choosing to come to this country.

Chapter 2, in part, has been submitted for publication of the material as it may appear in Molecular Endocrinology, 2008, Minh-Ha T. Do, Sharon J. Santos and Mark A. Lawson. The dissertation author was the primary investigator and author of this paper.

Chapter 4, in part, has been submitted for publication of the material as it may appear in Molecular Endocrinology, 2008, Minh-Ha T. Do, Sharon J. Santos and Mark A. Lawson. The dissertation author was the primary investigator and author of this paper.

VITA

2008 Ph.D., Biomedical Sciences, University of California, San Diego

2002 B.S., Molecular, Cell and Developmental Biology, University of California, Los Angeles

AWARDS AND HONORS

2007 ASBMB Graduate and Postdoctoral Travel Award

2003-2006 National Institutes of Health Genetics Training Grant

2004 International Society of Endocrinology Crowned Travel Award

2001-2002 Newfield Scholarship

2001 Phi Beta Kappa Honor Society

2000 Golden Key International Honor Society

PUBLICATIONS

Do MT, SJ Santos and MA Lawson. Activation of the unfolded protein response by gonadotropin-releasing hormone in pituitary gonadotropes. *Molecular Endocrinology*, *in revision.*

Navratil AM, **MT Do**, SJ Santos, JM Low, H Song, JB Hernandez, and MA Lawson. Insulin augments gonadotropin-releasing hormone induction of translation in LβT2 cells. *In preparation.*

ABSTRACTS

Do MT, R Intriago, SJ Santos, and MA Lawson. 2008. Activation of the unfolded protein response by gonadotropin-releasing hormone in pituitary gonadotropes. 90th Annual Meeting of the Endocrine Society, San Francisco, CA

Do MT, S Jain, KA Nguyen, SJ Santos, F He, and MA Lawson. 2007. Translational regulation of specific mRNAs by reproductive hormone GnRH. Experimental Biology Annual Meeting, Washington D.C.

Do MT, S Jain, KA Nguyen, SJ Santos, F He, and MA Lawson. 2007. GnRH induces redistribution of specific mRNA subpopulations in gonadotropes. 89th Annual Meeting of the Endocrine Society, Toronto, Ontario, Canada

Do MT, KA Nguyen, SJ Santos, S Jain, and MA Lawson. 2006. Differential redistribution of specific mRNAs in ribosome complexes by GnRH Translational Control Meeting, Cold Spring Harbor, NY

Do MT, SJ Santos, KA Nguyen, S Jain, and MA Lawson. 2006. GnRH induces specific translational regulation of LHβ mRNA in LβT2 cells. 88th Annual Meeting of the Endocrine Society, Boston, MA

Do MT, SJ Santos, KA Nguyen, and MA Lawson. 2005. Specificity of mRNA utilization in response to GnRH stimulation in LβT2 cells. 87th Annual Meeting of the Endocrine Society, San Diego, CA

Do MT, SJ Santos, KA Nguyen, and MA Lawson. 2004. Regulation of translation and mRNA utilization by GnRH. 12th International Congress of Endocrinology, Lisbon, Portugal

ABSTRACT OF THE DISSERTATION

Stress, Mixed Messages, and Hormone Signaling:
Regulation of Translation and the Unfolded Protein Response in Pituitary Gonadotropes

by

Minh-Ha T. Do

Doctor of Philosophy in Biomedical Sciences

University of California, San Diego, 2008

Professor Mark A. Lawson, Chair

The reproductive axis is controlled by release of GnRH from the hypothalamus, which stimulates gonadotrope cells in the anterior pituitary to activate and maintain the synthesis of one of their main secretory outputs, luteinizing hormone (LH). While the transcriptional regulation of the subunits of LH is well described, very little work has focused on the post-transcriptional regulatory pathways induced by GnRH. The work described in this dissertation addresses the hypothesis that GnRH activates a pathway called the unfolded protein response (UPR) in pituitary gonadotropes and through this pathway exerts specific translational regulation of gonadotrope mRNAs. The work utilizes ribosomal profiling in conjunction with quantitative PCR and bioinformatic analysis in order to examine mRNAs that are sensitive to translational regulation by GnRH and uses pharmacological inhibitors of known GnRH signaling pathways to dissect the pathways contributing to the regulation. Overall the work shows that GnRH activates markers of the UPR, including ER-stress sensor PERK, translation factor eIF2, and transcription factor Xbp1. The work shows that GnRH mobilizes calcium to cause a transient attenuation of translation of Lhb and Cga, the LH subunits. In addition to this, GnRH is shown to regulate the translation of a specific population of other gonadotrope mRNAs, stimulating the translation of some mRNAs

while attenuating the translation of others. This specificity is defined by signaling to the UPR as well as the MAPK ERK. This body of work blends the fields of reproductive endocrinology and translational control to provide a novel physiological function for the UPR and establish that GnRH exerts specific and bidirectional regulation of translation.

CHAPTER 1

INTRODUCTION

The hypothalamic-pituitary-gonadal axis

The reproductive axis is controlled by pulsatile release of the decapeptide gonadotropin-releasing hormone (GnRH) from the hypothalamus into the hypophyseal-portal circulation of the pituitary. GnRH stimulation of its G protein-coupled receptor on gonadotrope cells in the anterior pituitary activates and maintains the synthesis of gonadotropin hormones luteinizing hormone (LH) and follicle-stimulating hormone (FSH) and stimulates release of pre-formed stores of LH. LH and FSH act on the gonads to regulate the reproductive processes of folliculogenesis, ovulation, spermatogenesis, and steroidogenesis (1-3). The absolutely critical role this axis plays in regulating reproductive function is well established. The hypogonadal (*hpg*) mouse or animal models where the hypothalamic-pituitary input is severed reveal the dependence of gonadotropin gene expression and of fertility on GnRH input. Loss of LH results in infertility due to hypogonadism (1).

LH and FSH are glycoprotein heterodimers each comprised of a common alpha subunit (gene name Cga, also known as αGSU) and a unique beta (Lhb or Fshb, gene names, also known as LHβ or FSHβ) subunit. The beta subunit confers binding specificity. These genes are encoded on separate chromosomes and their gene products are non-covalently linked. After synthesis, the heterodimeric hormones are glycosylated, assembled, and stored in secretory granules (1-3). LH is released from these pre-formed stores in a pulsatile manner in response to GnRH stimulation, and FSH is released constitutively (3). This differential regulation of the gonadotropin hormones is also observed at the level of synthesis (2, 4). The transcriptional regulation of the subunits, in particular, is well characterized. Many studies have defined the promoter elements and binding proteins that are involved in both basal and GnRH-induced transcription (1, 2).

Gonadotropes comprise only approximately 10% of the cell population of the anterior pituitary (5), and thus studies are made possible by the LβT2 cell model. This cell line was created through immortalization of mouse gonadotropes by targeted tumorigenesis using SV-40 large T antigen driven by the rat Lhb promoter. These cells are one of the clonal isolates derived from the resulting tumors. They express Cga, Lhb, as well as the receptor for GnRH (gene name Gnrhr) (6). LβT2 cells have been shown to respond to GnRH by raising intracellular calcium levels and stimulating exocytosis (7). Much of what is known regarding the signal transduction pathways and transcriptional responses induced by GnRH, including of Lhb and Cga amongst other genes important to gonadotrope function, has been extensively characterized in part by utilizing this and other gonadotrope models (5).

GnRH signaling

The hypothalamic form of GnRH is designated GnRH-I, and the classical GnRH receptor is referred to as the type I GnRH receptor. For the purposes of this dissertation, these will be referred to simply as GnRH and GnRH receptor. Structural variants for both GnRH (3) and its receptor (3, 8) exist, but are not expressed in humans or rodents. GnRH signaling originates with binding of the peptide to its G protein-coupled receptor on gonadotropes, which leads to activation of $G\alpha_q$ and phospholipase C-β1 (PLC-β1). Activation of PLC mediates hydrolysis of phosphatidylinositol 4,5-bisphosphate to produce inositol 1,4,5-triphosphate (IP_3) and diaglycerol (DAG) signaling intermediates.

DAG activates several isoforms of protein kinase C (PKC), including ε and δ. LβT2 cells express multiple conventional, novel, as well as non-conventional isoforms of PKC (9). DAG/PKC signaling leads to stimulation of all four mitogen-activated protein kinases (MAPK): extracellular signal-regulated kinase (ERK), Jun N-terminal kinase (JNK), p38, and big MAPK (BMK), to varying degrees. The contribution of MAPK to the transcriptional response of the gonadotropin subunits has been studied extensively (1-4, 10). In LβT2, ERK is the most strongly

activated MAPK, compared to p38 or JNK. Activated ERK accumulates in the nucleus within minutes of stimulation (9).

In contrast to DAG, signaling intermediate IP_3 mediates calcium mobilization. Binding of IP_3 to its receptor on the endoplasmic reticulum (ER) membrane results in release of calcium and stimulation of LH secretion. This release from intracellular stores is followed by an influx of calcium from the extracellular environment into the cell through L-type voltage-gated calcium channels on the plasma membrane, required mainly for renewal of internal calcium stores. While calcium mobilization does play a role in activating MAPK and stimulating transcriptional responses, the main and immediate function of calcium mobilization is to stimulate secretion of LH (1-4, 10). LH secretion is wholly dependent on pulsatile GnRH input (3).

Translation

While much work focuses on the transcriptional response of hormone input, translation is also an important component of gene regulation. In translation, messenger RNAs (mRNAs) serve as a template from which to guide the process of protein synthesis, which is catalyzed by ribosomes each with a 40S (small) and 60S (large) subunit of multiple ribosomal RNAs (rRNA) and proteins and aided by a multitude of other mRNA binding proteins. A eukaryotic mRNA is comprised of a 5' untranslated region (UTR) of, on average, 186 bp, followed by the codons of its protein coding sequence, and then an average 3'UTR of 607 bp (11). The 5'UTR is capped at the 5' end by a 7-methylguanosine and the 3' end of the 3'UTR is polyadenylated. Translation can be broken into stages of initiation, elongation, and termination. Initiation can occur through two distinct mechanisms, cap-dependent and cap-independent. During cap-dependent initiation, an mRNA is bound by cap-binding factors, the ribosomal subunits are recruited and assembled, and protein synthesis begins once the mRNA is scanned for the appropriate AUG start codon. During cap-independent initiation, ribosomes bind to internal ribosomal entry sites (IRESs) in the 5'UTR and do not require cap-binding factors in order to initiate translation (12). Elongation occurs next, during which the mRNA is threaded through the ribosome and decoded such that the appropriate

peptide bonds of the nascent polypeptide are formed. Termination occurs when the stop codon is reached, and the nascent polypeptide released. Finally, the ribosomes and mRNA binding factors are released from the mRNA and recycled, allowing the factors to be available for synthesis off another mRNA template (13, 14). Multiple ribosomes typically synthesize polypeptides off a single mRNA, forming polysomes.

Of particular importance for secretory cells, protein synthesis is compartmentalized. Soluble proteins are synthesized on free ribosomes in the cytosol and secretory, integral membrane proteins or endoplasmic reticulum (ER)-resident proteins are translated on ER-bound ribosomes. For secretory proteins, this allows for the growing polypeptide to be co-translationally shunted towards the secretory pathway, to be folded, post-translationally modified, and packaged into secretory vesicles. The signal sequence on a nascent polypeptide chain destined for the ER is bound by the signal recognition particle (SRP) during the first round of translation, at which time chain growth is arrested. Translation resumes when the nascent chain and ribosomes are routed and bound to the ER and the nascent chain is translocated into the ER lumen (15).

Translation initiation

Initiation in eukaryotes is facilitated by at least 12 mRNA-binding eukaryotic initiation factors (eIFs). Amongst these are eIF4G, eIF4E, and eIF4E, which together comprise the heterotrimeric eIF4F complex. eIF4E specifically binds to the 5' cap, eIF4A is a DEAD-box RNA-dependent ATPase that functions as a helicase to unwind RNA duplexes, and eIF4G is a scaffold protein, bridging eIF4E and eIF4A. eIF4G also interacts with poly(A)-binding protein (PABP), which binds to the 3' poly(A) tail of an mRNA, and thus eIF4G serves to circularize mRNAs. Binding of the eIF4F complex to the 5' cap facilitates eIF4G recruitment of the 43S preinitiation complex, which includes the 40S ribosome bound to the ternary complex (eIF2, initiator tRNA Met-$tRNA_i^{Met}$ and GTP) and eIF3, with which eIF4G interacts. This entire complex can then scan the 5' end of the mRNA until the initiating AUG codon is recognized. This codon is optimally within the context of the Kozak consensus sequence CGG(A/G)CCAUGG. At this point the 60S

ribosome binds and elongation begins. Detailed information on translation initiation can be found in several reviews (13, 14).

Regulation of cap-binding factors

Translation is typically regulated at the level of initiation, and in particular, through targeting the activity or availability of cap-binding initiation factors. eIF4E is regulated at both of these levels. The phosphorylation of eIF4E is correlated with increased translation rates and appears to enhance its activity, since the phosphorylated form has higher affinity for the 5' cap and is the form predominantly found in pre-initiation complexes. The availability of eIF4E is regulated through phosphorylation of its binding protein and negative regulator, 4E-binding protein (4EBP1, or PHAS1). 4EBP1 competes with eIF4G for eIF4E binding and its phosphorylation facilitates eIF4E release, allowing eIF4E to be available to complex with eIF4G and thus available for binding and initiation at the 5' cap (16, 17).

Modulation of protein synthesis through regulation of the cap-binding factors can occur through signaling to mTOR (target of rapamycin). Signaling through mTOR results in a positive effect on translation through mTOR phosphorylation of 4EBP1, affecting eIF4E availability, and through phosphorylation of ribosomal protein S6 kinase ($p70^{s6k}$), stimulating mRNAs containing 5' terminal oligopyrimidines, such as ribosomal proteins. mTOR can also affect translation through phosphorylation of a third effector, the kinase for elongation factor 2 (eEF2), stimulating elongation (17-19). mTOR is a target of RTK-coupled hormones as well as GPCR agonists (20). MAPK activation may also target translation, by affecting 4EBP1 or eIF4E. The latter is regulated by MAPK activation of the eIF4E kinase Mnk1 (17).

Regulation of ternary complex

Translation initiation is also targeted through regulation of the ternary complex. Formation of the ternary complex is regulated through phosphorylation of eIF2 at its α subunit. In its GTP-bound state, eIF2 associates with an initiator tRNA and delivers it to the 40S ribosomal

subunit. Once the complex binds an mRNA and scans to the start codon, the 60S subunit joins the complex and translation then occurs. At this point, the eIF2α-associated GTP is hydrolyzed to GDP and eIF2 dissociates from the mRNA. The guanine nucleotide exchange factor (GEF) eIF2B recycles the GDP back to GTP, allowing eIF2 to bind another initiator tRNA. When eIF2 is phosphorylated at its α subunit, it is a competitive inhibitor of eIF2B, not releasing the GEF after GDP/GTP exchange. Thus, phosphorylation of eIF2α inhibits eIF2B and its own activation, resulting in a general decrease in translation. Very little eIF2α needs to be phosphorylated to exert a translational effect, since eIF2B is limiting compared to eIF2 (16, 17).

There are four known mammalian eIF2α kinases, all of which are responsible for attenuating translation during various stress conditions: heme-regulated inhibitor (HRI, or eIF2a-kinase 1), protein kinase R (PKR, or eIF2a-kinase 2), PKR-like ER kinase (PERK, PEK or eIF2a-kinase 3), and general amino acid control of gene expression non-derepressing 2 (GCN2, eIF2a-kinase 4). HRI is a heme-sensitive kinase responsible for regulating translation of globins in reticulocytes. PKR is activated by double-stranded RNA, important for cellular responses to viral infection. PERK senses ER stress and is integral to the unfolded protein response (UPR). GCN2 is found in eukaryotes from yeast to mammals and is responsible for sensing amino acid conditions (21).

GnRH and translation

A few studies have implicated the regulation of post-transcriptional processes, including translation, by GnRH. GnRH has been shown to impact mRNA stability, increasing the stability of Lhb (22) as well as Cga message (22, 23). Gnrhr was also previously shown to be targeted, at the level of translation (24). Egr1, a transcription factor highly upregulated by GnRH (1), has been shown to downregulate 4EBP1 mRNA in hematopoetic cells (25). Finally, studies have also implicated regulation of translation directly by examining the activation of cap-binding factors by GnRH (26, 27). Despite these studies, translation is by no means a well-established mode of gene regulation by GnRH and thus the work presented in this dissertation sought to further

explore this facet of GnRH action. The goals were to first examine the potential of GnRH to regulate the ternary complex as an additional arm of translational control outside of its known regulation of cap-binding factors and then to further understand the multiple layers of GnRH regulation by examining the specificity of translational regulation and determine the mRNAs that might be targeted by GnRH at the global level.

CHAPTER 2

Activation of the unfolded protein response by GnRH

INTRODUCTION

Regulation of the LH and FSH glycoprotein subunits has been well described at the level of transcription (2). Very little work has focused on post-transcriptional regulatory pathways induced by GnRH, however. One such pathway is the unfolded protein response (UPR), which incorporates both transcriptional and post-transcriptional mechanisms in a multifaceted response to minimize endoplasmic reticulum (ER) stress. The ER is an oxidative environment where protein folding and post-translational modification of proteins that are secreted or targeted to the plasma membrane occurs (15). Because of the compartmentalization of translation of these proteins to the ER, the integrity of the ER becomes important to maintain the fidelity of translation. The UPR is a quality control pathway that maintains this integrity by monitoring changes in the ER lumen that perturb protein folding capacity. Disruption of the ER lumen can be a result of pathological conditions such as hypoxia, viral infection and starvation, or a result of normal physiological processes such as secretion or a high protein synthetic demand. ER stress can also be induced experimentally by the overexpression of misfolded proteins, which overwhelm the ER, or by pharmacological insults that target glycosylation, calcium, or oxidative balance. The UPR seeks to reestablish balance by decreasing the burden through attenuating translation and degrading misfolded proteins, as well as increasing synthetic capacity by increasing the size of the ER and the capacity of the protein-folding machinery. If balance is not reached, the UPR induces apoptosis.

Stress in the ER lumen is sensed by three ER-resident proteins, PKR-like ER kinase (PERK), Inositol-requiring enzyme 1 (IRE1), and Activating transcription factor 6 (ATF6). Activation of PERK leads to an immediate attenuation of general translation through phosphorylation of translation initiation factor eIF2α, which reduces protein synthesis demand on the ER. Phosphorylation of eIF2α also causes translation stimulation of Atf4, a bZIP transcription factor that stimulates genes that further the UPR program, including those involved in amino acid

transport/synthesis, metabolism, and the antioxidant response. PERK activation is followed temporally by proteolytic activation of the basic leucine-zipper transcription factor ATF6, which regulates genes with ER stress response elements (ERSE), such as chaperones. Finally, the UPR activates the kinase/endoribonuclease IRE1, which splices Xbp1 mRNA, another bZIP transcription factor important for UPR transcriptional responses. Xbp1 acts on promoters at unfolded protein response elements and is thought to be responsible for regulating genes that mediate ER-associated degradation (ERAD) of misfolded proteins. The UPR signaling pathway has been studied extensively and is the subject of multiple reviews (28-31). Another, recently discovered arm of the stress response is inhibition of translational complexes at the ER translocon (32).

The UPR has been shown to be crucial for the function of secretory cells, including plasma cells, β cells, hepatocytes, and osteoblasts, all which have heavy protein synthesis demands and thus rely on the proper function of the ER in order to maintain secretory output. Secretory cells must also face the unique challenge of having to re-establish the balance in the ER upon stimulation to secrete. This stimulation causes profound changes in the ER, including potentially causing concurrent increases in protein synthetic demand, disrupting oxidative balance due to the generation of reactive oxygen species, and causing an acute loss of calcium to the cytosol (33). Loss of Xbp1 in B lymphocytes in mice results in failure to differentiate into immunoglobulin-secreting plasma cells and ultimately failure to mount an immune response to polyoma virus infection (34). Ire1 is also required for proper immunoglobulin production and plasma cell differentiation (35). Mice that lack functional PERK in insulin-secreting pancreatic β cells have elevated serum glucose levels compared to wild-type littermates and eventually experience β cell apoptosis and diabetes (36, 37). Transgenic mice harboring a mutation in eIF2α that does not allow it to be phosphorylated show impaired insulin production and loss of insulin-positive β cells. Most transgenic neonates died within 18 hours of birth (38).

Since gonadotropes are endocrine secretory cells that experience heavy secretion and protein synthesis demand, and GnRH may impact these demands, it can be hypothesized that

GnRH targets the UPR as a means to regulate genes and function in gonadotropes. Such a role is unexplored, though indirect evidence indicates that this may be the case. Microarray studies have shown that GnRH induces Atf3 (39-41), a transcription factor upregulated by the Perk/Atf4 arm of the UPR (42). GnRH has been shown to transcriptionally regulate genes involved in amino acid synthesis, metabolism, and oxidative stress (39, 40), also consistent with activation of Perk. Finally, Xbp1 predicted targets such as DnaJ (43) are upregulated by GnRH (40, 41). To meet the demands of hormone secretion, it is likely that gonadotropes may mount a UPR-like response to GnRH. This hypothesis is addressed in this study by examining the activation of UPR effectors in LβT2 cells and primary pituitary gonadotropes and by ribosome profiling to examine the general status of translation. Besides utilization of LβT2 cells for determination of signaling events and transcriptional regulation leading to Lhb mRNA, these cells have been shown to respond to GnRH by raising intracellular calcium levels and stimulating exocytosis (7), indicating that the LH synthetic and secretory pathway are intact. The results indicate that the UPR is a target of GnRH action within the gonadotrope.

RESULTS

GnRH activates the ER stress sensor, PERK

The sensors of ER stress are mediated by three ER-resident proteins, IRE1, PERK, and ATF6. RT-PCR of mRNA isolated from LβT2 cells indicates that all three sensors are expressed in the cell line (Figure 2-1A). An immediate effect of ER stress is activation of the UPR through PERK. Activated PERK oligomerizes (44) and autophosphorylates at 10 different sites in its kinase domain (45). To determine whether GnRH exposure leads to the phosphorylation of PERK, LβT2 cells were treated with GnRH or dithiothreitol (DTT) for 30 minutes. DTT severely disrupts the ER's oxidative environment required for proper protein folding (31) and is commonly used to disrupt translation and activate the UPR (32, 46, 47). The proteins were harvested and subjected to Western blotting. A shift in PERK mobility (Figure 2-1B) is consistent with hyper-phosphorylation of the protein, with DTT causing a slightly greater shift than seen with GnRH. To

confirm that this shift is indeed due to phosphorylation events, protein extracts were treated with phosphatase and then subjected to Western blotting. The mobility shift of PERK is abrogated when extracts are treated with phosphatase (Figure 2-1C). Under basal conditions PERK exists in a moderately phosphorylated state, with the level of phosphorylation increasing with GnRH or DTT treatment.

Activated PERK directly phosphorylates the α subunit of translation initiation factor eIF2. Phosphorylation of eIF2α prevents initiation complex formation, leading to free monosome and ribosomal subunit accumulation and a decrease in general translation (13). To check the phosphorylation status of eIF2α in response to GnRH, antibodies specific to total and phosphorylated eIF2α were used in Western blotting of vehicle, GnRH and DTT-treated extracts. GnRH treatment resulted in an increase in eIF2α phosphorylation, and greater phosphorylation was observed after DTT treatment (Figure 2-1D, 2-1E).

GnRH causes splicing of the UPR transcription factor Xbp1

To confirm that GnRH is activating ER stress, a different arm of the UPR was explored. Signaling to the kinase/endoribonuclease IRE1 leads to activation of Xbp1, which encodes a bZIP transcription factor important for UPR transcriptional responses. Xbp1 acts as an activator at unfolded protein response elements (29). Xbp1 is activated through a cytoplasmic mRNA splicing event, where removal of a small intron allows translation of an active transcription factor (48). The unspliced mRNA contains a PstI site in the intron that is removed by the splicing event (49). Xbp1 cDNA prepared from LβT2 cells treated with vehicle, GnRH, or DTT (Figure 2-2A) was subjected to PstI digestion. GnRH caused splicing of Xbp1 mRNA, although to a lesser degree than DTT treatment (Figure 2-2B), which resulted in splicing of all the available Xbp1 mRNA.

To confirm that the UPR is activated by GnRH in primary gonadotrope cells, pituitaries were isolated from wild-type, sexually mature nine-week old male mice, dissociated, and cultured. Only gonadotropes express the receptor for GnRH (50) and thus should be the only cell type

responding to GnRH. The cells were treated with GnRH for 30 minutes and the splicing of Xbp1 was measured through quantitative PCR using primers specific to the spliced form of Xbp1. Splicing of Xbp1 increased four-fold in response to GnRH (Figure 2-2C). Gapdh was assayed as an unregulated internal control mRNA. Using the GnRH-receptor (Gnrhr) mRNA as an internal control also resulted in the same observation (data not shown). PCR amplification of Lhb from the cultured pituitary cells indicates that indeed gonadotropes were amongst the cells isolated (Figure 2-2D).

GnRH causes an accumulation of RNP complexes

The observation that GnRH causes eIF2α phosphorylation (Figure 2-1D) indicates that GnRH may attenuate translation. To determine the general translational status of the LβT2 cells, ribosome and mRNA complexes were separated on sucrose gradients. Complexes were fractionated according to density while monitoring absorption at 254 nm. Presence of the 28S and 18S rRNAs was used to facilitate combining fractions to represent the actively translating polysome pool, consisting of mRNAs complexed with two or more ribosomes, or the heterogeneous ribonucleoprotein (RNP) pool, consisting of mRNAs complexed with initiation factors or a single ribosome (monosome), and free 60S or 40S ribosomal subunits (Figure 2-3A). These mRNAs could potentially be associated also with proteins involved in maturation, export, and localization, as well as translation initiation (51, 52). Enrichment of the ER-membrane bound protein Calnexin in the supernatant (Figure 2-3B) prior to layering on the gradient, as opposed to in the cell pellet, indicates that the extraction technique was able to isolate membrane-associated proteins, such as ribosomal complexes docked to the ER. This would be of particular interest for gonadotropin mRNAs, where compartmentalized protein synthesis routes translation of soluble proteins on free ribosomes in the cytosol and routes secretory proteins, such as the glycoprotein subunits Lhb and Cga, to ER-bound ribosomes (15). ERK was also enriched in the supernatant, but, like Calnexin, some was present in the cell pellet. This indicates that at least some of the

Calnexin detected in the cell pellet could be due to supernatant that was not completely collected for layering, as expected, as opposed to inefficient membrane extraction.

To determine the effect of GnRH on general translation, cells were treated with GnRH for 30 minutes and then ribosomes were fractionated and pooled. The relative abundance of RNA in each pool was compared using the absorption profiles to evaluate the extent of translational regulation. This comparison indicated a marked redistribution of RNA in response to acute GnRH, reflecting a general shift from actively translating polysomes to RNP complexes (Figure 2-3C). The areas under the ribosome profile curves of the pools were integrated as a measure of the amount of RNA present in each pool. The RNP pool shifted from being about 60% of the polysome pool to being equivalent to the polysome pool with GnRH exposure (Figure 2-3D).

As a comparison, cells were treated with epidermal growth factor (EGF), a mitogen known to stimulate translation (53), and an increase in polysomes compared to RNP was observed (Figure 2-3C). In contrast, treatment of the cells with DTT resulted in the expected depletion of polysomes (Figure 2-3C), similar in direction but much greater in magnitude than that of GnRH.

RNP accumulation by GnRH is mimicked by disruption of intracellular calcium

GnRH is responsible for inducing secretion and *de novo* synthesis of gonadotropins in gonadotropes. GnRH acts through its GPCR to activate $G\alpha_q$ and PLC, mediating production of IP_3 and DAG signaling intermediates. DAG leads to activation of PKC and all four MAPK cascades, ERK, JNK, p38, and BMK (4). ERK has been implicated in regulation of translation by GnRH (27). The IP_3 mediated release of calcium from internal stores triggers secretion, while influx from the extracellular environment renews internal stores (4). Modulation of protein synthesis in response to mitogenic signals is often regulated through PI3K and mTOR, whose downstream targets include 4EBP1 and ribosomal protein S6 kinase $p70^{s6k}$ (18). mTOR is a target of RTK-coupled hormones as well as GPCR agonists (20).

To understand the effect on translation mediated by GnRH, pharmacological inhibitors of the various signaling pathways were used prior to GnRH exposure to determine which signaling pathways are required. The use of U0126 (Figure 2-4B) or PD98059 to block ERK, SB203580 to block p38, SP600125 to block JNK, phorbol-12-myristate-13-acetate (PMA) to directly activate PKC, or bisindolylmaleimide I to block PKC activation (Figure 2-4B) had no effect on GnRH-induced RNP accumulation (Figure 2-4A). This indicates that PKC and MAPK signaling pathways are not required for the observed ribosome remodeling. Similarly, inhibiting CaMk II activation via KN62 and voltage-gated calcium channel activation via nimodipine had no effect (data not shown). The use of translation inhibitors LY 294002 to block PI3K or rapamycin to block mTOR were not informative, since these agents alone caused translation attenuation (data not shown). Furthermore, although GnRH has been shown to activate P13K via transactivation of the EGF receptor (54), signaling through P13K and/or mTOR would result in a positive effect on translation, which is not consistent with an accumulation of RNP complexes. In LβT2 cells, P13K appears to diverge from the classical RTK-signaling cascade, not utilizing Akt (and presumably, then, mTOR) in its direct downstream effects on cell survival (54), gonadotropin synthesis (55), or translation initiation factors (27). For these reasons, the P13K/mTOR arm was not pursued further.

In contrast, ER calcium disrupters such as thapsigargin, which blocks calcium reuptake by the SERCA pump (SR/ER Ca^{2+} ATPase), 2-APB, which blocks IP_3 receptors, and the calcium ionophore ionomycin, which increases intracellular calcium levels and is a known LH secretagogue (56), were all sufficient to induce RNP remodeling, similar to GnRH (Figure 2-4C). Chelation of calcium through BAPTA also had the same effect (Figure 2-4C). The calcium disrupters caused RNP accumulation to varying degrees, with ionomycin eliciting accumulation most similar in magnitude to GnRH (Figure 2-4D). Pharmacological agents that disrupt ER calcium stores have been shown to induce the UPR (57). The ER and intracellular calcium levels appear to be involved in mediating RNP accumulation in response to GnRH stimulation.

Lhb, Cga, and Gapdh mRNAs redistribute to RNP complexes

To evaluate if the overall ribosome changes seen after exposure to GnRH are reflected in the manner in which specific mRNAs relevant to gonadotrope function behave, Lhb and Cga mRNAs were examined. In the differentiated gonadotrope, GnRH stimulates transcription and synthesis of the LH subunits, which are modified and exported through the ER and are therefore dependent on proper ER function.

The behavior of Lhb and Cga mRNA was determined by measuring their mass ratio between the polysome and RNP pools. Redistribution of an mRNA species was calculated by comparing these ratios in GnRH-treated and control samples. The calculated fold-redistribution is thus a measurement of the change in transcript representation in each of the pools after GnRH treatment. In agreement with the overall shift of ribosomes, Lhb, Cga and Gapdh mRNAs all redistributed to RNP complexes after GnRH exposure (Figure 2-5). This behavior was recapitulated by ionomycin (Figure 2-5A) and DTT (Figure 2-5B) treatment. The magnitude of RNP accumulation caused by ionomycin of the three mRNAs was similar to that observed with GnRH, while the redistribution caused by DTT was much greater, consistent with the degree of general ribosome movement induced by these agents (Figures 2-4C and 2-3C).

GnRH attenuates translation initiation

The observed accumulation of RNP complexes after treatment with GnRH may be a result of two distinct responses. First, the stimulatory effect of GnRH on transcription of various genes has been well described (39-41, 58, 59) and so GnRH could be stimulating production of new mRNA and ribosomes that are assembling in new translation initiation complexes, resulting in an increase of RNP complexes. In this scenario, inhibition of transcription would block any GnRH-induced redistribution. To test this possibility, LβT2 cells were treated with actinomycin D to block transcriptional events prior to treatment with GnRH, and ribosomes were fractionated. Actinomycin D alone caused a slight redistribution of RNA into the RNP pool (Figure 2-6B). However, GnRH caused an additional influx, similar in magnitude to that seen without

actinomycin D pre-treatment (Figure 2-6A, 2-6B). Measurement of the distribution of Lhb, Cga, and Gapdh mRNA was also consistent with this behavior (Figure 2-8A). The concentration and duration of actinomycin D used was sufficient to inhibit transcription, as confirmed through its ability to inhibit Egr1 induction by GnRH (Figure 2-6C). Since actinomycin D did not block the ribosome remodeling, this indicates that the rise in RNP complexes and accumulation of mRNAs within those complexes is independent of transcriptional events.

The second cause of RNP accumulation may be ribosome dissociation from polysomal mRNA after exposure to GnRH, thus redistributing mRNAs as RNPs, such as predicted by an inhibition of translation initiation through activation of the UPR. In this scenario, inhibition of translation elongation would prevent ribosomes from dissociating, thus blocking any GnRH effect. To test this, LβT2 cells were pre-treated with cycloheximide to inhibit translation elongation prior to treatment with GnRH. Inhibition of translation elongation indeed blocked the redistribution of ribosomes (Figure 2-7A, 2-7B) as well as the redistribution of Lhb, Cga, and Gapdh mRNAs (Figure 2-8B). Cycloheximide pre-treatment alone caused a slight change in the distribution of RNA (Figure 2-7B). However, GnRH did not cause a further redistribution. Additionally, no differences in the total integrated areas (RNP and polysome) under the ribosomal curves (Figure 2-7C) or in the total mass of extracted RNA (Figure 2-7D) were detected between vehicle and GnRH-treated cells, consistent with ribosome redistribution rather than influx of newly synthesized RNA. Overall the results confirm that the RNP increase caused by GnRH is indicative of an attenuation of translation.

Attenuation of translation is transient

The primary function of pituitary gonadotropes is to produce LH and FSH and thus it seems paradoxical that GnRH would decrease the translation of mRNAs that are important for the production of these hormones. It was of interest to determine whether this attenuation is permanent or transient. To test this, LβT2 cells were exposed to a ten-minute pulse of GnRH and fractionated at various times after stimulation. Integration of the areas under curve of the

resulting ribosome profiles indicates that a 10-minute pulse exposure to 10 nM GnRH is sufficient to cause an accumulation of RNP complexes similar in magnitude to a tonic 30-minute exposure (Figure 2-9A, compare to Figure 2-3D). A 10-minute pulse of GnRH pulse is also sufficient to cause phosphorylation of PERK (Figure 2-11) and eIF2α (Figure 2-10C). Additionally, the RNP accumulation appears to be dose dependent, with a 1 nM pulse of GnRH sufficient to cause accumulation (Figure 2-10A, 2-10B). After 60 minutes, redistribution into RNP complexes subsides, but does not return to basal levels (Figure 2-9A) and PERK also remains phosphorylated (Figure 2-11). However, using quantitative PCR to follow the distribution of Lhb, Cga, and Gapdh mRNAs between polysomes and RNP complexes revealed that while the RNP accumulation does not completely resolve, the translation of the specific transcripts examined does return to basal levels within 60 minutes (Figure 2-9B).

DISCUSSION

The data show that in pituitary gonadotropes, GnRH, a central regulator of reproduction, induces the unfolded protein response pathway through activation of at least two of the three known ER stress sensors: PERK, which leads to translation attenuation through phosphorylation of eIF2α, and IRE1, which leads to splicing of transcription factor Xbp1 mRNA. Initial characterization of signal transduction in the UPR comes from experiments using agents that severely stress ER homeostasis and rapidly induce all three arms of the UPR. However, evidence is mounting that the UPR is crucial to normal physiological function, especially in the development or function of secretory cells (33). The data presented here support this hypothesis and is the first to examine activation of the UPR in gonadotropes.

Unlike pharmacological agents that severely disrupt ER function, physiological processes may be more subtle and utilize only specific UPR components or activate the UPR to a lesser degree or duration (33). This is observed in plasma cell differentiation, which requires activation of Ire1 but not Perk or eIF2α phosphorylation (35). Loss of Perk in mice results in loss of β-cell function (36), but loss of Xbp1 shows defects in liver growth (60) and lymphocyte differentiation

(34). In myocytes, vasopressin at physiological concentrations activates the UPR but not to the same degree as pharmacological agents. It also does not result in chaperone synthesis or condition the cells to tolerate future ER stressors (61), as pharmacological UPR activation has been shown to do. While GnRH appears to target Perk and Ire1, it is unknown whether it targets Atf6. Atf6 acts on ERSEs to stimulate transcription of Chop and Xbp1 (62) and chaperones, such as BiP/Grp78, Grp94, and Calreticulin (63). GnRH has been shown to induce Xbp1 (40, 41) and Chop (40). Induction of Xbp1 or Chop, however, may also occur via XBP1 itself. Like ATF6, XBP1 can bind to ERSEs, though with less affinity (64). Therefore, GnRH may activate all three arms of the UPR, or just Perk and Ire1, bypassing Atf6 and utilizing XBP1 instead to upregulate Chop and its own mRNA. This remains to be investigated in gonadotropes. Initial attempts to detect Atf6 and its activation through Western blotting have been unsuccessful (see Appendix, Figure 5-1).

The model presented in Figure 2-12 illustrates that GnRH, through activation of the IP_3 receptor, causes calcium to leave the ER and thus signals to activate Perk and attenuate translation. The involvement of intracellular calcium, but not other signal transducers of the known GnRH signaling pathways, is consistent with the hypothesis that it is the loss of calcium from the ER that elicits the UPR. While all of the pharmacological agents used in these studies are known to impact intracellular calcium levels in various ways, the common thread may be that they all at some level cause ER calcium loss. Ionomycin is an ionophore that carries Ca^{2+} ions across the plasma membrane into the cytosol but also facilitates release of the ions from intracellular stores, as demonstrated in a recent study (65). In the current studies, attempts to show that ionomycin causes LH release using IRMA have been inconclusive, though the effect of ionomycin on calcium and LH release under the same conditions used in these studies has been demonstrated elsewhere (56). The data here is consistent with data from others that show exposure of cells to ionophores such as ionomycin inhibits translation and causes an increase in monosomes and free ribosomal subunits (61, 66). While the experiments in sum were not conclusive in determining how GnRH may signal to the UPR since disruption of calcium alone

caused RNP accumulation, the consistent observation that only ER calcium loss appears to mimic GnRH action is revealing.

How PERK is activated, mechanistically, is not clear. Multiple signals may integrate to activate the UPR. First, secretory protein production and secretion results in acute loss of amino acids and continued production of reactive oxygen species (ROS) generated by disulfide bond formation. The ER may act as a sensor to combat oxidative stress caused by accumulated ROS (67, 68). Cells lacking UPR components accumulate higher levels of ROS that contribute to cell death (69). Alternatively, the stimulus to secrete (β cells) or differentiate (B cells) may be accompanied by an increase in demand for protein synthesis that the ER is not yet prepared for, resulting in accumulation of misfolded proteins that activate the UPR (33). The ER-resident chaperone BIP/GRP78 associates with PERK and IRE1 to prevent their dimerization and activation. Dissociation of BIP/GRP78 from these sensors caused by BIP association with unfolded proteins during stress allows PERK and IRE1 dimerization and activation (44). Unfolded proteins may also bind directly to IRE1 or PERK (28). The demonstration that uncontrolled upregulation of mTOR, which presumably leads to increased protein synthesis (as shown by phosphorylation of ribosomal protein S6 and its kinase), causes activation of the UPR and thapsigargin-induced apoptosis that is rescued by cycloheximide (70) is consistent with the idea that increased protein synthesis and misfolded proteins activate ER stress. How this might be involved in GnRH action will be explored further in Chapter 4. Finally, calcium may be the primary integrator of stress. Loss of calcium from the ER lumen during secretion may disrupt folding of proteins that require calcium to fold properly, particularly glycoproteins (61), resulting in misfolded proteins. Calcium loss may also directly disrupt chaperones, such as BIP, which bind calcium and are involved in maintaining ER calcium levels (71). Perk itself has been implicated in integrating calcium-mediated ER stress responses (47). Loss of ER calcium has been linked to UPR activation in myocytes upon vasopressin stimulation (61). For gonadotropes, calcium facilitates secretion (7) and transcriptional responses (1), and now it appears to play a role in translational control, giving greater credence to its importance in normal pituitary function. The

data support the idea that signaling to the UPR by ER-disrupting agents can be thought of as an extension of the UPR's physiological role in sensing calcium and maintaining the proper function of the ER. It is of interest to determine the mechanism of PERK activation and how exactly calcium may be involved, especially in the context of physiological processes such as secretion.

Activation of the UPR by GnRH is consistent with the known actions of GnRH and gonadotrope biology. First, Perk activation leads to cell cycle arrest (31), which is thought to protect cells by rerouting energy to allow for recovery of cell function and expansion of the ER. This might explain the anti-proliferative effects of GnRH observed in LβT2 and conferred by GnRH-receptor action in other cells (73). Secondly, activation of the UPR by GnRH is transient in LβT2 cells and is induced at a lower magnitude than by DTT. This is consistent with the idea that GnRH is not activating an acute, extreme stress response but rather modulating the level of protein production in the ER to match synthetic capacity, adapting to physiological ER stress. Similarly, myocytes rapidly recover protein synthesis after vasopressin stimulation of the UPR (61). A situation could be hypothesized where immediate exposure to GnRH causes gonadotropin hormone secretion and a temporary attenuation in secretory gene translation in order for the cell to lower the ER load and deal with metabolic changes. This matching of ER synthetic capacity with ER synthetic demand in order to reduce stress would be consistent with the pulsatile stimulation of gonadotropes by GnRH *in vivo*, which theoretically would place the gonadotrope under high, continual ER strain. It is unclear whether two 10-minute pulses of GnRH in the LβT2 cells results in the same degree of PERK phosphorylation as one pulse (Figure 2-11). Nonetheless, whereas perturbations in the ER by pharmacological agents can be categorized as acute insults, physiological processes such as periodic hormonal input for secretion can be viewed as chronic ER stress, indicating a potential necessity for the UPR. The role of the UPR in gonadotrope biology, particular in the context of pulsatile GnRH action, needs to be directly explored. The UPR may be involved in gonadotrope development to help expand the ER to prepare for protein synthesis and secretion, or, it may be signaled to in order to prevent apoptosis from periodic GnRH stimulation. These possibilities will be discussed in Chapter 4.

Finally, while these studies are the first to show that GnRH activates the UPR, GnRH has previously been shown to regulate translation and other post-transcriptional processes, including gonadotropin message stability (22, 23). Interestingly, microarray data in HeLa cells shows that mRNAs that are translationally attenuated during ER stress are also stabilized (72). This is consistent with the known increase in stability and now observed translational attenuation of Lhb and Cga mRNAs upon GnRH exposure. Evidence also suggests that GnRH targets translation through activating cap-binding initiation factors, including 4EBP-1 (26, 27), eIF4E and eIF4G (27). How these two seemingly opposing translational pathways work in concert to provide specificity to the translational regulation induced by GnRH will be addressed in the next chapter.

MATERIALS AND METHODS

LβT2 and primary pituitary cell culture

The LβT2 (6) mouse gonadotrope line was maintained in high-glucose HEPES-buffered DMEM supplemented with penicillin/streptomycin and 10% fetal bovine serum. The cells were incubated at 37°C in a humidified atmosphere of 5% CO_2.

For primary pituitary culture, pituitaries were isolated from nine-week old wild-type male mice (C57BL/6). Mice were sacrificed using CO_2 asphyxiation followed by cervical dislocation, in accordance with UCSD Institutional Animal Care and Use Committee regulations. Whole pituitaries were isolated into ice-cold PBS and then dissociated through incubation in trypsin containing collagenase in a shaking 37°C bath for 15 minutes. Afterwards, the pituitaries were gently pipetted to facilitate dissociation and then returned to the bath for another 15 minutes. Finally, DNase was added for 10 minutes and then the cells were pelleted at 2000 x g for 5 minutes. The pelleted cells were resuspended, plated on poly-lysine coated dishes, and then maintained in the same culture conditions described for the LβT2 cells.

To plate cells for experiments, cells were plated, grown overnight for 36 hours, and then the media was changed to serum-free media (SFM) and the cells were incubated overnight for an additional 16-18 hours. Cells were treated with hormones/drugs in SFM on the third day.

Hormone and drug treatments

Plated, serum-starved cells were treated with vehicle, 10 nM GnRH (unless otherwise indicated), 1 uM ionomycin (Calbiochem, La Jolla, CA) for 30 min, 50 nM thapsigargin for 1 hour, 75 uM 2-APB (Calbiochem) for 10 min, 50 uM BAPTA (Calbiochem) for 30 min, 2 mM dithiothreitol (DTT) for 30 min, or 10 nM EGF for 30 min. Where appropriate, 5 uM actinomycin D (Calbiochem) was added to the media for 1 hour, 100 ug/ml cycloheximide for 5 minutes, 1 uM U0126 (Calbiochem) for 30 min, or 100 nM bisindolylmaleimide I (Calbiochem) for 30 min, prior to GnRH treatment. All reagents were from Sigma-Aldrich (St. Louis, MO) unless otherwise indicated. GnRH at 10 nM was previously shown to induce calcium flux and exocytosis in LβT2 (7). The drugs/hormones were left in the media for the duration of treatment. For the GnRH pulse treatments, GnRH was added to the media for 5 or 10 minutes, as indicated, after which the media was removed, the cells were washed with PBS, and fresh media was added back until a second pulse was applied or the cells were harvested at the times indicated.

RNA isolation and RT-PCR

LβT2 and primary pituitary cells were plated at a density of $1x10^7$ cells per 10-cm dish or $3x10^5$ cells per 48-well plate, respectively. Total RNA was harvested using Trizol LS (Invitrogen, Carlsbad, CA). The RNA was DNase-treated and then reverse transcribed using QuantiTect Reverse Transcription Kit (Qiagen, Valencia, CA). For regular PCR, PCR was performed using HotStarTaq Mastermix (Qiagen, Valencia, CA) and transcript-specific primers, as outlined below. Parallel control PCRs were performed using all components except for reverse transcriptase. PCR products were subjected to agarose electrophoresis in the presence of ethidium bromide.

Primer sequences were designed against murine mRNA sequences as available through PubMed. The primer sequences were: Atf6 fwd 5'-AAAGTCCCAAGTCCAAAGC-3', Atf6 rev 5'-CTGAAAATTCCAAGAGATGC-3'; Ire1 fwd 5'-AACTCCTCTGTCTGCATCC-3', Ire1 rev 5'-GCCAACTATGTTGATAACTTCC-3'; Perk fwd 5'-AGCACGCAGATCACAGTCAGG-3', Perk rev 5'-TGGCTACGATGCAAAGCAGG-3'; Lhb fwd 5'-CTGTCAACGCAACTCTGG-3', Lhb rev 5'-

ACAGGAGGCAAAGCAGC-3'; Xbp1 fwd 5'-TACGGGAGAAAACTCACG-3', Xbp1 rev 5'-TCTGAAGAGCTTAGAGGTGC-3'.

Ribosome fractionation and mRNA isolation

Two 10-cm plates were used for each experimental condition with $2x10^7$ LβT2 cells seeded per plate and treated as described. After treatment, 100 ug/ml cycloheximide was added to all the plates (except for any plates already pre-treated with cycloheximide) and the cells were incubated on ice for 5 minutes. The cells were then harvested in 500 ul of ice-cold polysome extraction buffer (PEB) containing 140 mM KCl, 5 mM $MgCl_2$, 1 mg/ml heparin sodium salt, and 20 mM Tris-HCl pH 8, supplemented with fresh 0.5 mM DTT and 100 ug/ml cycloheximide on the day of the experiment. Cells from two plates of the same experimental condition were collected and pooled at this step. The cells were spun down at 1000 X g for 3 minutes and then each pellet was resuspended in 200 ul PEB containing 1% Triton-X. The pellets were allowed to lyse on ice for 20 minutes with gentle inversion by hand every few minutes. Finally, the cellular debris was collected by centrifugation at 10,000 X g for 10 minutes. The supernatants were layered onto 5 ml 10-50% sucrose gradients made with PEB lacking Triton-X. An aliquot of the supernatant or of the cell pellet, resuspended, was used to examine Calnexin and ERK presence via Western blotting. The layered supernatants were centrifuged in a SW-55 swing-bucket rotor for 1.5 hours at 150,000 X g.

A 21-guage needle was used to collect fractions from the bottom of the gradient. Fractions were collected using a peristaltic pump while monitoring real-time absorption at 254 nm through a UVM-II monitor (GE Healthcare, Fairfield, CT). Fractions of 250 ul volume each were collected using a FC 203B fraction collector (Gilson, Middleton, WI). Monitoring of UV absorption and fraction collection was controlled through a Labview virtual instrument (National Instruments, Austin, TX) and a KPCI 3108 DAQ card (Keithley Instruments, Cleveland, OH). Fractions were dripped directly into SDS for a final SDS concentration of 1%. Each fraction was then treated with 0.2 mg/ml proteinase K at 37° C for 1.5 hours. RNA was purified from each fraction by

phenol-chloroform extraction and ethanol precipitation. An aliquot (1 ul) of RNA from each fraction was subjected to agarose electrophoresis in the presence of ethidium bromide to verify the presence of the large and small ribosomal subunits through presence of the 28S and 18S rRNAs, respectively. The rest of the RNA from the fractions was pooled into polysome and RNP pools according to the gradient's UV absorption profile. The quality and mass of total extracted RNA from each pool was measured by absorption at 260 nm prior to mRNA isolation. Poly(A) RNA was then isolated using Oligotex mRNA Mini Kit oligo-dT columns (Qiagen, Valencia, CA) according to the manufacturer's recommendations and eluted into a final volume of 40 ul for each pool. A 10 ul aliquot of mRNA was used for reverse-transcription for quantitative PCR analysis.

Quantitative real-time PCR

For quantitative PCR analysis of fractionated, ribosome-bound mRNA, cDNA was synthesized using Omniscript Reverse Transcriptase (Qiagen, Valencia, CA) and 10 uM of random hexamer primers (Applied Biosystems, Foster City, CA). For analysis of primary pituitary RNA, cDNA was synthesized using QuantiTect Reverse Transcription Kit (Qiagen, Valencia, CA). Quantitative real-time PCR was carried out using the MyIQ Single-Color Real-Time Detection System (Bio-Rad Laboratories, Hercules, CA). The PCR products were amplified in the presence of SYBR Green using the QuantiTect SYBR Green PCR kit (Qiagen, Valencia, CA) supplemented with 300 nM of transcript specific primers and 1 uM fluorescein for proper instrument calibration. The cycling conditions used were those recommended by the PCR kit manufacturer. A melt curve was performed after each PCR run to ensure that just a single product was amplified in each assay and the size of the products were verified using agarose gel electrophoresis.

Primer sequences were designed against murine mRNA sequences as available through PubMed. The Xbp1s primer set only recognizes the spliced Xbp1 mRNA. The primer sequences were: Cga fwd 5'-GGTTCCAAAGAATATTACCTCG-3', Cga rev 5'-GTCATTCTGGTCATGCTGTCC-3'; Egr1 fwd 5'-ATTTTTCCTGAGCCCCAAAGC-3', Egr1 rev 5'-ATGGGAACCTGGAAACCACC-3'; Gapdh fwd 5'-TGCACCACCAACTGCTTAG-3', Gapdh rev 5'-

GATGCAGGGATGATGTTC-3'; Lhb fwd 5'-CTGTCAACGCAACTCTGG-3', Lhb rev 5'-ACAGGAGGCAAAGCAGC-3'; Xbp1s fwd 5'-GAGTCCGCAGCAGGTG-3', Xbp1s rev 5'-GAATCTGAAGAGGCAACAGTG-3'.

Primers were designed to generate an 80-150 bp amplicon that crossed intron/exon boundaries where possible in order to avoid amplification of any contaminating unspliced RNA or genomic DNA. All PCR reactions were performed in triplicate, except for those involving cDNA from primary pituitary cells, which were performed in duplicate. A larger cDNA fragment of Cga, Egr1, Gapdh, and Lhb was inserted into pCR2.1 (Invitrogen, Carlsbad, CA) and used to generate a standard curve and assess PCR efficiency for each run. The mass values for each transcript were extrapolated from the standard curve. For Xbp1s PCR reactions, cDNA from DTT-treated LβT2 cells were diluted serially and run alongside primary pituitary reactions in order to assess efficiency. In this case, the Pfaffl method (74) was used to calculate relative mass levels of Xbp1s with respect to Gapdh as an internal control.

To calculate a fold-redistribution value for an mRNA's movement within the ribosome profile, the mass of each transcript in each ribosome pool (polysome or RNP) was measured and a ratio was calculated for the mass of that transcript in the RNP pool compared to the polysome pool. A ratio was calculated for both the treated and control (vehicle treated) conditions. A fold-redistribution value was then generated by taking a ratio of the ratios: the RNP/polysome ratio in treated compared to the RNP/polysome ratio in control cells. Statistics were performed as indicated in each figure legend on these values. For ease of representation in the histograms only, the negative inverse was calculated and reported for fold-redistribution values between 0 and 1, such that movement of an mRNA into the polysome pool would report a negative redistribution value and movement into RNP complexes would report a positive value.

Xbp1 splicing assay

Xbp1 splicing was detected through PCR amplification of Xbp1 by primers that recognize both the spliced and unspliced mRNA, followed by PstI digestion. The primers used were Xbp1

fwd 5'-TACGGGAGAAAACTCACG-3' and Xbp1 rev 5'-TCTGAAGAGCTTAGAGGTGC-3'. After PCR amplification, Xbp1 cDNA (10 ul of a 50 ul PCR reaction) was treated with 20-40 units of PstI (New England BioLabs, Ipswich, MA) for 1 hour and then resolved by agarose electrophoresis in the presence of ethidium bromide. The expected PCR band sizes were 549 bp for the unspliced and 523 bp for the spliced form. PstI digestion of unspliced Xbp1 yields fragments of 172 and 381 bp while the spliced mRNA is resistant to PstI.

Western blotting

Cells were plated ($1x10^7$) in 10-cm dishes. After treatment, protein was harvested using standard RIPA lysis buffer supplemented with phosphatase inhibitors. Standard SDS-PAGE and semi-dry transfer method (Bio-Rad Laboratories, Hercules, CA) was used to transfer the extracts onto PVDF membranes (Bio-Rad Laboratories, Hercules, CA). Species specific antibodies were used for all subsequent blotting.

For detecting phosphorylated and total eIF2α, membranes were blocked with 5% non-fat dry milk and the primary antibodies delivered in 5% BSA. The antibodies (Cell Signaling, Danvers, MA) were diluted 1:1000 and incubated overnight. For PERK, blocking and primary antibody delivery was performed in 5% milk. The primary antibody (Rockland Immunochemicals, Gilbertsville, PA) was diluted 1:1000 and incubated overnight. For detecting phosphorylated ERK, blocking and primary antibody delivery was performed in 1X casein (Vector Laboratories, Burlingame, CA). Antibody against phosphorylated ERK (Santa Cruz Biotechnology, Santa Cruz, CA) was diluted 1:1000 and incubated for 1 hour.

For Western blotting of Calnexin and total ERK in extracts prepared for ribosomal profiling, an equal mass of protein from the ribosome fractionation supernatant and pellet was used for blotting. Blocking and Calnexin primary antibody (Cell Signaling, Danvers, MA) delivery was performed in 5% milk. The primary antibody was diluted 1:2000 and incubated overnight. The blot was then stripped and re-probed for total ERK. Blocking and ERK primary antibody

delivery was performed in 1X casein (Vector Laboratories, Burlingame, CA). Antibody against total ERK (Millipore, Billerica, MA) was diluted 1:2500 and incubated for 1 hour.

All the blots were developed using 1:2000 dilution of biotinylated secondary antibodies (Santa Cruz Biotechnology, Santa Cruz, CA) and Chemiglow chemiluminescence (Alpha Innotech, San Leandro, CA). Chemiluminescence was visualized and quantified using the GeneSnap BioImaging System (Syngene, Frederick, MD).

For confirmation of the phosphorylation status of PERK, extracts were lysed in RIPA buffer supplemented with protease inhibitors (Roche, Basel, Switzerland) but not phosphatase inhibitors. Extracts were then treated with 2000 units of Lambda Protein Phosphatase (New England BioLabs, Ipswich, MA) for 15 minutes prior to SDS-PAGE.

Statistical Analysis

The areas under the curves of the ribosome profiles were integrated using SigmaPlot v9.01 (Systat Software, Richmond, CA). Any ratio or fold-redistribution data was transformed using $\log_2$ and a value of 10 was added to those values to ensure positive values prior to analysis. All subsequent analysis was conducted using JMP IN (SAS Institute, Cary, NC) on untransformed (other than $\log_2 + 10$ for ratio or fold-redistribution values) or optimally Box-Cox transformed values. P-value ≤ 0.05 was considered significantly different. All experiments were repeated at least three independent times and reported values are the means +/- SEM, unless otherwise indicated.

ACKNOWLEDGEMENTS

Chapter 2, in part, has been submitted for publication of the material as it may appear in Molecular Endocrinology, 2008, Minh-Ha T. Do, Sharon J. Santos and Mark A. Lawson. The dissertation author was the primary investigator and author of this paper.

This work was supported by the National Institutes of Health grants R01 HD 43758 and K02 HD 40708. M.T.D. was supported by the NIH grant T32 GM08666. The LβT2 cells were a gift from Dr. Pamela Mellon.

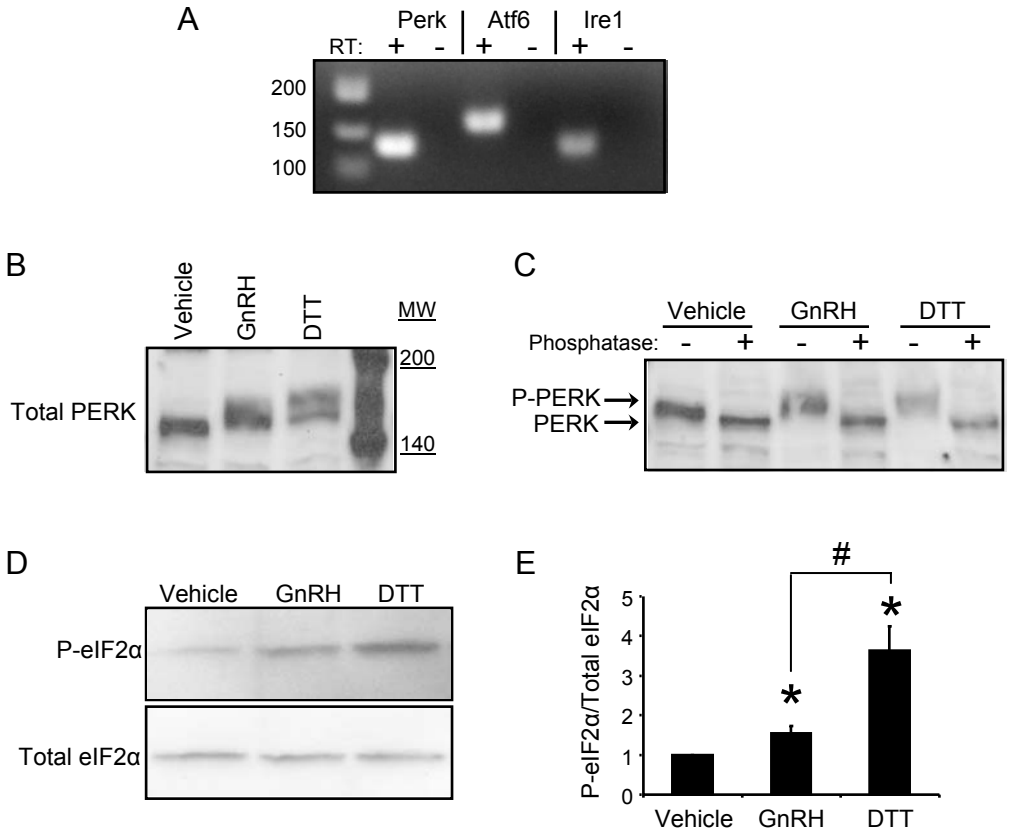

Figure 2-1. Expression of ER stress sensors and activation of PERK by GnRH in LβT2 gonadotropes. (A) Total RNA was isolated from untreated cells and PCR was performed using transcript-specific primers to determine the presence of the three known ER stress sensors Perk, Atf6, and Ire1. RT = reverse transcriptase. **(B)** Total protein was harvested from LβT2 cells treated with vehicle, 10 nM GnRH, or 2 mM DTT for 30 minutes and subjected to Western blotting using antibody directed against total PERK. Hyperphosphorylation of PERK (P-PERK) is indicated by decreased electrophoretic mobility. **(C)** The phosphorylation-dependent decrease in PERK mobility was confirmed by treatment of protein extracts with lambda protein phosphatase prior to Western blotting. **(D)** Phosphorylation of the PERK target eIF2α (P-eIF2α) was detected by Western blotting with antibodies specific to the phosphorylated and total forms of the protein. **(E)** Quantitative chemiluminescent image analysis of eIF2α Western blot band intensities. Reported values are the means +/- SEM. Asterisks indicate statistical significance from a value of 1 and pound (#) indicates groups are significantly different from each other, as determined by a Student's t-test.

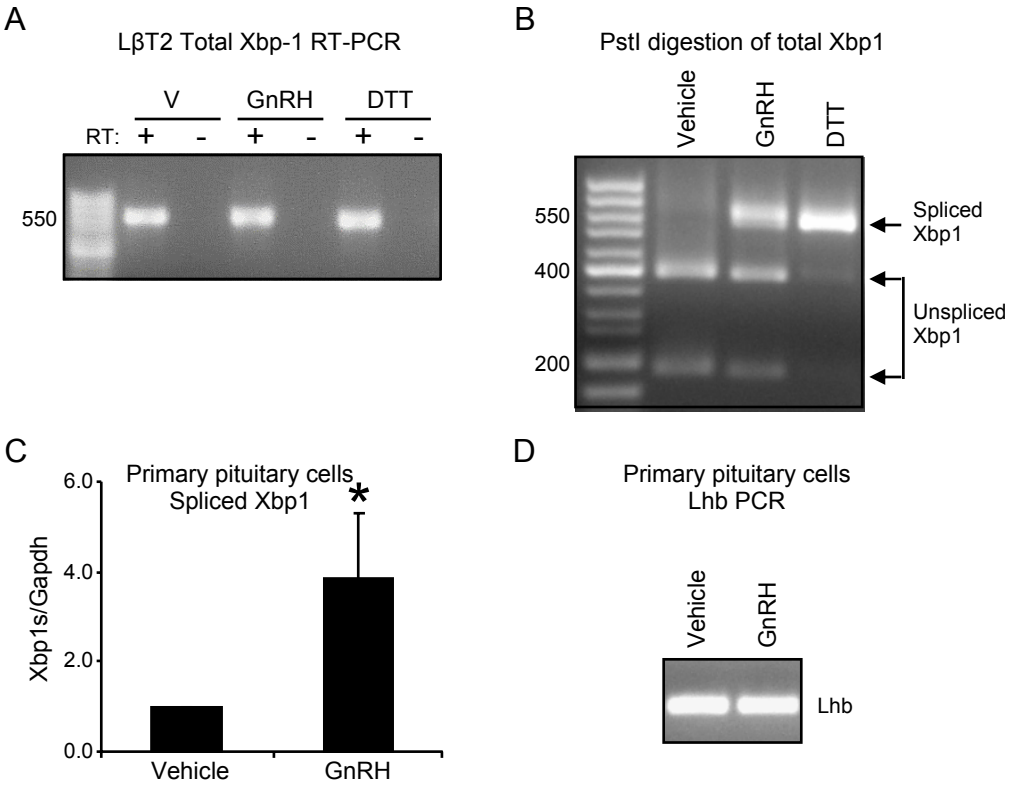

Figure 2-2. GnRH causes splicing of the UPR transcription factor Xbp1 mRNA in LβT2 and mouse primary gonadotropes. (A) LβT2 cells were treated for 30 minutes and total RNA harvested. Xbp1 mRNA was reverse transcribed and amplified using gene-specific primers. The resulting cDNA was subjected to agarose electrophoresis to confirm appropriate amplicon size. RT = reverse transcriptase. **(B)** Amplified Xbp1 cDNA was digested with PstI to confirm the loss of a PstI restriction site within the intron sequence. Spliced Xbp1 cDNA is insensitive to PstI digestion. **(C)** Primary pituitary cells cultured from wild-type, nine week old male mice were plated and treated for 30 minutes. RNA was isolated and reverse transcribed and quantitative PCR was used to measure the spliced form of Xbp1 specifically (Xbp1s). Gapdh was used as an internal control. **(D)** Lhb was PCR amplified to confirm the successful isolation of gonadotropes in the primary pituitary cell harvest. The reported values are the means +/- SEM of three independent experiments. Asterisks indicate statistical significance from a value of 1 as determined by a Student's t-test.

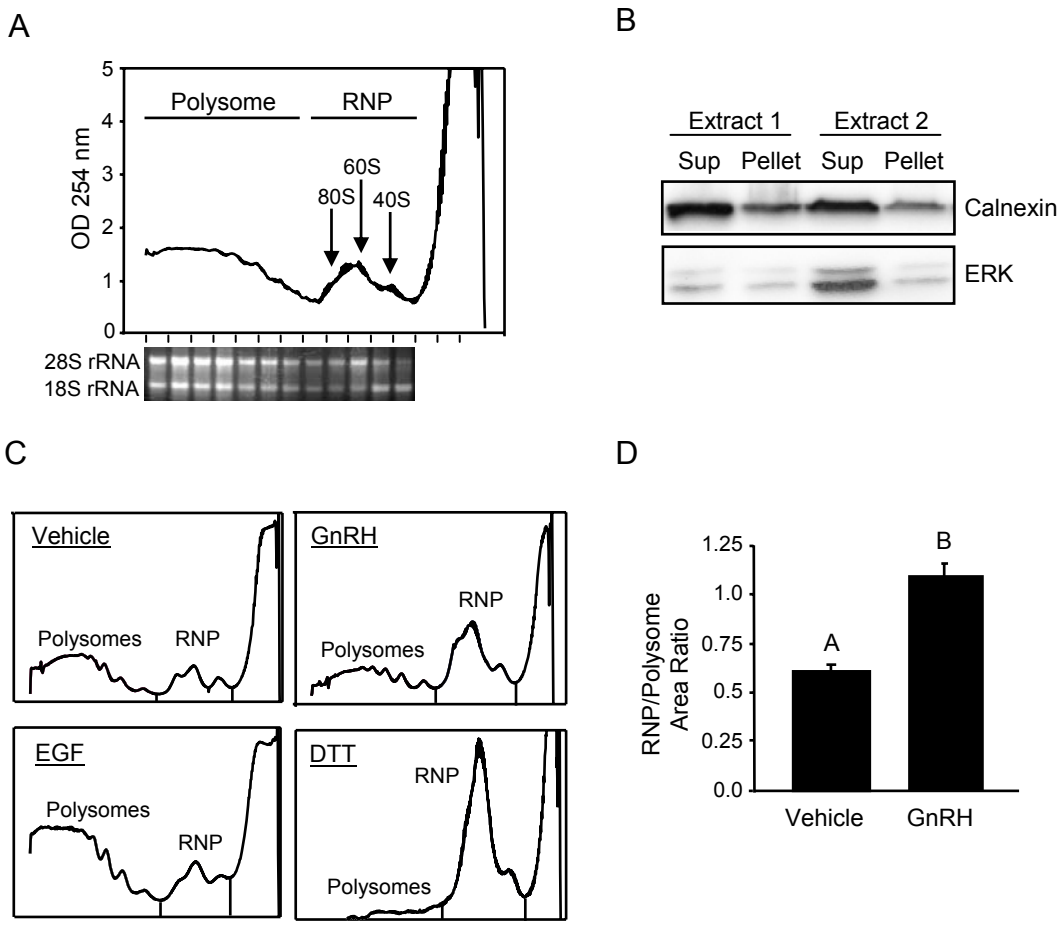

Figure 2-3. GnRH exposure causes an accumulation of RNP complexes in LβT2 cells. Cells were treated for 30 minutes and then extracts were harvested and layered onto sucrose gradients. RNA and ribosome complexes were pulled from the sucrose gradients and fractionated while monitoring UV absorption at 254 nm. **(A)** A representative profile from untreated cells. Fractions were pooled to represent polysomes (RNA with two or more ribosomes) and RNP complexes (ribosomal subunits, monosomes, initiation complexes), as shown. The peaks in the RNP pool correspond to the individual ribosomal subunits and full 80S monosomes, as indicated by the relative proportions of 28S and 18S rRNA, representing the large and small ribosomal subunits, respectively, present in the various fractions. **(B)** Aliquots from the supernatant (sup) prior to layering on the gradient or the cell pellet prior to discard, of two representative extracts, was subjected to Western blotting for ER-membrane bound protein Calnexin and nuclear/cytoplasmic protein ERK. The presence of Calnexin in the supernatant demonstrates the fractionation protocol was sufficient to isolate membrane-bound proteins. **(C)** Representative ribosomal profiles. **(D)** The ratio (RNP/polysome) of the integrated area under the curve from the profiles, as an indication of the level of redistribution of ribosomes. The reported values are the means +/- SEM of six independent experiments. Groups not connected by the same letter are significantly different as determined by ANOVA and *post hoc* Tukey's HSD test.

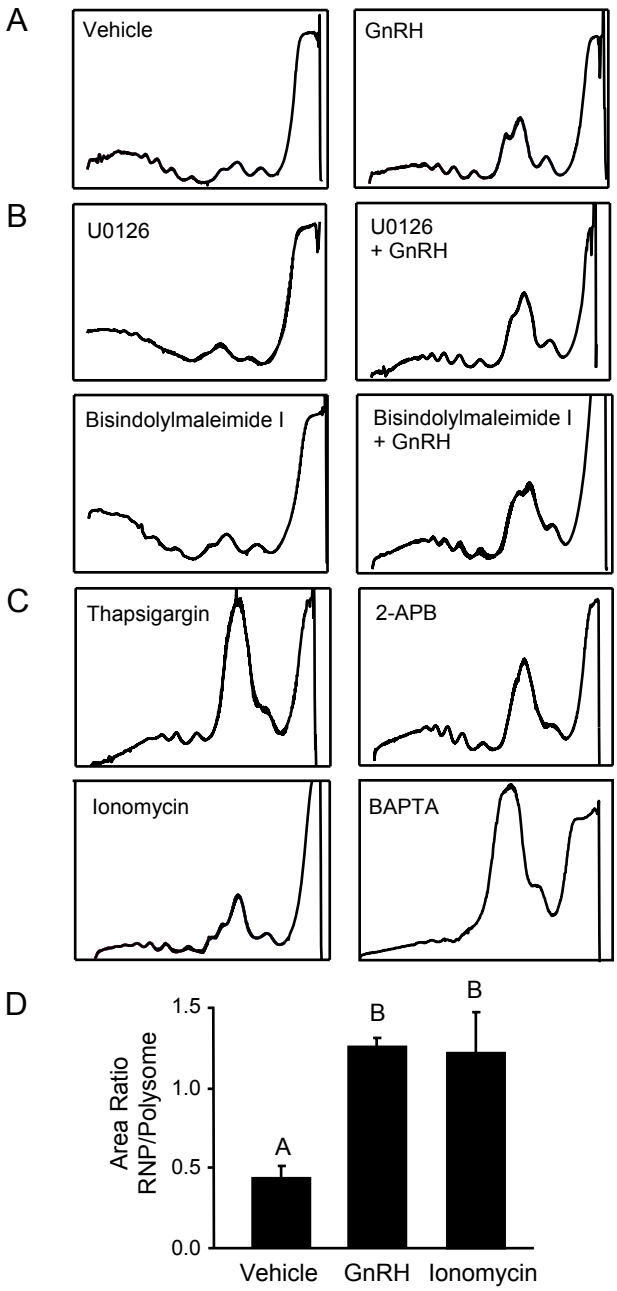

Figure 2-4. Accumulation of RNP complexes is mimicked by disruption of intracellular calcium. LβT2 cells were treated and ribosomes were fractionated while monitoring UV absorption. **(A)** Representative profiles from cells treated with vehicle or 10 nM GnRH for 30 minutes. **(B)** Profiles from cells treated with U0126 to inhibit ERK or bisindolylmaleimide I to inhibit PKC activation, prior to GnRH exposure for 30 minutes. **(C)** Profiles from cells treated with SERCA antagonist thapsigargin, IP_3-receptor antagonist 2-APB, calcium ionophore and secretagogue ionomycin, or calcium chelator BAPTA. **(D)** The ratio (RNP/polysome) of the integrated area under the curve from the profiles, as an indication of the level of redistribution of RNA. The reported values are the means +/- SEM of four independent experiments. Groups not connected by the same letter are significantly different as determined by ANOVA and *post hoc* Tukey's HSD test.

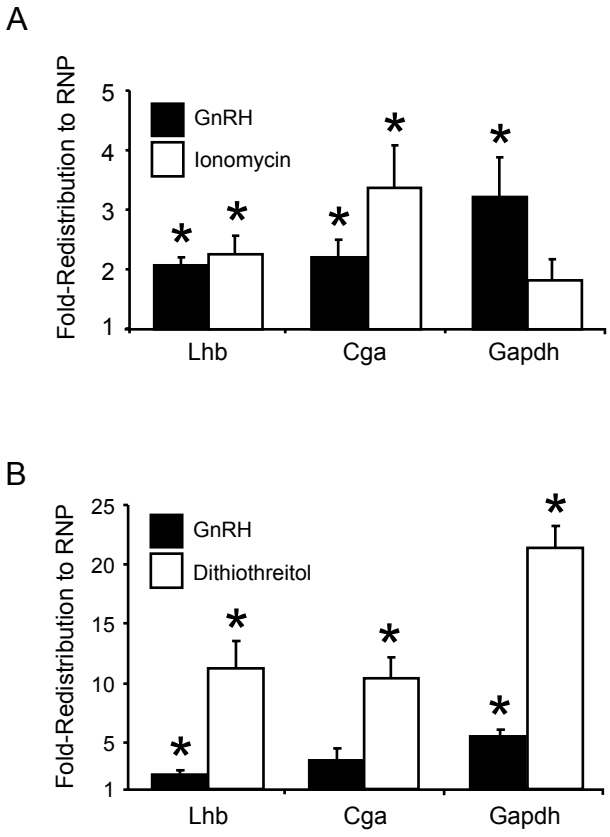

Figure 2-5. Lhb, Cga and Gapdh mRNAs redistribute to RNP complexes in response to GnRH. LβT2 cells were treated and ribosome complexes fractionated. Messenger RNA was isolated from the RNP and polysome pools of the fractionated extracts and measured using quantitative PCR. A fold-redistribution value was calculated as a measurement of the change in transcript representation in the pools after treatment, as compared to control (vehicle) treatment. The data is represented in the histogram such that a positive value indicates movement into the RNP pool and a negative value indicates movement into the polysome pool. A fold-redistribution value of 1 represents no change after treatment. **(A)** The redistribution of mRNAs was calculated for cells exposed to 30 minutes of GnRH (black) or ionomycin (white). The reported values are the means +/- SEM of four independent experiments. **(B)** The redistribution of mRNAs was calculated for cells exposed to 30 minutes of GnRH (black) or dithiothreitol (white). The reported values are the means +/- SEM of three independent experiments. Asterisks indicate statistical significance from a value of 1 as determined by a Student's t-test.

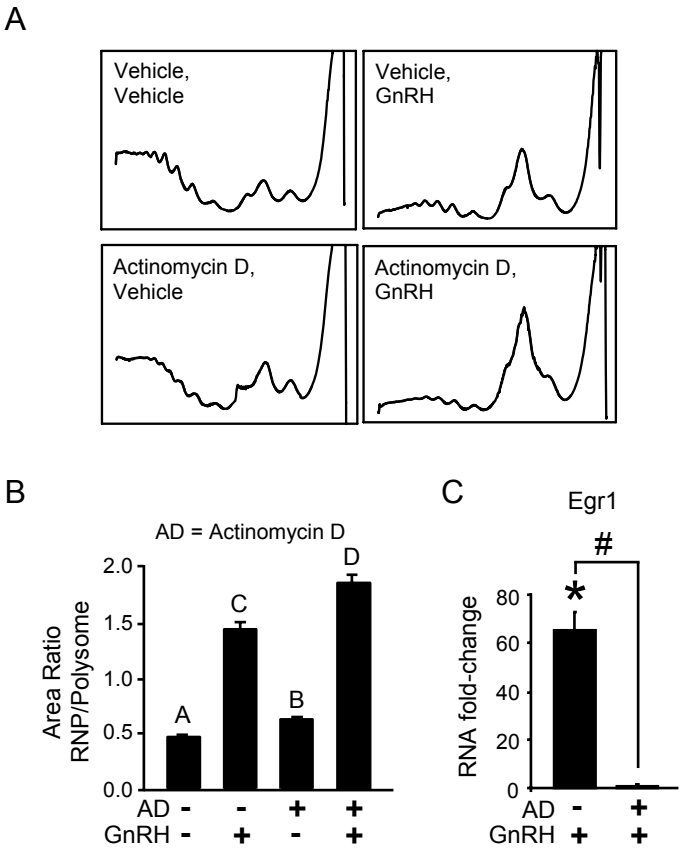

Figure 2-6. Accumulation of RNP complexes by GnRH does not involve transcriptional events. LβT2 cells were pre-treated with actinomycin D (AD) to block transcription and then treated with GnRH or PBS for 30 minutes. **(A)** Representative profiles from fractionation of ribosomal complexes while monitoring UV absorption. **(B)** The ratio (RNP/polysome) of the integrated area under the curve from the profiles, as an indication of the level of redistribution of ribosomes. Groups not connected by the same letter are significantly different as determined by ANOVA and *post hoc* Tukey's HSD test. **(C)** Efficacy of AD treatment was confirmed by quantitative PCR amplification of Egr1 from isolated RNA and comparing the levels in the GnRH-treated cells to those in the respective vehicle-treated cells. The reported values are the means +/- SEM of four or more independent experiments. Asterisks indicate statistical significance from a value of 1 and pound (#) indicates groups are significantly different from each other, as determined by a Student's t-test.

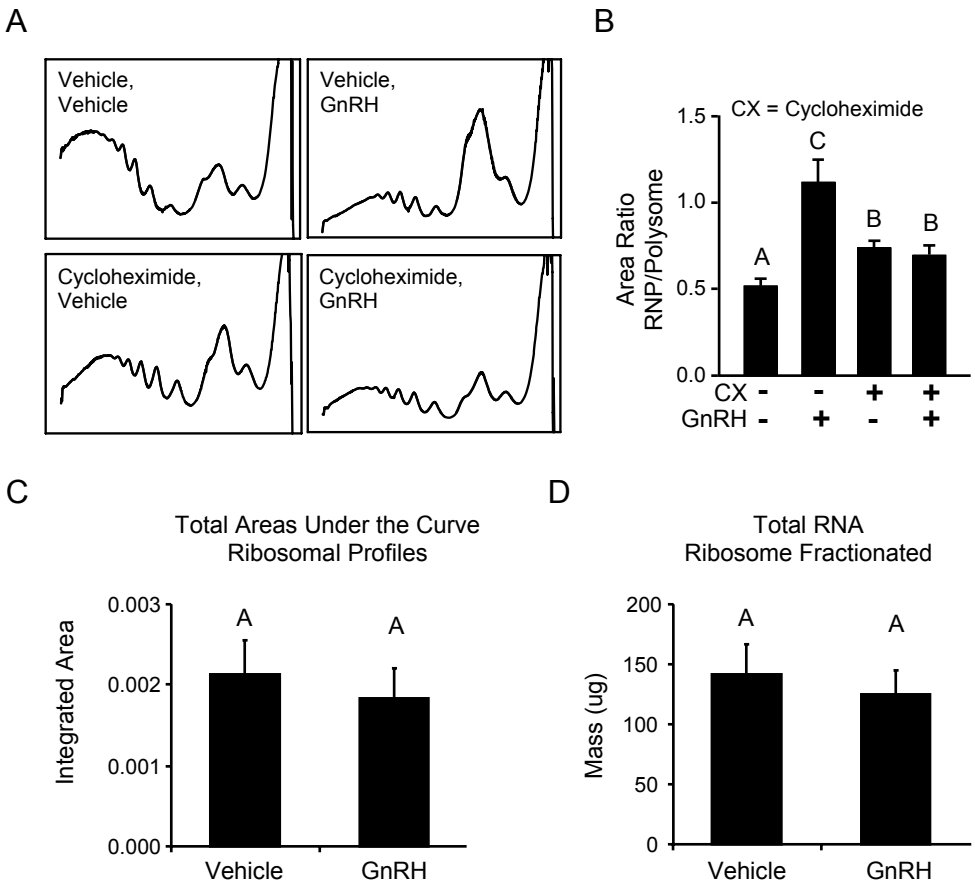

Figure 2-7. GnRH attenuates translation by redistributing ribosomes to RNP complexes. LβT2 cells were pre-treated with cycloheximide (CX) to block translation elongation and then treated with GnRH or PBS for 30 minutes. **(A)** Representative profiles from fractionation of ribosomal complexes while monitoring UV absorption. **(B)** The ratio (RNP/polysome) of the integrated area under the curve from the profiles, as an indication of the level of redistribution of ribosomes. **(C)** The sum (RNP+polysome) of the integrated areas under the curve from the profiles, as indication of the total RNA fractionated. **(D)** The sum (RNP+polysome) of the total RNA extracted from the ribosomal fractionated extracts. The reported values are the means +/- SEM of six or more independent experiments. Groups not connected by the same letter are significantly different as determined by ANOVA and *post hoc* Tukey's HSD test.

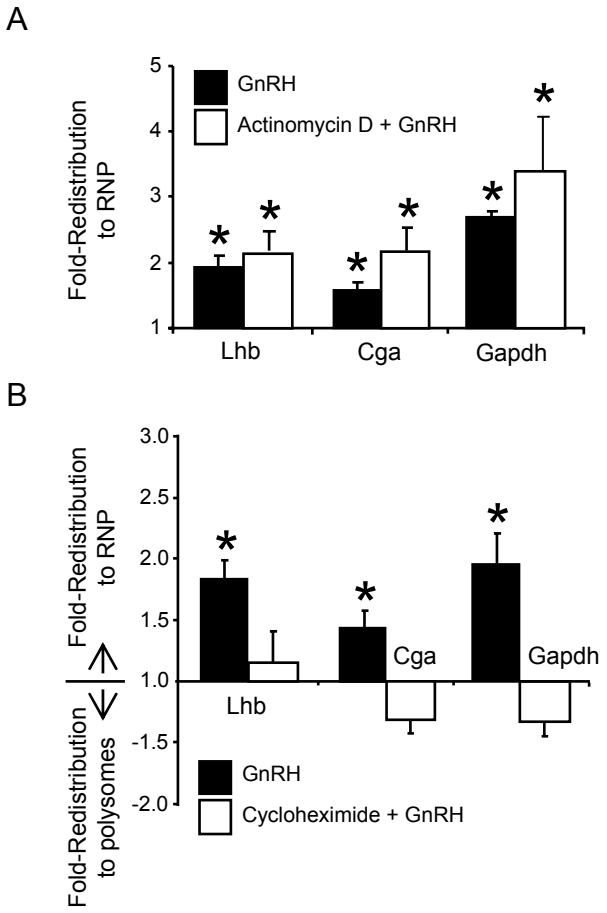

Figure 2-8. Translation of Lhb, Cga and Gapdh mRNAs is attenuated. LβT2 cells were pre-treated with actinomycin D (AD) to block transcription or cycloheximide (CX) to block translation elongation and then treated with 10 nM GnRH or PBS for 30 minutes. Ribosome complexes were fractionated. Messenger RNA was isolated from the RNP and polysome pools and measured using quantitative PCR. A fold-redistribution value was calculated as a measurement of the change in transcript representation in the pools after treatment, as compared to control (vehicle) treatment. The data is represented in the histogram such that a positive value indicates movement into the RNP pool and a negative value indicates movement into the polysome pool. A fold-redistribution value of 1 represents no change after treatment. **(A)** The redistribution of mRNAs was calculated for cells exposed to 30 minutes of GnRH (black) or pre-treated with AD prior to GnRH (white). **(B)** The redistribution of mRNAs was calculated for cells exposed to 30 minutes of GnRH (black) or pre-treated with CX prior to GnRH (white). The reported values are the means +/- SEM of four or more independent experiments. Asterisks indicate statistical significance from a value of 1 as determined by a Student's t-test.

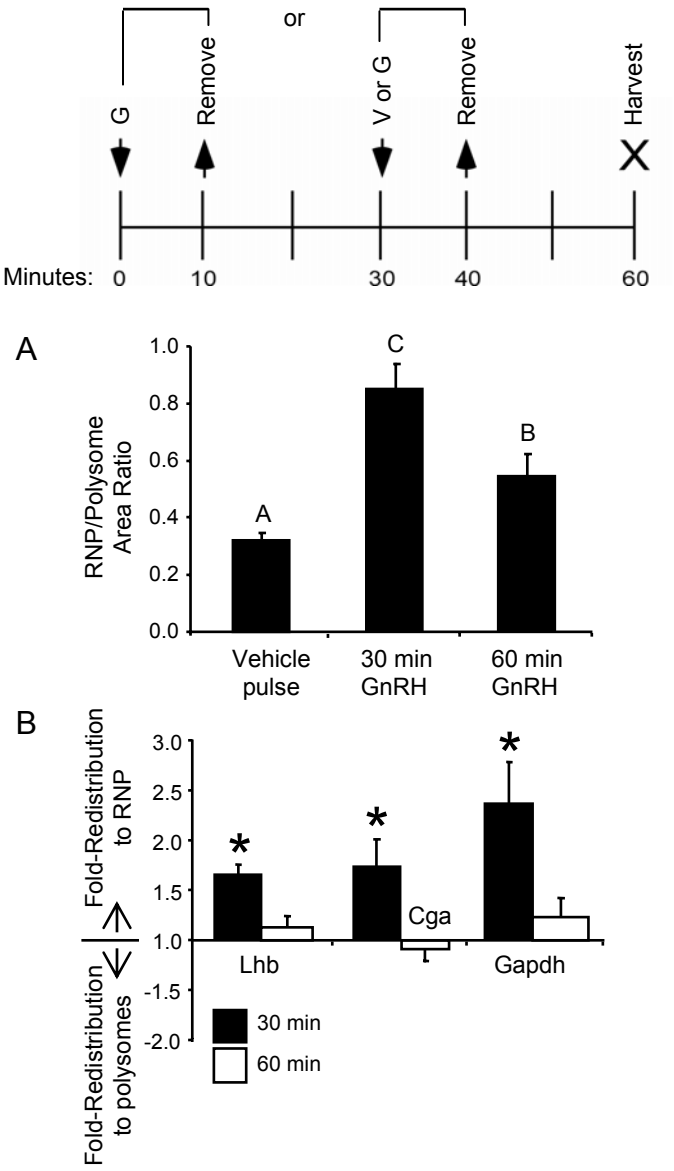

Figure 2-9. Attenuation of Lhb, Cga and Gapdh translation by GnRH is transient. LβT2 cells were treated with vehicle (V) or GnRH (G) for 10 minutes and then the cells were placed in fresh media and incubated until the time indicated prior to harvest. Ribosome complexes were then fractionated. **(A)** The ratio (RNP/polysome) of the integrated area under the curve from the profiles, as an indication of the level of redistribution of ribosomes. Groups not connected by the same letter are significantly different as determined by ANOVA and *post hoc* Tukey's HSD test. **(B)** Messenger RNA from the RNP and polysome pools of the fractionated extracts was measured using quantitative PCR. A fold-redistribution value was calculated as a measurement of the change in transcript representation in the pools after GnRH treatment, as compared to control (vehicle) treatment. The data is represented in the histogram such that a positive value indicates movement into the RNP pool and a negative value indicates movement into the polysome pool. A fold-redistribution value of 1 represents no change. Asterisks indicate statistical significance from a value of 1 as determined by a Student's t-test. The reported values are the means +/- SEM of six independent experiments.

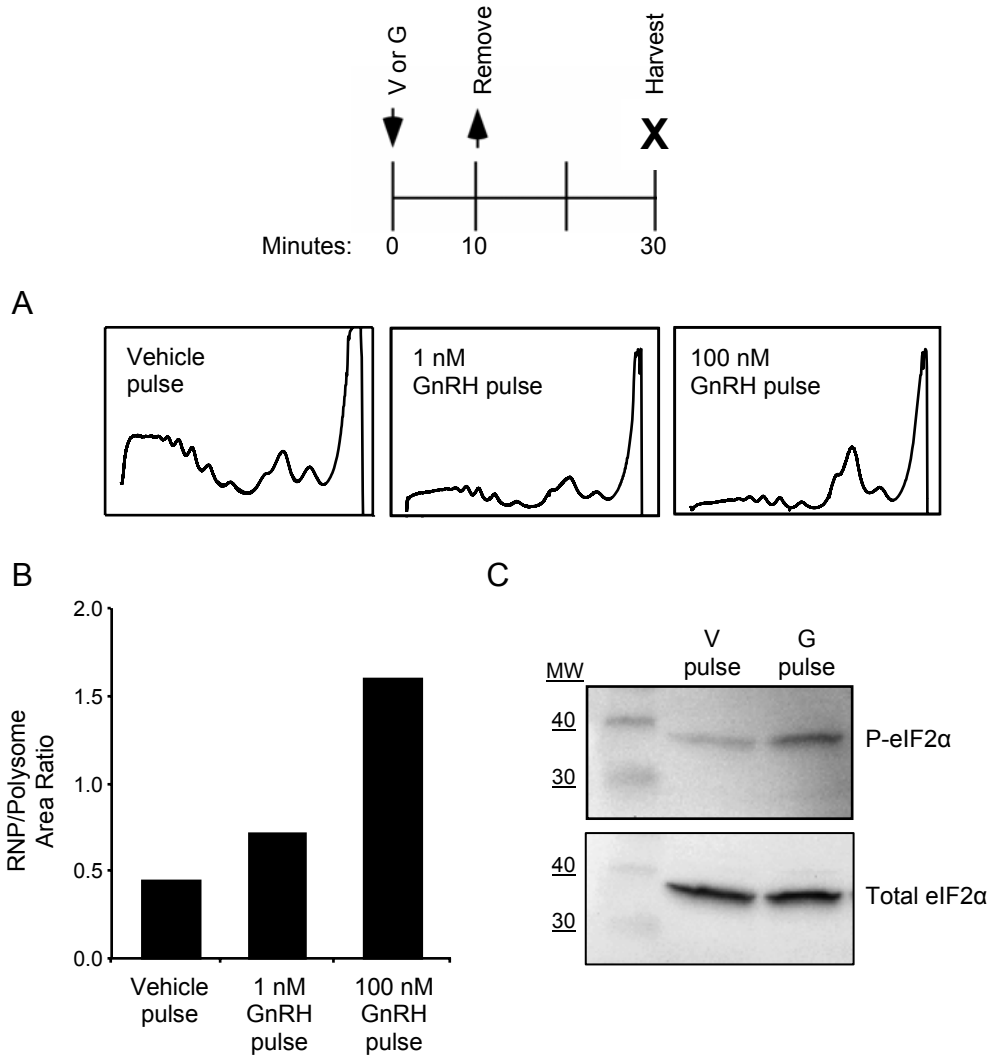

Figure 2-10. A 10-minute pulse of GnRH is sufficient to cause accumulation of RNP complexes and phosphorylation of eIF2α. Cells were treated for 10 minutes (vehicle, V, or GnRH, G), the media was removed, and then cells were replaced with fresh media without any GnRH. Extracts were harvested 30 minutes after the pulse. **(A)** Ribosomal complexes were fractionated while monitoring UV absorption at 254 nm. **(B)** The ratio (RNP/polysome) of the integrated area under the curve from the profiles, as an indication of the level of redistribution of ribosomes. The reported values are from one experiment. **(C)** After a vehicle or 10 nM GnRH pulse, total protein was subjected to Western blotting. Shown is a representative blot. The phosphorylation of PERK target eIF2α was detected using antibody directed against the phosphorylated (P-eIF2α) and total forms of the protein. Three independent experiments were performed.

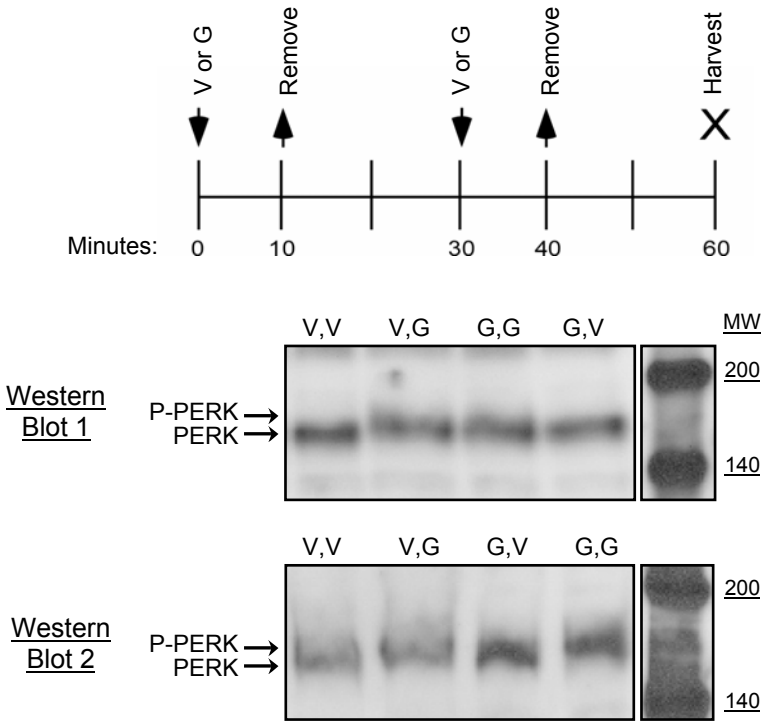

Figure 2-11. A 10-minute pulse of GnRH is sufficient to cause and sustain phosphorylation of PERK. LβT2 cells were treated with one or two 10-minute pulses of vehicle (V) or 10 nM GnRH (G). After each pulse, the media was replaced by fresh media without GnRH. Protein was harvested at the time point indicated and subjected to Western blotting using antibody directed against total PERK. Two independent experiments were performed, as shown. Phosphorylation of PERK (P-PERK) is indicated by the decrease in electrophoretic mobility. V,V = two vehicle pulses; V,G = 30 min after one GnRH pulse; G,G = 30 min after two GnRH pulses; G,V = 60 min after one GnRH pulse.

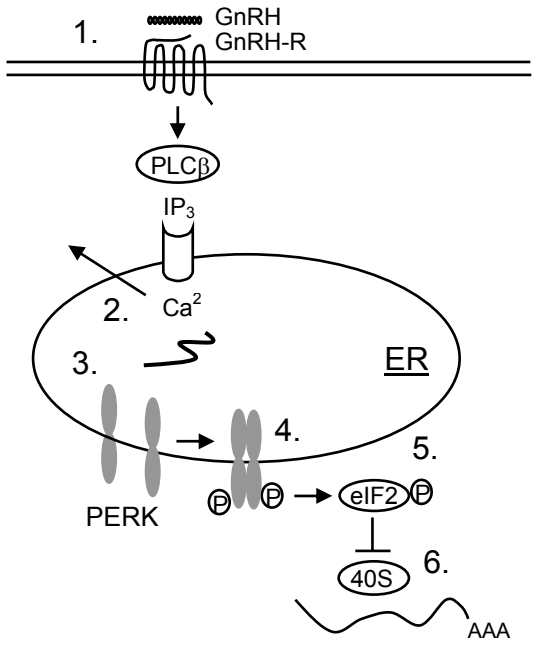

Figure 2-12. Proposed model for transient attenuation of translation induced by GnRH. GnRH acting on its receptor (1) to induce calcium efflux from the ER (2) leads to the loss of calcium and/or accumulation of unfolded proteins (3) that allows dimerization and activation by auto-phosphorylation of PERK (4). Activated PERK phosphorylates translation initiator eIF2 at its α subunit (5), leading to translation attenuation through inhibition of initiation complex formation and binding to mRNA (6).

CHAPTER 3

Specificity of the regulation of translation by GnRH

INTRODUCTION

Regulation of translation is typically targeted at the rate-limiting step of initiation. In particular, this regulation targets the components of the eIF4F cap-binding complex, comprised of cap-binding eIF4E, RNA helicase eIF4A and the eIF4E/eIF4A scaffolding protein eIF4G. eIF4E is targeted through regulation of its activity as well as availability. Phosphorylation of eIF4E is correlated with increased translation rates and phosphorylation of its binding protein 4EBP1 makes it available to interact with eIF4G and thus initiate translation (16, 17). Targeting 4EBP1 typically occurs through RTK signaling to PI3K/Akt/mTOR (17-19), though mTOR is also a target of GPCR agonists (20) and 4EBP1 may be targeted by MAPK activation (17). Phosphorylation of eIF4E is typically mediated by MAPK activation of eIF4E kinase Mnk1 (17).

Multiple layers of cross-talk exist between RTKs and GPCRs (75-77), and GnRH has been shown to cross-talk with EGF receptor (54). Given this complexity, it would not be surprising to find that GnRH may activate multiple cap-binding factors, and indeed this has been shown. In gonadotropes, GnRH causes the phosphorylation (activation) of Mnk1 and phosphorylation of eIF4E and eIF4G (27), as well as phosphorylation and thus inactivation of 4EBP1 (26, 27). The phosphorylation of Mnk1 and its target eIF4E were shown to be dependent on ERK activation (27). In LβT2, ERK is the MAPK most strongly activated by GnRH (9), and its activation is known to be important for mediating transcriptional responses of the gonadotropin subunits (1, 10). Thus, while the ERK pathway is well-established in transcriptional regulation, it appears to play a role in mediating translational responses involving the cap-binding initiation machinery as well.

The data shown in Chapter 2 presents evidence that GnRH targets yet another arm of translational regulation, one that is not dependent on ERK but instead involves calcium mobilization. This transient attenuation of translation was shown to be mediated by

phosphorylation of PERK and initiation factor eIF2α. It remains unclear then how stimulation of general regulatory factors, especially factors whose translational outcome appear to be opposing, can result in the preferential regulation of specific mRNAs. Recent studies have utilized cDNA arrays to address the role of translation at the global level. Microarrays have made possible the study of gene expression at the post-transcriptional level, including stability, translation, and the identification of RNA binding proteins (78). In the case of translation, this technology, combined with techniques of density centrifugation to separate mRNAs according to their ribosome complement, has provided powerful tools to investigate both global and specific regulation of protein synthesis (79). These technologies have been applied to studies of metabolic stress in yeast, as well as stress, apoptosis, development, cell growth, differentiation and viral infection in mammalian models.

To address the specificity of translational regulation by GnRH in this study, quantitative real-time PCR and microarray technology were used in combination with polysome fractionation in the LβT2 gonadotrope cell model (6). The hypothesis is that through stimulation of general regulatory factors, including those that appear to be opposing in regards to general translational outcome, GnRH preferentially regulates the translation of specific mRNAs. The results indicate that the stimulation of translation by GnRH is not general but specific, targeting a subset of mRNAs relevant to the differentiated function of gonadotropes, stimulating the translation of some mRNAs while attenuating the translation of others. Additionally, this bidirectional regulation appears to be mediated, at least in part, through signaling to the UPR and eIF2 as well as simultaneous signaling to ERK.

RESULTS

GnRH induces differential redistribution of gonadotrope-specific mRNAs

It was shown previously that cap-dependent translation initiation factors are activated within minutes of GnRH treatment in LβT2 cells, with maximal phosphorylation of several factors, including eIF4E, eIF4G, and 4EBP1, occurring within 30 minutes of exposure (27). The work

described in Chapter 2 also describes the targeting of eIF2α initiation factor within 30 minutes. To examine specific mRNAs targeted by translational regulation by GnRH, LβT2 cells were treated with vehicle or GnRH for 30 minutes and then ribosome and mRNA complexes were separated on sucrose gradients. Complexes were fractionated according to density while monitoring absorption at 254 nm. Fractions were combined to represent the actively translating polysome pool, consisting of mRNAs complexed with two or more ribosomes, or the RNP pool, consisting of mRNAs complexed with initiation factors, a single ribosome, and free 60S or 40S ribosomal subunits. As established in Chapter 2, stimulation of LβT2 gonadotrope cells with GnRH for 30 minutes causes an accumulation of RNP complexes (Figure 3-1A).

To determine whether the overall RNA changes seen after acute stimulation with GnRH are reflected in the manner in which specific mRNAs behave, the distribution of specific mRNAs between the RNP and polysome pools was measured. The redistribution of transcripts between the pools after exposure to GnRH was calculated by determining the ratio of the mass of the particular mRNA in the RNP pool compared to the polysome pool, and then a fold-redistribution was calculated by comparing these ratios in GnRH-treated and untreated samples. This fold-redistribution is thus a measurement of the change in transcript representation in each of the pools after GnRH treatment. In the differentiated gonadotrope, GnRH released from the hypothalamus acts on its G protein-coupled receptor (Gnrhr) to induce the synthesis and secretion of the hormone LH. LH is composed of two subunits, alpha (Cga) and beta (Lhb) (2). GnRH-induced regulation of Lhb transcription is dependent on Egr1, an immediate-early gene highly upregulated by GnRH (1).

Gnrhr, Egr1 and Cmyc mRNAs were measured using quantitative PCR analysis of the fractionated extracts. This revealed that in contrast to the RNP accumulation of Lhb, Cga, and Gapdh (Figure 2-5), Gnrhr is not translationally regulated, and Cmyc, which contains an IRES in its 5'UTR (80), and Egr1 were both recruited to polysomes in response to GnRH (Figure 3-1B).

To evaluate if active translation or transcription is required for the redistribution of the transcripts, cycloheximide to inhibit translation elongation or actinomycin D to inhibit transcription

were used to treat LβT2 cells prior to exposure to GnRH and ribosomal fractionation. Cycloheximide but not actinomycin D was shown in Chapter 2 to block the accumulation of Lhb, Cga and Gapdh in RNP complexes (Figure 2-8B), suggesting that translation elongation is required for their accumulation, and moreover, that their accumulation is indicative of an attenuation in translation. In contrast to this, Cmyc and Egr1 show differential sensitivity. The recruitment of Egr1 into polysomes requires translation (Figure 3-2C), as expected, but also transcription (Figure 3-2A). Cmyc recruitment to polysomes also shows dependence on transcription. Both Egr1 and Cmyc are stimulated transcriptionally within 30 minutes of GnRH exposure, by 60-fold (Figure 2-6C) and 3-fold (Figure 3-2B), respectively. The coupling of transcription and translation for Cmyc and Egr1 may be examples of potentiation (78, 81), in which new synthesis of an mRNA contributes to or is required for changes in the translation status of that mRNA. Overall, the results indicate that regulation of translation by GnRH is specific, with respect to the mRNAs that are regulated as well as the direction in which they are regulated.

Translational regulation by GnRH targets a specific subset of genes

In order to assess how widespread the regulation of translation by GnRH is, Affymetrix MOE430A chips were used to analyze the distribution of mRNAs in fractionated samples. Twelve chips in total were used to assay mRNAs in the RNP (R) and polysome (P) pools of each treatment group, GnRH or untreated, in three independent experiments. Unsupervised hierarchical clustering (Figure 3-3A) of the data sets showed that the samples clustered such that the treatment groups were recovered, indicating the reproducibility of the replicates. As another means of quality control, MA plots comparing the two different treatments were generated to assess the signal intensity variability (σ^2) between replicates and between GnRH-treated and untreated data sets (Figure 3-3B, 3-3C). Between biological replicates there was little variation, with σ^2 values ranging from 0.080 to 0.194 (Figure 3-3B), again demonstrating reproducibility. Additionally, plots comparing the GnRH-treated and untreated samples also showed little

variation, with σ^2 values ranging from 0.066 to 0.090 (Figure 3-3C). This indicates that GnRH treatment does not cause significant overall changes in mRNA distribution, providing evidence that redistribution of mRNAs induced by GnRH are more specific in nature, affecting potentially only a small subset of mRNAs as opposed to inducing global changes in translational status.

Using the same fold-redistribution calculation applied towards the quantitative PCR data for individual transcript analysis and the bioweight method of array analysis (Figure 3-4), a list of the top 5% (800) of the most translationally regulated genes amongst those found to be expressed in LβT2 cells was generated (Appendix, Table 5-1). This confirmed that a small subset of genes is regulated, and their regulation involves movement of specific mRNAs into both the polysome and RNP pools, not just the RNP pool as the ribosomal profiles alone might suggest. Of the top 5% of regulated probes, 37.9% redistributed to the polysome pool. The top 100 genes are listed in Table 3-1. Differential gene expression was also carried out using a permutation method, Significance Analysis of Microarrays (SAM, see Materials and Methods), with a False Discovery Rate set at 0.2. Of the 873 genes found to be differentially regulated using SAM (Appendix, Table 5-2), 496 of these were found amongst the top 800 bioweight genes (Figure 3-5A and see Appendix for list, Table 5-3), indicating significant overlap and similarity between the two methods. A heatmap was generated from the top 5% of regulated genes as determined by bioweight (Figure 3-5B). The heatmap indicates that the top regulated genes fall into distinct patterns of bidirectional mRNA redistribution, again demonstrating that some mRNAs become enriched in polysomes and others accumulate as RNP complexes after GnRH exposure. Conversely, there were no discernible patterns of movement with the lowest bioweight mRNAs (Figure 3-5C). The heatmaps show that the top genes separate the chips according to treatment, while the lowest bioweight genes could not clearly separate any experimental variables.

Amongst the top regulated genes were Lhb (Table 3-1, 5-1) and Gapdh (Table 5-1), confirming their regulation. Their fold-redistribution was measured to be 1.65 and 1.32, respectively. The top 800 regulated genes were further characterized by mapping them to biological pathways using the Kyoto Encyclopedia of Genes and Genomes (KEGG) pathway

database and analysis tool (Figure 3-6, see Appendix Figure 5-4 for full list). Overall, the genes that were regulated fell into pathways that include signal transduction, cell communication, cell growth, translation, and metabolism. Of the pathways identified, generally only a small subset of genes in each pathway was sensitive to regulation by GnRH, and of those regulated genes, redistribution to both the RNP and polysome pool was observed. Exceptions to this were mRNAs encoding proteins that constitute the ribosome or are involved in protein export, as well as those that are translated on ER-bound ribosomes such as proteins involved in oxidative phosphorylation or the citrate cycle, where the majority if not all of the regulated mRNAs accumulated in RNP complexes. This confirms the overall tone of attenuating translation, especially translation that occurs on the ER, consistent with activation of the UPR. The KEGG analysis also revealed pathways previously known to be important for GnRH signaling, including MAPK, Jak-STAT, and insulin. For MAPK, most of the mRNAs redistributing the RNP pool were intermediate signal transducers (Map4k4, Mapkapk2, Mknk2, Rras), while feedback regulators (Dusp1, Pla2g2d) redistributed to the polysome pool.

Activation of PKC and ERK by GnRH modulates translational attenuation

The stimulation of translation of some mRNAs and the attenuation of others by GnRH treatment indicates that at the translational level, specificity may be defined by multiple signaling inputs. The phosphorylation of eIF2α may explain the attenuated mRNAs, while upregulating eIF4E through its activity or availability may explain the stimulation of some mRNAs. 4EBP1 and eIF4E phosphorylation have been shown to be dependent on ERK activation (27), and ERK is downstream target of PKC (4). To determine the impact of ERK activation on ribosome remodeling, cells were treated with PD98059 or U0126 to block ERK activation prior to stimulation with GnRH and ribosome fractionation. Inhibition of ERK activation through U0126 results in greater GnRH-induced RNP remodeling (Figure 3-7B). PD98059 (Figure 3-7A) shows a similar trend, although this was not statistically significant. This suggests that ERK signaling may modulate the overall degree of translational attenuation induced by the UPR. Inhibition of

ERK activation by PD98059 or U0126 was confirmed by Western blotting for phosphorylated ERK after GnRH treatment (Figure 3-7C).

Quantitative PCR analysis was used to assess the role of ERK activation on the stimulation of translation of specific transcripts. The microarray analysis revealed that Dusp1 (also known as Mkp1) is recruited into polysomes after GnRH exposure (Table 3-1, 5-1). This recruitment of Dusp1 was confirmed through quantitative PCR analysis of ribosomal fractionated extracts (Figure 3-8). PD98059 or U0126 treatment prior to GnRH exposure partially inhibits this recruitment. Lhb, on the other hand, accumulates in RNP complexes in response to GnRH, and is not affected by ERK inhibition (Figure 3-8). The impact of ERK activation on the polysomal recruitment of Egr1 and Cmyc mRNAs was also examined (Figure 3-9) but in general the data was quite variable and thus inconclusive, although does indicate that Cmyc recruitment involves a PD98059-sensitive component (Figure 3-9B).

In a complementary experiment, cells were treated with PMA to bypass the GnRH-receptor and activate PKC directly, presumably leading to ERK activation, and then ribosomes were fractionated and the behavior of specific transcripts examined. Whereas PMA did not affect the distribution of Lhb, Cga and Gapdh mRNAs, it stimulated the polysomal recruitment of Egr1 and Cmyc, similar to GnRH (Figure 3-10). These data suggest that GnRH leads to the polysomal recruitment of particular transcripts at least partially by way of activating PKC/ERK signaling.

UPR activation is not responsible for Dusp1 mRNA recruitment to polysomes by GnRH

If the PKC/ERK arm of GnRH signaling contributes to the translational activation of particular mRNAs, then activation of the UPR signaling arm alone would be predicted to cause the RNP accumulation of Lhb, Cga, and Gapdh, but not affect or have the opposite effect on those mRNAs that are recruited to polysomes. The first prediction was shown to be true in Chapter 2, where UPR activating agents cause general RNP accumulation and specific attenuation of Lhb, Cga and Gapdh mRNAs. To examine the second prediction, vehicle, GnRH, DTT or ionomycin-treated cells were subjected to ribosome fractionation and Dusp1 distribution in

the fractionated RNP and polysome pools was examined. While GnRH causes redistribution of Dusp1 to polysomes, DTT treatment resulted in marked RNP accumulation (2.5-fold, Figure 3-11A), and ionomycin treatment had no effect (Figure 3-11B). GnRH stimulation of the UPR alone cannot account for the translational regulation of Dusp1, suggesting that other signaling arms activated by GnRH may be responsible for polysomal recruitment of Dusp1 and perhaps of some other mRNAs as well.

The 5'UTR of Lhb mRNA is not sufficient to confer sensitivity to translational regulation by GnRH

Because LH is one of the main outputs of the gonadotrope and plays a crucial role in reproductive biology, it was of interest to examine what defines the sensitivity of Lhb to translational attenuation. The regulation of translation initiation would be expected to target the 5'UTR of an mRNA, since it is here that translation begins. In order to examine whether the 5'UTR of Lhb confers its sensitivity, the 8 bp 5'UTR of the mouse Lhb mRNA was cloned upstream of a luciferase reporter gene and transfected into LβT2 cells. In comparison to an IRES-containing UTR, the construct containing the 5'UTR of Lhb showed greater basal activity. This is consistent with the known low translational efficiency of 5'UTRs containing IRES sequences (12) and also indicates that Lhb's 5'UTR can still direct translation despite its notably shorter-than-average 5'UTR length and predicted inefficiency of short 5'UTRs (16). However, after 4 hours of GnRH treatment, luciferase activity of the Lhb 5'UTR containing construct was not different from the activity in untreated cells (Figure 3-12). Thus, it appears that the 5'UTR of Lhb alone is not sufficient to confer its translational sensitivity to GnRH or thus affect its overall protein levels.

Consistent with proteins that are destined for secretion or for insertion into the plasma membrane, the 5' end of Lhb mRNA encodes a signal peptide (82). To test whether the signal peptide confers translational sensitivity, the sequence encoding the 20 amino acids of the signal peptide of LHβ was cloned upstream in frame with GFP (pLhbSignal-GFP) and transfected into

cells treated with vehicle or GnRH. The RNP and polysome distribution of the signal peptide-containing GFP was compared to the distribution of GFP without the signal peptide (pGFP) as well as endogenous Lhb mRNA. pLhbSignal-GFP does not appear to be sensitive to GnRH, implying that the signal peptide is not sufficient to explain the attenuation of endogenous Lhb mRNA. However, the complementary and more appropriate comparison of pLhbSignal-GFP with control vector pGFP reveals that these experiments may not be informative since pGFP may be sensitive to GnRH and accumulates in RNP complexes (Figure 3-13).

Contribution of transcription to LH protein levels

It was previously hypothesized that stimulation of Lhb translation is responsible for the increase in LH protein levels induced by GnRH (27). The number of LβT2 cells staining positive for LH protein has been shown to approximately double in response 100 nM tonic GnRH stimulation after 8 hours (9, 83) and 10 nM tonic GnRH stimulation after 16 hours (9). *In vivo* models including the *hpg* mouse or those where the hypothalamic-pituitary connection is lost demonstrate the crucial role of GnRH on LH levels (1). Chapter 2 shows that Lhb mRNA is attenuated in response to GnRH, albeit transiently. However, the time course of Lhb attenuation (Figure 2-8) shows that while the attenuation recovers to basal translational levels by 60 minutes, GnRH never increased association of Lhb with polysomes, even 90 minutes after a 10-minute pulse (Figure 3-14A) or 4 hours after a 5-minute pulse (Figure 3-14B). In fact, GnRH may still cause slight attenuation of Lhb mRNA at these time points, although this was not statistically significant (Figure 3-14A) or the experiment was only performed once (Figure 3-14B). In any case, these results indicate that the increase in LH protein levels observed in response to GnRH may not be a result of a stimulation of Lhb translation. Thus, the role of Lhb transcription was explored as the possible explanation for this increase. Treating the cells with GnRH for 30 minutes and measuring Lhb mRNA levels showed that Lhb mRNA increases 2-fold within 30 minutes, and Cga by 1.25-fold (Figure 3-15A, 3-15B). Both of these increases were abrogated in the presence of actinomycin D. An acute transcriptional response to GnRH could counter-

balance the transient attenuation of Lhb translation and ultimately lead to increased LH protein levels at later time points.

To further examine the role of transcription, intracellular LH protein content was measured via immunoradiometric assays (IRMA) in a time course after 10-min GnRH pulse stimulation in the presence of actinomycin D (Figure 3-15C). As would be expected by secretion of LH, total LH levels decreased to 50% 30 minutes after stimulation. These levels recovered to basal, pre-stimulation levels by 4 hours. By 6 hours, LH levels were the same as observed at 4 hours, not observed to increase over pre-stimulation levels. Interestingly, in the presence of actinomycin D, intracellular LH levels did not appear to decrease initially at 30 minutes or otherwise change in response to GnRH at any other time point.

DISCUSSION

The regulation of immediate-early genes Egr1 and Dusp1 are consistent with what has been previously shown in the regulation these genes. Egr1 is a transcription factor required for GnRH-induced Lhb expression (1). The finding that GnRH induces Egr1 transcription (Figure 2-6C) is consistent with other studies (39, 40, 59), and coupled with translational stimulation, this provides a mechanism for the rapid increase in Egr1 expression, potentially leading to increased Lhb mRNA. The stimulation of Dusp1 has also been shown previously. The activation of MAPK pathways involves negative feedback by nuclear localized phosphatases, including the dual-specificity kinases of the MKP (MAPK phosphatases) family (84, 85). Several studies show that Mkp1 (Dusp1) and Mkp2 (Dusp4) levels are rapidly elevated in response to GnRH (59, 86-88). The recruitment of Dusp1 mRNA in polysomes indicates that GnRH is also acting at the level of translation to temper its own signaling by increasing abundance of downstream phosphatases.

In these studies Gnrhr mRNA was not regulated by GnRH exposure. However, Gnrhr was previously shown to shift from heavy polysomes to less-efficient light polysomes in response to GnRH (24). Several reasons may explain this discrepancy. First, the down-regulation of Gnrhr was observed after exposure of cells to 24 hours tonic treatment with high, super-physiological

concentration (1 uM) of GnRH, unlike the 30 min of 10 nM GnRH used here. Secondly, the experiments were performed in the αT3-1 cell line, a model of an immature, less differentiated gonadotrope compared to LβT2 (6, 89). Finally, the studies presented here only examined mRNAs that redistribute between the polysome and RNP pools. Examining mRNAs that are occupied by light compared to heavy polysomes may reveal mRNAs such as Gnrhr that may be more subtlely regulated by GnRH.

In response to GnRH, Cmyc mRNA increased in abundance in polysomes. Cmyc is a proto-oncogene transcription factor that targets genes involved in cell growth and metabolism. Interestingly, Cmyc may also play a direct role in regulating translation initiation, based on the finding that it can bind and activate the eIF4E promoter (90). The translation of Cmyc is IRES-mediated. IRESs were first identified in viruses but since then several eukaryotic mRNAs, including Cmyc, have been demonstrated to initiate this way (80). The mechanism of translational stimulation of Cmyc is unclear. It may be due to activation of ERK and cap-binding factors or due to its IRES, allowing escape from the UPR, or a combination of both. During poliovirus infection, when overall protein synthesis is inhibited, Cmyc sediments with polysomes and its protein synthesized. This is thought to be conferred by its IRES (91). Unlike the fate of the cap-binding factors caused by GnRH, however, this was shown to occur despite a reduction in the cap binding complex eIF4F (92), and the current studies suggest that Cmyc stimulation may be a result of cap-binding factor stimulation via PKC/ERK (Figure 3-9B, 3-10). Cmyc translation has been shown to occur by a cap-dependent mechanism as well (93).

Examination of translational regulation beyond the few hand-picked genes was provided by the microarray analysis, which reveals regulation that is consistent with what has already been demonstrated for GnRH action. First, GnRH has been shown to negatively affect metabolism genes at the transcriptional level (39). Of the mRNAs determined to be translationally regulated by GnRH in this study, the KEGG analysis reveals that a large majority are involved in metabolism, including oxidative phosphorylation and the citrate cycle, and the majority accumulated in RNP complexes (Figure 3-6). The overall reduction in metabolism may be

consistent with the anti-proliferative effects of GnRH (73). The current studies also confirm the stimulation of the UPR by GnRH. An immediate effect of the UPR is to attenuate translation. Some transcripts escape this regulation, and this appears to occur with some regularity in GnRH induction of the UPR, as demonstrated by the microarray data. One well-established example of escape in other systems is transcription factor Atf4 (30). Indeed, the current studies revealed that Atf4 mRNA was amongst the top-regulated genes, associating with polysomes in response to GnRH (Appendix, Table 5-1). Additionally, Atf3 and Chop, transcription factors upregulated by Atf4 (94), are transcriptionally induced by GnRH, as observed in this study (discussed below) and by others (39, 40). Finally, the marked movement of ribosomal mRNAs, mRNAs involved in protein export, and mRNAs translated on ER-bound ribosomes into the RNP pool (Figure 3-6) is consistent with an overall tone of attenuating translation. To meet the demands of hormone secretion, the gonadotrope may mount a UPR-like response to GnRH, decreasing translation to allow recovery of the ER environment. Simultaneously, transcription factors, such as Egr1, may be immediately transcriptionally and translationally stimulated in order for longer term responses to GnRH to occur. Future studies addressing the role of the UPR in GnRH action, and what attenuation may mean for LH levels specifically, should reveal the significance of the UPR in gonadotrope function. The possibilities will be discussed in Chapter 4.

The validity of the microarray results can also be assessed by comparing the mRNAs revealed to be transcriptionally regulated by GnRH in this study with those revealed in previous studies. Using the RNP/polysome ratio calculation measures how an mRNA is distributed between different ribosomal complexes and is thus a measure of translational sensitivity that is independent of changes in overall level of the mRNA. However, the role of transcription can also be assessed, by examining genes that are significantly different between the polysome pool of GnRH-treated cells and the polysome pool of control-treated cells, instead of examining the RNP/polysome ratio. When approached this way, genes that are known to be regulated transcriptionally by GnRH and that were not deemed to be regulated translationally were identified. These included Fos, Jun, Egr1, Egr2, Egr4, Klf4, Dusp1, and Atf3 (data not shown), all

of which are documented transcriptional targets of GnRH (39, 40, 58, 59, 86-88, 95). The corroboration of this work with the work of others in uncovering the intricate network of gene regulation by GnRH, both at the level of transcription and of translation, illustrates the robustness of the current microarray analysis.

The ability to glean transcriptional regulation in addition to translational regulation also suggests that potentiation is not very widespread, since the transcriptional and translational analyses revealed different regulated genes. Potentiation describes the coupled regulation of an mRNA both at the level of transcription and translation such that both processes influence the production of the resulting protein in the same direction (81). However, the two processes do not necessarily have to be co-regulated. For example, upon switching carbon sources in yeast, the regulated yeast mRNAs show great potentiation, where almost all mRNAs whose transcription increased also redistributed to polysomes. However, specific transcripts were shown to accumulate in RNPs without a change in overall abundance, and lowering the level of a reporter mRNA did not result in decreased translation efficiency (96). In another yeast model, minimal overlap was observed between mRNAs that change at the transcript level and that are translationally responsive as well (97). In poliovirus-infected HeLa cells, very few mRNAs showed a change in overall abundance but the change in association of mRNAs with polysomes was dramatic (92). A direct assessment of potentiation from this study also comes from the genes that were assayed using quantitative PCR. These results showed that while the transcription of Cmyc (Figure 3-2B) and Egr1 (Figure 2-6C) and translation (Figure 3-1B) increase, indicating potentiation, Lhb and Cga mRNA levels also increased (Figure 3-15) but their translation was attenuated (Figure 2-5). Gapdh, also translationally attenuated (Figure 2-5), and Gnrhr, translationally unresponsive (Figure 3-1B), did not show a change in transcript levels in response to GnRH (Appendix, Figure 5-2).

While the microarray results revealed many mRNAs that are translationally regulated by GnRH, there were some discrepancies. The microarray results confirmed the regulation of Gapdh and Lhb, as determined by quantitative PCR, but not Egr1, Cmyc or Cga. The

discrepancy indicates that the microarray analysis may be conservative and potentially missing mRNAs that are indeed targets of regulation. For Egr1, the inability of the microarray to determine its regulation is not surprising, since Egr1 regulation was variable even using quantitative PCR analysis (compare 3-1B and 3-9). However, while Cga, Cmyc and Egr1 were not found amongst the top 800 mRNAs, their fold-redistribution value indicated movement in the same direction determined by PCR (Figure 3-4). Some of the discrepancy may also be explained by the different measurement methodologies. For the quantitative PCR data, the absolute mass of a specific mRNA in each pool was measured to examine redistribution of the mRNA between the pools despite any overall changes in mRNA level. In the microarray data, however, the mass of a specific mRNA as a proportion of total mRNA in each pool was used in calculating fold-redistribution. Although the calculated fold-redistribution for Lhb, for instance, is very similar using either method, this difference in methodology could lend to the discrepancies observed, at least for some mRNAs.

The overall data set is also expected to be conservative with respect to the ability to determine all the genes or pathways that are translationally regulated, for several reasons. First, only one treatment paradigm was used in these studies. Second, measuring RNP/polysome ratios only examines genes that move relatively dramatically between the polysome and RNP pools. Further dividing the polysomal pool into heavy and light pools (or even individual polysomal fractions) may pick up genes that are moving in more subtle yet still important ways. Third, both the amount of an mRNA in polysomes, as studied here, or the average number of ribosomes (polysome size) of a particular mRNA affects its translational efficiency and thus dissecting the latter may provide insight as well. Finally, for the microarray KEGG pathways analysis, characterization of the genes is limited to those that are previously defined in the KEGG database to be part of a particular pathway. Of the 800 top regulated genes, only about half had KEGG pathway information available.

Despite some discrepancies and potential shortcomings of the analyses performed, the regulation of Lhb was confirmed and is of specific interest because of its crucial role in

reproductive biology. Initial attempts to define the elements that confer its translational sensitivity to GnRH were presented in this chapter, and the data suggests that the signal peptide or the 5'UTR of Lhb are not sufficient to confer sensitivity. The signal peptide experiment has its shortcomings, as discussed. For the UTR experiment, the finding that the 5'UTR is not sufficient to alter reporter protein levels after GnRH treatment (Figure 3-12) is consistent with intracellular levels of LH not changing after four hours of GnRH exposure, compared to untreated conditions (Figure 3-15C). So, the question of whether the 5'UTR affects translation is either inconsequential because LH protein levels do not change in response to GnRH, or more likely, these experiments are not sufficient to answer the question. First, the four hour treatments potentially miss any acute regulation, since the attenuation is transient (Figure 2-9B). It would be more appropriate to transfect a reporter containing the 5'UTR of Lhb and use ribosomal fractionation and quantitative PCR to determine the ribosomal distribution of the reporter after 30 minutes of GnRH treatment, in a similar fashion to the signal peptide and all the other experiments. Secondly, it would be important to establish necessity of the 5'UTR or whatever other sequence, first, rather than just sufficiency, given that many components may affect translation and picking just one that would confer sufficiency may be difficult.

Overall the results show that GnRH exerts specific, bidirectional translational control by stimulating or attenuating translation of a selected pool of transcripts. The genes determined by quantitative PCR or microarray to be translationally regulated by GnRH include those important for the differentiated function of the gonadotrope. The specificity lies in the mRNAs regulated as well as the direction of movement of those mRNAs within ribosome complexes. GnRH appears to simultaneously target both eIF2α through calcium and cap-binding factors through ERK in order to elicit a specific translational response. The specificity of the signaling events mediating this bidirectional fate of the various mRNAs and the unanswered questions regarding the fate of LH protein levels in face of this regulation will be addressed in the concluding chapter.

MATERIALS AND METHODS

LβT2 cell culture

The LβT2 (6) mouse gonadotrope line was maintained in high-glucose HEPES-buffered DMEM supplemented with penicillin/streptomycin and 10% fetal bovine serum. The cells were incubated at 37°C in a humidified atmosphere of 5% CO_2. For the experiments, cells were plated, grown overnight for 36 hours, and then the media was changed to serum-free media (SFM) and the cells were incubated overnight for an additional 16-18 hours. Cells were treated with hormones/drugs in SFM on the third day.

For fractionation for microarray analysis, total RNA isolation or 5'UTR transfection experiments, after SFM starvation overnight, the media was changed to Earle's Balanced Salt Solution (EBSS) for amino acid starvation for one hour prior to GnRH treatment. Subsequent treatment was performed in EBSS. Although the degree of RNP remodeling was greatest for the EBSS starved cells, followed by the degree in SFM alone and then finally the 1% serum-containing media, the general remodeling of ribosomes to RNP complexes was observed under all of these conditions (Appendix, Figure 5-3).

Hormone and drug treatments

After starvation, the cells were treated with vehicle, 10 nM GnRH, 1 uM ionomycin (Calbiochem, La Jolla, CA) for 30 min, 2 mM dithiothreitol (DTT) for 30 min, or 100 nM PMA (Calbiochem) for 30 min. Where appropriate, 5 uM actinomycin D (Calbiochem) was added to the media for 1 hour, 100 ug/ml cycloheximide for 5 minutes, 1 uM U0126 (Calbiochem) for 30 min, or 30 uM PD98059 (Calbiochem) for 30 min, prior to GnRH treatment. All reagents were from Sigma-Aldrich (St. Louis, MO) unless otherwise indicated. The drugs/hormones were left in the media for the duration of treatment. For the GnRH pulse treatments, GnRH was added to the media for 5 or 10 minutes, as indicated, after which the media was removed, the cells were washed with PBS, and fresh media was added back until the cells were harvested.

Total RNA isolation

LβT2 cells were plated at a density of $1x10^7$ cells per 10-cm dish. On the third day, the cells were treated with 10 nM GnRH or vehicle (PBS) for 30 minutes. Where appropriate, actinomycin D at 5 uM was added to the media one hour prior to treatment with GnRH. Total RNA was harvested using Trizol LS (Invitrogen, Carlsbad, CA). A 2 ug aliquot of RNA was treated with DNase to remove any contaminating DNA and then used for reverse-transcription for quantitative real-time PCR analysis.

Ribosome fractionation and mRNA isolation

Two 10-cm plates were used for each experimental condition with $2x10^7$ LβT2 cells seeded per plate and treated as described. After treatment, 100 ug/ml cycloheximide was added to all the plates (except for any plates already pre-treated with cycloheximide) and the cells were incubated on ice for 5 minutes. The cells were then harvested in 500 ul of ice-cold polysome extraction buffer (PEB) containing 140 mM KCl, 5 mM $MgCl_2$, 1 mg/ml heparin sodium salt, and 20 mM Tris-HCl pH 8, supplemented with fresh 0.5 mM DTT and 100 ug/ml cycloheximide on the day of the experiment. Cells from two plates of the same experimental condition were collected and pooled at this step. The cells were spun down at 1000 X g for 3 minutes and then each pellet was resuspended in 200 ul PEB containing 1% Triton-X. The pellets were allowed to lyse on ice for 20 minutes with gentle inversion by hand every few minutes. Finally, the cellular debris was collected by centrifugation at 10,000 X g for 10 minutes. An aliquot of the supernatant and the debris pellet was collected and resuspended in Laemmli sample buffer for Western blot analysis. The rest of the supernatant was layered onto 5 ml 10-50% sucrose gradients made with PEB lacking Triton-X. The samples were centrifuged in a SW-55 swing-bucket rotor for 1.5 hours at 150,000 X g.

A 21-guage needle was used to collect fractions from the bottom of the gradient. Fractions were collected using a peristaltic pump while monitoring real-time absorption at 254 nm through a UVM-II monitor (GE Healthcare, Fairfield, CT). Fractions of 250 ul volume each were

collected using a FC 203B fraction collector (Gilson, Middleton, WI). Monitoring of UV absorption and fraction collection was controlled through a Labview virtual instrument (National Instruments, Austin, TX) and a KPCI 3108 DAQ card (Keithley Instruments, Cleveland, OH). Fractions were dripped directly into SDS for a final SDS concentration of 1%. Each fraction was then treated with 0.2 mg/ml proteinase K at 37° C for 1.5 hours. RNA was purified from each fraction by phenol-chloroform extraction and ethanol precipitation. The RNA from the fractions was pooled into polysome and RNP pools according to the gradient's UV absorption profile. Poly(A) RNA was then isolated using Oligotex mRNA Mini Kit oligo-dT columns (Qiagen, Valencia, CA) according to the manufacturer's recommendations and eluted into a final volume of 40 ul for each pool. A 10 ul aliquot of mRNA was used for reverse-transcription for quantitative PCR analysis.

Quantitative real-time PCR

For quantitative PCR analysis of fractionated, ribosome-bound mRNA, cDNA was synthesized using Omniscript Reverse Transcriptase (Qiagen, Valencia, CA) and 10 uM of random hexamer primers (Applied Biosystems, Foster City, CA). For analysis of total RNA, cDNA was synthesized using QuantiTect Reverse Transcription Kit (Qiagen, Valencia, CA). Quantitative real-time PCR was carried out using the MyIQ Single-Color Real-Time Detection System (Bio-Rad Laboratories, Hercules, CA). The PCR products were amplified in the presence of SYBR Green using the QuantiTect SYBR Green PCR kit (Qiagen, Valencia, CA) supplemented with 300 nM of transcript specific primers and 1 uM fluorescein for proper instrument calibration. The cycling conditions used were those recommended by the PCR kit manufacturer. A melt curve was performed after each PCR run to ensure that just a single product was amplified in each assay and the size of the products were verified using agarose gel electrophoresis.

Primer sequences were designed against murine mRNA sequences as available through PubMed. The primer sequences were: Lhb fwd 5'-CTGTCAACGCAACTCTGG-3', Lhb rev 5'-ACAGGAGGCAAAGCAGC-3'; Cga fwd 5'-GGTTCCAAAGAATATTACCTCG-3', Cga rev 5'-GTCATTCTGGTCATGCTGTCC-3'; Gnrhr fwd 5'-GCCCCTTGCTGTACAAAGC-3', Gnrhr rev 5'-

CCGTCTGCTAGGTAGATCATCC-3'; Egr1 fwd 5'-ATTTTTCCTGAGCCCCAAAGC-3', Egr1 rev 5'-ATGGGAACCTGGAAACCACC-3'; Cmyc fwd 5'-GCTGCATGAGGAGACACCG-3', Cmyc rev 5'-CCTCGGGATGGAGATGAGC-3'; Gapdh fwd 5'-TGCACCACCAACTGCTTAG-3', Gapdh rev 5'-GATGCAGGGATGATGTTC-3'; Dusp1 fwd 5'-TGGTTCAACGAGGCTATTGAC-3', Dusp1 rev 5'-GGCAATGAACAAACACTCTCC-3'; GFP fwd 5'-CAGCACGACTTCTTCAAGTCC-3', GFP rev 5'-TCTTGTAGTTGCCGTCGTCC-3'.

Primers were designed to generate an 80-150 bp amplicon that crossed intron/exon boundaries where possible in order to avoid amplification of any contaminating unspliced RNA or genomic DNA. All PCR reactions were performed in triplicate, except for those involving cDNA from primary pituitary cells, which were performed in duplicate. A larger cDNA fragment of all the genes assayed was inserted into pCR2.1 (Invitrogen, Carlsbad, CA) and used to generate a standard curve and assess PCR efficiency for each run. The mass values for each transcript were extrapolated from the standard curve.

To calculate a fold-redistribution value for an mRNA's movement within the ribosome profile, the mass of each transcript in each ribosome pool (polysome or RNP) was measured and a ratio was calculated for the mass of that transcript in the RNP pool compared to the polysome pool. A ratio was calculated for both the treated and control (vehicle treated) conditions. A fold-redistribution value was then generated by taking a ratio of the ratios: the RNP/polysome ratio in treated compared to the RNP/polysome ratio in control cells. Statistics were performed as indicated in each figure legend on these values. For ease of representation in the histograms only, the negative inverse was calculated and reported for fold-redistribution values between 0 and 1, such that movement of an mRNA into the polysome pool would report a negative redistribution value and movement into RNP complexes would report a positive value.

ERK Western blotting

Cells were plated ($1x10^7$) in 10-cm dishes and after treatment, protein was harvested using standard RIPA lysis buffer supplemented with phosphatase inhibitors. Standard SDS-

PAGE and semi-dry transfer method (Bio-Rad Laboratories, Hercules, CA) was used to transfer the extracts onto PVDF membranes (Bio-Rad Laboratories, Hercules, CA). Blocking and primary antibody delivery was performed in 1X casein (Vector Laboratories, Burlingame, CA). Antibody directed against mouse phosphorylated ERK (Santa Cruz Biotechnology, Santa Cruz, CA) was diluted 1:1000 and incubated for 1 hour. Blots were developed using 1:2000 dilution of biotinylated secondary antibodies (Santa Cruz Biotechnology, Santa Cruz, CA) and Chemiglow chemiluminescence (Alpha Innotech, San Leandro, CA). Chemiluminescence was visualized using the GeneSnap BioImaging System (Syngene, Frederick, MD).

Plasmid construction and transfection

pTK-EMCV-Luc was made by synthesizing 80 bp of the TK promoter and inserting it upstream of the EMCV IRES and luciferase coding sequence in the pGL3 vector (Promega, Madison, WI). pTK-mLhb5'-Luc was made by synthesizing 80 bp of the TK promoter immediately followed by the 8 bp mouse Lhb mRNA 5'UTR sequence and inserting this upstream of the luciferase coding sequence of pGL3 (Promega). pCMV-EMCV-Gal was made by cloning the Spe fragment of CMV from pCDNA3.1 (Invitrogen, Carlsbad, CA) upstream of the EMCV IRES and b-galactosidase coding sequence. $2x10^5$ cells were seeded per 24-well plate. Twenty-four hours later, the cells were co-transfected with pCMV-EMCV-Gal and either pTK-mLhb5'-Luc or pTK-EMCV-Luc using Fugene 6 (Roche, Basel, Switzerland). 0.1 ug of each plasmid was transfected, using a 3:1 DNA:Fugene 6 ratio. Twenty-four hours after transfection the media was changed to SFM and the cells were incubated another 16-18 hours. On the day of GnRH treatment, the media was changed to EBSS containing actinomycin D for 1 hour and then GnRH or PBS was added for 4 hours. After treatment, the cells were lysed and b-galactosidase activity determined using the Galacto-Light Plus system (Applied Biosystems, Foster City, CA). Luciferase activity was determined using the Luciferase Assay System (Promega, Madison, WI). Assay reagent injection and activity measurements were carried out on LMax and SOFTmax software (Molecular Devices, Sunnyvale, CA).

pLhbSignal-GFP was made by synthesizing the sequence encoding the 20 amino acid signal peptide of LHβ and cloning it immediately upstream and in frame of the coding sequence for GFP in the pEGFP-N1 vector (Clontech Laboratories, Mountain View, CA). Cells were transfected with this construct or GFP alone (pEGFP-N1, referred to as pGFP in this work). Cells plated in 10-cm plates were transfected with 6.0 ug of plasmid using Fugene 6 (Roche, Basel, Switzerland) at a 3:1 DNA:Fugene 6 ratio. Twenty-four hours after transfection the media was changed to SFM and the cells were incubated another 16-18 hours. Cells were treated with vehicle or 10 nM GnRH for 30 minutes and ribosomes were fractionated.

Intracellular LH Content

3.5×10^6 cells were plated in 6-well plates and starved as described. On the day of treatment, after 1 hour of vehicle or actinomycin D pre-treatment followed by vehicle or pulse GnRH exposure, cells were replaced with fresh media containing actinomycin D until harvest. To harvest, the cells were washed twice in ice cold PBS and then 150 ul of PBS was used to scrape the cells. Another 150 ul was used to rinse each well, and the cells were collected into pre-chilled tubes. The cells were sonicated and then centrifuged at 17000 x g for 2 min. The supernatant was collected and protein concentration was determined through the D_c Protein Assay kit (Bio-Rad, Hercules, CA). LH protein content was determined by immunoradiometric assay (IRMA) by the Ligand Assay and Analysis Core at University of Virginia's Center for Research in Reproduction. The amount of LH in each sample was normalized to total protein level in that sample, as determined by the protein assay.

Statistical Analysis

The areas under the curves of the ribosome profiles were integrated using SigmaPlot v9.01 (Systat Software, Richmond, CA). Any ratio or fold-redistribution data was transformed using $\log_2$ and a value of 10 was added to those values to ensure positive values prior to analysis. All subsequent analysis was conducted using JMP IN (SAS Institute, Cary, NC) on

untransformed (other than $\log_2$ + 10 for ratio or fold-redistribution values) or optimally Box-Cox transformed values. P-value ≤ 0.05 was considered significantly different. All experiments were repeated at least three independent times unless otherwise indicated and reported values are the means +/- SEM.

Affymetrix microarray analysis

The RNP (R) and polysome (P) fractionated mRNA collected from three independent experiments of GnRH or vehicle-treated LβT2 was used for Affymetrix GeneChip analysis. The integrity of the mRNA was checked by agarose gel electrophoresis, 200 ng of mRNA was processed, and 15 ug of cRNA was hybridized to Affymetrix mouse MOE430A array chips according to the manufacturer's recommended protocol (GeneChip Expression Analysis Technical Manual). These procedures were performed by the GeneChip Microarray Core at the University of California, San Diego.

Gene expression profiles were compared between the GnRH-treated R/P and untreated R/P groups. Three independent experiments were analyzed, resulting in a total of twelve microarray sets (six R/P sets). Affymetrix chip image files were converted to probe set data (.CEL files) using the Gene Chip Operating System (GCOS) v.1.2 (Affymetrix, Santa Clara, CA). The MOE430A Affymetrix chip consists of 22,690 probes. 6556 probes had Absent Calls that were consistent across all twelve chips and were removed, leaving 16,134 probes for analysis. Raw expression values in the .CEL files were pre-processed via the Robust Multichip Average (RMA) method (98), as implemented in Bioconductor (www.bioconductor.org), a suite of programs for the R statistical programming language (http://cran.r-project.org). RMA default values were employed to pre-process the twelve chips simultaneously.

The $\log_2$ gene expression values obtained from RMA pre-processing were analyzed as follows. First, genes that were differentially expressed between the GnRH-treated R/P and untreated R/P groups were identified via two different criteria: fold change and t-statistics. Fold-change analysis highlights potentially biologically interesting genes. The t-statistics were used to

compute the magnitude of the variation among biological replicates as compared to the variation between the treated and untreated groups. A large absolute value in the t-statistic is indicative that there is larger statistical variation between treated and untreated groups than variation within a specific group. A composite measure of fold-change and t-statistics, called bioweight (99), was used to produce a list of the top 5% (800) of the most regulated genes amongst those that are found to be expressed in LβT2. The bioweight measure is a product of the across-replicate fold change and the negative $\log_{10}$ of p-values for the gene specific t-tests. The advantage of bioweight analysis is that the impacts of fold-change analysis and gene specific t-test analysis are studied simultaneously.

Confirmatory differential gene expression analysis was conducted via the permutation method Significance Analysis of Microarrays (SAM). The SAM method detects genes with statistically significant differences in expression by computing a score for each gene relative to the gene specific standard deviation (100). Genes with scores greater than an adjustable threshold are declared significant. The percentage of genes that are identified by chance is the False Discovery Rate (FDR), which was set at 0.2. Since non-parametric, permutation-based techniques, such as SAM, are hindered by experiments with small sample sizes, it is reasonable to compare the results from SAM to other methods such as bioweight. The SAM technique was computed in Bioconductor via the siggenes library. The q-values generated by SAM are an FDR-adjusted equivalent to the p-value (101).

Confirmatory analysis employed unsupervised clustering to determine if the treatment groups could be recovered. Dendograms of expression patterns and samples were computed via hierarchical clustering using complete-linkage as the between-cluster distance criteria and Pearson's correlation as the similarity measure (102). Heatmaps (false color images) of the top 800 and bottom 800 bioweight genes were generated such that the rows (samples) and columns (genes) were clustered independently using hierarchical clustering via Pearson's correlation for within-cluster distance and complete linkage for between-cluster distance. Red indicates strong positive correlation and green indicates strong negative correlation.

The top regulated genes were further characterized by the Kyoto Encyclopedia of Genes and Genomes (KEGG) pathway analysis (http://www.kegg.org) via the Bioconductor package, annffy (103). The annffy package is designed to interface between Affymetrix chip analysis results and web-based databases by gathering annotation data from diverse resources. Probes that were not associated with a KEGG pathway (approximately 400) were not summarized in Figure 3-6. Genes with multiple probes or that were associated with multiple pathways were consolidated.

ACKNOWLEDGEMENTS

The microarray analysis and the figures generated from it, as well as the writing of the corresponding Materials and Methods section, were completed in collaboration with Dr. Sonia Jain and Feng He from the Division of Biostatistics and Bioinformatics in the Department of Family and Preventive Medicine of the University of California, San Diego.

This work was supported by the National Institutes of Health grants R01 HD 43758 and K02 HD 40708. M.T.D. was supported by the NIH grant T32 GM08666. The LβT2 cells were a gift from Dr. Pamela Mellon.

The IRMA for LH was performed by the University of Virginia Ligand Core and was supported by the NICHD/NIH through cooperative agreement (U54 HD28934) as part of the Specialized Cooperative Centers Program in Reproductive Research.

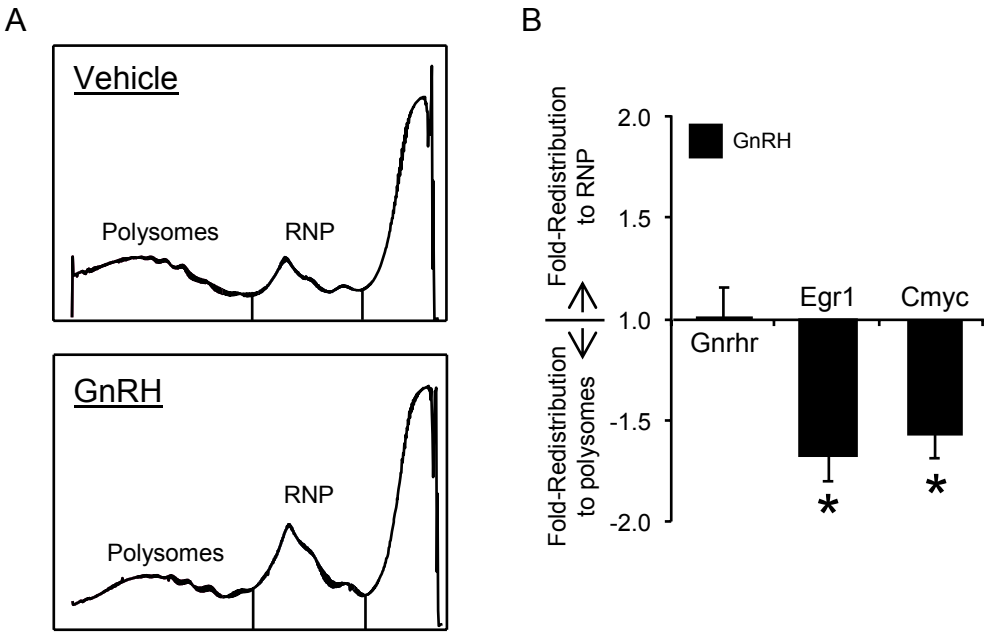

Figure 3-1. Gnrhr, Egr1 and Cmyc mRNAs differentially redistribute in ribosome complexes in response to GnRH. LβT2 cells were treated for 30 minutes and then cell extracts were fractionated on sucrose gradients while monitoring UV absorption at 254 nm. Fractions were pooled to represent polysomes (RNA with two or more ribosomes) and RNP complexes (ribosomal subunits, monosomes, initiation complexes). **(A)** Representative profiles. **(B)** Messenger RNA was isolated from the RNP and polysome pools of the fractionated extracts and measured using quantitative PCR. A fold-redistribution value was calculated as a measurement of the change in transcript representation in the pools after GnRH treatment, as compared to control (vehicle) treatment. The data is represented in the histogram such that a positive value indicates movement into the RNP pool and a negative value indicates movement into the polysome pool. A fold-redistribution value of 1 represents no change after treatment. The reported values are the means +/- SEM of six independent experiments. Asterisks indicate statistical significance from a value of 1 as determined by a Student's t-test.

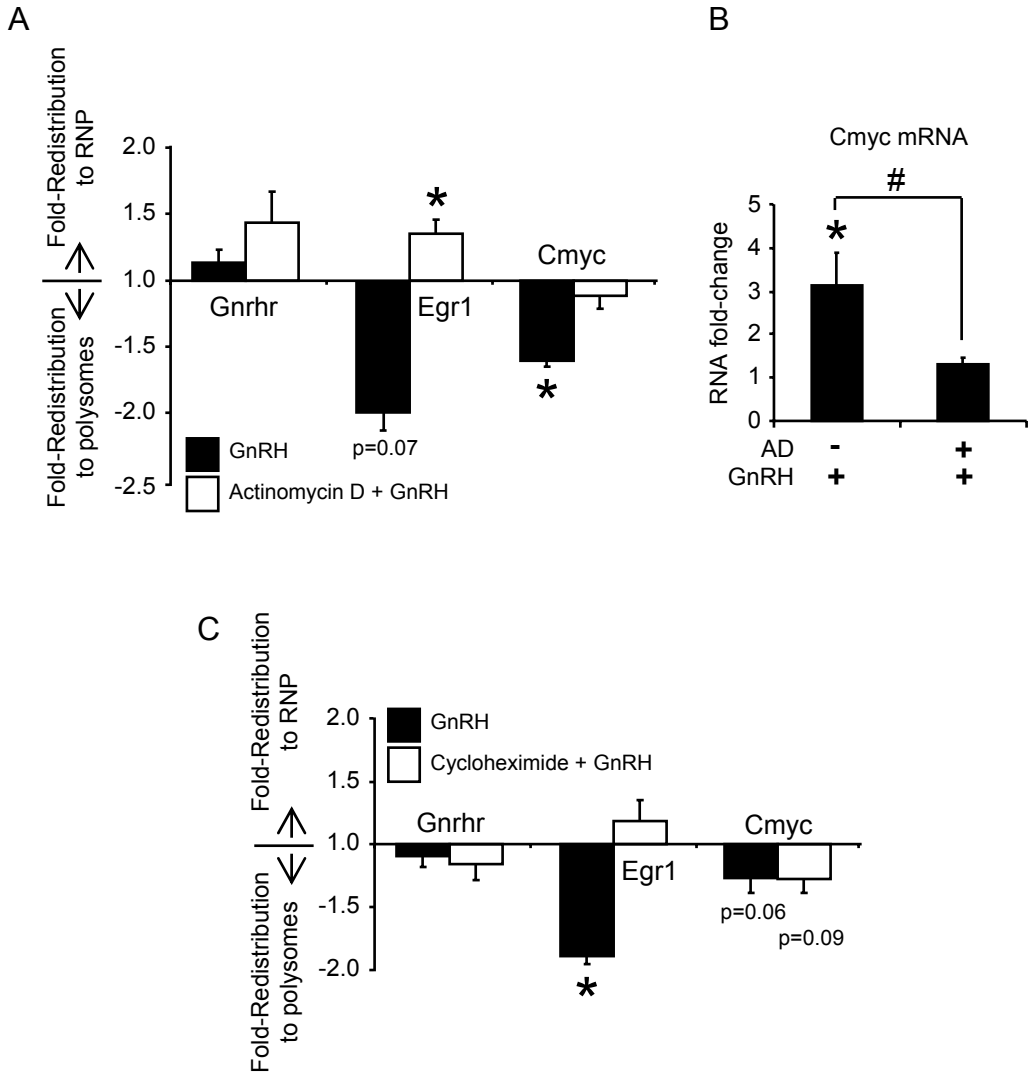

Figure 3-2. Gnrhr, Egr1 and Cmyc are differentially sensitive to translational and transcriptional regulation by GnRH. LβT2 cells were treated with actinomycin D (AD) to block transcription or cycloheximide to block translation elongation and then treated with GnRH or PBS (vehicle) for 30 minutes. **(A and C)** Ribosome complexes were fractionated and mRNA isolated from the RNP and polysome pools was measured using quantitative PCR. A fold-redistribution value was calculated as a measurement of the change in transcript representation in the pools after treatment, as compared to control (vehicle) treatment. The data is represented in the histogram such that a positive value indicates movement into the RNP pool and a negative value indicates movement into the polysome pool. A fold-redistribution value of 1 represents no change after treatment. **(B)** Total RNA was isolated from unfractionated extracts and Cmyc mRNA was measured by quantitative PCR, comparing its level in the GnRH-treated cells to that in the respective vehicle-treated cells. All the reported values are the means +/- SEM of four or more independent experiments. Asterisks indicate statistical significance from a value of 1; the p-value of selected groups is shown. For (B) only, pound (#) indicates groups are significantly different from each other, as determined by a Student's t-test.

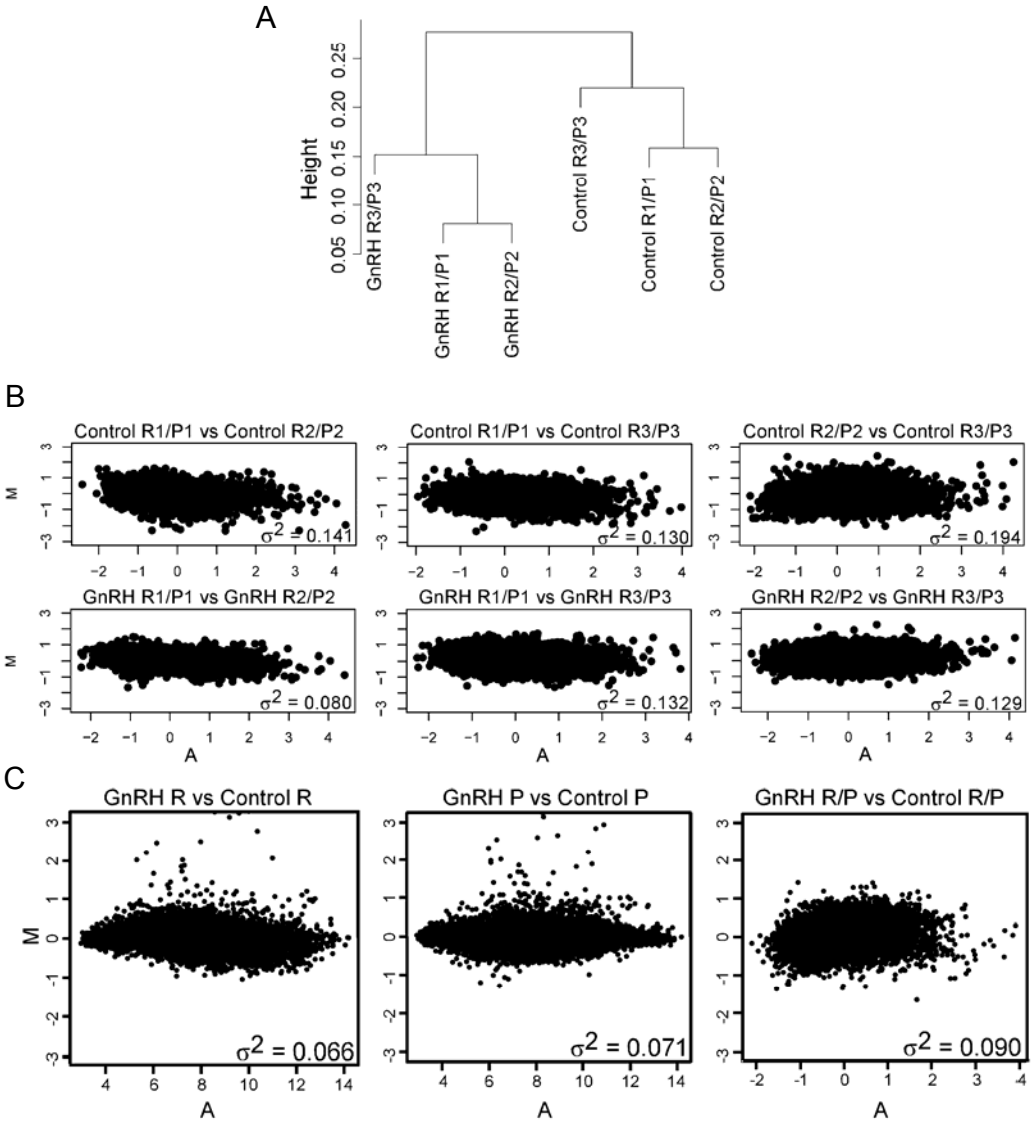

Figure 3-3. mRNA redistribution in ribosomal complexes is reproducible and not global. Three sets of messenger RNA from vehicle or GnRH-treated ribosomal-complex fractionated extracts were processed and hybridized to mouse Affymetrix MOE430A chips. **(A)** Unsupervised hierarchical clustering of the six RNP/polysome (R/P) groups using Pearson's correlation and complete-linkage. GnRH-treated and untreated control samples from the three experiments (1,2,3) were compared. **(B)** MA plots were generated to examine the variance between the different datasets. "M" on the y-axis is the $\log_2$ of the ratio of the intensities between the two arrays or the two sets of arrays being compared. A value of 0 indicates that the intensity for a particular probe between the two arrays is the same. "A" on the x-axis and is the average of the $\log_2$ intensities of the two arrays being compared. The σ^2 value is a measure of the variance in M. The R/P intensity ratio of each probe between replicate experiments was compared. **(C)** MA plots comparing the average R, P, or R/P intensity of all three replicates between GnRH-treated and untreated samples.

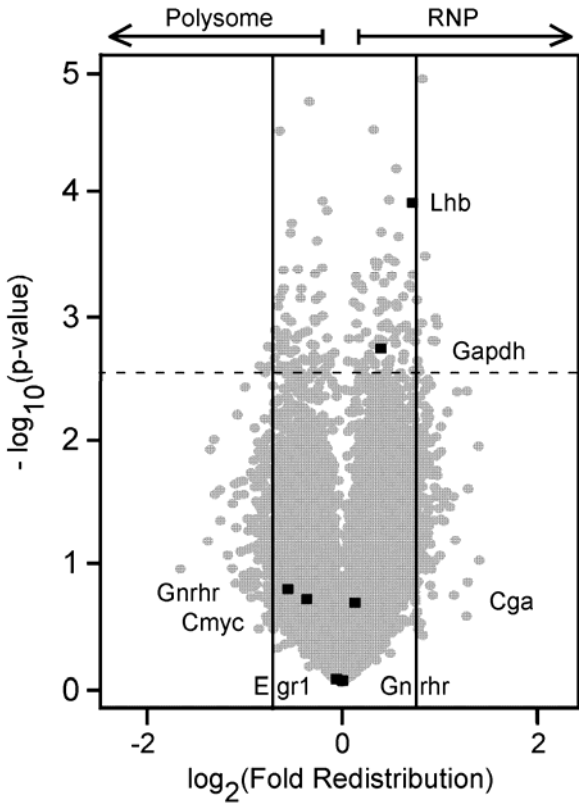

Figure 3-4. GnRH causes bidirectional redistribution of a specific subset of mRNAs. Volcano plot of expressed genes across the three datasets according to their bioweight, a combined measurement of GnRH fold-redistribution (x-axis) and confidence (y-axis). The plotted fold-redistribution is the $\log_2$ value of the fold-redistribution and the plotted confidence value is the $-\log_{10}$ of the p-value as determined by a Student's t-test. The highlighted spots are those corresponding to mRNAs assayed by quantitative real-time PCR. The horizontal and vertical lines represent the 99% quantile of the p-values and fold-redistributions, respectively.

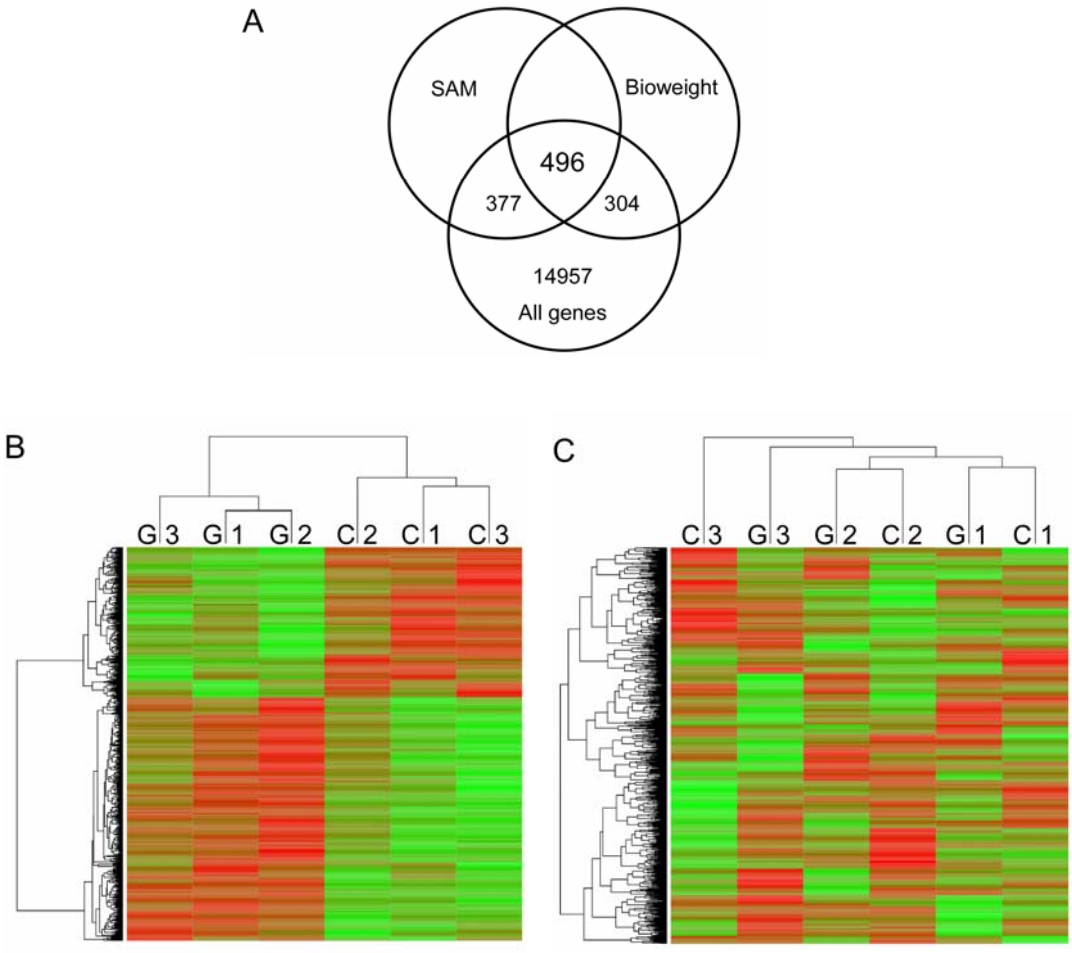

Figure 3-5. The top regulated genes show distinct patterns of mRNA redistribution. **(A)** The number of genes found to be in common between the top 800 genes as determined by bioweight and the 873 genes identified using SAM. A total of 16,134 genes were found to be expressed in LβT2 cells. **(B)** A heatmap of the top 800 regulated mRNAs as determined by bioweight shows that the mRNAs fall into distinct patterns of redistribution. The patterns cluster the chips appropriately into the three control samples (C1-3) and the three GnRH-treated samples (G1-3). **(C)** A heatmap of the 800 mRNAs with the lowest bioweight show no discernible expression patterns and the chips do not cluster in any meaningful manner. Red indicates strong positive correlation (greater representation of an mRNA as an RNP complex) and green indicates strong negative correlation (greater representation of an mRNA as a polysome). The heatmaps were generated using Pearson's correlation and complete linkage.

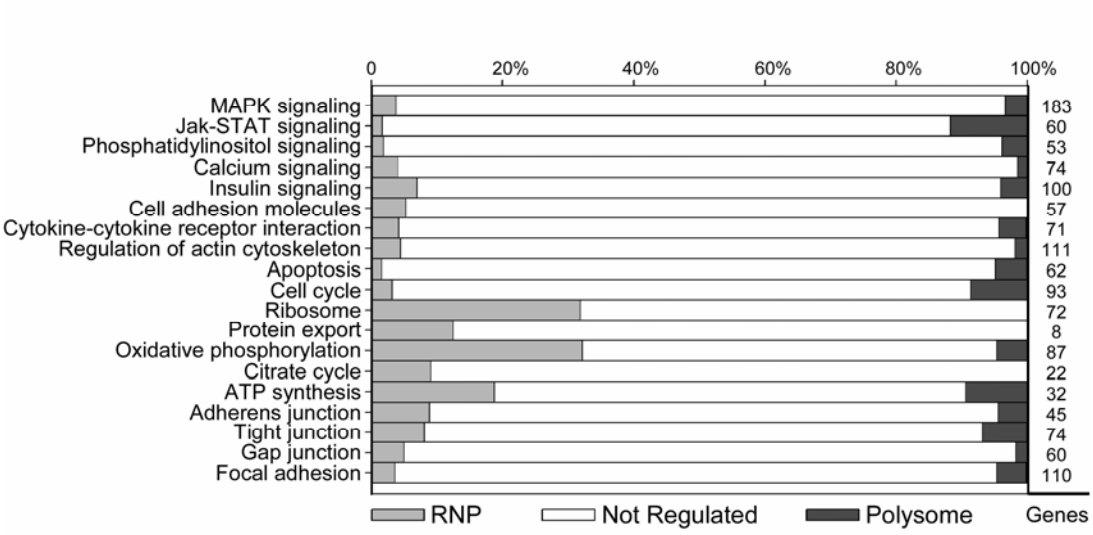

Figure 3-6. Summary of KEGG pathways identified by the top 5% of bioweight genes. The top 800 bioweight genes were organized into available KEGG pathways. The number of genes in a particular pathway is indicated as 100%. Represented is the percentage of genes moving into the RNP pool (light gray) or polysome pool (dark gray) after GnRH stimulation. The percentage of genes in each pathway showing no translational response to GnRH is represented in white.

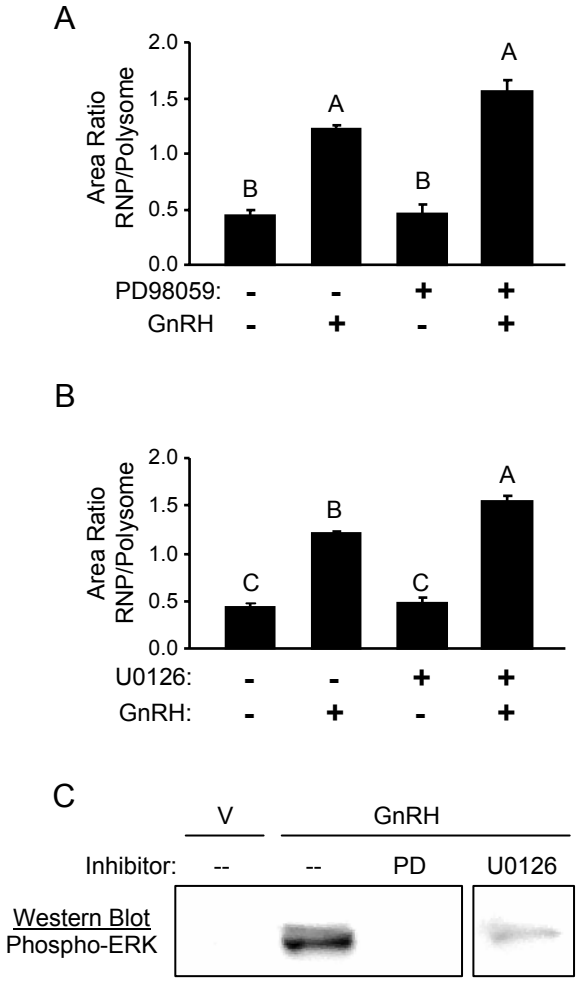

Figure 3-7. Inhibition of ERK activation by GnRH exacerbates RNP accumulation. LβT2 cells were treated with PD98059 (PD) or U0126 to block MEK/ERK activation and then treated with GnRH or PBS for 30 minutes. **(A and B)** Ribosome/RNP complexes were isolated and fractionated while monitoring UV absorption. The ratio (RNP/polysome) of the integrated area under the curve was calculated from the absorption profiles, as an indication of the level of redistribution of ribosomes. The reported values are the means +/- SEM of three or more independent experiments. Groups not connected by the same letter are significantly different as determined by ANOVA and *post hoc* Tukey's HSD test. **(C)** The efficacy of PD or U0126 was confirmed by Western blotting of protein extracts using antibody directed against the phosphorylated form of ERK (phospho-ERK).

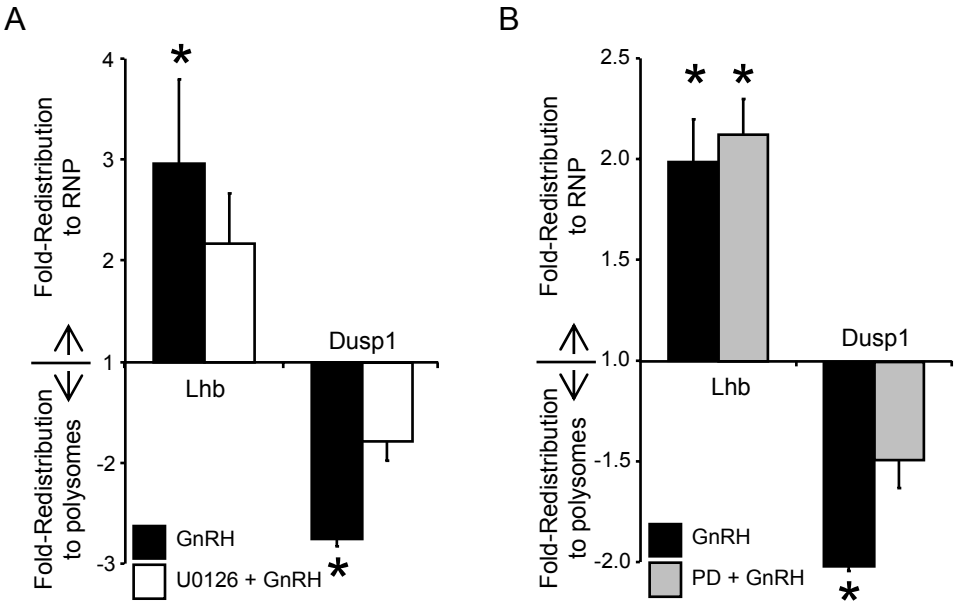

Figure 3-8. ERK activation by GnRH contributes to association of Dusp1 with polysomes. LβT2 cells were treated with U0126 or PD98059 (PD) to block MEK/ERK activation and then treated with GnRH or PBS (vehicle) for 30 minutes. Ribosomes were fractionated and mRNA isolated from the RNP and polysome pools was measured using quantitative PCR. A fold-redistribution value was calculated as a measurement of the change in transcript representation in the pools after treatment, as compared to control (vehicle) treatment. The data is represented in the histogram such that a positive value indicates movement into the RNP pool and a negative value indicates movement into the polysome pool. A fold-redistribution value of 1 represents no change after treatment. **(A)** Redistribution of mRNA in response to GnRH (black) or U0126 prior to GnRH (white) treatment. Three independent experiments. **(B)** Redistribution of mRNA in response to GnRH (black) or PD prior to GnRH (gray) treatment. Two independent experiments. The reported values are the means +/- SEM. As determined by a Student's t-test, asterisks indicate statistical significance from a value of 1. None of the treatment groups for each gene were different from each other using a Student's t-test.

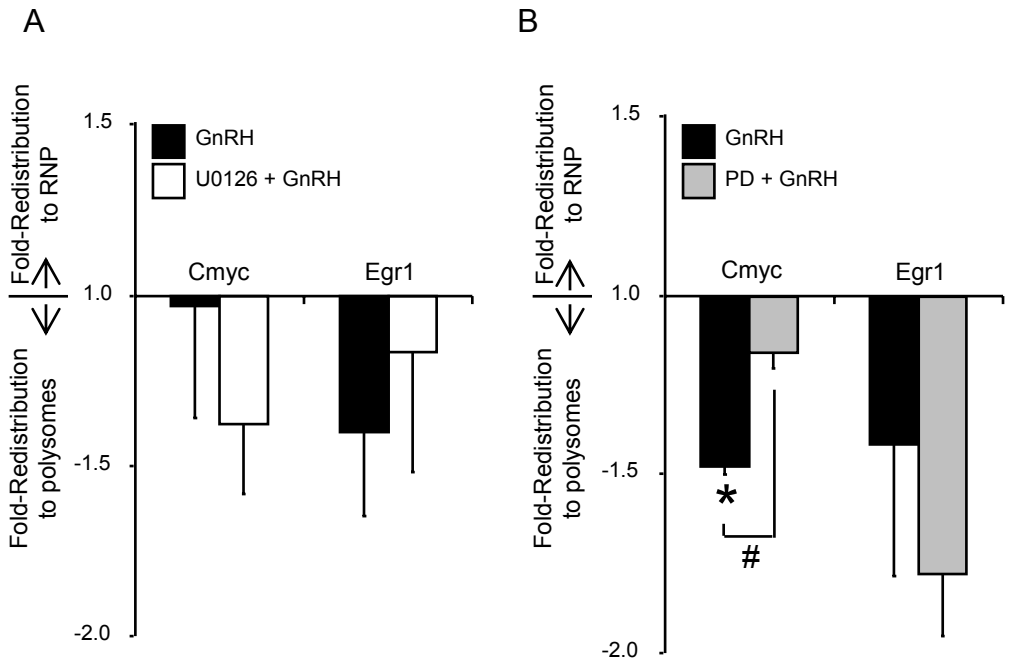

Figure 3-9. Role of ERK activation on Cmyc and Egr1 recruitment to polysomes is not clear. LβT2 cells were treated with U0126 or PD98059 (PD) to block MEK/ERK activation and then treated with GnRH or PBS (vehicle) for 30 minutes. Ribosomes were fractionated and mRNA isolated from the RNP and polysome pools was measured using quantitative PCR. A fold-redistribution value was calculated as a measurement of the change in transcript representation in the pools after treatment, as compared to control (vehicle) treatment. The data is represented in the histogram such that a positive value indicates movement into the RNP pool and a negative value indicates movement into the polysome pool. A fold-redistribution value of 1 represents no change after treatment. **(A)** Redistribution of mRNA in response to GnRH (black) or U0126 prior to GnRH (white) treatment. **(B)** Redistribution of mRNA in response to GnRH (black) or PD prior to GnRH (gray) treatment. The reported values are the means +/- SEM of at least three independent experiments. Asterisks indicate statistical significance from a value of 1 and pound (#) indicates groups are significantly different from each other, as determined by a Student's t-test.

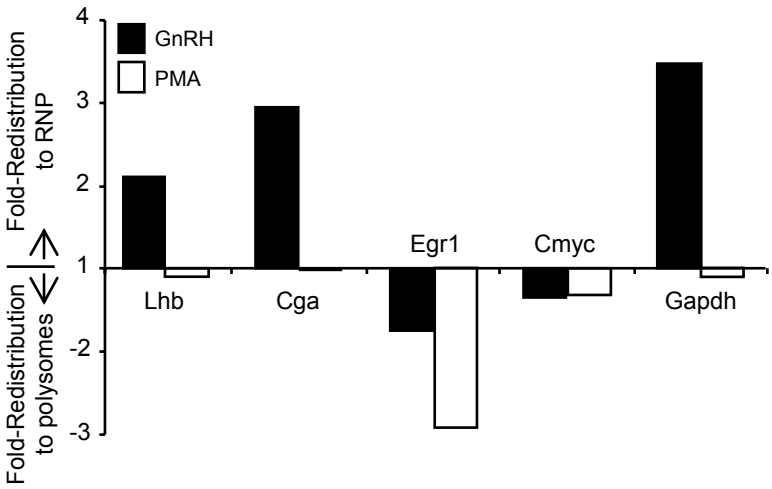

Figure 3-10. PKC activation promotes polysomal recruitment but not RNP accumulation of an mRNA. LβT2 cells were treated for 30 minutes and ribosome/RNA complexes were fractionated. Messenger RNA was isolated from the RNP and polysome pools and measured using quantitative PCR. A fold-redistribution value was calculated as a measurement of the change in transcript representation in the pools after treatment, as compared to control (vehicle) treatment. The data is represented in the histogram such that a positive value indicates movement into the RNP pool and a negative value indicates movement into the polysome pool. A fold-redistribution value of 1 represents no change. The reported values are from one experiment.

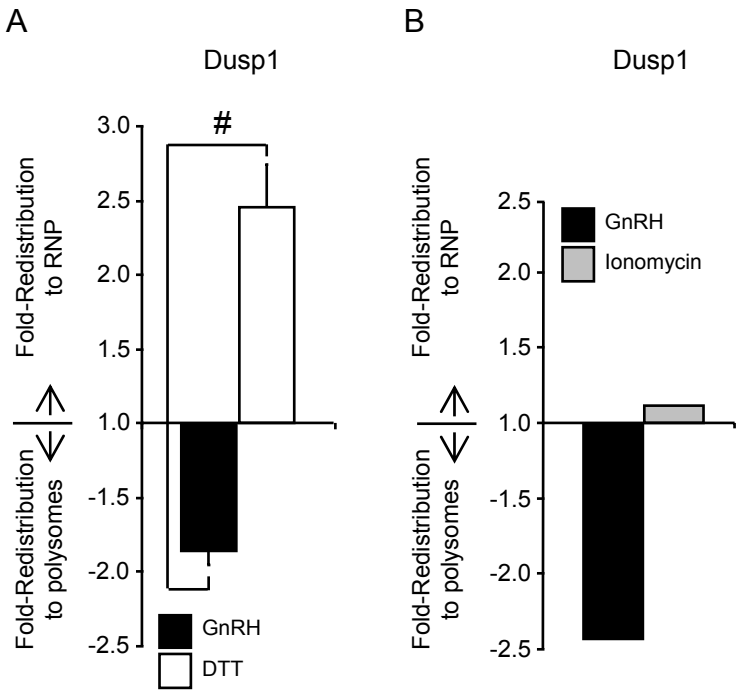

Figure 3-11. Activation of the UPR does not induce polysomal recruitment of Dusp1 mRNA by GnRH. LβT2 cells were treated for 30 minutes and ribosome/RNA complexes were fractionated. Messenger RNA was isolated from the RNP and polysome pools of the fractionated extracts and measured using quantitative PCR. A fold-redistribution value was calculated as a measurement of the change in transcript representation in the pools after treatment, as compared to control (vehicle) treatment. The data is represented in the histogram such that a positive value indicates movement into the RNP pool and a negative value indicates movement into the polysome pool. A fold-redistribution value of 1 represents no change after treatment. **(A)** Redistribution of Dusp1 mRNA in response to DTT or GnRH. The reported values are the means +/- SEM of three independent experiments. Pound (#) indicates statistical significance between the treatments, as determined by a Student's t-test. **(B)** Redistribution of Dusp1 mRNA in response to ionomycin or GnRH. The reported value is from one experiment.

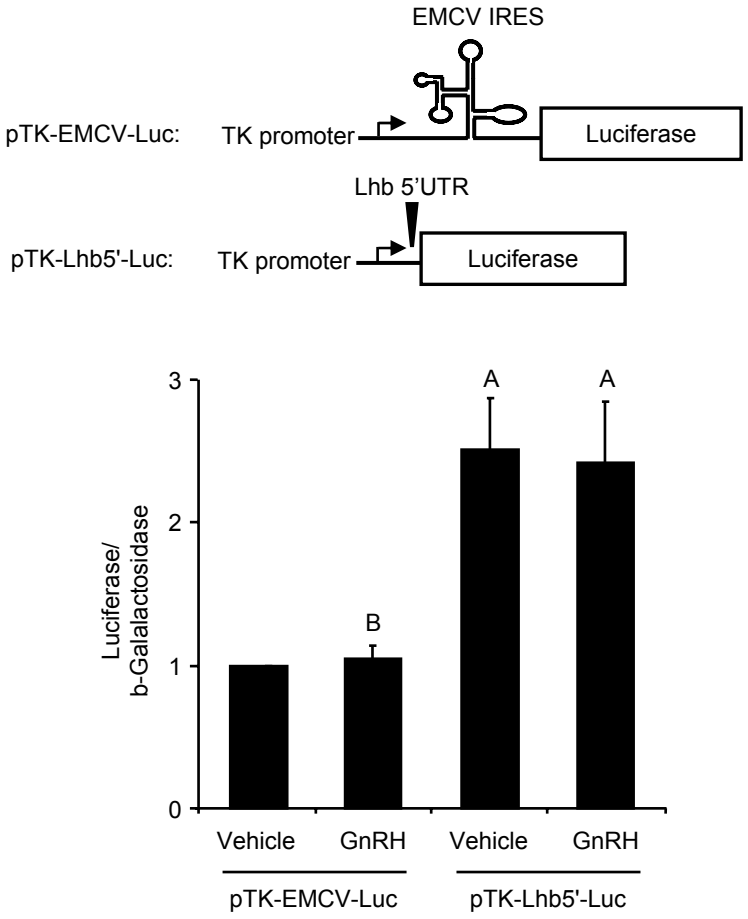

Figure 3-12. The 5'UTR of mouse Lhb is not sufficient to confer sensitivity to translational regulation by GnRH. Constructs containing the thymidine kinase (TK) promoter driving luciferase with either the EMCV IRES or the 5'UTR of mouse Lhb mRNA cloned upstream were transfected into LβT2 cells. The cells were co-transfected with the same b-galactosidase-encoding construct as an internal control for transfection efficiency. After transfection the cells were treated with vehicle or GnRH for 4 hours and then harvested and assayed for luciferase and b-galactosidase activity. The reported values are the means +/- SEM of four independent experiments. Groups not connected by the same letter are significantly different as determined by ANOVA and *post hoc* Tukey's HSD test.

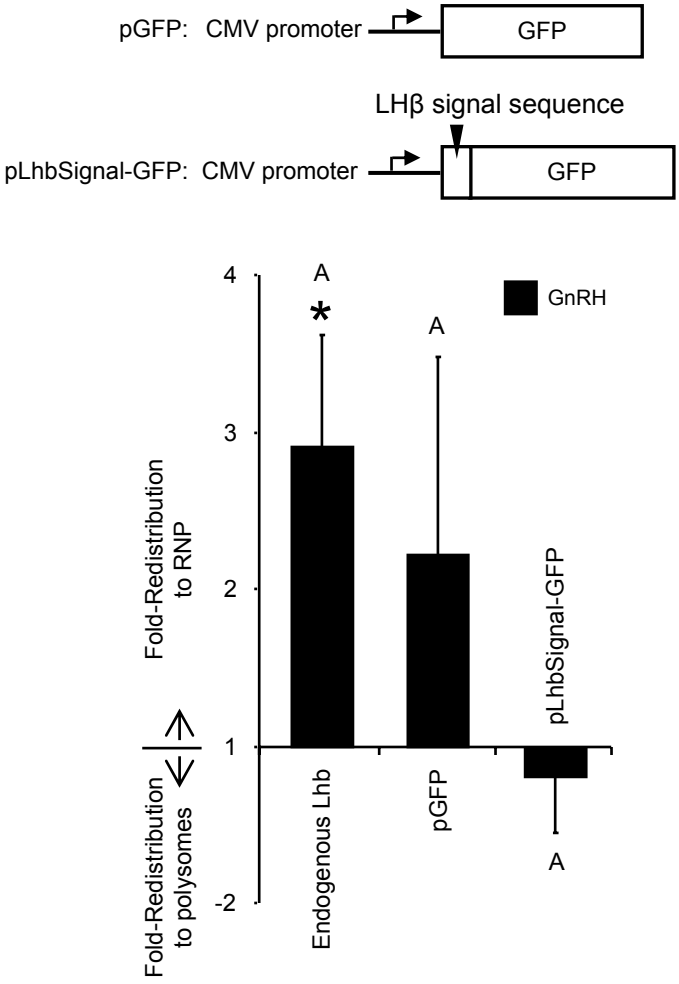

Figure 3-13. The signal peptide of LHβ is not sufficient to confer sensitivity of Lhb mRNA to translational regulation by GnRH. Constructs encoding the signal peptide of LHβ fused to GFP or GFP alone were transfected into LβT2 cells. After treatment with vehicle or 10 nM GnRH for 30 minutes, ribosomal complexes were fractionated. Messenger RNA was isolated from the RNP and polysome pools of the fractionated extracts and endogenous Lhb mRNA or transfected GFP was measured using quantitative PCR. A fold-redistribution value was calculated as a measurement of the change in transcript representation in the pools after treatment, as compared to control (vehicle) treatment. The data is represented in the histogram such that a positive value indicates movement into the RNP pool and a negative value indicates movement into the polysome pool. A fold-redistribution value of 1 represents no change after treatment. The reported values are the means +/- SEM of four independent experiments. Asterisks indicate statistical significance from a value of 1 and groups connected by the same letter are not significantly different as determined by ANOVA and *post hoc* Tukey's HSD test.

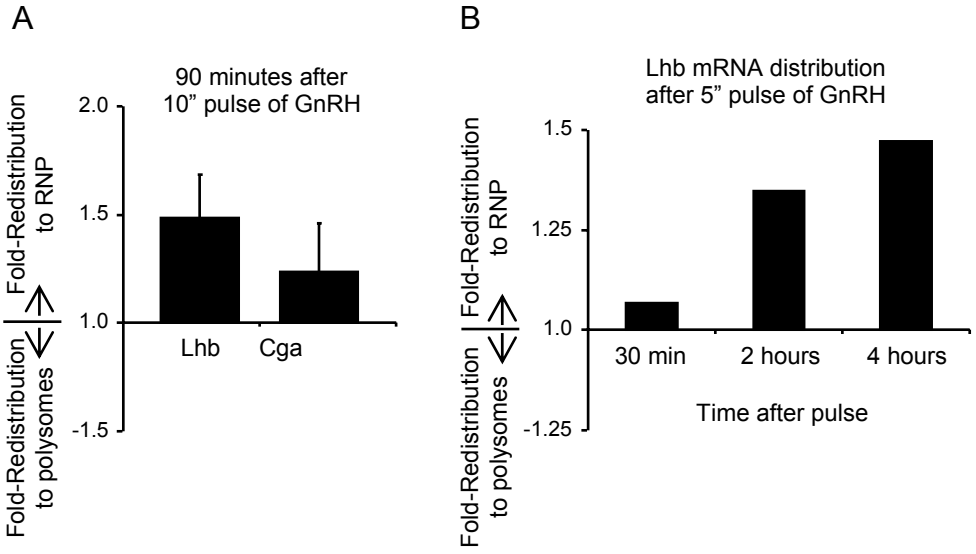

Figure 3-14. GnRH does not stimulate Lhb mRNA recruitment to polysomes. Cells were treated with a **(A)** 10 min pulse or **(B)** 5 min pulse of 10 nM GnRH (or vehicle), the media was removed, and the cells were replaced with fresh media without GnRH until harvest at the various times indicated. Ribosomal complexes were fractionated and mRNA isolated from the RNP and polysome pools was measured using quantitative PCR. A fold-redistribution value was calculated as a measurement of the change in transcript representation in the pools after GnRH treatment, as compared to control (vehicle) treatment. The data is represented in the histogram such that a positive value indicates movement into the RNP pool and a negative value indicates movement into the polysome pool. A fold-redistribution value of 1 represents no change after treatment. **(A)** The reported values are the means +/- SEM of six independent experiments. None of the groups are statistically different from a value of 1, as determined by a Student's t-test. **(B)** The reported values are from one experiment.

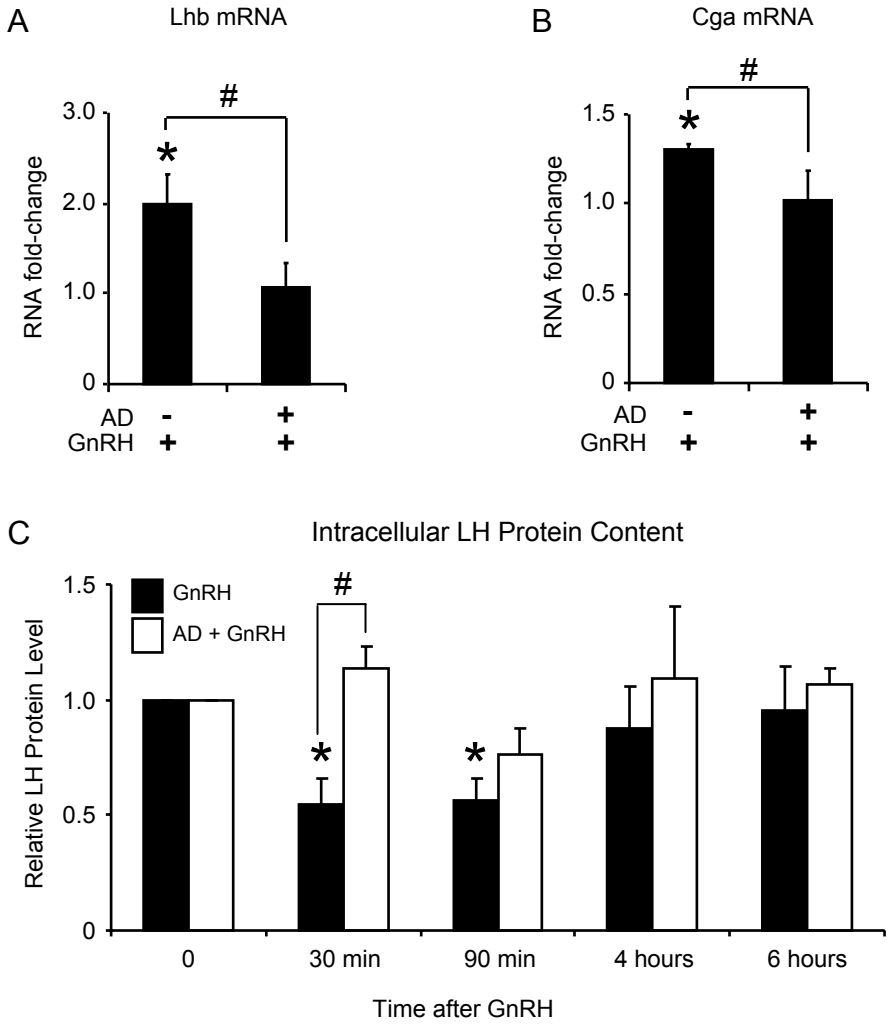

Figure 3-15. Contribution of Lhb and Cga mRNA transcription on intracellular LH protein levels. LβT2 cells were pre-treated with vehicle or actinomycin D (AD) to block transcription then treated with vehicle or GnRH. **(A and B)** Cells were treated with GnRH for 30 minutes and then total RNA was harvested, reverse transcribed, and quantitative PCR was used to measure the levels of the specific transcripts in the GnRH-treated cells compared to in the respective vehicle-treated cells. **(B)** Cells were exposed to a 10 minute pulse of GnRH, the media was replaced with fresh media, and then intracellular protein was harvested at the times indicated. Intracellular LH protein was measured by immunoradiometric assay as a proportion of the total protein present. All the reported values are the means +/- SEM of four or more independent experiments. Asterisks indicate statistical significance from a value of 1 and pound (#) indicates the treatment groups are significantly different from each other, as determined by a Student's t-test.

Table 3-1. Top 100 bioweight (BW) genes

Probe ID	R/P[a]	BW	Gene	Description
1452790_x_at	R	4.068	Ndufa3	NADH dehydrogenase (ubiquinone) 1 alpha subcomplex, 3
1422586_at	R	3.041	Ecel1	endothelin converting enzyme-like 1
1448685_at	R	2.975	2900010M23Rik	RIKEN cDNA 2900010M23 gene
1418300_a_at	R	2.861	Mknk2	MAP kinase-interacting serine/threonine kinase 2
1456109_a_at	R	2.860	Mrps15	mitochondrial ribosomal protein S15
1450795_at	R	2.837	Lhb	luteinizing hormone beta
1416134_at	R	2.792	Aplp1	amyloid beta (A4) precursor-like protein 1
1418255_s_at	R	2.695	Srf	serum response factor
1437164_x_at	R	2.657	Atp5o	ATP synthase, H+ transporting, mitochondrial F1 complex, O subunit
1428464_at	R	2.585	Ndufa3	NADH dehydrogenase (ubiquinone) 1 alpha subcomplex, 3
1436064_x_at	R	2.425	Rps24	ribosomal protein S24
1455950_x_at	R	2.404	Rpl35	RIKEN cDNA 1700123D08 gene
1422532_at	R	2.396	Xpc	xeroderma pigmentosum, complementation group C
1460711_at	R	2.388	9930116P15Rik	ES cells cDNA, RIKEN clone:C330022M23
1451307_at	R	2.355	1110006I11Rik	RIKEN cDNA 1110006I11 gene
1437621_x_at	R	2.308		RIKEN clone 2410167D16 similar to L21027 Mus musculus
1423948_at	R	2.242	Bag2	Bcl2-associated athanogene 2
1433603_at	R	2.210	BC059730	CDNA clone IMAGE:6772417, with apparent retained intron
1422614_s_at	R	2.192	Bloc1s1	GCN5 general control of amino acid synthesis-like 1 (yeast)
1416367_at	R	2.175	1110001J03Rik	RIKEN cDNA 1110001J03 gene
1417657_s_at	R	2.121	Zrf2	zuotin related factor 2
1455106_a_at	R	2.120	Ckb	creatine kinase, brain
1416584_at	R	2.109	Man2b2	mannosidase 2, alpha B2
1416494_at	R	2.091	Ndufs5	NADH dehydrogenase (ubiquinone) Fe-S protein 5
1418256_at	R	2.043	Srf	serum response factor
1427294_a_at	R	2.036	1810073N04Rik	RIKEN cDNA 1810073N04 gene
1417348_at	R	2.034	2310039H08Rik	male enhanced antigen 1
1418910_at	R	2.011	Bmp7	bone morphogenetic protein 7
1452367_at	R	2.008	Coro2a	tripartite motif-containing 14
1454674_at	R	1.994	Fez1	fasciculation and elongation protein zeta 1 (zygin I)
1428494_a_at	R	1.985	Polr2i	polymerase (RNA) II (DNA directed) polypeptide I
1428869_at	R	1.961	Nolc1	nucleolar and coiled-body phosphoprotein 1
1419292_at	R	1.938	9530081K03Rik	RIKEN cDNA 9530081K03 gene
1424871_s_at	R	1.930	1500031H01Rik	cDNA sequence BC013706
1416713_at	R	1.917	2700055K07Rik	RIKEN cDNA 2700055K07 gene
1434646_s_at	R	1.916	Sap18	Sin3-associated polypeptide 18
1423857_at	R	1.914	Mrpl30	mitochondrial ribosomal protein L30
1418448_at	R	1.914	Rras	Harvey rat sarcoma oncogene, subgroup R
1424018_at	R	1.910	Hint1	histidine triad nucleotide binding protein 1
1437450_x_at	R	1.877	2700060E02Rik	RIKEN cDNA 2700060E02 gene
1425248_a_at	R	1.875	Tyro3	TYRO3 protein tyrosine kinase 3
1424002_at	R	1.874	Pdcl3	phosducin-like 3
1450466_at	R	1.867		Adult male corpora quadrigemina cDNA, RIKEN clone:B230310J22
1448917_at	R	1.865	Thrap6	thyroid hormone receptor associated protein 6
1423676_at	R	1.861	Atp5h	ATP synthase, H+ transporting, mitochondrial F0 complex, subunit d
1416495_s_at	R	1.849	Ndufs5	NADH dehydrogenase (ubiquinone) Fe-S protein 5
1428076_s_at	R	1.843	Ndufb4	NADH dehydrogenase (ubiquinone) 1 beta subcomplex 4
1420368_at	R	1.830	Denr	Mus musculus RIKEN clone:2410004J11, density regulated protein
1418709_at	R	1.785	Cox7a1	cytochrome c oxidase, subunit VIIa 1
1418273_a_at	R	1.770	Rpl30	ribosomal protein L30

Table 3-1. Top 100 bioweight (BW) genes (continued)

1416859_at	R	1.766	Fkbp3	FK506 binding protein 3
1424172_at	R	1.763	Hagh	hydroxyacyl glutathione hydrolase
1437133_x_at	R	1.751	Akr1b3	2 days pregnant female oviduct cDNA, RIKEN E230024H01
1424391_at	R	1.750	Nrd1	nardilysin, N-arginine dibasic convertase, NRD convertase 1
1424830_at	R	1.739	Ccnk	cyclin K
1434396_a_at	R	1.739	Myl6	myosin light chain, alkali, nonmuscle
1435755_at	R	1.734	1110001A16Rik	RIKEN cDNA 1110001A16 gene
1448794_s_at	R	1.730	Zrf2	zuotin related factor 2
1460724_at	R	1.729	Ap2a1	adaptor protein complex AP-2, alpha 1 subunit
1416337_at	R	1.719	Uqcrb	ubiquinol-cytochrome c reductase binding protein
1422480_at	R	1.710	Snx3	sorting nexin 3
1460581_a_at	R	1.701	Rpl13	Similarity to protein NP_150254.1 (H.sapiens)
1423090_x_at	R	1.698	Sec61g	Similarity to protein P38384 (H.sapiens)
1421260_a_at	R	1.697	Srm	spermidine synthase
1434053_x_at	R	1.681	Atp5k	ATP synthase, H+ transporting mitochondrial F1F0 complex, subunit e
1425300_at	R	1.670	BC021917	cDNA sequence BC021917
1439389_s_at	R	1.659	Myadm	BB500055 RIKEN clone D630024J02 similar to AJ001616
1417394_at	R	1.658	Klf4	Kruppel-like factor 4 (gut)
1438563_s_at	R	1.650	Mrps24	AV069725 Mus musculus cDNA clone 2010312F15
1427074_at	P	2.834	5330414D10Rik	Clone L0848C02-3 NIA Mouse Newborn Brain cDNA Library
1448830_at	P	2.578	Dusp1	dual specificity phosphatase 1
1427985_at	P	2.541	9630042H07Rik	RIKEN cDNA 9630042H07 gene
1450008_a_at	P	2.365	Catnb	catenin beta
1437354_at	P	2.316		0 day neonate cerebellum cDNA, RIKEN cloneC230091D08
1415823_at	P	2.143	Scd2	stearoyl-Coenzyme A desaturase 2
1424766_at	P	2.044	BC004701	cDNA sequence BC004701
1429144_at	P	1.994	2310032D16Rik	RIKEN cDNA 2310032D16 gene
1419277_at	P	1.984	Usp31	ubiquitin specific protease 31
1419529_at	P	1.976	Il23a	interleukin 23, alpha subunit p19
1418025_at	P	1.969	Bhlhb2	basic helix-loop-helix domain containing, class B2
1415996_at	P	1.961	Txnip	thioredoxin interacting protein
1420922_at	P	1.945	Usp9x	Similar to ubiquitin specific protease 9 (LOC240170), mRNA
1434392_at	P	1.930	Usp34	U2af1-rs1 region 2
1429850_x_at	P	1.921	2010004B12Rik	RIKEN cDNA 2010004B12 gene
1415945_at	P	1.915	Mcm5	minichromosome maintenance deficient 5, cell division cycle 46
1424522_at	P	1.912	BC019693	cDNA sequence BC019693
1427413_a_at	P	1.901	Cugbp1	CUG triplet repeat, RNA binding protein 1; RIKEN clone:4432412L08
1426750_at	P	1.895	Flnb	filamin, beta
1417363_at	P	1.888	Zfp61	zinc finger protein 61
1438809_at	P	1.833	Atp5c1	ATP synthase, H+ transporting, mitochondrial F1 complex, γ polypeptide1
1424723_s_at	P	1.799	Cstf3	cleavage stimulation factor, 3' pre-RNA, subunit 3
1425514_at	P	1.783	Pik3r1	phosphatidylinositol 3-kinase, regulatory subunit, polypeptide 1 (p85 alpha)
1435934_at	P	1.752	9330101J02Rik	RIKEN cDNA 9330101J02 gene
1454686_at	P	1.703	6430706D22Rik	RIKEN cDNA 6430706D22 gene
1437175_at	P	1.696	BC027088	cDNA sequence BC027088
1417155_at	P	1.691	Nmyc1	neuroblastoma myc-related oncogene 1
1423828_at	P	1.688	Fasn	fatty acid synthase
1460429_at	P	1.685	Cdc5l	cell division cycle 5-like (S. pombe)
1427490_at	P	1.679	Abcb7	ATP-binding cassette, sub-family B (MDR/TAP), member 7
1420811_a_at	P	1.664	Catnb	catenin beta

[a] Movement into the RNP pool (R) or polysome pool (P)

CHAPTER 4

CONCLUSIONS

Mechanisms of gene regulation by GnRH

The regulation of translation allows for rapid, reversible and fine control of gene expression in response to changes in the cellular environment. This regulation may involve either changes that affect mRNAs at the global level, or those that affect a subset of mRNAs (104-106). Translation control is utilized to make diverse developmental decisions in many organisms, ranging from the translational repression of tra-2 mRNA to allow spermatogenesis to occur in males and hermaphrodites of *C. elegans*, to the translational activation of 15-lipoxygenase mRNA to promote the destruction of mitochondria, critical in the maturation of reticulocytes into erythrocytes in mammals (107). The regulation of translation is also not a foreign subject in reproductive endocrinology. In castrated rats receiving exogenous testosterone, androgen receptor mRNA accumulates in polysomes isolated from the prostate (108). In breast and prostate cancer cell models, androgen exposure decreases overall androgen receptor mRNA level but androgen receptor protein level increases (109). Testosterone has also been implicated in regulating the translation of Fgf-2 mRNA through its IRES during development of testes in mice (110). The data here firmly establishes the regulation of translation as a mode of gene regulation by GnRH, and establishes that the regulation is specific, in terms of the mRNAs that are regulated and the direction of their regulation. As shown by the bidirectional regulation of the targeted mRNAs, global responses in translation as measured by ribosome profiles, bicistronic reporters or the activation of phosphorylation factors do not reflect the behavior of specific mRNAs. The specificity of translational regulation by GnRH is defined, at least to one end, by signaling to the UPR. This work is the first to establish the involvement of this pathway in GnRH action. The specificity on the other end may be defined by activation of ERK and cap-binding initiation factors, although certainly this remains to be fully explored.

This body of work does not rule out the possibility that other post-transcriptional processes may be involved in gene regulation by GnRH. One is the process of translation elongation, which may provide some explanation of the accumulation of RNP complexes, if initiation is rate-limiting and cannot accommodate increased elongation rates. Translation elongation is often stimulated, as in the case with insulin, through regulation of eEF2 by way of mTOR and $p70^{S6K}$ (19). Although not directly addressed here, elongation does not appear to be a mode of GnRH action. As discussed earlier, mTOR may not be a significant GnRH target, and $p70^{S6K}$ phosphorylation status does change after GnRH exposure (Kathryn Nguyen, unpublished data). There is also the question of mRNA stability. GnRH increases the stability of Lhb (22) and Cga message (22, 23). In cultured rat primary pituitary cells, the half-life of Cga is 6 hours and Lhb is stable for a half-life of 44 hours (111). In αT3-1 cells, the half-life of Cga mRNA is 1.2 hours and increases to 8 hours with GnRH (23). While the discrepancy in mRNA half-life between the different culture methods is unclear, the short time-frame used in the study should reveal translational regulation that is independent of mRNA decay. Also, any observed GnRH-induced increases in mRNA levels in this study were sensitive to inhibition of transcriptional events (Figure 2-6C, 3-2B, 3-15A, 3-15B).

When this body of work began, a question existed concerning whether translation stimulation contributes to the increase in LH protein levels observed in gonadotropes in response to GnRH exposure (9, 27, 56, 112). Indirect evidence through the discrepancy of the timing and degree of increase of transcriptional events compared to that of observed protein changes implicated translation. In rats administered pulsatile GnRH every 30 minutes, Lhb mRNA level increases by 1.5 fold in 6 hours, and Cga levels remained unchanged. However, in this time the serum level of LH hormone rises by 100-fold. At one hour, no changes in Cga or Lhb mRNA levels are observed, but LH serum increases 10-15-fold (113). While secretion of previously synthesized hormone may explain the bulk of this serum increase, the role of translation was not directly addressed or excluded at the time. *In vitro*, utilizing the LβT2 cell model, this discrepancy was also observed. By one hour after GnRH stimulation, there is an increase in the number of

cells staining positive for intracellular LHβ protein (9). However, in this time, microarray analysis revealed that Lhb mRNA level did not change, either in response to GnRH (59), or an analogue (39). Additionally, with two hours of GnRH stimulation, there is no increase in the activity of a rat Lhb promoter reporter (95). *In vivo* data also indicate moderate transcriptional responses (113).

The small transcriptional responses coupled with the increase in LHβ protein in response to GnRH and the demonstration that GnRH activates cap-binding factors and a cap-dependent bicistronic translational reporter (26, 27) led to the hypothesis that GnRH may stimulate general translation and specific protein synthesis of the LH subunits. However, translational stimulation of Lhb and Cga mRNAs was never observed in these studies, even four hours after a GnRH pulse (Figure 3-14B). Furthermore, Lhb and Cga mRNA levels acutely increase in response to GnRH (Figure 3-15A, 3-15B). The slight transcriptional increases may be enough to compensate for the slight translational attenuation, resulting in the same net protein synthesis, and/or may also eventually be responsible for increasing LH protein levels. This is in agreement with other studies that have demonstrated acute transcriptional increases of Lhb mRNA (114) or primary transcript (113) within 30 min or one hour of GnRH exposure. Certainly, the longer-term transcriptional responses of Lhb have been defined, recently demonstrated by measuring mRNA (113) or by Lhb promoter activity (115) within several hours of GnRH treatment. Transcriptional responses of Lhb would also be in agreement with the acute stimulation of transcription factor Egr1 observed here (Figure 2-6C) and in microarrays (39, 40, 59), and in agreement with the established importance of Egr1 on Lhb subunit transcription, shown by loss of Egr1 in mice (116) and in other studies (1).

This body of work also sought to demonstrate the role of transcription through measuring total intracellular LH protein levels with IRMA, different in methodology from the studies mentioned above that addressed LH levels by determining the percentage of cells staining positive for LHβ. The IRMA data show that indeed LH is immediately lost to the media in response to GnRH, but the level of LH was never observed to increase over basal levels in the time frame examined (Figure 3-15C). Perhaps the difference in methodology or the single pulse administration of GnRH is responsible for the difference in results between this study and the

previously mentioned studies, which used tonic GnRH stimulation. Several recent studies have shown that Lhb mRNA levels are sensitive to the pulsatile pattern of GnRH (113, 115, 117). While the increase in protein can be observed as early as one hour in some studies, the changes are moderate and after 8 hours of chronic 100 nM stimulation the number of cells staining positive for LH only doubles (9). The chronic stimulation may mimic the effects of pulsatile administration. These moderate protein changes and the time frame in which they occur demonstrate two things. First is that an acute and transient attenuation in Lhb translation through the UPR is not in direct conflict with these observations, especially because the previously observed increase in protein levels coincides with the timing of the known longer-term increases in transcription. Secondly, it suggests that perhaps the question of whether LH protein levels is defined by a stimulation in Lhb transcription or Lhb translation is best answered only under administration of pulsatile GnRH, and as such an increase in gonadotropin subunit transcription has not been unequivocally ruled out as a contributing mechanism. Interestingly, the use of actinomycin D in the IRMA data to address this question suggests that transcriptional inhibition prevents or perhaps delays the acute loss of LH into the media by GnRH. This is perplexing, as secretion in response to GnRH should be independent of transcriptional events, only driven by release of pre-formed stores of LH (3). It is possible that the inability to release LH is an unexpected secondary effect of the drug. The role of transcriptional or translational stimulation of Lhb remains unresolved.

Specificity of translational regulation

This body of work establishes, using microarray and quantitative PCR of mRNAs in ribosomal complexes, that within the seemingly global regulation of translation through the general translation factor eIF2, GnRH in fact exerts specific mRNA regulation. Global and specific regulation need not be mutually exclusive. Besides the many studies now established in mammalian systems addressing the specificity of the UPR response, studies using models of stress in yeast have also addressed the extent of both global and specific regulation of translation in response to a single stimulus. For example, during amino acid deprivation, protein synthesis is

globally inhibited, but the translation efficiency of *GCN4* increases (105, 118). The transfer of yeast from glucose, a fermentable carbon source, to glycerol, a non-fermentable carbon source, results in a global reduction of translation. However, some transcripts sediment with heavier polysomes (96). Under conditions of nitrogen starvation induced by amino acid deprivation, butanol addition (97), or rapamycin treatment (81), specific mRNAs accumulate in polysomes or in RNP complexes, despite a general remodeling of RNA to RNP complexes observed through ribosomal profiling.

For GnRH, the stimulation of translation initiation factors can be reconciled with a UPR response to attenuate translation, and understanding how these two forces are reconciled may lead to understanding the bidirectional and specific regulation of translation by GnRH. First, while the activation or availability of initiation factors may serve to select the translation of transcripts, the UPR may play an important role in regulating the fidelity of their translation. With compromised ER integrity, translation of ER-bound mRNAs, in particular, would not be fruitful. Secondly, activation of protein synthesis through activation of cap-binding factors by GnRH may in fact contribute to ER stress. As discussed in Chapter 2, how the UPR is signaled to by GnRH is unclear, though the use of cycloheximide to ameliorate dysregulated mTOR-induced ER stress suggests that increased protein synthesis may be responsible (70). For GnRH, this may not be the case since cycloheximide does not prevent PERK activation by GnRH (Figure 5-5), and the data in Chapter 3 illustrate that inhibition of ERK signaling and presumably of activation cap-binding factors exacerbates, but does not ameliorate, the degree of attenuation of translation caused by GnRH (Figure 3-7). Nevertheless, the mTOR study illustrates that translation initiation and the UPR are linked, and thus suggests a third possibility with which to reconcile signaling to the UPR with activation of cap-binding factors, which is that the simultaneous activation by GnRH may be necessary to maintain homeostatic balance. The specific regulation of mRNAs in both directions by GnRH may be a demonstration of this fine balance. As shown with GnRH action in Chapter 3, the translation attenuation induced by GnRH does not result in attenuation of all mRNAs and ERK signaling contributes to at least some of the mRNA stimulation. The activation

of cap-binding initiation factors by GnRH within the context of the UPR appears to lend specificity to the translational response. In the current studies, ERK is implicated in mediating this counter-balance to the UPR, although it probably is not the complete other half of the equation.

At the individual mRNA level, specificity may be understood from the standpoint that many factors define the inherent translational efficiency of an mRNA and therefore its sensitivity to overall changes in the translational machinery. In particular, the efficiency may be affected by structure in its 5' and 3' UTRs, the presence of upstream open reading frames (uORF), IRES elements, and specific binding sites for regulatory complexes that may include both proteins and small RNAs (105, 106). These motifs may mediate translational stimulation as a result of ERK stimulation of cap-binding factors, or may mediate stimulation as a result of escape from eIF2α phosphorylation. Specific structural motifs, for example IRESs and uORFs, mediating escape from general translational attenuation is well-established. During poliovirus infection, when polysomes decrease in abundance and overall protein synthesis is inhibited, an estimated 3% of genes, including those with IRES sequences, become associated with polysomes (92). During mitosis-induced translational arrest, 3% of mRNAs are associated with the same or a greater number of ribosomes. Seven of these mRNAs demonstrated a functional IRES (119). Preferential translation of IRES-containing mRNAs has also been shown to occur during stress and apoptosis (80, 118) and mitosis (80, 120). Specifically during the UPR, the use of uORFs is an established mechanism of translational stimulation of Atf4 mRNA (30) and the related yeast gene Gcn4 (105). Whether IRESs, uORFs or other specific structural or sequence motifs mediate escape from translation attenuation during the UPR induced by GnRH is currently unknown. Establishing this will be difficult in part because of the lack of UTR information, although this is being gathered (121). Overall, however, coupling cis-regulatory elements of mRNAs with changes in activation status or availability of initiation factors or other trans-acting factors may provide a balance that determines which mRNAs are sensitive to translation attenuation or other changes in the general translational machinery. These contributing factors for GnRH regulation are summarized in Figure 4-1. Future studies may also take into account

another possible layer of specificity, which lies in the compartmentalization of protein synthesis (15). At first glance of the microarray data shown and discussed in Chapter 3, it may be tempting to draw the conclusion that GnRH exposure attenuates and thus protects the fidelity of translation occurring on the ER-membrane. However, not all the mRNAs attenuated are those that are translated on the ER and not all the mRNAs stimulated are those that encode proteins destined for the cytosol. The question of specificity may be complicated by the idea that the ER may play a more crucial role in mediating compartmentalization than previously realized, where instead of the SRP mediating docking of nascent peptides with a signal sequence to the ER translocon, the ER may be the initiating site for all proteins, regardless of whether they are destined for the membrane, secretory vesicles, or the cytosol (122). Additionally, studies have also shown that during stress-induced translational attenuation, as induced by Coxsackie B viral infection (123) or by DTT or thapsigargin-induced UPR (124) in mammalian cells, the ER is the preferred site of reduced but sustained protein synthesis.

Especially now, given the demonstrated specificity of translational regulation by GnRH, it is important to mention that caution must be taken in interpreting translational status using general initiation factors or bicistronic translational reporter data alone. It is clear that GnRH causes bidirectional regulation, and examination of the status of cap-binding factors or eIF2 alone would not reflect this. Additionally, while the outcome of phosphorylation of eIF2 is more straight-forward, the phosphorylation of cap-binding initiation factors is generally associated with increases in overall translation efficiency but phosphorylation does not always correlate with this increase (17) and the physiological consequence of phosphorylation is still unclear (125, 126). Assessment of whether eIF4E is complexed with eIF4G may be better way of determining the competency of the cap-binding machinery to initiate translation (127, 128). Studies using bicistronic reporters of cap-dependent translation are also not straight-forward, due to the potential that bicistronic vectors may be influenced by the ORF type and position, affecting the translation of the second, IRES-dependent cistron, and thereby affecting the interpretation of relative regulation (129). In addition, bicistronic reporters were designed for assessing cap-

binding complex activation but the status of eIF2, for instance, would not be reflected using such reporters, and thus activity of those reporters may not accurately represent the general status of translation. Finally, the previous studies on the impact of GnRH on cap-binding factors and bicistronic activity were performed after amino acid starvation to reduce translational background prior to treatment with GnRH, operating on the assumption that GnRH activates translation. The studies here also used amino acid starvation for some experiments, including the microarray data, and it appears that amino acid starvation does not affect the direction (Appendix, Figure 5-3A, 5-3B) of ribosome remodeling induced by GnRH. However, this is not ideal, since nutrient conditions would certainly be expected to alter the translational status of the cell and may affect the magnitude, in particular, of the GnRH response, as observed through ribosome profiling (Figure 5-3B) and the assessment of translational status of specific mRNAs (Figure 5-4). Additionally, amino acid starvation is known to attenuate translation through GCN2-mediated phosphorylation of eIF2 (21) and may affect other initiation factors as well (130), and was in these studies sometimes observed to cause accumulation of RNP complexes within the time frame used for GnRH treatments and certainly within two hours of starvation (Figure 5-3C). Given these cautions and the multitude of signaling arms and UTR or other mRNA motifs that contribute to translational specificity, full understanding of translational regulation should examine the status of mRNAs at the individual level and under consistent treatment paradigms, and will in this way remain a challenge.

Role of the UPR in gonadotropes

This work is the first to define specificity of translational regulation by GnRH and is also the first to describe activation of the UPR in gonadotropes. It remains unknown, however, what function the UPR serves in gonadotrope biology. On one hand, activation of the UPR could be considered an acute developmental response to adapt the capacity of the ER of gonadotropes. In culture, perhaps the LβT2 cells can be considered naïve to GnRH and activation of the UPR may be necessary for ER expansion, as is the case in plasma cells (31). Recently, generation of

β cell-specific Perk knockout mice has led to the hypothesis that Perk is critical for β cell proliferation and differentiation during a short window in fetal development, rather than for preventing overburdening of the ER and apoptosis postnatally (131). Perk and the UPR may be important for postnatal gonadotrope biology, however, since the primary pituitary cells used in this study were from sexually mature mice that have already experienced GnRH and yet still splice Xbp1 upon GnRH exposure (Figure 2-2C). On the other hand, then, the UPR may serve to regulate translational fidelity and in the long run, protect gonadotropes from apoptosis. Tunicamycin and thapsigargin impair cell growth in embryonic stem cells lacking PERK and this effect is ameliorated by cycloheximide, indicating that translational attenuation induced by PERK is protective, aimed to prevent the accumulation of misfolded proteins (132). *In vivo* models also demonstrate a protective effect, particularly evident in secretory cell types. Global knockout of Perk (36, 37) or of the ability to phosphorylate eIF2α (38) in mice leads to β cell loss and the development of diabetes. Other secretory cells such as hepatocytes and osteoblasts also show defects with the loss of Perk or other UPR components (33). Additionally, induction of the UPR protects cells from injury by future stress (133, 134). This would fit in well with the pulsatile action of GnRH. As measured in rats (135) and sheep (136), GnRH is released once every 30 minutes to 1 hour and pulses last for less than 10 minutes. Two 10-minute pulses of GnRH in the LβT2 cells appears to result in the same degree of PERK phosphorylation as one pulse (Figure 2-11), although activation of PERK may not in itself be an indicator of the protective effect of repeated signaling to the UPR, if that protection exists.

Paradoxically, the UPR can also signal to apoptotic pathways, such as through induction of CHOP, through calcium-mediated release of cytochrome C from the mitochondria, and through Ire1 activation of JNK, all which lead to activation of caspases, or through direct caspase activation by IRE1 (137). GnRH has been shown to activate JNK, and signaling to JNK has been shown to require intracellular calcium and be independent of PKC (138). Activation of JNK through IRE1 of the UPR is consistent with this finding. Mechanistically, the UPR in gonadotropes might exert protective effects in several ways. Central to mediating apoptosis is

the induction of Chop, which is thought to be upregulated by all three arms of the UPR (29). GnRH highly induces Atf3 (39-41), an inhibitor of Chop (139). Microarray studies using various concentrations and durations of GnRH treatment do not reveal Chop as a target of GnRH action, except in one study where Chop was induced when GnRH was administered chronically in conjunction with activin (40). It is possible that Atf3 prevents induction of Chop, thus conferring protection from apoptosis. In agreement with this, while non-physiological exposure of LβT2 cells to GnRH agonist for 96 hours increases apoptosis (73), one hour of tonic 10 nM GnRH stimulation does not result in apoptosis-induced laddering of DNA (Figure 5-6) and GnRH has been shown to be protective *in vivo* (140).

On the other hand, if indeed GnRH does induce CHOP, perhaps after longer, chronic stimulation or multiple pulses, the protective effect might be mediated through CHOP activation of GADD34 (growth arrest and DNA damage-inducible gene 34), a stress-inducible eIF2α phosphatase. GADD34 feeds back to turn off eIF2α phosphorylation to ensure recovery of protein synthesis and that the UPR is not activated excessively or for too long, potentially tipping the threshold of the cell to trigger apoptosis (31, 141). This balance is delicate, however, because overexpression of GADD34 hypersensitizes cells to ER stress (134). Pro-apoptotic mRNAs and proteins such as eIF2α phosphatases GADD34 and CReP (constitutive repressor of eIF2α phosphorylation) have been shown to be labile (142, 143), and this intrinsic stability compared to those proteins that are adaptive, such as chaperones, might explain how continued stress stimulation, leading to prolonged pro-apoptotic protein induction, would eventually induce apoptosis (143). Thus, the UPR in gonadotropes might serve to prevent or limit the degree of apoptosis, both from GnRH as well as from the apoptotic signals that are induced by the UPR itself, and this remains to be determined. Interestingly, outside of the UPR, or perhaps in conjunction with the UPR, ERK itself might play a role in protecting cells from apoptosis. ERK activation has been shown to increase in magnitude with repeated ER stress (133). In LβT2, multiple pulses of GnRH results in increased ERK activation (117).

Overall, the UPR signals to both apoptotic and anti-apoptotic pathways, and how this balance is tipped to determine cell fate is not yet well understood. Also of great interest, in particular regards to GnRH action, is how this balance would be affected by pulsatile GnRH signaling. GnRH pulsatility modulates gonadotropin gene transcription (113, 115) as well as signal transduction (117). The 30 minute treatment and concentration of GnRH used in this study were chosen to correspond with maximal activation of translation initiation factors eIF4E, eIF4G, and 4EBP1 (27). *In vivo* studies in female rats show that duration of a single pulse of GnRH in normal physiological conditions lasts about 10-15 minutes (135). This duration however appears to be variable and may last as long as 20 minutes (144). In sheep, the concentration of pituitary exposure to GnRH was estimated to be approximately 0.1 nM (136, 145). It is very possible that the degree of translational regulation would vary in response to different pulse amplitudes, as suggested in comparing GnRH pulses of 1 nM and 100 nM (Figure 2-10A, 2-10B), as well as different pulse durations. The LβT2 cell line may not be the appropriate model with which to study the effects of pulsatility on the UPR, since the cells do not mobilize calcium or secrete in a pulsatile manner in response to GnRH (146, 147), which may be integral to signaling to the UPR. That aside, how the continued, episodic exposure of gonadotropes to GnRH would affect the specificity, magnitude and timing of UPR activation and translational control is intriguing.

Concluding remarks

The data here show that GnRH exerts specific, acute translational regulation, targeting gonadotropins and other mRNAs relevant to the function of the differentiated gonadotrope. This work is the first to examine at the global level the specificity of translational regulation as it pertains to the physiologically relevant and important process of controlling reproductive function. The translational regulation specificity is defined, at least at one end, by translational regulation through the UPR. As a neuropeptide hormone, GnRH in part utilizes a regulatory mechanism previously associated with starvation or stress to modulate gene expression. The UPR has been established to be in important for insulin secretion and immune cell development and now this

work further expands the role of the UPR to include regulation of reproductive endocrinology. It also supports the idea that the UPR plays a general physiological role in sensing calcium and thereby maintaining the integrity of the ER and the quality of proteins leaving it. This work leads to a more complete understanding of the integration of multiple levels of gene regulation by GnRH and adds to the physiological relevance of the UPR in maintaining cellular homeostasis.

ACKNOWLEDGEMENTS

Chapter 4, in part, has been submitted for publication of the material as it may appear in Molecular Endocrinology, 2008, Minh-Ha T. Do, Sharon J. Santos and Mark A. Lawson. The dissertation author was the primary investigator and author of this paper.

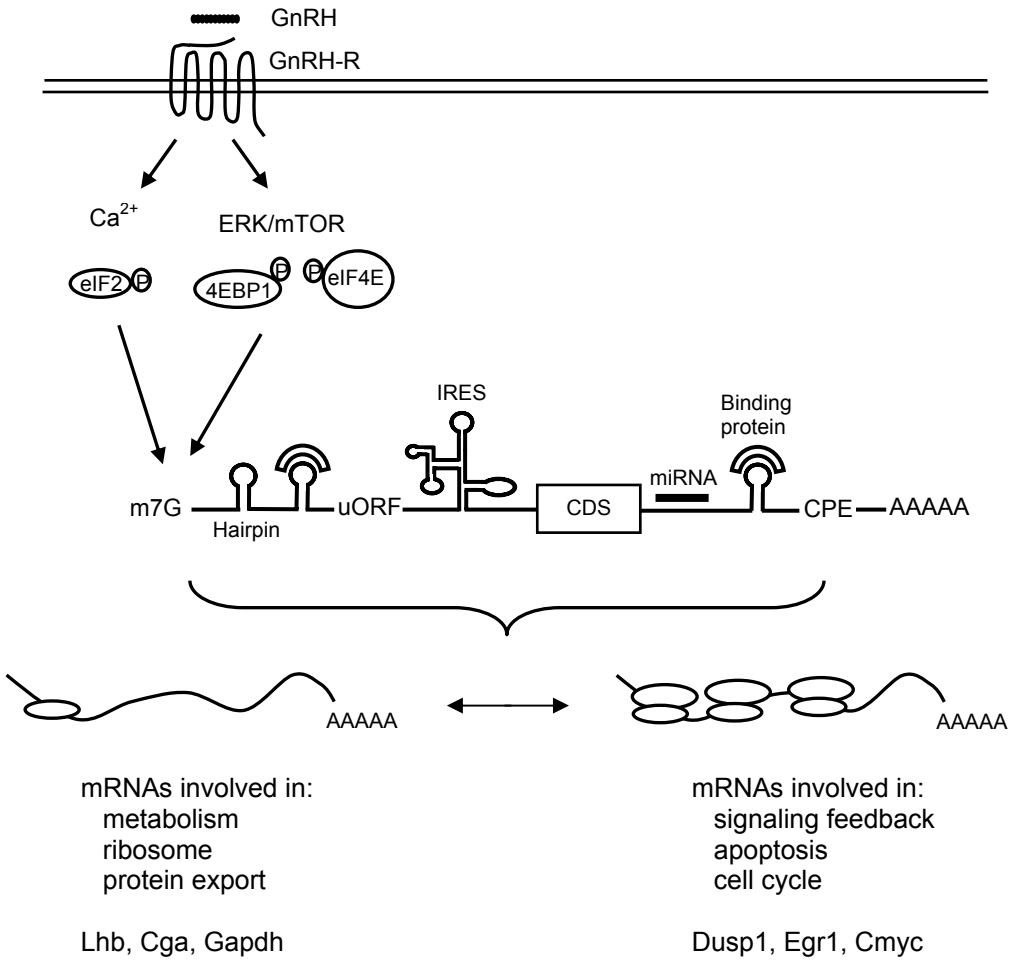

Figure 4-1. Summary of specificity of acute translational regulation by GnRH. CDS = coding sequence. GnRH acts on its receptor to induce calcium flux from the ER, leading to phosphorylation of eIF2α, and activates ERK (and possibly mTOR), leading to activation of cap-binding initiation factors. Whether an mRNA is translationally stimulated, attenuated, or unaffected within the context of these initiation factors may depend on secondary structures, structures or sequences that bind trans-regulatory factors, presence of upstream open reading frames (uORFs), the availability or activity of trans-regulatory factors, and the stability of the mRNA, as defined by the poly(A) tail and any cytoplasmic polyadenylation element (CPE). All of these may act together to confer specificity to the translational response exerted by GnRH.

CHAPTER 5

APPENDIX

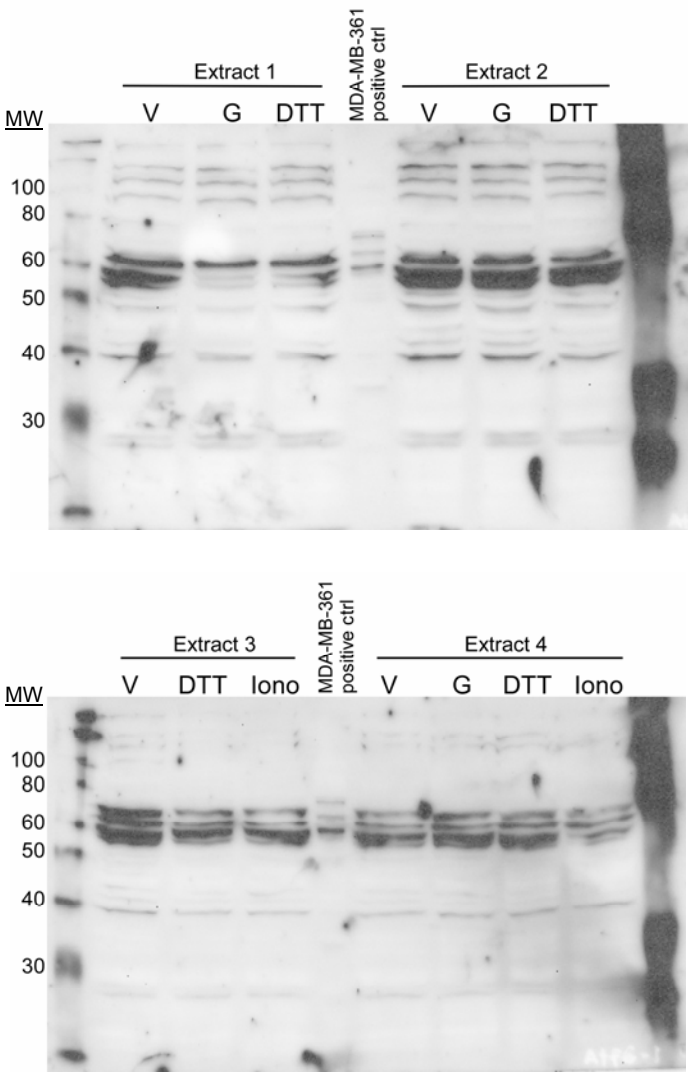

Figure 5-1. ATF6 Western blotting attempts. Total protein was harvested from LβT2 cells treated with vehicle, 10 nM GnRH, 2 mM DTT or 1 uM ionomycin (iono) for 30 minutes and subjected to Western blotting. The membranes were blocked in 2X casein for 1 hour prior to incubation overnight with a 1:1000 dilution of antibody directed against total ATF6 (Abcam, Cambridge, MA) in 1X casein. The blots were developed using 1:2000 dilution of biotinylated secondary antibody (Santa Cruz Biotechnology, Santa Cruz, CA) and Chemiglow chemiluminescence (Alpha Innotech, San Leandro, CA). Full-length ATF6 is approximately 85 kDa and is proteolytically activated to a 50 kDa form. MDA-MB-361 whole cell lysate from a human breast adenocarcinoma cell line (Abcam, Cambridge, MA) served as a positive control. Four independent experiments were performed, as shown.

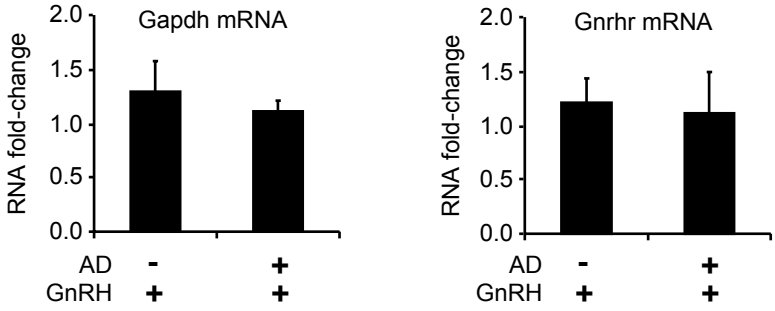

Figure 5-2. Gnrhr and Gapdh mRNA levels do not change in response to GnRH treatment. LβT2 cells were treated with ethanol (vehicle) or actinomycin D (AD) to block transcription and then treated with GnRH or PBS (vehicle) for 30 minutes. Total RNA was isolated and mRNA levels were measured by quantitative PCR, comparing levels in the GnRH-treated cells to those in the respective vehicle-treated cells. All the reported values are the means +/- SEM of five independent experiments. None of the groups were determined to be statistically significant from a value of 1 or different from each other, as determined by a Student's t-test.

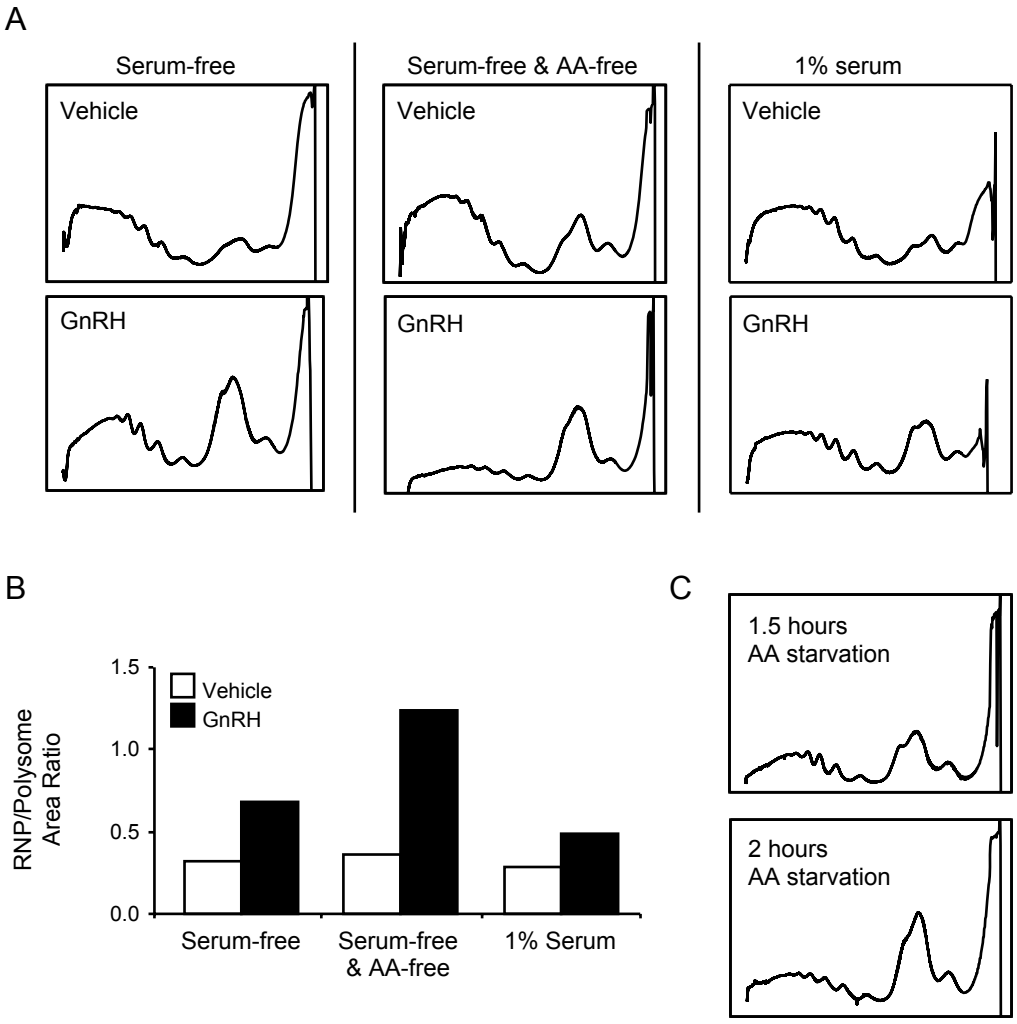

Figure 5-3. Effect of various starvation conditions on ribosomal remodeling. (A and B) LβT2 cells were starved and treated in serum-free media, or starved in serum-free media and treated after 1 hour of amino acid (AA) starvation, or starved and treated in 1% serum. Cells were treated with vehicle or 10 nM GnRH for 30 minutes. **(A)** Profiles from fractionation of ribosomal complexes while monitoring UV absorption. **(B)** The ratio (RNP/polysome) of the integrated area under the curve from the profiles, as an indication of the level of redistribution of ribosomes. The reported values are from one experiment. **(C)** Cells were starved in serum-free media overnight and then starved of amino acids the next day for various times, as shown, and ribosomal complexes were fractionated while monitoring UV absorption.

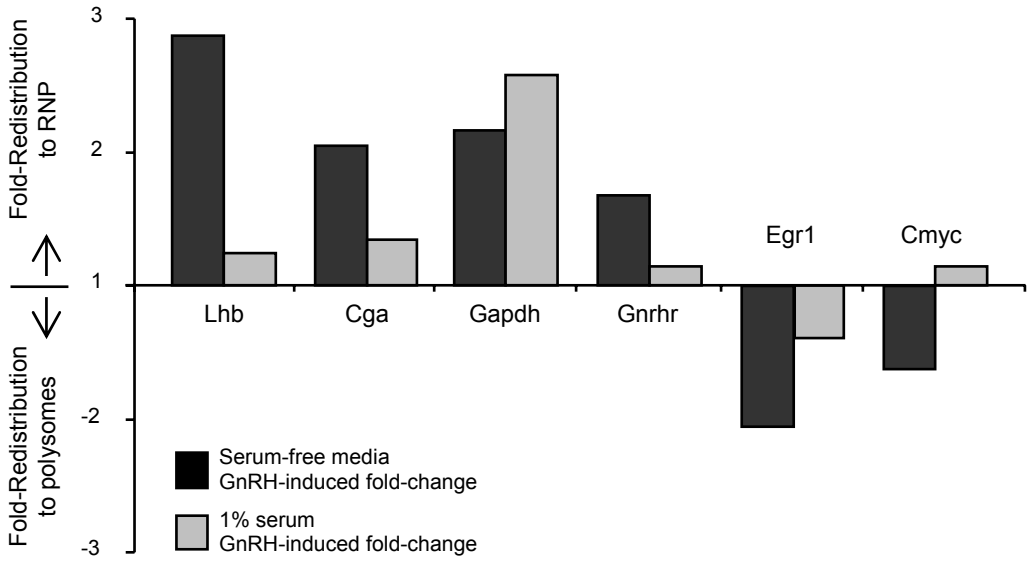

Figure 5-4. Effect of various starvation conditions on GnRH-induced ribosomal redistribution of specific mRNAs. LβT2 cells were starved and treated in serum-free media or starved and treated in 1% serum. Cells were treated with vehicle or 10 nM GnRH for 30 minutes and then ribosomal complexes were fractionated. Quantitative PCR was used to measure mRNA isolated from the fractionated RNP and polysome pools. A fold-redistribution value was calculated as a measurement of the change in transcript representation in the pools after GnRH treatment, as compared to control (vehicle) treatment. The data is represented in the histogram such that a positive value indicates movement into the RNP pool and a negative value indicates movement into the polysome pool. A fold-redistribution value of 1 represents no change after treatment. The reported values are from one experiment.

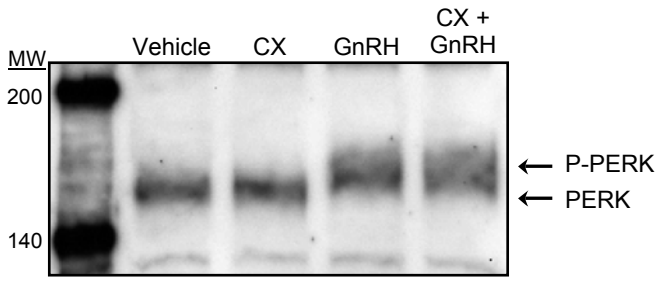

Figure 5-5. An acute increase in protein synthesis is not responsible for activation of ER stress by GnRH. Cells were treated with vehicle or cycloheximide (CX) for 5 minutes to inhibit translation and then treated with vehicle or GnRH for 30 minutes. Total protein was isolated and subjected to Western blotting using antibody directed against PERK protein (details for the blotting are available in the Materials and Methods section of Chapter 2). The phosphorylation status of PERK (P-PERK) is indicated by electrophoretic mobility. The primary trigger for PERK activation by GnRH does not appear to be an acute increase in new protein synthesis that may lead to misfolded proteins. However, this does not rule out the possibility that proteins that are already translated and in the ER compartment contribute to activation of PERK, by way of misfolding when the calcium balance in the ER is disrupted by GnRH induction of calcium mobilization (see model in Figure 2-12). Shown is a representative blot from two independent experiments.

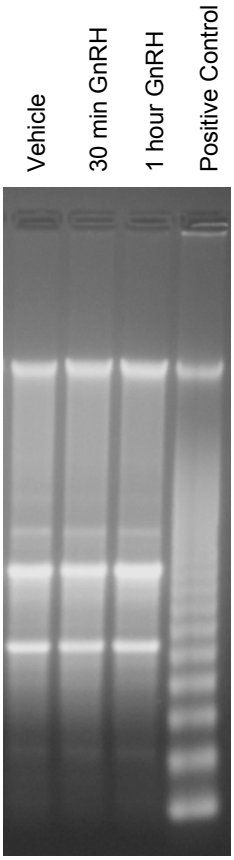

Figure 5-6. One hour of tonic 10 nM GnRH treatment does not cause apoptosis-induced DNA fragmentation. $2x10^6$ LβT2 cells were plated in 6-well plates. Twenty-four hours later, the media was changed to media without serum and the cells were starved overnight. On the third day, the cells were treated with vehicle or GnRH for the times indicated. For DNA harvest, the cells were scraped into 200 ul of 1X PBS and then DNA was isolated using the Apoptotic DNA Ladder Kit (Roche, Basel, Switzerland). 5 ug of DNA and 15 ul of the provided positive control were subjected to 1% agarose gel electrophoresis in the presence of ethidium bromide. The laddering observed in the positive control indicates DNA that has undergone fragmentation due to induction of apoptosis.

Table 5-1. Top 800[a] bioweight (BW) genes

Probe ID	R/P[b]	BW	Gene	Description	Accession
1452790_x_at	R	4.068	Ndufa3	NADH dehydrogenase (ubiquinone) 1 alpha subcomplex 3	AV048277
1422586_at	R	3.041	Ecel1	endothelin converting enzyme-like 1	NM_021306
1448685_at	R	2.975	2900010M23Rik	RIKEN cDNA 2900010M23 gene	NM_026063
1418300_a_at	R	2.861	Mknk2	MAP kinase-interacting serine/threonine kinase 2	NM_021462
1456109_a_at	R	2.860	Mrps15	mitochondrial ribosomal protein S15	BB314055
1450795_at	R	2.837	Lhb	luteinizing hormone beta	NM_008497
1416134_at	R	2.792	Aplp1	amyloid beta (A4) precursor-like protein 1	NM_007467
1418255_s_at	R	2.695	Srf	serum response factor	BI662291
1437164_x_at	R	2.657	Atp5o	ATP synthase, H+ transporting, mitochondrial F1 complex, O subunit	AV066932
1428464_at	R	2.585	Ndufa3	NADH dehydrogenase (ubiquinone) 1 alpha subcomplex, 3	AV048277
1436064_x_at	R	2.425	Rps24	ribosomal protein S24	AV004977
1455950_x_at	R	2.404	Rpl35	RIKEN cDNA 1700123D08 gene	AV172221
1422532_at	R	2.396	Xpc	xeroderma pigmentosum, complementation group C	NM_009531
1460711_at	R	2.388	9930116P15Rik	ES cells cDNA, RIKEN clone:C330022M23	BG071611
1451307_at	R	2.355	1110006I11Rik	RIKEN cDNA 1110006I11 gene	BC027021
1437621_x_at	R	2.308		AV216768 RIKEN clone 2410167D16 3' similar to L21027	AV216768
1423948_at	R	2.242	Bag2	Bcl2-associated athanogene 2	BC016230
1433603_at	R	2.210	BC059730	CDNA clone IMAGE:6772417, with apparent retained intron	C88200
1422614_s_at	R	2.192	Bloc1s1	GCN5 general control of amino acid synthesis-like 1 (yeast)	NM_015740
1416367_at	R	2.175	1110001J03Rik	RIKEN cDNA 1110001J03 gene	NM_025363
1417657_s_at	R	2.121	Zrf2	zuotin related factor 2	BG067003
1455106_a_at	R	2.120	Ckb	creatine kinase, brain	BG967663
1416584_at	R	2.109	Man2b2	mannosidase 2, alpha B2	NM_008550
1416494_at	R	2.091	Ndufs5	NADH dehydrogenase (ubiquinone) Fe-S protein 5	NM_134104
1418256_at	R	2.043	Srf	serum response factor	BI662291
1427294_a_at	R	2.036	1810073N04Rik	RIKEN cDNA 1810073N04 gene	BB406585
1417348_at	R	2.034	2310039H08Rik	male enhanced antigen 1	NM_025966
1418910_at	R	2.011	Bmp7	bone morphogenetic protein 7	NM_007557
1452367_at	R	2.008	Coro2a	tripartite motif-containing 14	AI316747
1454674_at	R	1.994	Fez1	fasciculation and elongation protein zeta 1 (zygin I)	AU067669
1428494_a_at	R	1.985	Polr2i	polymerase (RNA) II (DNA directed) polypeptide I	BB284638
1428869_at	R	1.961	Nolc1	nucleolar and coiled-body phosphoprotein 1	BM213850
1419292_at	R	1.938	9530081K03Rik	RIKEN cDNA 9530081K03 gene	NM_030127
1424871_s_at	R	1.930	1500031H01Rik	cDNA sequence BC013706	BC013706
1416713_at	R	1.917	2700055K07Rik	RIKEN cDNA 2700055K07 gene	NM_026481
1434646_s_at	R	1.916	Sap18	Sin3-associated polypeptide 18	AV023865
1423857_at	R	1.914	Mrpl30	mitochondrial ribosomal protein L30	BC004614
1418448_at	R	1.914	Rras	Harvey rat sarcoma oncogene, subgroup R	NM_009101
1424018_at	R	1.910	Hint1	histidine triad nucleotide binding protein 1	U60001
1437450_x_at	R	1.877	2700060E02Rik	RIKEN cDNA 2700060E02 gene	AV167877
1425248_a_at	R	1.875	Tyro3	TYRO3 protein tyrosine kinase 3	AB000828
1424002_at	R	1.874	Pdcl3	phosducin-like 3	BC005601
1450466_at	R	1.867		Adult male corpora quadrigemina cDNA, RIKEN full-length enriched library, clone:B230310J22 product:unclassifiable, full insert	BI739719

Table 5-1. Top 800[a] bioweight (BW) genes (continued)

1448917_at	R	1.865	Thrap6	thyroid hormone receptor associated protein 6	NM_027212
1423676_at	R	1.861	Atp5h	ATP synthase, H+ transporting, mitochondrial F0 complex, subunit d	AF354051
1416495_s_at	R	1.849	Ndufs5	NADH dehydrogenase (ubiquinone) Fe-S protein 5	NM_134104
1428076_s_at	R	1.843	Ndufb4	NADH dehydrogenase (ubiquinone) 1 beta subcomplex 4	BG968046
1420368_at	R	1.830	Denr	Mus musculus ES cells cDNA, RIKEN full-length enriched library, clone:2410004J11:Density-Regulated Protein, full insert sequence.	AK010394
1418709_at	R	1.785	Cox7a1	cytochrome c oxidase, subunit VIIa 1	AF037370
1418273_a_at	R	1.770	Rpl30	ribosomal protein L30	NM_009083
1416859_at	R	1.766	Fkbp3	FK506 binding protein 3	NM_013902
1424172_at	R	1.763	Hagh	hydroxyacyl glutathione hydrolase	BC004749
1437133_x_at	R	1.751	Akr1b3	2 days pregnant female oviduct cDNA, RIKEN full-length enriched library, clone:E230024H01:unknown EST, full insert sequence	AV127085
1424391_at	R	1.750	Nrd1	nardilysin, N-arginine dibasic convertase, NRD convertase 1	BC026832
1424830_at	R	1.739	Ccnk	cyclin K	BC027297
1434396_a_at	R	1.739	Myl6	myosin light chain, alkali, nonmuscle	AU017189
1435755_at	R	1.734	1110001A16Rik	RIKEN cDNA 1110001A16 gene	BB609468
1448794_s_at	R	1.730	Zrf2	zuotin related factor 2	BG067003
1460724_at	R	1.729	Ap2a1	adaptor protein complex AP-2, alpha 1 subunit	NM_007458
1416337_at	R	1.719	Uqcrb	ubiquinol-cytochrome c reductase binding protein	NM_026219
1422480_at	R	1.710	Snx3	sorting nexin 3	NM_017472
1460581_a_at	R	1.701	Rpl13	Transcribed sequence with strong similarity to protein ref:NP_150254.1 (H.sapiens) ribosomal protein L13; 60S ribosomal protein L13; breast basic conserved protein 1 [Homo sapiens]	AI506565
1423090_x_at	R	1.698	Sec61g	Transcribed sequence with strong similarity to protein sp:P38384 (H.sapiens) S61G_HUMAN Protein transport protein SEC61 gamma subunit	AV216331
1421260_a_at	R	1.697	Srm	spermidine synthase	NM_009272
1434053_x_at	R	1.681	Atp5k	ATP synthase, H+ transporting mitochondrial F1F0 complex, subunit e	AV216686
1425300_at	R	1.670	BC021917	cDNA sequence BC021917	BC021917
1439389_s_at	R	1.659	Myadm	BB500055 RIKEN full-length enriched, 0 day neonate kidney Mus musculus cDNA clone D630024J02 3' similar to AJ001616 Mus musculus mRNA for myeloid associated differentiation protein, mRNA sequence.	BB500055
1417394_at	R	1.658	Klf4	Kruppel-like factor 4 (gut)	BG069413
1438563_s_at	R	1.650	Mrps24	AV069725 Mus musculus small intestine C57BL/6J adult Mus musculus cDNA clone 2010312F15, mRNA sequence.	AV069725
1449029_at	R	1.648	Mknk2	MAP kinase-interacting serine/threonine kinase 2	NM_021462
1416098_at	R	1.648	Syngr3	synaptogyrin 3	NM_011522
1448440_x_at	R	1.631	D17Wsu104e	interleukin 25	NM_080837
1427943_at	R	1.629	Acyp2	acylphosphatase 2, muscle type	BI730288
1448319_at	R	1.628	Akr1b3	aldo-keto reductase family 1, member B3 (aldose reductase)	NM_009658
1422608_at	R	1.625	Arpp19	cAMP-regulated phosphoprotein 19	BE648432
1452184_at	R	1.620	Ndufb9	NADH dehydrogenase (ubiquinone) 1 beta subcomplex, 9	W29413

Table 5-1. Top 800[a] bioweight (BW) genes (continued)

1456691_s_at	R	1.614	Srd5a2l	BB825787 RIKEN full-length enriched, mammary gland RCB-0526 Jyg-MC(A) cDNA Mus musculus cDNA clone G830039K08 3', mRNA	BB825787
1418226_at	R	1.607	Orc2l	origin recognition complex, subunit 2-like (S. cerevisiae)	BB830976
1434442_at	R	1.607	D5Ertd593e	DNA segment, Chr 5, ERATO Doi 593, expressed	BB667844
1423610_at	R	1.605	Metap2	Adult retina cDNA, RIKEN full-length enriched library, clone:A930035J23 product:unknown EST, full insert sequence	BG086961
1416673_at	R	1.600	Bace2	beta-site APP-cleaving enzyme 2	NM_019517
1416765_s_at	R	1.598	Magmas	mitochondria-associated protein involved in granulocyte-macrophage colony-stimulating factor signal transduction	NM_025571
1417432_a_at	R	1.596	Gnb1	guanine nucleotide binding protein, beta 1	NM_008142
1418942_at	R	1.591	Ccdc2	coiled-coil domain containing 2	NM_026319
1435041_at	R	1.582	Myl6	myosin light chain, alkali, nonmuscle	BI108818
1426659_a_at	R	1.571	BC029892	Similar to 60S ribosomal protein L23a (LOC268449), mRNA	BF178310
1452357_at	R	1.569	Sept5	septin 5	AF033350
1456471_x_at	R	1.569	Phgdh	Transcribed sequence with strong similarity to protein sp:Q61753 (M.musculus) SERA_MOUSE D-3-phosphoglycerate dehydrogenase	BB204486
1448483_a_at	R	1.569	Ndufb2	NADH dehydrogenase (ubiquinone) 1 beta subcomplex, 2	NM_026612
1453362_x_at	R	1.567	Rps24	ribosomal protein S24	AK008386
1448050_s_at	R	1.566	Map4k4	mitogen-activated protein kinase kinase kinase kinase 4	BF450398
1422507_at	R	1.552	Cstb	cystatin B	NM_007793
1427939_s_at	R	1.551	Mycbp	c-myc binding protein	BB046347
1436510_a_at	R	1.547	Lrrfip2	leucine rich repeat (in FLII) interacting protein 2	BE456782
1427913_at	R	1.546	Rwdd1	RWD domain containing 1	AK003262
1417389_at	R	1.545	Gpc1	glypican 1	NM_016696
1448353_x_at	R	1.534	Rpn1	ribophorin I	NM_133933
1426657_s_at	R	1.522	Phgdh	3-phosphoglycerate dehydrogenase	L21027
1426964_at	R	1.521	3110003A17Rik	RIKEN cDNA 3110003A17 gene	AK013984
1415761_at	R	1.521	Mrpl52	mitochondrial ribosomal protein L52	AV021593
1435857_s_at	R	1.520	Aplp1	amyloid beta (A4) precursor-like protein 1	AI848048
1416850_s_at	R	1.519	D10Ertd214e	DNA segment, Chr 10, ERATO Doi 214, expressed	NM_134007
1448439_at	R	1.515	D17Wsu104e	interleukin 25	NM_080837
1438001_x_at	R	1.510	Dp1	deleted in polyposis 1	AV054377
1422794_at	R	1.503	Cul3	cullin 3	AV273804
1428340_s_at	R	1.503	1110012E06Rik	RIKEN cDNA 1110012E06 gene	BM944122
1449482_at	R	1.498	Hist3h2ba	histone 3, H2ba	NM_030082
1448784_at	R	1.496	Taf10	TAF10 RNA polymerase II, TATA box binding protein (TBP)-associated factor	NM_020024
1452584_at	R	1.495	1500032L24Rik	RIKEN cDNA 1500032L24 gene	BG915677
1418327_at	R	1.495	1110058L19Rik	RIKEN cDNA 1110058L19 gene	NM_026503
1424110_a_at	R	1.486	Nme1	expressed in non-metastatic cells 1, protein	BC005629
1423972_at	R	1.482	Etfa	electron transferring flavoprotein, alpha polypeptide	BC003432
1436840_x_at	R	1.471	Rpl35	Transcribed sequence with strong similarity to protein sp:P42766 (H.sapiens) RL35_HUMAN 60S ribosomal protein L35	AV124739
1416834_x_at	R	1.469	Ndufb2	NADH dehydrogenase (ubiquinone) 1 beta subcomplex, 2	NM_026612
1428679_s_at	R	1.461	0610010K14Rik	RIKEN cDNA 0610010K14 gene	AK003842

Table 5-1. Top 800[a] bioweight (BW) genes (continued)

1448623_at	R	1.456	2310075C12Rik	RIKEN cDNA 2310075C12 gene	NM_133739
1423804_a_at	R	1.455	Idi1	isopentenyl-diphosphate delta isomerase	BC004801
1431771_a_at	R	1.446	Irak1bp1	interleukin-1 receptor-associated kinase 1 binding protein 1	AK014712
1424121_at	R	1.444	Commd1	COMM domain containing 1	AB076722
1437013_x_at	R	1.433	Atp6v0b	AV339131 RIKEN full-length enriched, adult male olfactory bulb Mus musculus cDNA clone 6430502C13 3', mRNA sequence.	AV339131
1437908_a_at	R	1.432	1200007D18Rik	RIKEN cDNA 1200007D18 gene	BB095626
1423916_s_at	R	1.429	Mlf2	myeloid leukemia factor 2	BC003975
1422718_at	R	1.427	Ap3s2	adaptor-related protein complex 3, sigma 2 subunit	NM_009682
1417501_at	R	1.425	Fbxo6b	F-box only protein 6b	NM_015797
1451259_at	R	1.424	Smfn	small fragment nuclease	BC003445
1428360_x_at	R	1.419	Ndufa7	NADH dehydrogenase (ubiquinone) 1 alpha subcomplex, 7 (B14.5a)	BI558499
1448595_a_at	R	1.416	Rex3	reduced expression 3	NM_009052
1422432_at	R	1.412	Dbi	diazepam binding inhibitor	NM_007830
1448331_at	R	1.411	Ndufb7	calmegin	NM_025843
1428122_s_at	R	1.410	2610528K11Rik	RIKEN cDNA 2610528K11 gene	AK012178
1424396_a_at	R	1.407	Asrgl1	asparaginase like 1	AU040643
1427938_at	R	1.407	Mycbp	c-myc binding protein	BB046347
1419398_a_at	R	1.406	Dp1	deleted in polyposis 1	NM_007874
1460670_at	R	1.399	Riok3	RIO kinase 3 (yeast)	NM_024182
1418577_at	R	1.396	Trim8	tripartite motif protein 8	BG063064
1449080_at	R	1.394	Hdac2	histone deacetylase 2	NM_008229
1428075_at	R	1.386	Ndufb4	NADH dehydrogenase (ubiquinone) 1 beta subcomplex 4	BG968046
1451045_at	R	1.379	Syt13	synaptotagmin 13	BE648447
1417652_a_at	R	1.376	Tbca	tubulin cofactor a	NM_009321
1460701_a_at	R	1.371	Mrpl52	mitochondrial ribosomal protein L52	AV021593
1434872_x_at	R	1.369	Rpl37	AV170241 Mus musculus head C57BL/6J 13-day embryo Mus musculus cDNA clone 3110094P05, mRNA sequence.	AV170241
1423686_a_at	R	1.364	1110020C13Rik	RIKEN cDNA 1110020C13 gene	BC016234
1456244_x_at	R	1.359	Txnl2	thioredoxin-like 2	BB458835
1418896_a_at	R	1.359	Rpn2	ribophorin II	NM_019642
1455749_x_at	R	1.359	Ndufa7	NADH dehydrogenase (ubiquinone) 1 alpha subcomplex, 7 (B14.5a)	C88880
1437907_a_at	R	1.352	Tbca	tubulin cofactor a	BB559082
1449294_at	R	1.348	Mrps15	mitochondrial ribosomal protein S15	NM_025544
1452646_at	R	1.347	1110029F20Rik	RIKEN cDNA 1110029F20 gene	AK003956
1419455_at	R	1.346	Il10rb	interleukin 10 receptor, beta	NM_008349
1426660_x_at	R	1.345	BC029892	Similar to 60S ribosomal protein L23a (LOC268449), mRNA	BF178310
1439415_x_at	R	1.345	Rps21	ribosomal protein S21	AV151252
1426297_at	R	1.344	Tcfe2a	transcription factor E2a	AF352579
1450638_at	R	1.342	Pdcd5	programmed cell death 5	AF161074
1438503_x_at	R	1.339	Edf1	AV102509 Mus musculus C57BL/6J ES cell Mus musculus cDNA clone 2410098K03, mRNA sequence.	AV102509
1426744_at	R	1.339	Srebf2	sterol regulatory element binding factor 2	BM123132
1416057_at	R	1.335	Np15	nuclear protein 15.6	BC027265
1415716_a_at	R	1.321	Rps27	ribosomal protein S27	AA208652
1422615_at	R	1.315	Map4k4	mitogen-activated protein kinase kinase kinase kinase 4	NM_008696
1449256_a_at	R	1.313	Rab11a	RAB11a, member RAS oncogene family	BC010722

Table 5-1. Top 800[a] bioweight (BW) genes (continued)

1422778_at	R	1.312	Taf9	TAF9 RNA polymerase II, TATA box binding protein (TBP)-associated factor	NM_027139
1424684_at	R	1.310	Rab5c	RAB5C, member RAS oncogene family	BC023027
1428257_s_at	R	1.305	Dncl2a	dynein, cytoplasmic, light chain 2A	BG791323
1417103_at	R	1.298	Ddt	D-dopachrome tautomerase	NM_010027
1416910_at	R	1.296	Dnajd1	DnaJ (Hsp40) homolog, subfamily D, member 1	NM_025384
1415919_at	R	1.295	Npdc1	neural proliferation, differentiation and control gene 1	NM_008721
1417510_at	R	1.293	Vps4a	vacuolar protein sorting 4a (yeast)	NM_126165
1426209_at	R	1.291	Strn4	striatin, calmodulin binding protein 4	AF414080
1435431_at	R	1.289	2310047M15Rik	RIKEN cDNA 2310047M15 gene	AW558989
1448427_at	R	1.283	Ndufa6	NADH dehydrogenase (ubiquinone) 1 alpha subcomplex, 6 (B14)	NM_025987
1417399_at	R	1.280	Gas6	growth arrest specific 6	NM_019521
1456663_x_at	R	1.273	2410018G23Rik	BB718785 RIKEN full-length enriched, adult male liver tumor Mus musculus cDNA clone C730019F01 3', mRNA sequence.	BB718785
1449429_at	R	1.273	Fkbp1b	FK506 binding protein 1b	NM_016863
1429708_at	R	1.271	Ndufa11	NADH dehydrogenase (ubiquinone) 1 alpha subcomplex	AA596846
1449046_a_at	R	1.270	1110007C05Rik	RIKEN cDNA 1110007C05 gene	NM_025368
1420842_at	R	1.269	Ptprf	protein tyrosine phosphatase, receptor type, F	BF235516
1435517_x_at	R	1.266	Ralb	BB465250 RIKEN full-length enriched, 12 days embryo spinal ganglion Mus musculus cDNA clone D130097N13 3' similar to L19699 Rat GTP-binding protein (ral B) mRNA, mRNA sequence.	BB465250
1420878_a_at	R	1.264	Ywhab	tyrosine 3-monooxygenase/tryptophan 5-monooxygenase activation protein, beta polypeptide	NM_018753
1448320_at	R	1.256	Stim1	stromal interaction molecule 1	NM_009287
1424285_s_at	R	1.254	Arl6ip4	ADP-ribosylation factor-like 6 interacting protein 4	AB035383
1435873_a_at	R	1.253	Rpl13a	Transcribed sequence with strong similarity to protein pir:S29539 (H.sapiens) S29539 ribosomal protein L13a, cytosolic - human	AI324936
1416816_at	R	1.253	Nek7	NIMA (never in mitosis gene a)-related expressed kinase 7	NM_021605
1416845_at	R	1.252	Hspa5bp1	heat shock 70kDa protein 5 binding protein 1	NM_133804
1451232_at	R	1.250	Cd151	CD151 antigen	U89772
1452111_at	R	1.247	Mrps35	mitochondrial ribosomal protein S35	AV304074
1426475_at	R	1.244	Hmbs	Similar to Hydroxymethylbilane synthase (LOC383565), mRNA	AI325144
1451573_a_at	R	1.243	Stx4a	syntaxin 4A (placental)	BC011491
1427903_at	R	1.242	Phpt1	RIKEN cDNA 1700008C22 gene	BB650419
1418888_a_at	R	1.239	Sepr	selenoprotein R	NM_013759
1418991_at	R	1.235	Bak1	BCL2-antagonist/killer 1	NM_007523
1416782_s_at	R	1.235	DXImx39e	DNA segment, Chr X, Immunex 39, expressed	NM_138602
1416050_a_at	R	1.232	Scarb1	scavenger receptor class B, member 1	NM_016741
1427119_at	R	1.230	Spink4	serine protease inhibitor, Kazal type 4	AV066321
1417285_a_at	R	1.230	Ndufa5	NADH dehydrogenase (ubiquinone) 1 alpha subcomplex, 5	NM_026614
1417340_at	R	1.223	Txnl2	thioredoxin-like 2	NM_023140
1422527_at	R	1.221	H2-DMa	histocompatibility 2, class II, locus DMa	NM_010386
1456628_x_at	R	1.221	Rps24	ribosomal protein S24	AV111319
1454870_x_at	R	1.218	D15Ertd747e	DNA segment, Chr 15, ERATO Doi 747, expressed	BB251205
1451399_at	R	1.218	Brp17	brain protein 17	BC008274

Table 5-1. Top 800[a] bioweight (BW) genes (continued)

1460739_at	R	1.217	D11Bwg0280e	DNA segment, Chr 11, Brigham & Women's Genetics 0280e expressed	BQ174371
1460718_s_at	R	1.216	Mtch1	mitochondrial carrier homolog 1 (C. elegans)	AF192558
1418225_at	R	1.215	Orc2l	origin recognition complex, subunit 2-like (S. cerevisiae)	BB830976
1427173_a_at	R	1.213	Mrps33	mitochondrial ribosomal protein S33	Y17852
1449188_at	R	1.211	Midn	midnolin	NM_021565
1454856_x_at	R	1.211	Rpl35	ribosomal protein L35	AV066335
1426940_at	R	1.209	BC023957	cDNA sequence BC023957	BI412808
1418439_at	R	1.208	2900055D03Rik	RIKEN cDNA 2900055D03 gene	NM_026065
1449855_s_at	R	1.206	Uchl3	ubiquitin carboxyl-terminal esterase L3 (ubiquitin thiolesterase)	AB033370
1416243_a_at	R	1.203	Rpl35	ribosomal protein L35	NM_025592
1418567_a_at	R	1.200	Srp14	signal recognition particle 14	NM_009273
1451385_at	R	1.199	2310056P07Rik	RIKEN cDNA 2310056P07 gene	BC010826
1453634_a_at	R	1.196	Erp29	endoplasmic reticulum protein 29	AK013303
1438177_x_at	R	1.193	Lysal1	AV255351 RIKEN full-length enriched, adult male testis (DH10B) Mus musculus cDNA clone 4921519B12 3', mRNA sequence.	AV255351
1424351_at	R	1.191	1600023A02Rik	RIKEN cDNA 1600023A02 gene	AF334269
1416109_at	R	1.190	Fuca	fucosidase, alpha-L- 1, tissue	NM_024243
1427764_a_at	R	1.189	Tcfe2a	transcription factor E2a	D29919
1424708_at	R	1.188	1110014C03Rik	RIKEN cDNA 1110014C03 gene	BI409239
1424269_a_at	R	1.187	Myl6	myosin light chain, alkali, nonmuscle	BC026760
1435067_at	R	1.187	B230208H17Rik	RIKEN cDNA B230208H17 gene	BG075288
1448604_at	R	1.185	AA407809	expressed sequence AA407809	NM_030724
1424380_at	R	1.185	BC026744	cDNA sequence BC026744	BC026744
1433472_x_at	R	1.182	Rpl38	RIKEN cDNA 0610025G13 gene	AA050777
1426534_a_at	R	1.182	Arfgap3	ADP-ribosylation factor GTPase activating protein 3	BG067878
1423717_at	R	1.177	Ak3l	adenylate kinase 3 alpha-like	BC019174
1418049_at	R	1.174	Ltbp3	latent transforming growth factor beta binding protein 3	NM_008520
1435232_x_at	R	1.173	Mrpl15	mitochondrial ribosomal protein L15	BI791064
1425194_a_at	R	1.173	6330577E15Rik	RIKEN cDNA 6330577E15 gene	BC024403
1424204_at	R	1.173	Mrpl13	mitochondrial ribosomal protein L13	AB049641
1448217_a_at	R	1.171	Rpl27	ribosomal protein L27	NM_011289
1448357_at	R	1.169	Snrpg	small nuclear ribonucleoprotein polypeptide G	NM_026506
1415762_x_at	R	1.164	Mrpl52	mitochondrial ribosomal protein L52	AV021593
1452061_s_at	R	1.164	Strbp	spermatid perinuclear RNA binding protein	AK006314
1423035_s_at	R	1.163	Txnl5	thioredoxin-like 5	AK004219
1448543_at	R	1.163	2310042G06Rik	RIKEN cDNA 2310042G06 gene	NM_025531
1417320_at	R	1.161	Grpel1	GrpE-like 1, mitochondrial	NM_024478
1434120_a_at	R	1.159	Metap2	methionine aminopeptidase 2	AW742814
1437679_a_at	R	1.159	Glrx2	BB172698 RIKEN full-length enriched, adult male hypothalamus Mus musculus cDNA clone A230040G05 3', mRNA sequence.	BB172698
1423764_s_at	R	1.158	Mrpl37	mitochondrial ribosomal protein L37	BC011065
1428842_a_at	R	1.155	Ngfrap1	nerve growth factor receptor (TNFRSF16) associated protein 1	BI407690
1423680_at	R	1.155	Fads1	RIKEN cDNA 0710001O03 gene	BC026831
1421861_at	R	1.155	Clstn1	calsyntenin 1	BG065300
1439454_x_at	R	1.152	2410018G23Rik	RIKEN cDNA 2410018G23 gene	AV337733
1416108_a_at	R	1.150	1200002G13Rik	RIKEN cDNA 1200002G13 gene	NM_025360
1434924_at	R	1.149	Phf2	PHD finger protein 2	BF468039
1426480_at	R	1.148	Sbds	Shwachman-Bodian-Diamond syndrome homolog (human)	BB773592

Table 5-1. Top 800[a] bioweight (BW) genes (continued)

1417481_at	R	1.146	Ramp1	receptor (calcitonin) activity modifying protein 1	NM_016894
1452272_a_at	R	1.144	Gfer	growth factor, erv1 (S. cerevisiae)-like (augmenter of liver regeneration)	BI901126
1428310_at	R	1.142	D3Wsu161e	RIKEN cDNA C330027G06 gene	BF321707
1428823_at	R	1.140	2310057G13Rik	RIKEN cDNA 2310057G13 gene	AK009957
1424773_at	R	1.140	1110012M11Rik	RIKEN cDNA 1110012M11 gene	BC020119
1418248_at	R	1.140	Gla	galactosidase, alpha	NM_013463
1418123_at	R	1.140	Unc119	unc-119 homolog (C. elegans)	BC001990
1417773_at	R	1.139	Nans	602916387F1 NCI_CGAP_Lu29 Mus musculus cDNA clone IMAGE:5067068 5', mRNA sequence.	BI151886
1416493_at	R	1.136	Ddost	dolichyl-di-phosphooligosaccharide-protein glycotransferase	NM_007838
1423240_at	R	1.134	Src	Rous sarcoma oncogene	BG868120
1422579_at	R	1.132	Hspe1	heat shock protein 1 (chaperonin 10)	NM_008303
1448292_at	R	1.129	Uqcr	ubiquinol-cytochrome c reductase (6.4kD) subunit	NM_025650
1455288_at	R	1.128	1110036O03Rik	RIKEN cDNA 1110036O03 gene	BE951265
1450106_a_at	R	1.127	Evl	Ena-vasodilator stimulated phosphoprotein	NM_007965
1416807_at	R	1.125	Rpl36a	ribosomal protein L36a	NM_019865
1417344_at	R	1.123	2900064A13Rik	RIKEN cDNA 2900064A13 gene	BE915256
1418572_x_at	R	1.122	Tnfrsf12a	tumor necrosis factor receptor superfamily, member 12a	NM_013749
1418704_at	R	1.122	S100a13	S100 calcium binding protein A13	NM_009113
1426648_at	R	1.122	Mapkapk2	MAP kinase-activated protein kinase 2	BG918951
1416519_at	R	1.120	Rpl36	ribosomal protein L36	NM_018730
1452039_a_at	R	1.118	Bap1	Brca1 associated protein 1	AK009033
1417368_s_at	R	1.116	Ndufa2	NADH dehydrogenase (ubiquinone) 1 alpha subcomplex, 2	NM_010885
1435413_x_at	R	1.115	2700060E02Rik	AV167958 Mus musculus head C57BL/6J 13-day embryo Mus musculus cDNA clone 3110059K19, mRNA sequence.	AV167958
1418000_a_at	R	1.115	Itm2b	integral membrane protein 2B	NM_008410
1419550_a_at	R	1.113	Stk39	6 days neonate head cDNA, RIKEN full-length enriched library, clone:5430411A13 product:serine/threonine kinase 39, STE20/SPS1 homolog (yeast), full insert sequence	BG919998
1450640_x_at	R	1.109	Atp5k	ATP synthase, H+ transporting, mitochondrial F1F0 complex, subunit e	NM_007507
1451602_at	R	1.105	Snx6	sorting nexin 6	BC025911
1424073_at	R	1.100	5430437P03Rik	RIKEN cDNA 5430437P03 gene	BC005692
1426811_at	R	1.099	Ppp2r5b	glycoprotein hormone alpha 2	BB080065
1434019_at	R	1.099	Pdap1	PDGFA associated protein 1	BG065186
1437976_x_at	R	1.097	BC029892	Similar to 60S ribosomal protein L23a (LOC268449), mRNA	C87154
1417026_at	R	1.096	Pfdn1	prefoldin 1	BC024693
1448346_at	R	1.095	Cfl1	cofilin 1, non-muscle	NM_007687
1450668_s_at	R	1.094	Hspe1	heat shock protein 1 (chaperonin 10)	NM_008303
1416636_at	R	1.093	Rheb	RAS-homolog enriched in brain	NM_053075
1416285_at	R	1.093	Ndufc1	NADH dehydrogenase (ubiquinone) 1, subcomplex unknown, 1	NM_025523
1456205_x_at	R	1.092	Tbca	tubulin cofactor a	BB559082
1418625_s_at	R	1.090	LOC14433	glyceraldehyde-3-phosphate dehydrogenase	NM_008084
1415879_a_at	R	1.088	Rplp2	ribosomal protein, large P2	BC012413
1416074_a_at	R	1.088	Rpl28	ribosomal protein L28	NM_009081
1424488_a_at	R	1.087	1110013G13Rik	RIKEN cDNA 1110013G13 gene	BC011417
1454760_at	R	1.086	2600017A12Rik	RIKEN cDNA 2600017A12 gene	AW543705

Table 5-1. Top 800[a] bioweight (BW) genes (continued)

1449108_at	R	1.086	Fdx1	ferredoxin 1	D43690
1417585_at	R	1.085	Nup210	nucleoporin 210	NM_018815
1423133_at	R	1.085	0610040D20Rik	RIKEN cDNA 0610040D20 gene	BG071645
1435112_a_at	R	1.083	Atp5h	ATP synthase, H+ transporting, mitochondrial F0 complex, subunit d	AV154755
1456373_x_at	R	1.079		ribosomal protein S20	AV046829
1437767_s_at	R	1.079	Fts	retinoblastoma-like 2	AA138720
1426244_at	R	1.079	Mapre2	microtubule-associated protein, RP/EB family, member 2	BC027056
1451747_a_at	R	1.075	Apg12l	autophagy 12-like (S. cerevisiae)	AK016474
1451425_a_at	R	1.075	Mkrn1	makorin, ring finger protein, 1	BC003329
1460428_at	R	1.074	1100001D10Rik	RIKEN cDNA 1100001D10 gene	BC003286
1450878_at	R	1.074	Sri	RIKEN cDNA 2210417O06 gene	AK008404
1436949_a_at	R	1.073	Tceb2	AV068352 Mus musculus small intestine C57BL/6J adult Mus musculus cDNA clone 2010303D07, mRNA sequence.	AV068352
1448971_at	R	1.070	2410022L05Rik	RIKEN cDNA 2410022L05 gene	NM_025556
1416480_a_at	R	1.070	Hig1	hypoxia induced gene 1	NM_019814
1439462_x_at	R	1.068	1110014C03Rik	AV060550 Mus musculus pancreas C57BL/6J adult Mus musculus cDNA clone 1810063I09, mRNA sequence.	AV060550
1426323_x_at	R	1.064	Siva	Cd27 binding protein (Hindu God of destruction)	AF033112
1417511_at	R	1.062	Lyar	Ly1 antibody reactive clone	NM_025281
1418901_at	R	1.058	Cebpb	CCAAT/enhancer binding protein (C/EBP), beta	NM_009883
1448656_at	R	1.057	Cacnb3	calcium channel, voltage-dependent, beta 3 subunit	NM_007581
1452585_at	R	1.057	Mrps28	mitochondrial ribosomal protein S28	AK011036
1456243_x_at	R	1.056	Mcl1	BB374534 RIKEN full-length enriched, 16 days embryo head Mus musculus cDNA clone C130075I17 3' similar to U35623 Mus musculus EAT/MCL-1 mRNA, mRNA sequence.	BB374534
1426529_a_at	R	1.052	Tagln2	transgelin 2	C76322
1417075_at	R	1.052	2010309E21Rik	RIKEN cDNA 2010309E21 gene	NM_025591
1448284_a_at	R	1.051	Ndufc1	NADH dehydrogenase (ubiquinone) 1, subcomplex unknown, 1	NM_025523
1460354_a_at	R	1.050	Mrpl13	mitochondrial ribosomal protein L13	AB049641
1415950_a_at	R	1.048	Pbp	phosphatidylethanolamine binding protein	NM_018858
1422134_at	R	1.047	Fosb	FBJ osteosarcoma oncogene B	NM_008036
1417774_at	R	1.045	Nans	602916387F1 NCI_CGAP_Lu29 Mus musculus cDNA clone IMAGE:5067068 5', mRNA sequence.	BI151886
1424894_at	R	1.045	Rab13	RAB13, member RAS oncogene family	BC027214
1437975_a_at	R	1.043	BC029892	Similar to 60S ribosomal protein L23a (LOC268449), mRNA	C87154
1439234_a_at	R	1.042	2410018G23Rik	RIKEN cDNA 2410018G23 gene	BE200117
1418029_at	R	1.042	Faim	Fas apoptotic inhibitory molecule	NM_011810
1423080_at	R	1.042	Tomm20	translocase of outer mitochondrial membrane 20 homolog (yeast)	AK002902
1449245_at	R	1.042	Grin2c	glutamate receptor, ionotropic, NMDA2C (epsilon 3)	NM_010350
1438058_s_at	R	1.041	Ptov1	prostate tumor over expressed gene 1	BG073526
1418714_at	R	1.041	Dusp8	dual specificity phosphatase 8	NM_008748
1417893_at	R	1.039	Sfxn3	sideroflexin 3	NM_053197
1424456_at	R	1.037	Pvrl2	poliovirus receptor-related 2	BC009088
1433549_x_at	R	1.036	Rps21	ribosomal protein S21	AV123618

Table 5-1. Top 800[a] bioweight (BW) genes (continued)

1435712_a_at	R	1.033	Rps18	Transcribed sequence with strong similarity to protein ref:NP_072045.1 (H.sapiens) ribosomal protein S18; 40S ribosomal protein S18 [Homo sapiens]	AW907444
1451012_a_at	R	1.032	Csda	AV216648 RIKEN full-length enriched, ES cells Mus musculus cDNA clone 2410165I03 3' similar to D14485 Mouse mRNA for dbpA murine homologue, mRNA sequence.	AV216648
1418656_at	R	1.032	Lsm5	LSM5 homolog, U6 small nuclear RNA associated (S. cerevisiae)	NM_025520
1448592_at	R	1.031	Crtap	cartilage associated protein	NM_019922
1455129_at	R	1.030	2610103J23Rik	RIKEN cDNA 2610103J23 gene	AV083741
1433991_x_at	R	1.030	Dbi	diazepam binding inhibitor	AV007315
1438659_x_at	R	1.027	0710001P09Rik	BB458460 RIKEN full-length enriched, 12 days embryo spinal ganglion Mus musculus cDNA clone D130057E08 3', mRNA sequence.	BB458460
1455126_x_at	R	1.026	2310028O11Rik	Adult male xiphoid cartilage cDNA, RIKEN full-length enriched library, clone:5230400C04 product:unknown EST, full insert sequence	AV209841
1419351_a_at	R	1.025	0610007P06Rik	RIKEN cDNA 0610007P06 gene	BC003916
1433721_x_at	R	1.024	Rps21	ribosomal protein S21	AV123577
1416245_at	R	1.023	0610033H09Rik	RIKEN cDNA 0610033H09 gene	NM_025338
1421152_a_at	R	1.021	Gnao	guanine nucleotide binding protein, alpha o	NM_010308
1450981_at	R	1.020	Cnn2	calponin 2	BI663014
1450925_a_at	R	1.019	Rps27l	ribosomal protein S27-like	BB836796
1424771_at	R	1.019	E130307C13	hypothetical protein E130307C13	BF661121
1449289_a_at	R	1.018	B2m	RIKEN cDNA E130113K22 gene	BF715219
1428189_at	R	1.018	5730494M16Rik	RIKEN cDNA 5730494M16 gene	BQ174627
1456745_x_at	R	1.018	Sdbcag84	serologically defined breast cancer antigen 84	BB253632
1448372_a_at	R	1.014	Tmem4	transmembrane protein 4	NM_019953
1427511_at	R	1.014	B2m	beta-2 microglobulin	AA170322
1455364_a_at	R	1.013	Rps7	Similar to Rpl7a protein (LOC245667), mRNA	AI414989
1448589_at	R	1.011	Ndufb5	NADH dehydrogenase (ubiquinone) 1 beta subcomplex, 5	BC025155
1425196_a_at	R	1.011	Hint2	histidine triad nucleotide binding protein 2	AF356874
1451211_a_at	R	1.009	Lgtn	ligatin	BC025036
1424222_s_at	R	1.008	Rad23b	Mus musculus cDNA clone IMAGE:3256899, complete cds.	BC006751
1415673_at	R	1.007	Psph	phosphoserine phosphatase	NM_133900
1417102_a_at	R	1.007	Ndufb5	NADH dehydrogenase (ubiquinone) 1 beta subcomplex, 5	BC025155
1417879_at	R	1.007	1110060M21Rik	RIKEN cDNA 1110060M21 gene	NM_025424
1448344_at	R	1.003	Rps12	ribosomal protein S12	NM_011295
1437381_x_at	R	1.002	D15Ertd747e	BB236260 RIKEN full-length enriched, 3 days neonate thymus Mus musculus cDNA clone A630058C06 3', mRNA sequence.	BB236260
1448699_at	R	1.002	Mrpl54	mitochondrial ribosomal protein L54	NM_025317
1434736_at	R	1.001	Hlf	hepatic leukemia factor	BB744589
1426510_at	R	1.000	C330023F11Rik	RIKEN cDNA C330023F11 gene	AW537824
1452679_at	R	1.000	2410129E14Rik	Transcribed sequence with strong similarity to protein ref:NP_001060.1 (H.sapiens) tubulin, beta polypeptide [Homo sapiens]	AA986082
1448657_a_at	R	0.999	Dnajb10	DnaJ (Hsp40) homolog, subfamily B, member 10	NM_020266
1416247_at	R	0.999	Dctn3	dynactin 3	NM_016890

Table 5-1. Top 800[a] bioweight (BW) genes (continued)

1423907_a_at	R	0.997	Ndufs8	NADH dehydrogenase (ubiquinone) Fe-S protein 8	BC021616
1417183_at	R	0.996	Dnaja2	DnaJ (Hsp40) homolog, subfamily A, member 2	C77509
1452754_at	R	0.996	5730592L21Rik	RIKEN cDNA 5730592L21 gene	AK017880
1460697_s_at	R	0.995	2610209M04Rik	RIKEN cDNA 2610209M04 gene	BC027564
1417869_s_at	R	0.994	Ctsz		NM_022325
1434358_x_at	R	0.994	Rps21	Transcribed sequence with moderate similarity to protein ref:NP_001015.1 (H.sapiens) ribosomal protein S21; 40S ribosomal protein S21 [Homo sapiens]	AV124427
1433554_at	R	0.994	AU022870	hypothetical protein MGC56855	BM246500
1438986_x_at	R	0.994	Rps17	ribosomal protein S17	AV064451
1426680_at	R	0.993	Sepn1	RIKEN cDNA 1110019I12 gene	AK003819
1444952_a_at	R	0.991	8430423A01Rik	RIKEN cDNA 8430423A01 gene	BB260383
1452370_s_at	R	0.990	B230208H17Rik	RIKEN cDNA B230208H17 gene	BB449608
1451255_at	R	0.988	Lisch7	liver-specific bHLH-Zip transcription factor	BC004672
1428214_at	R	0.988	Tomm7	translocase of outer mitochondrial membrane 7 homolog (yeast)	BB609428
1423087_a_at	R	0.987	1110002E23Rik	RIKEN cDNA 1110002E23 gene	BB453951
1423365_at	R	0.987	Cacna1g	calcium channel, voltage-dependent, T type, alpha 1G subunit	AW494038
1434976_x_at	R	0.985	Eif4ebp1	AV216412 RIKEN full-length enriched, ES cells Mus musculus cDNA clone 2410160M04 3' similar to U28656 Mus musculus insulin-stimulated eIF-4E binding protein PHAS-I mRNA, mRNA sequence.	AV216412
1416971_at	R	0.985	Cox7a2	cytochrome c oxidase, subunit VIIa 2	NM_009945
1423736_a_at	R	0.985	4933427L07Rik	RIKEN cDNA 4933427L07 gene	BC018220
1456540_s_at	R	0.982	Mtmr6	BB297632 RIKEN full-length enriched, 9.5 days embryo parthenogenote Mus musculus cDNA clone B130063F15 3' similar to AF072928 Homo sapiens myotubularin related protein 6 mRNA, mRNA sequence.	BB297632
1415912_a_at	R	0.981	Rps13	ribosomal protein S13	NM_026533
1448498_at	R	0.981	Rps6ka4	ribosomal protein S6 kinase, polypeptide 4	NM_019924
1448876_at	R	0.978	Evc	Ellis van Creveld gene homolog (human)	NM_021292
1418545_at	R	0.978	Wasf1	WASP family 1	NM_031877
1452586_at	R	0.978	1810004D07Rik	RIKEN cDNA 1810004D07 gene	BM122700
1437947_x_at	R	0.976	Vdac1	AV036172 Mus musculus adult C57BL/6J placenta Mus musculus cDNA clone 1600017H06, mRNA sequence.	AV036172
1423294_at	R	0.972	Mest	Transcribed sequence with moderate similarity to protein sp:Q9UBF2 (H.sapiens) CPG2_HUMAN Coatomer gamma-2 subunit	AW555393
1460424_at	R	0.971	1810008O21Rik	RIKEN cDNA 1810008O21 gene	BI411309
1435277_x_at	R	0.971	Nme1	AV156640 Mus musculus head C57BL/6J 12-day embryo Mus musculus cDNA clone 3000003N22, mRNA sequence.	AV156640
1428029_a_at	R	0.971	H2av	H2A histone family, member V	BC028539
1422451_at	R	0.967	Mrps21	mitochondrial ribosomal protein S21	NM_078479
1422524_at	R	0.967	Abcb6	ATP-binding cassette, sub-family B (MDR/TAP), member 6	NM_023732
1417357_at	R	0.966	Emd	emerin	NM_007927
1426606_at	R	0.965	Crtac1	cartilage acidic protein 1	BB426194
1452181_at	R	0.965	Ckap4	BB312117 RIKEN full-length enriched, adult male corpora quadrigemina Mus musculus cDNA clone B230331K02 3' similar to X69910 H.sapiens p63 mRNA for transmembrane protein, mRNA sequence.	BB312117
1418986_a_at	R	0.964	Uxt	ubiquitously expressed transcript	NM_013840

Table 5-1. Top 800[a] bioweight (BW) genes (continued)

1451071_a_at	R	0.963	Atp1a1	ATPase, Na+/K+ transporting, alpha 1 polypeptide	BC025618
1438776_x_at	R	0.961	Rps17	AV046534 Mus musculus adult C57BL/6J testis Mus musculus cDNA clone 1700057O18, mRNA sequence.	AV046534
1424640_at	R	0.961	1110033P22Rik	RIKEN cDNA 1110033P22 gene	BC018479
1449040_a_at	R	0.960	Sephs2	selenophosphate synthetase 2	NM_009266
1417722_at	R	0.960	Pgls	6-phosphogluconolactonase	BC006594
1448869_a_at	R	0.956	Mrps16	mitochondrial ribosomal protein S16	NM_025440
1426782_at	R	0.955	3830613O22Rik	RIKEN cDNA 3830613O22 gene	BC019649
1422683_at	R	0.955	Irak1bp1	interleukin-1 receptor-associated kinase 1 binding protein 1	NM_022986
1448799_s_at	R	0.954	Mrps12	nuclear factor of kappa light chain gene enhancer in B-cells inhibitor, beta	NM_011885
1423181_s_at	R	0.954	Clns1a	chloride channel, nucleotide-sensitive, 1A	AK011789
1427282_a_at	R	0.952	Frda	Friedreich ataxia	AV007132
1416054_at	R	0.951	Rps5	ribosomal protein S5	NM_009095
1452621_at	R	0.948	2700061N24Rik	RIKEN cDNA 2700061N24 gene	AI324894
1428954_at	R	0.947	Slc9a3r2	solute carrier family 9 (sodium/hydrogen exchanger), isoform 3 regulator 2	AK004710
1418744_s_at	R	0.946	Tesc	tescalcin	NM_021344
1451291_at	R	0.946	2610036N15Rik	RIKEN cDNA 2610036N15 gene	BC026942
1415980_at	R	0.945	Atp5g2	ATP synthase, H+ transporting, mitochondrial F0 complex, subunit c (subunit 9), isoform 2	NM_026468
1451178_at	R	0.944	Mrpl53	mitochondrial ribosomal protein L53	BC022162
1416696_at	R	0.943	D17Wsu104e	interleukin 25	NM_080837
1451017_at	R	0.942	Sdbcag84	BB556862 RIKEN full-length enriched, 2 days pregnant adult female ovary Mus musculus cDNA clone E330025K14 3' similar to AL161963 Homo sapiens mRNA; cDNA DKFZp547A2190 (from clone DKFZp547A2190), mRNA sequence.	BB556862
1456293_s_at	R	0.941	Ccnh	cyclin H	AA068868
1434230_at	R	0.941	Polb	polymerase (DNA directed), beta	BG094331
1418579_at	R	0.940	Cetn2	centrin 2	BC013545
1424076_at	R	0.939	2610020H15Rik	RIKEN cDNA 2610020H15 gene	AK016023
1449267_at	R	0.939	3110023E09Rik	RIKEN cDNA 3110023E09 gene	BC006876
1417886_at	R	0.939	1810009A15Rik	RIKEN cDNA 1110055N21 gene	BE307471
1416412_at	R	0.937	Nsmaf	neutral sphingomyelinase (N-SMase) activation associated factor	NM_010945
1422520_at	R	0.936	Nef3	neurofilament 3, medium	NM_008691
1428179_at	R	0.935	Ndufv2	NADH dehydrogenase (ubiquinone) flavoprotein 2	BI692577
1420113_s_at	R	0.933	2410022L05Rik	RIKEN cDNA 2410022L05 gene	AA409325
1439466_s_at	R	0.933	Ptcd1	BB001490 RIKEN full-length enriched, 13 days embryo head Mus musculus cDNA clone 3110026K15 3' similar to AF058791 Rattus norvegicus G10 protein homolog (edg2) mRNA, mRNA sequence.	BB001490
1434883_at	R	0.929	2610103J23Rik	RIKEN cDNA 2610103J23 gene	AV083741
1435652_a_at	R	0.929	Gnai2	uz40a02.x1 NCI_CGAP_Mam5 Mus musculus cDNA clone IMAGE:3671498 3', mRNA sequence.	BF228116
1452246_at	R	0.929	Ostf1	osteoclast stimulating factor 1	U58888
1420513_at	R	0.928	1700073K01Rik	RIKEN cDNA 1700073K01 gene	BC025062
1430128_a_at	R	0.928	Dp1l1	deleted in polyposis 1-like 1	AK002562
1416605_at	R	0.927	Nola2	nucleolar protein family A, member 2	BC024944
1449194_at	R	0.926	Mrps25	mitochondrial ribosomal protein S25	AK004037

Table 5-1. Top 800[a] bioweight (BW) genes (continued)

1416349_at	R	0.926	Mrpl34	mitochondrial ribosomal protein L34	NM_053162
1448887_x_at	R	0.920	Fxc1	fractured callus expressed transcript 1	NM_019502
1424300_at	R	0.919	Gemin6	gem (nuclear organelle) associated protein 6	BC025157
1417959_at	R	0.918	Pdlim7	PDZ and LIM domain 7	NM_026131
1418743_a_at	R	0.918	Tesc	tescalcin	NM_021344
1422525_at	R	0.918	Atp5k	ATP synthase, H+ transporting, mitochondrial F1F0 complex, subunit e	NM_007507
1421817_at	R	0.913	Gsr	glutathione reductase 1	AK019177
1416769_s_at	R	0.912	Atp6v0b	ATPase, H+ transporting, V0 subunit B	NM_033617
1431036_a_at	R	0.912	1110032D12Rik	RIKEN cDNA 1110032D12 gene	BF121933
1427876_at	R	0.912	2610312B22Rik	RIKEN cDNA 2610312B22 gene	BB703070
1422977_at	R	0.912	Gp1bb	glycoprotein Ib, beta polypeptide	NM_010327
1448198_a_at	R	0.909	Ndufb8	NADH dehydrogenase (ubiquinone) 1 beta subcomplex 8	NM_026061
1433928_a_at	R	0.908	Rpl13a	ribosomal protein L13a	BF146301
1423897_at	R	0.907	2410016F01Rik	RIKEN cDNA 2410016F01 gene	AW488376
1439451_x_at	R	0.906	D15Ertd747e	BB487787 RIKEN full-length enriched, 13 days embryo lung Mus musculus cDNA clone D430044J16 3', mRNA sequence.	BB487787
1430295_at	R	0.906	Gna13	guanine nucleotide binding protein, alpha 13	BG094302
1423242_at	R	0.906	Mrps36	mitochondrial ribosomal protein S36	BE627004
1453651_a_at	R	0.904	Brp44l	AV223468 RIKEN full-length enriched, 18 days pregnant, placenta and extra embryonic tissue Mus musculus cDNA clone 3830411I18 3', mRNA sequence.	AV223468
1436803_a_at	R	0.903	Ndufb9	NADH dehydrogenase (ubiquinone) 1 beta subcomplex, 9	AV161987
1421266_s_at	R	0.902	Nfkbib	nuclear factor of kappa light chain gene enhancer in B-cells inhibitor, beta	NM_010908
1418589_a_at	R	0.902	Mlf1	myeloid leukemia factor 1	AF100171
1418588_at	R	0.902	Vmp	vesicular membrain protein p24	NM_009513
1448737_at	R	0.901	Tm4sf2	transmembrane 4 superfamily member 2	AF052492
1429265_a_at	R	0.900	Rnf130	ring finger protein 130	AK011088
1454859_a_at	R	0.899	Rpl23	Similar to ribosomal protein L23 (LOC384399), mRNA	AV124394
1416022_at	R	0.899	Fabp5	fatty acid binding protein 5, epidermal	BC002008
1456584_x_at	R	0.898	Phgdh	BB495884 RIKEN full-length enriched, 13 days embryo stomach Mus musculus cDNA clone D530050H10 3' similar to L21027 Mus musculus A10 mRNA, mRNA sequence.	BB495884
1417458_s_at	R	0.898	Cks2	CDC28 protein kinase regulatory subunit 2	NM_025415
1439410_x_at	R	0.897	3010027G13Rik	RIKEN cDNA 3010027G13 gene	BI966363
1416608_a_at	R	0.896	BC004004	cDNA sequence BC004004	NM_030561
1423321_at	R	0.896	Myadm	myeloid-associated differentiation marker	BI078799
1419765_at	R	0.896	Cul2	cullin 2	NM_029402
1454987_a_at	R	0.895	H2-Ke6	H2-K region expressed gene 6	AI323545
1416965_at	R	0.893	Pcsk1n	proprotein convertase subtilisin/kexin type 1 inhibitor	AF181560
1423653_at	R	0.893	Atp1a1	ATPase, Na+/K+ transporting, alpha 1 polypeptide	BC025618
1423993_at	R	0.890	Atp6v1f	ATPase, H+ transporting, V1 subunit F	BC016553
1419456_at	R	0.890	Dcxr	dicarbonyl L-xylulose reductase	BC012247
1451745_a_at	R	0.889	Znhit1	zinc finger, HIT domain containing 1	BC026751
1423746_at	R	0.889	Txndc5	thioredoxin domain containing 5	BC016252
1450389_s_at	R	0.889	Pip5k1a	phosphatidylinositol-4-phosphate 5-kinase, type 1 alpha	NM_008846
1433616_a_at	R	0.888	2310028O11Rik	Adult male xiphoid cartilage cDNA, RIKEN full-length enriched library, clone:5230400C04 product:unknown EST, full insert sequence	BG793007

Table 5-1. Top 800[a] bioweight (BW) genes (continued)

1425485_at	R	0.886	Mtmr6	myotubularin related protein 6	BC020019
1441866_s_at	R	0.884	Ptdss1	BB526117 RIKEN full-length enriched, 15 days embryo head Mus musculus cDNA clone D930031G20 3' similar to AF042731 Mus musculus phosphatidylserine synthase-1 mRNA, mRNA sequence.	BB526117
1435364_at	R	0.883		4 days neonate male adipose cDNA, RIKEN full-length enriched library, clone:B430101C18 product:HYPOTHETICAL 19.9 KDA PROTEIN homolog [Homo sapiens], full insert sequence	BB323901
1416394_at	R	0.883	Bag1	Bcl2-associated athanogene 1	NM_009736
1415880_a_at	R	0.883	Lamp1	lysosomal membrane glycoprotein 1	NM_010684
1421903_at	R	0.883	2810405O22Rik	RIKEN cDNA 2810405O22 gene	AK005112
1428526_at	R	0.882	1500034E06Rik	RIKEN cDNA 1500034E06 gene	AK018782
1437345_a_at	R	0.882	Bscl2	Bernardinelli-Seip congenital lipodystrophy 2 homolog (human)	BB223872
1449000_at	R	0.880	D10Jhu81e	DNA segment, Chr 10, Johns Hopkins University 81 expressed	NM_138601
1456616_a_at	R	0.880	Bsg	AV035166 Mus musculus adult C57BL/6J placenta Mus musculus cDNA clone 1600013O06, mRNA sequence.	AV035166
1424171_a_at	R	0.879	Hagh	hydroxyacyl glutathione hydrolase	BC004749
1423507_a_at	R	0.879	Sirt2	Transcribed sequence with moderate similarity to protein ref:NP_036369.2 (H.sapiens) sirtuin 2, isoform 1; SIR2	BB807595
1451386_at	R	0.879	Blvrb	biliverdin reductase B (flavin reductase (NADPH))	BC027279
1448824_at	R	0.878	Ube2j1	ubiquitin-conjugating enzyme E2, J1	NM_019586
1434325_x_at	R	0.877	Prkar1b	BB274009 RIKEN full-length enriched, 10 days neonate cortex Mus musculus cDNA clone A830086C24 3', mRNA sequence.	BB274009
1454807_a_at	R	0.877	Snx12	sorting nexin 12	BB414983
1416528_at	R	0.875	Sh3bgrl3	SH3 domain binding glutamic acid-rich protein-like 3	NM_080559
1425674_a_at	R	0.874	1500011L16Rik	RIKEN cDNA 1500011L16 gene	BC016544
1423959_at	R	0.874	AV047578	expressed sequence AV047578	AF305427
1427074_at	P	2.834	5330414D10Rik	L0848C02-3 NIA Mouse Newborn Brain cDNA Library Mus musculus cDNA clone L0848C02 3', mRNA sequence.	BM117243
1448830_at	P	2.578	Dusp1	dual specificity phosphatase 1	NM_013642
1427985_at	P	2.541	9630042H07Rik	RIKEN cDNA 9630042H07 gene	BC027796
1450008_a_at	P	2.365	Catnb	catenin beta	NM_007614
1437354_at	P	2.316		0 day neonate cerebellum cDNA, RIKEN full-length enriched library, clone:C230091D08 product:unclassifiable, full insert sequence	AI154956
1415823_at	P	2.143	Scd2	stearoyl-Coenzyme A desaturase 2	BG060909
1424766_at	P	2.044	BC004701	cDNA sequence BC004701	BC004701
1429144_at	P	1.994	2310032D16Rik	RIKEN cDNA 2310032D16 gene	AV291259
1419277_at	P	1.984	Usp31	ubiquitin specific protease 31	BG068704
1419529_at	P	1.976	Il23a	interleukin 23, alpha subunit p19	NM_031252
1418025_at	P	1.969	Bhlhb2	basic helix-loop-helix domain containing, class B2	NM_011498
1415996_at	P	1.961	Txnip	thioredoxin interacting protein	AF173681
1420922_at	P	1.945	Usp9x	Similar to ubiquitin specific protease 9, X-linked isoform 2; Drosophila fat facets related, X-linked; ubiquitin specific protease 9, X chromosome (fat facets-like Drosophila) (LOC240170), mRNA	AW107303
1434392_at	P	1.930	Usp34	U2af1-rs1 region 2	BM235696

Table 5-1. Top 800[a] bioweight (BW) genes (continued)

1429850_x_at	P	1.921	2010004B12Rik	RIKEN cDNA 2010004B12 gene	AK008083
1415945_at	P	1.915	Mcm5	minichromosome maintenance deficient 5, cell division cycle 46 (S. cerevisiae)	NM_008566
1424522_at	P	1.912	BC019693	cDNA sequence BC019693	BC019693
1427413_a_at	P	1.901	Cugbp1	unnamed protein product; CUG triplet repeat, RNA binding protein 1 (MGD|MGI:1342295) putative; Mus musculus 14 days embryo liver cDNA, RIKEN full-length enriched library, clone:4432412L08 product:CUG triplet repeat, RNA binding protein 1, full insert sequence.	AK014492
1426750_at	P	1.895	Flnb	filamin, beta	AW538200
1417363_at	P	1.888	Zfp61	zinc finger protein 61	NM_009561
1438809_at	P	1.833	Atp5c1	ATP synthase, H+ transporting, mitochondrial F1 complex, gamma polypeptide 1	AI644507
1424723_s_at	P	1.799	Cstf3	cleavage stimulation factor, 3' pre-RNA, subunit 3	BC003241
1425514_at	P	1.783	Pik3r1	phosphatidylinositol 3-kinase, regulatory subunit, polypeptide 1 (p85 alpha)	M60651
1435934_at	P	1.752	9330101J02Rik	RIKEN cDNA 9330101J02 gene	AI643884
1454686_at	P	1.703	6430706D22Rik	RIKEN cDNA 6430706D22 gene	BM248225
1437175_at	P	1.696	BC027088	cDNA sequence BC027088	BI691129
1417155_at	P	1.691	Nmyc1	neuroblastoma myc-related oncogene 1	BC005453
1423828_at	P	1.688	Fasn	fatty acid synthase	AF127033
1460429_at	P	1.685	Cdc5l	cell division cycle 5-like (S. pombe)	AK004547
1427490_at	P	1.679	Abcb7	ATP-binding cassette, sub-family B (MDR/TAP), member 7	U43892
1420811_a_at	P	1.664	Catnb	catenin beta	NM_007614
1426653_at	P	1.645	Mcm3	minichromosome maintenance deficient 3 (S. cerevisiae)	BI658327
1424571_at	P	1.635	Ddx46	DEAD (Asp-Glu-Ala-Asp) box polypeptide 46	BF023426
1448616_at	P	1.632	Dvl2	dishevelled 2, dsh homolog (Drosophila)	BF466091
1452519_a_at	P	1.621	Zfp36	unnamed protein product; TIS11 (AA 1 - 183); Mouse TPA-induced TIS11 mRNA.	X14678
1451959_a_at	P	1.617	Vegfa	vascular endothelial growth factor A	U50279
1456128_at	P	1.616	Atp5g2	ATP synthase, H+ transporting, mitochondrial F0 complex, subunit c (subunit 9), isoform 2	AW413339
1425326_at	P	1.610	Acly	ATP citrate lyase	BI456232
1449011_at	P	1.607	Slc12a7	solute carrier family 12, member 7	BB732135
1433451_at	P	1.592	Cdk5r	cyclin-dependent kinase 5, regulatory subunit (p35)	BB177836
1454626_at	P	1.589	Cltc	clathrin, heavy polypeptide (Hc)	BM211219
1417356_at	P	1.579	Peg3	paternally expressed 3	AB003040
1428087_at	P	1.573	Dnm1l	dynamin 1-like	BM249101
1422967_a_at	P	1.564	Tfrc	transferrin receptor	BB810450
1421455_at	P	1.558	Sntb1	syntrophin, basic 1	NM_016667
1448420_a_at	P	1.550	Fbxl12	F-box and leucine-rich repeat protein 12	NM_013911
1418768_at	P	1.550	Opa1	optic atrophy 1 homolog (human)	BC025160
1460631_at	P	1.549	Ogt	602117024T1 Soares_mammary_gland_NMLMG Mus musculus cDNA clone IMAGE:3468509 3', mRNA sequence.	BF681886
1427797_s_at	P	1.548		602099052F1 NCI_CGAP_Co24 Mus musculus cDNA clone IMAGE:4219044 5', mRNA sequence.	BF580235
1427795_s_at	P	1.534		Clone IMAGE:6494162, mRNA	BC021394
1425231_a_at	P	1.526	Zfp46	zinc finger protein 46	BC006587

Table 5-1. Top 800[a] bioweight (BW) genes (continued)

1417380_at	P	1.526	Iqgap1	IQ motif containing GTPase activating protein 1	NM_016721
1452143_at	P	1.524	Spnb2	spectrin beta 2	BQ174069
1448650_a_at	P	1.512	Pole	polymerase (DNA directed), epsilon	NM_011132
1428286_at	P	1.508	2900097C17Rik	13 days embryo forelimb cDNA, RIKEN full-length enriched library, clone:5930433F13 product:unknown EST, full insert sequence	AW545056
1425384_a_at	P	1.507	Ube4a	ubiquitination factor E4A, UFD2 homolog (S. cerevisiae)	BC006649
1421888_x_at	P	1.496	Aplp2	amyloid beta (A4) precursor-like protein 2	M97216
1452265_at	P	1.492	Clasp1	CLIP associating protein 1	AJ288061
1422581_at	P	1.491	Pias1	protein inhibitor of activated STAT 1	NM_019663
1449324_at	P	1.489	Ero1l	Transcribed sequences	BM234652
1452154_at	P	1.488	Iars	isoleucine-tRNA synthetase	BE915338
1455940_x_at	P	1.488	Wdr6	RIKEN cDNA 6330580J24 gene	BB453609
1434561_at	P	1.484	Asxl1	additional sex combs like 1 (Drosophila)	BI648411
1426677_at	P	1.481	Flna	filamin, alpha	BM233746
1415973_at	P	1.465	Marcks	myristoylated alanine rich protein kinase C substrate	AW546141
1420971_at	P	1.460	Ubr1	ubiquitin protein ligase E3 component n-recognin 1	BQ173927
1433804_at	P	1.453	Jak1	Janus kinase 1	BQ032637
1428848_a_at	P	1.450	Macf1	microtubule-actin crosslinking factor 1	BM248206
1449865_at	P	1.450	Sema3a	sema domain, immunoglobulin domain (Ig), short basic domain, secreted, (semaphorin) 3A	NM_009152
1454890_at	P	1.446	Amot	angiomotin	BG067039
1422685_at	P	1.446	Sec8l1	SEC8-like 1 (S. cerevisiae)	NM_009148
1421519_a_at	P	1.435	Zfp120	zinc finger protein 120	NM_023266
1448809_at	P	1.432	Cse1l	chromosome segregation 1-like (S. cerevisiae)	NM_023565
1426377_at	P	1.415	Zfp281	Adult male diencephalon cDNA, RIKEN full-length enriched library, clone:9330157H23 product:inferred: Mus musculus, Similar to zinc finger protein 281, clone MGC:7737 IMAGE:3498439, mRNA, complete cds, full insert sequence	AV071650
1450634_at	P	1.408	Atp6v1a1	ATPase, H+ transporting, V1 subunit A, isoform 1	NM_007508
1415899_at	P	1.405	Junb	Jun-B oncogene	NM_008416
1451109_a_at	P	1.404	Nedd4	neural precursor cell expressed, developmentally down-regulted gene 4	BG073415
1428847_a_at	P	1.403	Macf1	microtubule-actin crosslinking factor 1	BM248206
1419647_a_at	P	1.403	Ier3	immediate early response 3	NM_133662
1416129_at	P	1.391	1300002F13Rik	RIKEN cDNA 1300002F13 gene	NM_133753
1421333_a_at	P	1.390	Mynn	myoneurin	AK019238
1425188_s_at	P	1.387	Sel1h	Sel1 (suppressor of lin-12) 1 homolog (C. elegans)	BC026816
1417570_at	P	1.380	Anapc1	anaphase promoting complex subunit 1	NM_008569
1415758_at	P	1.377	2010313D22Rik	RIKEN cDNA 2510002A14 gene	BM118442
1454789_x_at	P	1.372	2610031L17Rik	RIKEN cDNA 2610031L17 gene	BB085604
1418023_at	P	1.366	Narg1	NMDA receptor-regulated gene 1	BG067031
1423645_a_at	P	1.363	Ddx5	DEAD (Asp-Glu-Ala-Asp) box polypeptide 5	BC009142
1453260_a_at	P	1.362	Ppp2r2a	protein phosphatase 2 (formerly 2A), regulatory subunit B (PR 52), alpha isoform	AK010380
1430533_a_at	P	1.351	Catnb	catenin beta	BI134907
1427407_s_at	P	1.347		RIKEN cDNA 6030460N08 gene	AV013785
1427456_at	P	1.346	Wdfy3	WD repeat and FYVE domain containing 3	BF150771
1430527_a_at	P	1.344	5730408C10Rik	RIKEN cDNA 5730408C10 gene	AK017523

Table 5-1. Top 800[a] bioweight (BW) genes (continued)

1451847_s_at	P	1.330	Arid4b	AT rich interactive domain 4B (Rbp1 like)	BC024724
1417592_at	P	1.330	Frap1	FK506 binding protein 12-rapamycin associated protein 1	NM_020009
1434846_at	P	1.323	1700065A05Rik	RIKEN cDNA 1700065A05 gene	AW557010
1460240_a_at	P	1.313	Hnrpc	heterogeneous nuclear ribonucleoprotein C	NM_016884
1422539_at	P	1.306	Extl2	exotoses (multiple)-like 2	BM203810
1456615_a_at	P	1.305	Falz	vx16a10.r1 Soares_thymus_2NbMT Mus musculus cDNA clone IMAGE:1264602 5', mRNA sequence.	AA867746
1448127_at	P	1.304	Rrm1	ribonucleotide reductase M1	BB758819
1437349_at	P	1.304	4930432B04Rik	RIKEN cDNA 4930432B04 gene	BE951922
1423711_at	P	1.300	Ndufaf1	NADH dehydrogenase (ubiquinone) 1 alpha subcomplex, assembly factor 1	BC018422
1448497_at	P	1.297	Ercc3	excision repair cross-complementing rodent repair deficiency, complementation group 3	NM_133658
1427140_at	P	1.297	Pvt1	H2A histone family, member Y2	BE956863
1423430_at	P	1.296	Mybbp1a	cDNA sequence BC011467	AW228043
1417279_at	P	1.289	Itpr1	inositol 1,4,5-triphosphate receptor 1	NM_010585
1455372_at	P	1.288	Cpeb3	cytoplasmic polyadenylation element binding protein 3	BB770826
1415916_a_at	P	1.285	Mthfd1	methylenetetrahydrofolate dehydrogenase (NADP+ dependent), methenyltetrahydrofolate cyclohydrolase, formyltetrahydrofolate synthase	NM_138745
1425721_at	P	1.283	Phip	pleckstrin homology domain interacting protein	BI737352
1419356_at	P	1.282	Klf7	Kruppel-like factor 7 (ubiquitous)	BB524597
1425702_a_at	P	1.280	Enpp5	ectonucleotide pyrophosphatase/phosphodiesterase 5	BC011294
1427199_at	P	1.279	2510002A14Rik	RIKEN cDNA 2510002A14 gene	BM118442
1419392_at	P	1.278	Pclo	piccolo (presynaptic cytomatrix protein)	NM_011995
1423086_at	P	1.275	Npc1	RIKEN cDNA 2400010D15 gene	BB769209
1448566_at	P	1.273	Slc40a1	solute carrier family 40 (iron-regulated transporter), member 1	AF226613
1425206_a_at	P	1.269	0610009M14Rik	BB224620 RIKEN full-length enriched, adult male aorta and vein Mus musculus cDNA clone A530087G20 3', mRNA sequence.	BB224620
1455958_s_at	P	1.267	9130017A15Rik	RIKEN cDNA 9130017A15 gene	AI881989
1418019_at	P	1.267	Cpd	carboxypeptidase D	NM_007754
1452496_at	P	1.255	Atp11c	RIKEN cDNA A330005H02 gene	AI593492
1425187_at	P	1.251	Sel1h	Sel1 (suppressor of lin-12) 1 homolog (C. elegans)	BC026816
1448135_at	P	1.247	Atf4	activating transcription factor 4	M94087
1421229_at	P	1.244	Dffb	DNA fragmentation factor, beta subunit	NM_007859
1420557_at	P	1.236	Epha5	Eph receptor A5	NM_007937
1455990_at	P	1.231	Kif23	kinesin family member 23	AW986176
1419099_x_at	P	1.230	Epb7.2	erythrocyte protein band 7.2	AF093620
1425767_a_at	P	1.228	Six4	sine oculis-related homeobox 4 homolog (Drosophila)	D50416
1448116_at	P	1.225	Ube1x	ubiquitin-activating enzyme E1, Chr X	NM_009457
1449138_at	P	1.222	Sf3b1	splicing factor 3b, subunit 1	BE951504
1418288_at	P	1.219	Lpin1	lipin 1	NM_015763
1450162_at	P	1.219	Dpf3	D4, zinc and double PHD fingers, family 3	NM_058212
1422430_at	P	1.212	Fignl1	fidgetin-like 1	NM_021891
1421144_at	P	1.207	Rpgrip1	retinitis pigmentosa GTPase regulator interacting protein 1	NM_023879
1419638_at	P	1.201	Efnb2	ephrin B2	U30244
1416062_at	P	1.196	Tbc1d15	TBC1 domain family, member 15	BF577643

Table 5-1. Top 800[a] bioweight (BW) genes (continued)

1415971_at	P	1.192	Marcks	myristoylated alanine rich protein kinase C substrate	AW546141
1434674_at	P	1.191	Lyst	lysosomal trafficking regulator	BB463428
1425516_at	P	1.189	Ogt	O-linked N-acetylglucosamine (GlcNAc) transferase (UDP-N-acetylglucosamine:polypeptide-N-acetylglucosaminyl transferase)	AF363030
1437203_at	P	1.185	Cbll1	Casitas B-lineage lymphoma-like 1	BB460904
1424988_at	P	1.184	Mylip	myosin regulatory light chain interacting protein	BC010206
1450021_at	P	1.182	Ubqln2	ubiquilin 2	AV171029
1421889_a_at	P	1.180	Aplp2	amyloid beta (A4) precursor-like protein 2	M97216
1418727_at	P	1.180	Nup155	nucleoporin 155	BG073833
1424617_at	P	1.178	Ifi35	interferon-induced protein 35	BC008158
1415997_at	P	1.170	Txnip	thioredoxin interacting protein	AF173681
1426814_at	P	1.168	AU024582	hypothetical protein MGC38812	BM248309
1417379_at	P	1.168	Iqgap1	IQ motif containing GTPase activating protein 1	NM_016721
1456005_a_at	P	1.167	Bcl2l11	BCL2-like 11 (apoptosis facilitator)	BB667581
1454904_at	P	1.166		602846904F1 NCI_CGAP_Mam6 Mus musculus cDNA clone IMAGE:4977457 5', mRNA sequence.	BG976607
1424515_at	P	1.162		BB440272 RIKEN full-length enriched, 9 days embryo Mus musculus cDNA clone D030020O16 3', mRNA sequence.	BB440272
1422198_a_at	P	1.160	Shmt1	serine hydroxymethyl transferase 1 (soluble)	NM_009171
1423030_at	P	1.153	Vcp	Transcribed sequence with strong similarity to protein ref:NP_009057.1 (H.sapiens) valosin-containing protein [Homo sapiens]	AI195225
1420628_at	P	1.145	Pura	purine rich element binding protein A	NM_008989
1423919_at	P	1.133	BC023882	cDNA sequence BC023882	BC027393
1418597_at	P	1.128	Top3a	topoisomerase (DNA) III alpha	NM_009410
1455899_x_at	P	1.127	Socs3	suppressor of cytokine signaling 3	BB241535
1422621_at	P	1.126	Ranbp2	RAN binding protein 2	BM507707
1426895_at	P	1.124	Zfp191	BB579760 RIKEN full-length enriched, 1 day pregnant adult female ovary Mus musculus cDNA clone 7230402O10 5', mRNA sequence.	BB579760
1452448_at	P	1.119	Aqr	aquarius	BE573695
1450034_at	P	1.119	Stat1	signal transducer and activator of transcription 1	AW214029
1417019_a_at	P	1.119	Cdc6	cell division cycle 6 homolog (S. cerevisiae)	NM_011799
1450396_at	P	1.119	Stag2	stromal antigen 2	NM_021465
1423431_a_at	P	1.117	Mybbp1a	cDNA sequence BC011467	AW228043
1451738_at	P	1.111	Ogt	O-linked N-acetylglucosamine (GlcNAc) transferase (UDP-N-acetylglucosamine:polypeptide-N-acetylglucosaminyl transferase)	AF363030
1437752_at	P	1.108	Lin28	BB706377 RIKEN full-length enriched, in vitro fertilized eggs Mus musculus cDNA clone 7420489F16 3', mRNA sequence.	BB706377
1421395_at	P	1.108	Zik1	zinc finger protein interacting with K protein 1	NM_009577
1426957_at	P	1.101	Trp53bp1	transformation related protein 53 binding protein 1	AJ414734
1435862_at	P	1.097	Son	Son cell proliferation protein	BG067046
1452099_at	P	1.097	AA408296	expressed sequence AA408296	BG070043
1424229_at	P	1.096	Dyrk3	dual-specificity tyrosine-(Y)-phosphorylation regulated kinase 3	BC006704
1428105_at	P	1.091	2610005B21Rik	RIKEN cDNA 2610005B21 gene	AK011311
1450700_at	P	1.088	Cdc42ep3	CDC42 effector protein (Rho GTPase binding) 3	BB012489

Table 5-1. Top 800[a] bioweight (BW) genes (continued)

1451137_a_at	P	1.085	Brd8	bromodomain containing 8	BC025644
1433834_at	P	1.085	F830029L24Rik	RIKEN cDNA F830029L24 gene	BQ176049
1423975_s_at	P	1.084	6720401E04Rik	expressed sequence AL022610	BC006631
1427888_a_at	P	1.081	Spna2	spectrin alpha 2	AK011566
1438808_at	P	1.080	Trp53	transformation related protein 53	BB450072
1460409_at	P	1.080	Cpt1a	carnitine palmitoyltransferase 1a, liver	AI987925
1451459_at	P	1.080	Elys	embryonic large molecule derived from yolk sac	BC023122
1418022_at	P	1.076	Narg1	NMDA receptor-regulated gene 1	BG067031
1449548_at	P	1.075	Efnb2	ephrin B2	U30244
1415811_at	P	1.073	Uhrf1	ubiquitin-like, containing PHD and RING finger domains, 1	BB702754
1451432_x_at	P	1.070	2010004B12Rik	RIKEN cDNA 2010004B12 gene	BC022729
1427143_at	P	1.060	Jarid1b	jumonji, AT rich interactive domain 1B (Rbp2 like)	BC019446
1436859_at	P	1.060	2700007P21Rik	RIKEN cDNA 2700007P21 gene	AV342631
1449414_at	P	1.058	Zfp53	Zinc finger protein 118	NM_013843
1450773_at	P	1.056	Kcnd2	potassium voltage-gated channel, Shal-related family, member 2	BB051684
1435369_at	P	1.054	C78212	RIKEN cDNA C330018L13 gene	BM244352
1417792_at	P	1.054	Np220	nuclear protein 220	BM238431
1438418_at	P	1.049	4932432K03Rik	RIKEN cDNA 4932432K03 gene	BB536931
1428225_s_at	P	1.048	Hnrpdl	heterogeneous nuclear ribonucleoprotein D-like	AV101245
1435114_at	P	1.047	D630024B06Rik	RIKEN cDNA D630024B06 gene	C77437
1415703_at	P	1.046	Ureb1	upstream regulatory element binding protein 1e	BM248615
1424516_at	P	1.045		BB440272 RIKEN full-length enriched, 9 days embryo Mus musculus cDNA clone D030020O16 3', mRNA sequence.	BB440272
1426804_at	P	1.045	Smarca4	SWI/SNF related, matrix associated, actin dependent regulator of chromatin, subfamily a, member 4	AW701251
1426842_at	P	1.042	9130022A11Rik	RIKEN cDNA 9130022A11 gene	BB183208
1448325_at	P	1.041	Myd116	myeloid differentiation primary response gene 116	NM_008654
1426002_a_at	P	1.039	Cdc7	cell division cycle 7 (S. cerevisiae)	AB018574
1422248_at	P	1.033	Irs4	insulin receptor substrate 4	NM_010572
1451254_at	P	1.032	Ikbkap	inhibitor of kappa light polypeptide enhancer in B-cells, kinase complex-associated protein	AF367244
1425463_at	P	1.032	Gata6	GATA binding protein 6	BM214048
1424144_at	P	1.030	Ris2	retroviral integration site 2	AF477481
1438211_s_at	P	1.029	Dbp	BB550183 RIKEN full-length enriched, 2 days pregnant adult female oviduct Mus musculus cDNA clone E230020M14 3', mRNA sequence.	BB550183
1427321_s_at	P	1.028	Cxadr	coxsackievirus and adenovirus receptor	AK004908
1433946_at	P	1.028	Zik1	zinc finger protein interacting with K protein 1	BE824681
1421131_a_at	P	1.028	Zfp111	zinc finger protein 111	AV174549
1416250_at	P	1.027	Btg2	B-cell translocation gene 2, anti-proliferative	NM_007570
1456302_at	P	1.023	Pex6	Transcribed sequence with moderate similarity to protein sp:Q13608 (H.sapiens) PEX6_HUMAN Peroxisome assembly factor-2	BB252740
1427923_at	P	1.023	Zmpste24	zinc metalloproteinase, STE24 homolog (S. cerevisiae)	BM233793
1426878_at	P	1.021	2610016F04Rik	RIKEN cDNA 2610016F04 gene	AK020971
1435122_x_at	P	1.019	Dnmt1	DNA methyltransferase (cytosine-5) 1	BB165431
1452002_at	P	1.018	BC024969	cDNA sequence BC024969	BC024969

Table 5-1. Top 800[a] bioweight (BW) genes (continued)

1427949_at	P	1.017	Zfp294	zinc finger protein 294	BM231649
1419354_at	P	1.017	Klf7	Kruppel-like factor 7 (ubiquitous)	BB524597
1418109_at	P	1.015	Gspt2	G1 to phase transition 2	NM_008179
1455534_s_at	P	1.009	Osbpl11	oxysterol binding protein-like 11	BM220135
1421955_a_at	P	1.008	Nedd4	neural precursor cell expressed, developmentally down-regulted gene 4	NM_010890
1425095_at	P	1.007	BC002059	cDNA sequence BC002059	BC002059
1427906_at	P	1.004	1110037F02Rik	RIKEN cDNA 1110037F02 gene	AK012768
1422453_at	P	1.003	Prpf8	pre-mRNA processing factor 8	NM_138659
1436480_at	P	1.001	Dpp7	dipeptidylpeptidase 7	BB746075
1448086_at	P	1.001	D1Ertd164e	Transcribed sequences	BG079429
1450163_a_at	P	1.000	Wrn	Werner syndrome homolog (human)	D86527
1424738_at	P	0.999	4932432K03Rik	RIKEN cDNA 4932432K03 gene	BE288551
1433924_at	P	0.998	Peg3	paternally expressed 3	BM200248
1454157_a_at	P	0.994	Pla2g2d	phospholipase A2, group IID	AK004232
1423550_at	P	0.993	Slc1a4	solute carrier family 1 (glutamate/neutral amino acid transporter), member 4	BB277461
1452315_at	P	0.992	Kif11	kinesin family member 11	BB827235
1452843_at	P	0.991	Il6st	interleukin 6 signal transducer	AK017211
1450690_at	P	0.989	Ranbp2	RAN binding protein 2	BM507707
1422720_at	P	0.989	Isl1	UI-M-DJ2-bwa-g-01-0-UI.s1 NIH_BMAP_DJ2 Mus musculus cDNA clone UI-M-DJ2-bwa-g-01-0-UI 3', mRNA sequence.	BQ176915
1451828_a_at	P	0.988	Acsl4	fatty acid-Coenzyme A ligase, long chain 4	AB033886
1423945_a_at	P	0.988	Pkig	protein kinase inhibitor, gamma	BC026550
1431337_a_at	P	0.986	1810055E12Rik	RIKEN cDNA 1810055E12 gene	AK004643
1417685_at	P	0.984	Ankfy1	ankyrin repeat and FYVE domain containing 1	NM_009671
1427334_s_at	P	0.983	2810474O19Rik	RIKEN cDNA 2810474O19 gene	BE196832
1420295_x_at	P	0.981	T25545	chloride channel 5	T25545
1451274_at	P	0.979	Ogdh	oxoglutarate dehydrogenase (lipoamide)	BC013670
1415985_at	P	0.978	D8Ertd633e	DNA segment, Chr 8, ERATO Doi 633, expressed	NM_133953
1449669_at	P	0.976	E130318E12Rik	RIKEN cDNA E130318E12 gene	AW549708
1422663_at	P	0.976	Orc1l	origin recognition complex, subunit 1-like (S.cereviaiae)	BC015073
1425517_s_at	P	0.974	Ogt	O-linked N-acetylglucosamine (GlcNAc) transferase (UDP-N-acetylglucosamine:polypeptide-N-acetylglucosaminyl transferase)	AF363030
1426817_at	P	0.974	Mki67	antigen identified by monoclonal antibody Ki 67	X82786
1417131_at	P	0.973	Cdc25a	C76119 Mouse 3.5-dpc blastocyst cDNA Mus musculus cDNA clone J0003H02 3' similar to Rat mRNA for cdc25A, mRNA sequence.	C76119
1450108_at	P	0.970	C630002N23Rik	kinesin family member 1A	NM_008440
1448361_at	P	0.970	Ttc3	tetratricopeptide repeat domain 3	BB833716
1436300_at	P	0.967	C430014H23Rik	RIKEN cDNA A930019K20 gene	BB435342
1452611_at	P	0.966	Zfp294	zinc finger protein 294	BM231649
1416791_a_at	P	0.966	Nxf1	nuclear RNA export factor 1 homolog (S. cerevisiae)	BC005594
1453550_a_at	P	0.961	3732409C05Rik	RIKEN cDNA 3732409C05 gene	AK011187
1452385_at	P	0.960	AA939927	expressed sequence AA939927	BG076275
1451317_at	P	0.960	9430020E02Rik	RIKEN cDNA 9430020E02 gene	BB455932
1426380_at	P	0.960	Eif4b	RIKEN cDNA 2310046H11 gene	AW741459
1426068_at	P	0.957	Slc7a4	solute carrier family 7 (cationic amino acid transporter, y+ system), member 4	BC016100

Table 5-1. Top 800[a] bioweight (BW) genes (continued)

1419397_at	P	0.955	Pola1	polymerase (DNA directed), alpha 1	NM_008892
1421881_a_at	P	0.954	Elavl2	ELAV (embryonic lethal, abnormal vision, Drosophila)-like 2 (Hu antigen B)	BB105998
1449099_at	P	0.953	Lrba	LPS-responsive beige-like anchor	NM_030695
1448952_at	P	0.948	A030009H04Rik	RIKEN cDNA A030009H04 gene	AK002962
1426815_s_at	P	0.947	AU024582	hypothetical protein MGC38812	BM248309
1448155_at	P	0.947	Pdcd6ip	programmed cell death 6 interacting protein	BC026823
1426117_a_at	P	0.946	Slc19a2	solute carrier family 19 (thiamine transporter), member 2	AF326916
1421698_a_at	P	0.946	Col19a1	procollagen, type XIX, alpha 1	NM_007733
1424252_at	P	0.944	Hnrpdl	heterogeneous nuclear ribonucleoprotein D-like	BC021374
1420617_at	P	0.941	Cpeb4	cytoplasmic polyadenylation element binding protein 4	NM_026252
1424750_at	P	0.939	Zbtb1	zinc finger and BTB domain containing 1	BC012239
1436908_at	P	0.939	Pcm1	pericentriolar material 1	BG076129
1418443_at	P	0.937	Xpo1	exportin 1, CRM1 homolog (yeast)	BC025628
1422630_at	P	0.936	Rad50	RAD50 homolog (S. cerevisiae)	NM_009012
1425617_at	P	0.935	Dhx9	DEAH (Asp-Glu-Ala-His) box polypeptide 9	U91922
1425242_at	P	0.934	1810006K21Rik	RIKEN cDNA 1810006K21 gene	BC024923
1430692_a_at	P	0.934	Sel1h	Sel1 (suppressor of lin-12) 1 homolog (C. elegans)	AK005023
1416061_at	P	0.933	Tbc1d15	TBC1 domain family, member 15	BF577643
1429745_at	P	0.932	F8a	unnamed protein product; putative weakly similar to UBE-1C2 [Mus musculus] (SPTR|Q9R1R7, evidence: FASTY, 48.7%ID, 99.2%length, match=783); Mus musculus adult female placenta cDNA, RIKEN full-length enriched library, clone:1600013E24 product:weakly similar to UBE-1C2 [Mus musculus], full insert sequence.	AK005439
1450061_at	P	0.929	Enc1	ectodermal-neural cortex 1	BM120053
1459885_s_at	P	0.929	D13Ertd332e	cytochrome c oxidase, subunit VIIc	AA190297
1416041_at	P	0.921	Sgk	serum/glucocorticoid regulated kinase	NM_011361
1417066_at	P	0.920	Cabc1	chaperone, ABC1 activity of bc1 complex like (S. pombe)	AK014605
1426379_at	P	0.918	Eif4b	RIKEN cDNA 2310046H11 gene	AW741459
1449510_at	P	0.917	Zfp467	zinc finger protein 467	NM_020589
1455740_at	P	0.917	Hnrpa1	heterogeneous nuclear ribonucleoprotein A1	BE685966
1420520_x_at	P	0.917	Eral1	Era (G-protein)-like 1 (E. coli)	NM_022313
1454633_at	P	0.912	Etnk1	ethanolamine kinase 1	BG066916
1433552_a_at	P	0.910	Polr2b	polymerase (RNA) II (DNA directed) polypeptide B	BQ177004
1449293_a_at	P	0.909	Skp2	AV259620 RIKEN full-length enriched, adult male testis (DH10B) Mus musculus cDNA clone 4930405J03 3' similar to AF083215 Mus musculus SCF complex protein Skp2 mRNA, mRNA sequence.	AV259620
1421064_at	P	0.905	Mpp5	membrane protein, palmitoylated 5 (MAGUK p55 subfamily member 5)	AW258373
1455904_at	P	0.904	Gas5	growth arrest specific 5	BI650268
1451688_s_at	P	0.902	Entpd8	ectonucleoside triphosphate diphosphohydrolase 6	BC020003
1422094_a_at	P	0.901	2810439M05Rik	RIKEN cDNA 2810439M05 gene	NM_026046
1421070_at	P	0.897	D3Ertd300e	DNA segment, Chr 3, ERATO Doi 300, expressed	NM_019995
1425650_at	P	0.896	Tle4	transducin-like enhancer of split 4, homolog of Drosophila E(spl)	AF229633
1426956_a_at	P	0.895	Trp53bp1	transformation related protein 53 binding protein 1	AJ414734

Table 5-1. Top 800[a] bioweight (BW) genes (continued)

1460562_at	P	0.894	6030468D11Rik	RIKEN cDNA 6030468D11 gene	BB042938
1427737_a_at	P	0.892	1200011M11Rik	RIKEN cDNA 1200011M11 gene	BC002247
1460203_at	P	0.889	Itpr1	inositol 1,4,5-triphosphate receptor 1	NM_010585
1417254_at	P	0.887	Spata5	spermatogenesis associated 5	NM_021343
1426641_at	P	0.887	Trib2	expressed sequence AW319517	BB354684
1430571_s_at	P	0.885	2410153K17Rik	unnamed protein product; hypothetical Armadillo repeat/Armadillo/plakoglobin ARM repeat profile containing protein (InterPro|IPR000225, PROSITE|PS50176, evidence: InterPro) putative; Mus musculus ES cells cDNA, RIKEN full-length enriched library, clone:2410153K17 product:hypothetical Armadillo repeat/Armadillo/plakoglobin ARM repeat profile containing protein, full insert sequence.	AK010815
1452316_at	P	0.884	1110020M19Rik	RIKEN cDNA 1110020M19 gene	AK003874
1426896_at	P	0.881	Zfp191	BB579760 RIKEN full-length enriched, 1 day pregnant adult female ovary Mus musculus cDNA clone 7230402O10 5', mRNA sequence.	BB579760
1435690_at	P	0.878	9030624J02Rik	RIKEN cDNA 9030624J02 gene	BB476775
1426288_at	P	0.878	Lrp4	RIKEN cDNA 6430526J12 gene	AF247637
1438637_x_at	P	0.877	Sf3b2	AV305279 RIKEN full-length enriched, 8 days embryo Mus musculus cDNA clone 5730526P08 3', mRNA sequence.	AV305279
1433685_a_at	P	0.875	6430706D22Rik	RIKEN cDNA 6430706D22 gene	BM248225
1433685_a_at	P	0.875	6430706D22Rik	RIKEN cDNA 6430706D22 gene	BM248225

[a] Five probes included by Affymetrix as controls were removed from this list

[b] Movement into the RNP pool (R) or polysome pool (P)

Table 5-2. Genes identified by SAM[a]

Probe ID	q.value	Gene	Description	Accession
1418255_s_at	0.0744	Srf	serum response factor	BI662291
1422586_at	0.0744	Ecel1	endothelin converting enzyme-like 1	NM_021306
1427985_at	0.0744	9630042H07Rik	RIKEN cDNA 9630042H07 gene	BC027796
1418256_at	0.1116	Srf	serum response factor	BI662291
1417657_s_at	0.1190	Zrf2	zuotin related factor 2	BG067003
1418448_at	0.1190	Rras	Harvey rat sarcoma oncogene, subgroup R	NM_009101
1419292_at	0.1190	9530081K03Rik	RIKEN cDNA 9530081K03 gene	NM_030127
1424002_at	0.1190	Pdcl3	phosducin-like 3	BC005601
1448830_at	0.1190	Dusp1	dual specificity phosphatase 1	NM_013642
1456109_a_at	0.1190	Mrps15	mitochondrial ribosomal protein S15	BB314055
1419529_at	0.1217	Il23a	interleukin 23, alpha subunit p19	NM_031252
1416134_at	0.1259	Aplp1	amyloid beta (A4) precursor-like protein 1	NM_007467
1420368_at	0.1328	Denr	Mus musculus ES cells cDNA, RIKEN full-length enriched library, clone:2410004J11 product:DENSITY-REGULATED PROTEIN (DRP), full insert sequence.	AK010394
1423610_at	0.1376	Metap2	Adult retina cDNA, RIKEN full-length enriched library, clone:A930035J23 product:unknown EST, full insert sequence	BG086961
1424871_s_at	0.1376	1500031H01Rik	cDNA sequence BC013706	BC013706
1425248_a_at	0.1376	Tyro3	TYRO3 protein tyrosine kinase 3	AB000828
1437354_at	0.1376		0 day neonate cerebellum cDNA, RIKEN full-length enriched library, clone:C230091D08 product:unclassifiable, full insert sequence	AI154956
1449029_at	0.1376	Mknk2	MAP kinase-interacting serine/threonine kinase 2	NM_021462
1451959_a_at	0.1376	Vegfa	vascular endothelial growth factor A	U50279
1421260_a_at	0.1381	Srm	spermidine synthase	NM_009272
1422967_a_at	0.1390	Tfrc	transferrin receptor	BB810450
1437133_x_at	0.1390	Akr1b3	2 days pregnant adult female oviduct cDNA, RIKEN full-length enriched library, clone:E230024H01 product:unknown EST, full insert sequence	AV127085
1430533_a_at	0.1456	Catnb	catenin beta	BI134907
1454686_at	0.1487	6430706D22Rik	RIKEN cDNA 6430706D22 gene	BM248225
1417394_at	0.1530	Klf4	Kruppel-like factor 4 (gut)	BG069413
1418300_a_at	0.1530	Mknk2	MAP kinase-interacting serine/threonine kinase 2	NM_021462
1420842_at	0.1530	Ptprf	protein tyrosine phosphatase, receptor type, F	BF235516
1421519_a_at	0.1530	Zfp120	zinc finger protein 120	NM_023266
1422532_at	0.1530	Xpc	xeroderma pigmentosum, complementation group C	NM_009531
1424121_at	0.1530	Commd1	COMM domain containing 1	AB076722
1424766_at	0.1530	BC004701	cDNA sequence BC004701	BC004701
1425188_s_at	0.1530	Sel1h	Sel1 (suppressor of lin-12) 1 homolog (C. elegans)	BC026816
1425231_a_at	0.1530	Zfp46	zinc finger protein 46	BC006587
1426653_at	0.1530	Mcm3	minichromosome maintenance deficient 3 (S. cerevisiae)	BI658327
1426657_s_at	0.1530	Phgdh	3-phosphoglycerate dehydrogenase	L21027
1427913_at	0.1530	Rwdd1	RWD domain containing 1	AK003262
1428076_s_at	0.1530	Ndufb4	NADH dehydrogenase (ubiquinone) 1 beta subcomplex 4	BG968046
1428310_at	0.1530	D3Wsu161e	RIKEN cDNA C330027G06 gene	BF321707
1428340_s_at	0.1530	1110012E06Rik	RIKEN cDNA 1110012E06 gene	BM944122
1433603_at	0.1530	BC059730	CDNA clone IMAGE:6772417, with apparent retained intron	C88200
1434120_a_at	0.1530	Metap2	methionine aminopeptidase 2	AW742814
1435857_s_at	0.1530	Aplp1	amyloid beta (A4) precursor-like protein 1	AI848048

Table 5-2. Genes identified by SAM[a] (continued)

1437621_x_at	0.1530		AV216768 RIKEN full-length enriched, ES cells Mus musculus cDNA clone 2410167D16 3' similar to L21027 Mus musculus A10 mRNA, mRNA sequence.	AV216768
1439415_x_at	0.1530	Rps21	ribosomal protein S21	AV151252
1448319_at	0.1530	Akr1b3	aldo-keto reductase family 1, member B3 (aldose reductase)	NM_009658
1448320_at	0.1530	Stim1	stromal interaction molecule 1	NM_009287
1448439_at	0.1530	D17Wsu104e	interleukin 25	NM_080837
1448440_x_at	0.1530	D17Wsu104e	interleukin 25	NM_080837
1451109_a_at	0.1530	Nedd4	neural precursor cell expressed, developmentally down-regulted gene 4	BG073415
1452519_a_at	0.1530	Zfp36	unnamed protein product; TIS11 (AA 1 - 183); Mouse TPA-induced TIS11 mRNA.	X14678
1455372_at	0.1530	Cpeb3	cytoplasmic polyadenylation element binding protein 3	BB770826
1456244_x_at	0.1530	Txnl2	thioredoxin-like 2	BB458835
1423948_at	0.1554	Bag2	Bcl2-associated athanogene 2	BC016230
1428464_at	0.1554	Ndufa3	NADH dehydrogenase (ubiquinone) 1 alpha subcomplex, 3	AV048277
1460711_at	0.1554	9930116P15Rik	ES cells cDNA, RIKEN full-length enriched library, clone:C330022M23 product:unclassifiable, full insert sequence	BG071611
1415761_at	0.1563	Mrpl52	mitochondrial ribosomal protein L52	AV021593
1415950_a_at	0.1563	Pbp	phosphatidylethanolamine binding protein	NM_018858
1415997_at	0.1563	Txnip	thioredoxin interacting protein	AF173681
1416845_at	0.1563	Hspa5bp1	heat shock 70kDa protein 5 binding protein 1	NM_133804
1417155_at	0.1563	Nmyc1	neuroblastoma myc-related oncogene 1	BC005453
1417389_at	0.1563	Gpc1	glypican 1	NM_016696
1417773_at	0.1563	Nans	602916387F1 NCI_CGAP_Lu29 Mus musculus cDNA clone IMAGE:5067068 5', mRNA sequence.	BI151886
1417774_at	0.1563	Nans	602916387F1 NCI_CGAP_Lu29 Mus musculus cDNA clone IMAGE:5067068 5', mRNA sequence.	BI151886
1418888_a_at	0.1563	Sepr	selenoprotein R	NM_013759
1419356_at	0.1563	Klf7	Kruppel-like factor 7 (ubiquitous)	BB524597
1419550_a_at	0.1563	Stk39	6 days neonate head cDNA, RIKEN full-length enriched library, clone:5430411A13 product:serine/threonine kinase 39, STE20/SPS1 homolog (yeast), full insert sequence	BG919998
1419647_a_at	0.1563	Ier3	immediate early response 3	NM_133662
1420628_at	0.1563	Pura	purine rich element binding protein A	NM_008989
1420811_a_at	0.1563	Catnb	catenin beta	NM_007614
1420878_a_at	0.1563	Ywhab	tyrosine 3-monooxygenase/tryptophan 5-monooxygenase activation protein, beta polypeptide	NM_018753
1422430_at	0.1563	Fignl1	fidgetin-like 1	NM_021891
1422527_at	0.1563	H2-DMa	histocompatibility 2, class II, locus DMa	NM_010386
1422718_at	0.1563	Ap3s2	adaptor-related protein complex 3, sigma 2 subunit	NM_009682
1423294_at	0.1563	Mest	Transcribed sequence with moderate similarity to protein sp:Q9UBF2 (H.sapiens) CPG2_HUMAN Coatomer gamma-2 subunit	AW555393
1423857_at	0.1563	Mrpl30	mitochondrial ribosomal protein L30	BC004614
1423916_s_at	0.1563	Mlf2	myeloid leukemia factor 2	BC003975
1424285_s_at	0.1563	Arl6ip4	ADP-ribosylation factor-like 6 interacting protein 4	AB035383
1424391_at	0.1563	Nrd1	nardilysin, N-arginine dibasic convertase, NRD convertase 1	BC026832
1424988_at	0.1563	Mylip	myosin regulatory light chain interacting protein	BC010206
1425196_a_at	0.1563	Hint2	histidine triad nucleotide binding protein 2	AF356874
1426648_at	0.1563	Mapkapk2	MAP kinase-activated protein kinase 2	BG918951

Table 5-2. Genes identified by SAM[a] (continued)

1426895_at	0.1563	Zfp191	BB579760 RIKEN full-length enriched, 1 day pregnant adult female ovary Mus musculus cDNA clone 7230402O10 5', mRNA sequence.	BB579760
1427490_at	0.1563	Abcb7	ATP-binding cassette, sub-family B (MDR/TAP), member 7	U43892
1428075_at	0.1563	Ndufb4	NADH dehydrogenase (ubiquinone) 1 beta subcomplex 4	BG968046
1428286_at	0.1563	2900097C17Rik	13 days embryo forelimb cDNA, RIKEN full-length enriched library, clone:5930433F13 product:unknown EST, full insert sequence	AW545056
1428869_at	0.1563	Nolc1	nucleolar and coiled-body phosphoprotein 1	BM213850
1429144_at	0.1563	2310032D16Rik	RIKEN cDNA 2310032D16 gene	AV291259
1429850_x_at	0.1563	2010004B12Rik	RIKEN cDNA 2010004B12 gene	AK008083
1448331_at	0.1563	Ndufb7	calmegin	NM_025843
1448346_at	0.1563	Cfl1	cofilin 1, non-muscle	NM_007687
1448566_at	0.1563	Slc40a1	solute carrier family 40 (iron-regulated transporter), member 1	AF226613
1448604_at	0.1563	AA407809	expressed sequence AA407809	NM_030724
1448784_at	0.1563	Taf10	TAF10 RNA polymerase II, TATA box binding protein (TBP)-associated factor	NM_020024
1449080_at	0.1563	Hdac2	histone deacetylase 2	NM_008229
1449294_at	0.1563	Mrps15	mitochondrial ribosomal protein S15	NM_025544
1449324_at	0.1563	Ero1l	Transcribed sequences	BM234652
1450008_a_at	0.1563	Catnb	catenin beta	NM_007614
1451425_a_at	0.1563	Mkrn1	makorin, ring finger protein, 1	BC003329
1452357_at	0.1563	Sept5	septin 5	AF033350
1452646_at	0.1563	1110029F20Rik	RIKEN cDNA 1110029F20 gene	AK003956
1454674_at	0.1563	Fez1	fasciculation and elongation protein zeta 1 (zygin I)	AU067669
1454760_at	0.1563	2600017A12Rik	RIKEN cDNA 2600017A12 gene	AW543705
1455288_at	0.1563	1110036O03Rik	RIKEN cDNA 1110036O03 gene	BE951265
1456128_at	0.1563	Atp5g2	ATP synthase, H+ transporting, mitochondrial F0 complex, subunit c (subunit 9), isoform 2	AW413339
1456471_x_at	0.1563	Phgdh	Transcribed sequence with strong similarity to protein sp:Q61753 (M.musculus) SERA_MOUSE D-3-phosphoglycerate dehydrogenase	BB204486
1417357_at	0.1568	Emd	emerin	NM_007927
1437907_a_at	0.1568	Tbca	tubulin cofactor a	BB559082
1452315_at	0.1568	Kif11	kinesin family member 11	BB827235
1415899_at	0.1571	Junb	Jun-B oncogene	NM_008416
1424750_at	0.1571	Zbtb1	zinc finger and BTB domain containing 1	BC012239
1450878_at	0.1571	Sri	RIKEN cDNA 2210417O06 gene	AK008404
1450981_at	0.1571	Cnn2	calponin 2	BI663014
1416250_at	0.1601	Btg2	B-cell translocation gene 2, anti-proliferative	NM_007570
1416859_at	0.1601	Fkbp3	FK506 binding protein 3	NM_013902
1424488_a_at	0.1601	1110013G13Rik	RIKEN cDNA 1110013G13 gene	BC011417
1428848_a_at	0.1606	Macf1	microtubule-actin crosslinking factor 1	BM248206
1416584_at	0.1607	Man2b2	mannosidase 2, alpha B2	NM_008550
1417792_at	0.1607	Np220	nuclear protein 220	BM238431
1418248_at	0.1607	Gla	galactosidase, alpha	NM_013463
1418545_at	0.1607	Wasf1	WASP family 1	NM_031877
1420971_at	0.1607	Ubr1	ubiquitin protein ligase E3 component n-recognin 1	BQ173927
1421152_a_at	0.1607	Gnao	guanine nucleotide binding protein, alpha o	NM_010308
1421333_a_at	0.1607	Mynn	myoneurin	AK019238
1421889_a_at	0.1607	Aplp2	amyloid beta (A4) precursor-like protein 2	M97216
1421955_a_at	0.1607	Nedd4	neural precursor cell expressed, developmentally down-regulted gene 4	NM_010890
1424269_a_at	0.1607	Myl6	myosin light chain, alkali, nonmuscle	BC026760

Table 5-2. Genes identified by SAM[a] (continued)

1424515_at	0.1607		BB440272 RIKEN full-length enriched, 9 days embryo Mus musculus cDNA clone D030020O16 3', mRNA sequence.	BB440272
1425194_a_at	0.1607	6330577E15Rik	RIKEN cDNA 6330577E15 gene	BC024403
1425206_a_at	0.1607	0610009M14Rik	BB224620 RIKEN full-length enriched, adult male aorta and vein Mus musculus cDNA clone A530087G20 3', mRNA sequence.	BB224620
1426297_at	0.1607	Tcfe2a	transcription factor E2a	AF352579
1427294_a_at	0.1607	1810073N04Rik	RIKEN cDNA 1810073N04 gene	BB406585
1448050_s_at	0.1607	Map4k4	mitogen-activated protein kinase kinase kinase kinase 4	BF450398
1448498_at	0.1607	Rps6ka4	ribosomal protein S6 kinase, polypeptide 4	NM_019924
1448794_s_at	0.1607	Zrf2	zuotin related factor 2	BG067003
1416247_at	0.1617	Dctn3	dynactin 3	NM_016890
1416636_at	0.1617	Rheb	RAS-homolog enriched in brain	NM_053075
1417510_at	0.1617	Vps4a	vacuolar protein sorting 4a (yeast)	NM_126165
1418709_at	0.1617	Cox7a1	cytochrome c oxidase, subunit VIIa 1	AF037370
1426606_at	0.1617	Crtac1	cartilage acidic protein 1	BB426194
1435041_at	0.1617	Myl6	myosin light chain, alkali, nonmuscle	BI108818
1415919_at	0.1632	Npdc1	neural proliferation, differentiation and control gene 1	NM_008721
1416098_at	0.1632	Syngr3	synaptogyrin 3	NM_011522
1416673_at	0.1632	Bace2	beta-site APP-cleaving enzyme 2	NM_019517
1416834_x_at	0.1632	Ndufb2	NADH dehydrogenase (ubiquinone) 1 beta subcomplex, 2	NM_026612
1417379_at	0.1632	Iqgap1	IQ motif containing GTPase activating protein 1	NM_016721
1417380_at	0.1632	Iqgap1	IQ motif containing GTPase activating protein 1	NM_016721
1417585_at	0.1632	Nup210	nucleoporin 210	NM_018815
1417959_at	0.1632	Pdlim7	PDZ and LIM domain 7	NM_026131
1418577_at	0.1632	Trim8	tripartite motif protein 8	BG063064
1418974_at	0.1632	Blzf1	basic leucine zipper nuclear factor 1	AK006544
1419351_a_at	0.1632	0610007P06Rik	RIKEN cDNA 0610007P06 gene	BC003916
1420922_at	0.1632	Usp9x	Similar to ubiquitin specific protease 9, X-linked isoform 2; Drosophila fat facets related, X-linked; ubiquitin specific protease 9, X chromosome (fat facets-like Drosophila) (LOC240170), mRNA	AW107303
1421395_at	0.1632	Zik1	zinc finger protein interacting with K protein 1	NM_009577
1422520_at	0.1632	Nef3	neurofilament 3, medium	NM_008691
1422614_s_at	0.1632	Bloc1s1	GCN5 general control of amino acid synthesis-like 1 (yeast)	NM_015740
1422720_at	0.1632	Isl1	UI-M-DJ2-bwa-g-01-0-UI.s1 NIH_BMAP_DJ2 Mus musculus cDNA clone UI-M-DJ2-bwa-g-01-0-UI 3', mRNA sequence.	BQ176915
1423086_at	0.1632	Npc1	RIKEN cDNA 2400010D15 gene	BB769209
1423804_a_at	0.1632	Idi1	isopentenyl-diphosphate delta isomerase	BC004801
1423919_at	0.1632	BC023882	cDNA sequence BC023882	BC027393
1424396_a_at	0.1632	Asrgl1	asparaginase like 1	AU040643
1424640_at	0.1632	1110033P22Rik	RIKEN cDNA 1110033P22 gene	BC018479
1424684_at	0.1632	Rab5c	RAB5C, member RAS oncogene family	BC023027
1424773_at	0.1632	1110012M11Rik	RIKEN cDNA 1110012M11 gene	BC020119
1428494_a_at	0.1632	Polr2i	polymerase (RNA) II (DNA directed) polypeptide I	BB284638
1430692_a_at	0.1632	Sel1h	Sel1 (suppressor of lin-12) 1 homolog (C. elegans)	AK005023
1433451_at	0.1632	Cdk5r	cyclin-dependent kinase 5, regulatory subunit (p35)	BB177836
1433549_x_at	0.1632	Rps21	ribosomal protein S21	AV123618
1433721_x_at	0.1632	Rps21	ribosomal protein S21	AV123577
1433946_at	0.1632	Zik1	zinc finger protein interacting with K protein 1	BE824681
1434396_a_at	0.1632	Myl6	myosin light chain, alkali, nonmuscle	AU017189
1434442_at	0.1632	D5Ertd593e	DNA segment, Chr 5, ERATO Doi 593, expressed	BB667844

Table 5-2. Genes identified by SAM[a] (continued)

1435067_at	0.1632	B230208H17Rik	RIKEN cDNA B230208H17 gene	BG075288
1435652_a_at	0.1632	Gnai2	uz40a02.x1 NCI_CGAP_Mam5 Mus musculus cDNA clone IMAGE:3671498 3', mRNA sequence.	BF228116
1435690_at	0.1632	9030624J02Rik	RIKEN cDNA 9030624J02 gene	BB476775
1436859_at	0.1632	2700007P21Rik	RIKEN cDNA 2700007P21 gene	AV342631
1438264_a_at	0.1632	Tpp2	tripeptidyl peptidase II	AW536258
1448086_at	0.1632	D1Ertd164e	Transcribed sequences	BG079429
1448592_at	0.1632	Crtap	cartilage associated protein	NM_019922
1449011_at	0.1632	Slc12a7	solute carrier family 12, member 7	BB732135
1449108_at	0.1632	Fdx1	ferredoxin 1	D43690
1449138_at	0.1632	Sf3b1	splicing factor 3b, subunit 1	BE951504
1450700_at	0.1632	Cdc42ep3	CDC42 effector protein (Rho GTPase binding) 3	BB012489
1452002_at	0.1632	BC024969	cDNA sequence BC024969	BC024969
1452099_at	0.1632	AA408296	expressed sequence AA408296	BG070043
1456615_a_at	0.1632	Falz	vx16a10.r1 Soares_thymus_2NbMT Mus musculus cDNA clone IMAGE:1264602 5', mRNA sequence.	AA867746
1456745_x_at	0.1632	Sdbcag84	serologically defined breast cancer antigen 84	BB253632
1418942_at	0.1634	Ccdc2	coiled-coil domain containing 2	NM_026319
1424172_at	0.1634	Hagh	hydroxyacyl glutathione hydrolase	BC004749
1451432_x_at	0.1634	2010004B12Rik	RIKEN cDNA 2010004B12 gene	BC022729
1421698_a_at	0.1640	Col19a1	procollagen, type XIX, alpha 1	NM_007733
1448427_at	0.1640	Ndufa6	NADH dehydrogenase (ubiquinone) 1 alpha subcomplex, 6 (B14)	NM_025987
1415811_at	0.1650	Uhrf1	ubiquitin-like, containing PHD and RING finger domains, 1	BB702754
1416057_at	0.1650	Np15	nuclear protein 15.6	BC027265
1416062_at	0.1650	Tbc1d15	TBC1 domain family, member 15	BF577643
1416129_at	0.1650	1300002F13Rik	RIKEN cDNA 1300002F13 gene	NM_133753
1416495_s_at	0.1650	Ndufs5	NADH dehydrogenase (ubiquinone) Fe-S protein 5	NM_134104
1416528_at	0.1650	Sh3bgrl3	SH3 domain binding glutamic acid-rich protein-like 3	NM_080559
1416782_s_at	0.1650	DXImx39e	DNA segment, Chr X, Immunex 39, expressed	NM_138602
1417594_at	0.1650	Gkap42	cGMP-dependent protein kinase anchoring protein	NM_019832
1418443_at	0.1650	Xpo1	exportin 1, CRM1 homolog (yeast)	BC025628
1419803_s_at	0.1650	2700094L05Rik	RIKEN cDNA 2700094L05 gene	C76605
1421266_s_at	0.1650	Nfkbib	nuclear factor of kappa light chain gene enhancer in B-cells inhibitor, beta	NM_010908
1421881_a_at	0.1650	Elavl2	ELAV (embryonic lethal, abnormal vision, Drosophila)-like 2 (Hu antigen B)	BB105998
1421903_at	0.1650	2810405O22Rik	RIKEN cDNA 2810405O22 gene	AK005112
1422597_at	0.1650	Mmp15	matrix metalloproteinase 15	NM_008609
1422683_at	0.1650	Irak1bp1	interleukin-1 receptor-associated kinase 1 binding protein 1	NM_022986
1422966_a_at	0.1650	Tfrc	transferrin receptor	BB810450
1424738_at	0.1650	4932432K03Rik	RIKEN cDNA 4932432K03 gene	BE288551
1425721_at	0.1650	Phip	pleckstrin homology domain interacting protein	BI737352
1425940_a_at	0.1650	Ssbp3	single-stranded DNA binding protein 3	AF170906
1427309_at	0.1650	BC027073	cDNA sequence BC027073	BF583012
1428842_a_at	0.1650	Ngfrap1	nerve growth factor receptor (TNFRSF16) associated protein 1	BI407690
1428954_at	0.1650	Slc9a3r2	solute carrier family 9 (sodium/hydrogen exchanger), isoform 3 regulator 2	AK004710
1430571_s_at	0.1650	2410153K17Rik	unnamed protein product; hypothetical Armadillo repeat/Armadillo/plakoglobin ARM repeat profile containing protein (InterPro|IPR000225, PROSITE|PS50176, evidence: InterPro) putative; Mus musculus ES cells cDNA, RIKEN full-length enriched library, clone:2410153K17 product:hypothetical Armadillo repeat/Armadillo/plakoglobin ARM repeat profile containing protein, full insert sequence.	AK010815

Table 5-2. Genes identified by SAM[a] (continued)

1433554_at	0.1650	AU022870	hypothetical protein MGC56855	BM246500
1434392_at	0.1650	Usp34	U2af1-rs1 region 2	BM235696
1434872_x_at	0.1650	Rpl37	AV170241 Mus musculus head C57BL/6J 13-day embryo Mus musculus cDNA clone 3110094P05, mRNA sequence.	AV170241
1448876_at	0.1650	Evc	Ellis van Creveld gene homolog (human)	NM_021292
1448917_at	0.1650	Thrap6	thyroid hormone receptor associated protein 6	NM_027212
1448952_at	0.1650	A030009H04Rik	RIKEN cDNA A030009H04 gene	AK002962
1450466_at	0.1650		Adult male corpora quadrigemina cDNA, RIKEN full-length enriched library, clone:B230310J22 product:unclassifiable, full insert sequence	BI739719
1450925_a_at	0.1650	Rps27l	ribosomal protein S27-like	BB836796
1452790_x_at	0.1650	Ndufa3	NADH dehydrogenase (ubiquinone) 1 alpha subcomplex, 3	AV048277
1453550_a_at	0.1650	3732409C05Rik	RIKEN cDNA 3732409C05 gene	AK011187
1455039_a_at	0.1650	Sin3b	transcriptional regulator, SIN3B (yeast)	BF017589
1433991_x_at	0.1660	Dbi	diazepam binding inhibitor	AV007315
1451291_at	0.1660	2610036N15Rik	RIKEN cDNA 2610036N15 gene	BC026942
1460675_at	0.1660	Igsf8	immunoglobulin superfamily, member 8	AF411055
1460718_s_at	0.1660	Mtch1	mitochondrial carrier homolog 1 (C. elegans)	AF192558
1416245_at	0.1678	0610033H09Rik	RIKEN cDNA 0610033H09 gene	NM_025338
1416910_at	0.1692	Dnajd1	DnaJ (Hsp40) homolog, subfamily D, member 1	NM_025384
1417652_a_at	0.1692	Tbca	tubulin cofactor a	NM_009321
1418123_at	0.1692	Unc119	unc-119 homolog (C. elegans)	BC001990
1418273_a_at	0.1692	Rpl30	ribosomal protein L30	NM_009083
1418714_at	0.1692	Dusp8	dual specificity phosphatase 8	NM_008748
1418918_at	0.1692	Igfbp1	insulin-like growth factor binding protein 1	NM_008341
1420402_at	0.1692	Atp2b2	ATPase, Ca++ transporting, plasma membrane 2	NM_009723
1420617_at	0.1692	Cpeb4	cytoplasmic polyadenylation element binding protein 4	NM_026252
1422134_at	0.1692	Fosb	FBJ osteosarcoma oncogene B	NM_008036
1422507_at	0.1692	Cstb	cystatin B	NM_007793
1425384_a_at	0.1692	Ube4a	ubiquitination factor E4A, UFD2 homolog (S. cerevisiae)	BC006649
1426659_a_at	0.1692	BC029892	Similar to 60S ribosomal protein L23a (LOC268449), mRNA	BF178310
1427173_a_at	0.1692	Mrps33	mitochondrial ribosomal protein S33	Y17852
1434053_x_at	0.1692	Atp5k	ATP synthase, H+ transporting, mitochondrial F1F0 complex, subunite	AV216686
1436510_a_at	0.1692	Lrrfip2	leucine rich repeat (in FLII) interacting protein 2	BE456782
1448685_at	0.1692	2900010M23Rik	RIKEN cDNA 2900010M23 gene	NM_026063
1451012_a_at	0.1692	Csda	AV216648 RIKEN full-length enriched, ES cells Mus musculus cDNA clone 2410165I03 3' similar to D14485 Mouse mRNA for dbpA murine homologue, mRNA sequence.	AV216648
1451211_a_at	0.1692	Lgtn	ligatin	BC025036
1451255_at	0.1692	Lisch7	liver-specific bHLH-Zip transcription factor	BC004672
1451602_at	0.1692	Snx6	sorting nexin 6	BC025911
1453362_x_at	0.1692	Rps24	ribosomal protein S24	AK008386
1415971_at	0.1702	Marcks	myristoylated alanine rich protein kinase C substrate	AW546141
1417131_at	0.1702	Cdc25a	C76119 Mouse 3.5-dpc blastocyst cDNA Mus musculus cDNA clone J0003H02 3' similar to Rat mRNA for cdc25A, mRNA sequence.	C76119
1421131_a_at	0.1702	Zfp111	zinc finger protein 111	AV174549
1424110_a_at	0.1702	Nme1	expressed in non-metastatic cells 1, protein	BC005629
1425702_a_at	0.1702	Enpp5	ectonucleotide pyrophosphatase/phosphodiesterase 5	BC011294
1426244_at	0.1702	Mapre2	microtubule-associated protein, RP/EB family, member 2	BC027056

Table 5-2. Genes identified by SAM[a] (continued)

1426641_at	0.1702	Trib2	expressed sequence AW319517	BB354684
1426660_x_at	0.1702	BC029892	Similar to 60S ribosomal protein L23a (LOC268449), mRNA	BF178310
1427335_at	0.1702	6720456H20Rik	BB238358 RIKEN full-length enriched, 3 days neonate thymus Mus musculus cDNA clone A630071E21 3', mRNA sequence.	BB238358
1428453_at	0.1702	4930487N19Rik	RIKEN cDNA 4930487N19 gene	AK017805
1439389_s_at	0.1702	Myadm	BB500055 RIKEN full-length enriched, 0 day neonate kidney Mus musculus cDNA clone D630024J02 3' similar to AJ001616 Mus musculus mRNA for myeloid associated differentiation protein, mRNA sequence.	BB500055
1450162_at	0.1702	Dpf3	D4, zinc and double PHD fingers, family 3	NM_058212
1417886_at	0.1707	1810009A15Rik	RIKEN cDNA 1110055N21 gene	BE307471
1434561_at	0.1709	Asxl1	additional sex combs like 1 (Drosophila)	BI648411
1448127_at	0.1709	Rrm1	ribonucleotide reductase M1	BB758819
1450350_a_at	0.1709	Jundm2	Jun dimerization protein 2	NM_030887
1452143_at	0.1709	Spnb2	spectrin beta 2	BQ174069
1439368_a_at	0.1719	Slc9a3r2	AV002797 Mus musculus C57BL/6J kidney Mus musculus cDNA clone 0610020H24, mRNA sequence.	AV002797
1449633_s_at	0.1721	C330027I04Rik	RIKEN cDNA C330027I04 gene	AI841843
1418019_at	0.1734	Cpd	carboxypeptidase D	NM_007754
1420909_at	0.1734	Vegfa	vascular endothelial growth factor A	NM_009505
1421255_a_at	0.1734	Cabp1	calcium binding protein 1	NM_013879
1422489_at	0.1734	Gcs1	glucosidase 1	NM_020619
1422807_at	0.1734	Arf5	ADP-ribosylation factor 5	NM_007480
1422882_at	0.1734	Sypl	synaptophysin-like protein	BE333485
1427876_at	0.1734	2610312B22Rik	RIKEN cDNA 2610312B22 gene	BB703070
1448483_a_at	0.1734	Ndufb2	NADH dehydrogenase (ubiquinone) 1 beta subcomplex, 2	NM_026612
1452184_at	0.1734	Ndufb9	NADH dehydrogenase (ubiquinone) 1 beta subcomplex, 9	W29413
1416367_at	0.1743	1110001J03Rik	RIKEN cDNA 1110001J03 gene	NM_025363
1416519_at	0.1743	Rpl36	ribosomal protein L36	NM_018730
1417348_at	0.1743	2310039H08Rik	male enhanced antigen 1	NM_025966
1418022_at	0.1743	Narg1	NMDA receptor-regulated gene 1	BG067031
1421052_a_at	0.1743	Sms	spermine synthase	NM_009214
1424315_at	0.1743	1110004E09Rik	RIKEN cDNA 1110004E09 gene	BC019533
1424456_at	0.1743	Pvrl2	poliovirus receptor-related 2	BC009088
1424894_at	0.1743	Rab13	RAB13, member RAS oncogene family	BC027214
1425617_at	0.1743	Dhx9	DEAH (Asp-Glu-Ala-His) box polypeptide 9	U91922
1427143_at	0.1743	Jarid1b	jumonji, AT rich interactive domain 1B (Rbp2 like)	BC019446
1427943_at	0.1743	Acyp2	acylphosphatase 2, muscle type	BI730288
1428164_at	0.1743	Nudt9	nudix (nucleoside diphosphate linked moiety X)-type motif 9	AK004444
1428214_at	0.1743	Tomm7	translocase of outer mitochondrial membrane 7 homolog (yeast)	BB609428
1428679_s_at	0.1743	0610010K14Rik	RIKEN cDNA 0610010K14 gene	AK003842
1429473_at	0.1743	1200003I07Rik	RIKEN cDNA 1200003I07 gene	AV292561
1430295_at	0.1743	Gna13	guanine nucleotide binding protein, alpha 13	BG094302
1433616_a_at	0.1743	2310028O11Rik	Adult male xiphoid cartilage cDNA, RIKEN full-length enriched library, clone:5230400C04 product:unknown EST, full insert sequence	BG793007
1435517_x_at	0.1743	Ralb	BB465250 RIKEN full-length enriched, 12 days embryo spinal ganglion Mus musculus cDNA clone D130097N13 3' similar to L19699 Rat GTP-binding protein (ral B) mRNA, mRNA sequence.	BB465250
1436121_a_at	0.1743	2510027N19Rik	RIKEN cDNA 2510027N19 gene	BI903760

Table 5-2. Genes identified by SAM[a] (continued)

1437013_x_at	0.1743	Atp6v0b	AV339131 RIKEN full-length enriched, adult male olfactory bulb Mus musculus cDNA clone 6430502C13 3', mRNA sequence.	AV339131
1437450_x_at	0.1743	2700060E02Rik	RIKEN cDNA 2700060E02 gene	AV167877
1438986_x_at	0.1743	Rps17	ribosomal protein S17	AV064451
1450638_at	0.1743	Pdcd5	programmed cell death 5	AF161074
1451017_at	0.1743	Sdbcag84	BB556862 RIKEN full-length enriched, 2 days pregnant adult female ovary Mus musculus cDNA clone E330025K14 3' similar to AL161963 Homo sapiens mRNA; cDNA DKFZp547A2190 (from clone DKFZp547A2190), mRNA sequence.	BB556862
1452164_at	0.1743	BC038286	cDNA sequence BC038286	BI647183
1452679_at	0.1743	2410129E14Rik	Transcribed sequence with strong similarity to protein ref:NP_001060.1 (H.sapiens) tubulin, beta polypeptide [Homo sapiens]	AA986082
1456590_x_at	0.1743	Akr1b3	BB469763 RIKEN full-length enriched, 12 days embryo eyeball Mus musculus cDNA clone D230028K07 3' similar to L39795 Mus musculus (clone MAR1) aldose reductase mRNA, mRNA sequence.	BB469763
1460697_s_at	0.1743	2610209M04Rik	RIKEN cDNA 2610209M04 gene	BC027564
1460739_at	0.1743	D11Bwg0280e	DNA segment, Chr 11, Brigham & Women's Genetics 0280e expressed	BQ174371
1416922_a_at	0.1751	Bnip3l	BCL2/adenovirus E1B 19kDa-interacting protein 3-like	AK018668
1422432_at	0.1751	Dbi	diazepam binding inhibitor	NM_007830
1423321_at	0.1751	Myadm	myeloid-associated differentiation marker	BI078799
1423087_a_at	0.1757	1110002E23Rik	RIKEN cDNA 1110002E23 gene	BB453951
1418910_at	0.1758	Bmp7	bone morphogenetic protein 7	NM_007557
1427938_at	0.1764	Mycbp	c-myc binding protein	BB046347
1427903_at	0.1765	Phpt1	RIKEN cDNA 1700008C22 gene	BB650419
1422524_at	0.1767	Abcb6	ATP-binding cassette, sub-family B (MDR/TAP), member 6	NM_023732
1418439_at	0.1774	2900055D03Rik	RIKEN cDNA 2900055D03 gene	NM_026065
1422608_at	0.1774	Arpp19	cAMP-regulated phosphoprotein 19	BE648432
1423507_a_at	0.1774	Sirt2	Transcribed sequence with moderate similarity to protein ref:NP_036369.2 (H.sapiens) sirtuin 2, isoform 1; SIR2	BB807595
1424753_at	0.1774	Nudt14	nudix (nucleoside diphosphate linked moiety X)-type motif 14	BC025444
1424771_at	0.1774	E130307C13	hypothetical protein E130307C13	BF661121
1431771_a_at	0.1774	Irak1bp1	interleukin-1 receptor-associated kinase 1 binding protein 1	AK014712
1436803_a_at	0.1774	Ndufb9	NADH dehydrogenase (ubiquinone) 1 beta subcomplex, 9	AV161987
1449040_a_at	0.1774	Sephs2	selenophosphate synthetase 2	NM_009266
1455950_x_at	0.1774	Rpl35	RIKEN cDNA 1700123D08 gene	AV172221
1456381_x_at	0.1774	Mcl1	myeloid cell leukemia sequence 1	AV274748
1418327_at	0.1775	1110058L19Rik	RIKEN cDNA 1110058L19 gene	NM_026503
1415879_a_at	0.1804	Rplp2	ribosomal protein, large P2	BC012413
1423653_at	0.1804	Atp1a1	ATPase, Na+/K+ transporting, alpha 1 polypeptide	BC025618
1426940_at	0.1804	BC023957	cDNA sequence BC023957	BI412808
1434325_x_at	0.1804	Prkar1b	BB274009 RIKEN full-length enriched, 10 days neonate cortex Mus musculus cDNA clone A830086C24 3', mRNA sequence.	BB274009
1451259_at	0.1804	Smfn	small fragment nuclease	BC003445
1452726_a_at	0.1804	1110061L23Rik	RIKEN cDNA 1110061L23 gene	AK016797
1456691_s_at	0.1804	Srd5a2l	BB825787 RIKEN full-length enriched, mammary gland RCB-0526 Jyg-MC(A) cDNA Mus musculus cDNA clone G830039K08 3', mRNA sequence.	BB825787

Table 5-2. Genes identified by SAM[a] (continued)

1422480_at	0.1805	Snx3	sorting nexin 3	NM_017472
1426744_at	0.1805	Srebf2	sterol regulatory element binding factor 2	BM123132
1448540_a_at	0.1805	0610012G03Rik	RIKEN cDNA 0610012G03 gene	BC021536
1451385_at	0.1805	2310056P07Rik	RIKEN cDNA 2310056P07 gene	BC010826
1423210_a_at	0.1808	Nola3	nucleolar protein family A, member 3	AK004120
1449267_at	0.1808	3110023E09Rik	RIKEN cDNA 3110023E09 gene	BC006876
1452246_at	0.1808	Ostf1	osteoclast stimulating factor 1	U58888
1454870_x_at	0.1808	D15Ertd747e	DNA segment, Chr 15, ERATO Doi 747, expressed	BB251205
1416480_a_at	0.1810	Hig1	hypoxia induced gene 1	NM_019814
1417320_at	0.1810	Grpel1	GrpE-like 1, mitochondrial	NM_024478
1417399_at	0.1810	Gas6	growth arrest specific 6	NM_019521
1418244_at	0.1810	Nat5	N-acetyltransferase 5 (ARD1 homolog, S. cerevisiae)	NM_026425
1422011_s_at	0.1810	Xlr	X-linked lymphocyte-regulated complex	BC005560
1422716_a_at	0.1810	Acp1	acid phosphatase 1, soluble	AW554436
1426510_at	0.1810	C330023F11Rik	RIKEN cDNA C330023F11 gene	AW537824
1438659_x_at	0.1810	0710001P09Rik	BB458460 RIKEN full-length enriched, 12 days embryo spinal ganglion Mus musculus cDNA clone D130057E08 3', mRNA sequence.	BB458460
1449190_a_at	0.1810	Lysal1	lysosomal apyrase-like 1	NM_026174
1449289_a_at	0.1810	B2m	RIKEN cDNA E130113K22 gene	BF715219
1449302_at	0.1810	Abca2	ATP-binding cassette, sub-family A (ABC1), member 2	NM_007379
1460670_at	0.1810	Riok3	RIO kinase 3 (yeast)	NM_024182
1426960_a_at	0.1813	Fa2h	fatty acid 2-hydroxylase	BM118638
1452111_at	0.1813	Mrps35	mitochondrial ribosomal protein S35	AV304074
1417026_at	0.1814	Pfdn1	prefoldin 1	BC024693
1421500_at	0.1826	Sts	steroid sulfatase	NM_009293
1423764_s_at	0.1826	Mrpl37	mitochondrial ribosomal protein L37	BC011065
1424073_at	0.1826	5430437P03Rik	RIKEN cDNA 5430437P03 gene	BC005692
1426209_at	0.1826	Strn4	striatin, calmodulin binding protein 4	AF414080
1436236_x_at	0.1826	Cotl1	coactosin-like 1 (Dictyostelium)	AI327078
1452272_a_at	0.1826	Gfer	growth factor, erv1 (S. cerevisiae)-like (augmenter of liver regeneration)	BI901126
1419299_at	0.1830	2010012O05Rik	RIKEN cDNA 2010012O05 gene	NM_025563
1439466_s_at	0.1830	Ptcd1	BB001490 RIKEN full-length enriched, 13 days embryo head Mus musculus cDNA clone 3110026K15 3' similar to AF058791 Rattus norvegicus G10 protein homolog (edg2) mRNA, mRNA sequence.	BB001490
1418229_s_at	0.1831	Hirip5	histone cell cycle regulation defective interacting protein 5	BC018355
1422977_at	0.1831	Gp1bb	glycoprotein Ib, beta polypeptide	NM_010327
1424708_at	0.1831	1110014C03Rik	RIKEN cDNA 1110014C03 gene	BI409239
1416231_at	0.1839	D8Wsu151e	synonyms: Trx, Vac14, Tax1bp2, BC032215, MGC38230; cDNA sequence BC032215; Tax1 (human T-cell leukemia virus type I) binding protein 1; Tax1 (human T-cell leukemia virus type I) binding protein 2; vacuole morphology 14 (yeast); Mus musculus DNA segment, Chr 8, Wayne State University 151, expressed (D8Wsu151e), mRNA.	NM_138588
1416494_at	0.1839	Ndufs5	NADH dehydrogenase (ubiquinone) Fe-S protein 5	NM_134104
1416881_at	0.1839	Mcl1	myeloid cell leukemia sequence 1	BC003839
1419352_at	0.1839	0610007P06Rik	RIKEN cDNA 0610007P06 gene	BC003916
1423133_at	0.1839	0610040D20Rik	RIKEN cDNA 0610040D20 gene	BG071645
1423737_at	0.1839	Ndufs3	NADH dehydrogenase (ubiquinone) Fe-S protein 3	BC027270
1438391_x_at	0.1839	Hadh2	hydroxyacyl-Coenzyme A dehydrogenase type II	AV078914

Table 5-2. Genes identified by SAM[a] (continued)

1449381_a_at	0.1839	Pacsin1	protein kinase C and casein kinase substrate in neurons 1	BI731319
1449855_s_at	0.1839	Uchl3	ubiquitin carboxyl-terminal esterase L3 (ubiquitin thiolesterase)	AB033370
1450389_s_at	0.1839	Pip5k1a	phosphatidylinositol-4-phosphate 5-kinase, type 1 alpha	NM_008846
1451045_at	0.1839	Syt13	synaptotagmin 13	BE648447
1451091_at	0.1839	Txndc5	thioredoxin domain containing 5	BC016252
1455640_a_at	0.1839	Txn2	AV053127 Mus musculus pancreas C57BL/6J adult Mus musculus cDNA clone 1810025B13, mRNA sequence.	AV053127
1417511_at	0.1841	Lyar	Ly1 antibody reactive clone	NM_025281
1418072_at	0.1841	Hist1h2bc	histone 1, H2bc	NM_023422
1419398_a_at	0.1841	Dp1	deleted in polyposis 1	NM_007874
1419456_at	0.1841	Dcxr	dicarbonyl L-xylulose reductase	BC012247
1460354_a_at	0.1841	Mrpl13	mitochondrial ribosomal protein L13	AB049641
1431208_a_at	0.1844	Slc9a3r2	solute carrier family 9 (sodium/hydrogen exchanger), isoform 3 regulator 2	BF468098
1424394_at	0.1846	Sepm	selenoprotein M	AY043488
1435695_a_at	0.1846	A030007L17Rik	RIKEN cDNA A030007L17 gene	AA673177
1416836_at	0.1851	Lrp10	low-density lipoprotein receptor-related protein 10	BC011058
1417368_s_at	0.1851	Ndufa2	NADH dehydrogenase (ubiquinone) 1 alpha subcomplex, 2	NM_010885
1418588_at	0.1851	Vmp	vesicular membrain protein p24	NM_009513
1418970_a_at	0.1851	Bcl10	B-cell leukemia/lymphoma 10	AF100339
1423501_at	0.1851	Max	Max protein	AA617392
1435873_a_at	0.1851	Rpl13a	Transcribed sequence with strong similarity to protein pir:S29539 (H.sapiens) S29539 ribosomal protein L13a, cytosolic - human	AI324936
1460257_a_at	0.1851	Mthfs	5, 10-methenyltetrahydrofolate synthetase	NM_026829
1416285_at	0.1862	Ndufc1	NADH dehydrogenase (ubiquinone) 1, subcomplex unknown, 1	NM_025523
1416795_at	0.1862	Cryl1	crystallin, lamda 1	NM_030004
1417467_a_at	0.1862	Tada3l	transcriptional adaptor 3 (NGG1 homolog, yeast)-like	AK003405
1417604_at	0.1862	Camk1	calcium/calmodulin-dependent protein kinase I	NM_133926
1418226_at	0.1862	Orc2l	origin recognition complex, subunit 2-like (S. cerevisiae)	BB830976
1421022_x_at	0.1862	Acyp1	acylphosphatase 1, erythrocyte (common) type	NM_025421
1422778_at	0.1862	Taf9	TAF9 RNA polymerase II, TATA box binding protein (TBP)-associated factor	NM_027139
1425300_at	0.1862	BC021917	cDNA sequence BC021917	BC021917
1426658_x_at	0.1862	Phgdh	3-phosphoglycerate dehydrogenase	L21027
1428023_at	0.1862	3110009E18Rik	RIKEN cDNA 3110009E18 gene	AA879840
1434976_x_at	0.1862	Eif4ebp1	AV216412 RIKEN full-length enriched, ES cells Mus musculus cDNA clone 2410160M04 3' similar to U28656 Mus musculus insulin-stimulated eIF-4E binding protein PHAS-I mRNA, mRNA sequence.	AV216412
1435712_a_at	0.1862	Rps18	Transcribed sequence with strong similarity to protein ref:NP_072045.1 (H.sapiens) ribosomal protein S18; 40S ribosomal protein S18 [Homo sapiens]	AW907444
1438655_a_at	0.1862	1100001I22Rik	RIKEN cDNA 1100001I22 gene	AV057789
1449372_at	0.1862	Dnajc3	DnaJ (Hsp40) homolog, subfamily C, member 3	BE624323
1452367_at	0.1862	Coro2a	tripartite motif-containing 14	AI316747
1416417_a_at	0.1881	Ndufb7	calmegin	NM_025843
1416945_at	0.1881	Ptov1	prostate tumor over expressed gene 1	NM_133949
1417098_s_at	0.1881	Nrbf1	nuclear receptor binding factor 1	NM_025297
1419259_at	0.1881	Rsu1	Ras suppressor protein 1	NM_009105

Table 5-2. Genes identified by SAM[a] (continued)

1434019_at	0.1881	Pdap1	PDGFA associated protein 1	BG065186
1437679_a_at	0.1881	Glrx2	BB172698 RIKEN full-length enriched, adult male hypothalamus Mus musculus cDNA clone A230040G05 3', mRNA sequence.	BB172698
1426241_a_at	0.1885	Scmh1	sex comb on midleg homolog 1	AB030906
1436949_a_at	0.1885	Tceb2	AV068352 Mus musculus small intestine C57BL/6J adult Mus musculus cDNA clone 2010303D07, mRNA sequence.	AV068352
1437164_x_at	0.1885	Atp5o	ATP synthase, H+ transporting, mitochondrial F1 complex, O subunit	AV066932
1415681_at	0.1889	Mrpl43	mitochondrial ribosomal protein L43	NM_053164
1415762_x_at	0.1889	Mrpl52	mitochondrial ribosomal protein L52	AV021593
1415932_x_at	0.1889	Atp9a	ATPase, class II, type 9A	NM_015731
1416074_a_at	0.1889	Rpl28	ribosomal protein L28	NM_009081
1416349_at	0.1889	Mrpl34	mitochondrial ribosomal protein L34	NM_053162
1416816_at	0.1889	Nek7	NIMA (never in mitosis gene a)-related expressed kinase 7	NM_021605
1416965_at	0.1889	Pcsk1n	proprotein convertase subtilisin/kexin type 1 inhibitor	AF181560
1417103_at	0.1889	Ddt	D-dopachrome tautomerase	NM_010027
1417124_at	0.1889	Dstn	destrin	NM_019771
1417340_at	0.1889	Txnl2	thioredoxin-like 2	NM_023140
1417487_at	0.1889	Fosl1	fos-like antigen 1	U34245
1417488_at	0.1889	Fosl1	fos-like antigen 1	U34245
1417722_at	0.1889	Pgls	6-phosphogluconolactonase	BC006594
1418000_a_at	0.1889	Itm2b	integral membrane protein 2B	NM_008410
1418901_at	0.1889	Cebpb	CCAAT/enhancer binding protein (C/EBP), beta	NM_009883
1420626_at	0.1889	2410016F19Rik	RIKEN cDNA 2410016F19 gene	BF782285
1422185_a_at	0.1889	Dia1	diaphorase 1 (NADH)	NM_029787
1422615_at	0.1889	Map4k4	mitogen-activated protein kinase kinase kinase kinase 4	NM_008696
1423090_x_at	0.1889	Sec61g	Transcribed sequence with strong similarity to protein sp:P38384 (H.sapiens) S61G_HUMAN Protein transport protein SEC61 gamma subunit	AV216331
1423967_at	0.1889	Palm	paralemmin	BC015297
1424204_at	0.1889	Mrpl13	mitochondrial ribosomal protein L13	AB049641
1424222_s_at	0.1889	Rad23b	Mus musculus cDNA clone IMAGE:3256899, complete cds.	BC006751
1427939_s_at	0.1889	Mycbp	c-myc binding protein	BB046347
1434882_at	0.1889	2610103J23Rik	RIKEN cDNA 2610103J23 gene	AV083741
1435800_a_at	0.1889	Csda	BB779100 RIKEN full-length enriched, bladder RCB-0544 MBT-2 cDNA Mus musculus cDNA clone G430050O16 3', mRNA sequence.	BB779100
1435807_at	0.1889	Cdc42	cell division cycle 42 homolog (S. cerevisiae)	BF467211
1438001_x_at	0.1889	Dp1	deleted in polyposis 1	AV054377
1448333_at	0.1889	Adprh	ADP-ribosylarginine hydrolase	AF244347
1448971_at	0.1889	2410022L05Rik	RIKEN cDNA 2410022L05 gene	NM_025556
1450795_at	0.1889	Lhb	luteinizing hormone beta	NM_008497
1451071_a_at	0.1889	Atp1a1	ATPase, Na+/K+ transporting, alpha 1 polypeptide	BC025618
1451399_at	0.1889	Brp17	brain protein 17	BC008274
1452596_at	0.1889	Polr2k	polymerase (RNA) II (DNA directed) polypeptide K	AA175187
1456584_x_at	0.1889	Phgdh	BB495884 RIKEN full-length enriched, 13 days embryo stomach Mus musculus cDNA clone D530050H10 3' similar to L21027 Mus musculus A10 mRNA, mRNA sequence.	BB495884
1452754_at	0.1898	5730592L21Rik	RIKEN cDNA 5730592L21 gene	AK017880
1424900_at	0.1903	Slc29a4	solute carrier family 29 (nucleoside transporters), member 4	BC025599
1448292_at	0.1903	Uqcr	ubiquinol-cytochrome c reductase (6.4kD) subunit	NM_025650
1423242_at	0.1904	Mrps36	mitochondrial ribosomal protein S36	BE627004

Table 5-2. Genes identified by SAM[a] (continued)

1426475_at	0.1904	Hmbs	Similar to Hydroxymethylbilane synthase (LOC383565), mRNA	AI325144
1449256_a_at	0.1904	Rab11a	RAB11a, member RAS oncogene family	BC010722
1429411_a_at	0.1907	1810057B09Rik	RIKEN cDNA 1810057B09 gene	AI595744
1435431_at	0.1907	2310047M15Rik	RIKEN cDNA 2310047M15 gene	AW558989
1439451_x_at	0.1907	D15Ertd747e	BB487787 RIKEN full-length enriched, 13 days embryo lung Mus musculus cDNA clone D430044J16 3', mRNA sequence.	BB487787
1448656_at	0.1907	Cacnb3	calcium channel, voltage-dependent, beta 3 subunit	NM_007581
1427282_a_at	0.1911	Frda	Friedreich ataxia	AV007132
1453467_s_at	0.1911	Rps15a	Transcribed sequence with strong similarity to protein sp:P39027 (H.sapiens) RS1A_HUMAN 40S ribosomal protein S15a	BM207059
1416021_a_at	0.1916	Fabp5	fatty acid binding protein 5, epidermal	BC002008
1416265_at	0.1916	Capn10	calpain 10	NM_011796
1418744_s_at	0.1916	Tesc	tescalcin	NM_021344
1425341_at	0.1916	Kcnk3	potassium channel, subfamily K, member 3	BF467278
1426403_at	0.1916	Actr1b	ARP1 actin-related protein 1 homolog B (yeast)	BG801851
1437976_x_at	0.1916	BC029892	Similar to 60S ribosomal protein L23a (LOC268449), mRNA	C87154
1448774_at	0.1916	Stoml2	stomatin (Epb7.2)-like 2	NM_023231
1417879_at	0.1917	1110060M21Rik	RIKEN cDNA 1110060M21 gene	NM_025424
1434970_a_at	0.1919	Mrpl15	AV216669 RIKEN full-length enriched, ES cells Mus musculus cDNA clone 2410165L09 3', mRNA sequence.	AV216669
1436064_x_at	0.1919	Rps24	ribosomal protein S24	AV004977
1438656_x_at	0.1919	Timm17b	AV157500 Mus musculus head C57BL/6J 12-day embryo Mus musculus cDNA clone 3010003E09, mRNA sequence.	AV157500
1460724_at	0.1919	Ap2a1	adaptor protein complex AP-2, alpha 1 subunit	NM_007458
1421861_at	0.1921	Clstn1	calsyntenin 1	BG065300
1435112_a_at	0.1921	Atp5h	ATP synthase, H+ transporting, mitochondrial F0 complex, subunit d	AV154755
1456243_x_at	0.1921	Mcl1	BB374534 RIKEN full-length enriched, 16 days embryo head Mus musculus cDNA clone C130075I17 3' similar to U35623 Mus musculus EAT/MCL-1 mRNA, mRNA sequence.	BB374534
1417432_a_at	0.1922	Gnb1	guanine nucleotide binding protein, beta 1	NM_008142
1421819_a_at	0.1924	Set	SET translocation	BF134272
1438563_s_at	0.1925	Mrps24	AV069725 Mus musculus small intestine C57BL/6J adult Mus musculus cDNA clone 2010312F15, mRNA sequence.	AV069725
1424171_a_at	0.1927	Hagh	hydroxyacyl glutathione hydrolase	BC004749
1416133_at	0.1929	C920006C10Rik	Adult male spinal cord cDNA, RIKEN full-length enriched library, clone:A330049K02 product:SIMILAR TO CONSERVED MEMBRANE PROTEIN AT 44E homolog [Mus musculus], full insert sequence	BB188557
1417562_at	0.1929	Eif4ebp1	eukaryotic translation initiation factor 4E binding protein 1	NM_007918
1417827_at	0.1929	Ngly1	N-glycanase 1	NM_021504
1418737_at	0.1929	Nudt2	nudix (nucleoside diphosphate linked moiety X)-type motif 2	NM_025539
1420820_at	0.1929	2900073G15Rik	RIKEN cDNA 2900073G15 gene	NM_026064
1448623_at	0.1929	2310075C12Rik	RIKEN cDNA 2310075C12 gene	NM_133739
1452925_a_at	0.1929	1810015H18Rik	RIKEN cDNA 1810015H18 gene	AK009364
1460348_at	0.1929	Mad2l2	MAD2 mitotic arrest deficient-like 2 (yeast)	BC011282
1416520_x_at	0.1936	Rpl36	ribosomal protein L36	NM_018730
1418896_a_at	0.1936	Rpn2	ribophorin II	NM_019642
1460701_a_at	0.1936	Mrpl52	mitochondrial ribosomal protein L52	AV021593

Table 5-2. Genes identified by SAM[a] (continued)

1415714_a_at	0.1938	2610209M04Rik	RIKEN cDNA 2610209M04 gene	BC027564
1449037_at	0.1940	Crem	cAMP responsive element modulator	AI467599
1424760_a_at	0.1942	Smyd2	SET and MYND domain containing 2	BC023119
1427764_a_at	0.1942	Tcfe2a	transcription factor E2a	D29919
1428515_at	0.1942	2410012H22Rik	RIKEN cDNA 2410012H22 gene	AK010472
1434155_a_at	0.1942	2310061I04Rik	RIKEN cDNA 2310061I04 gene	BB174350
1434679_at	0.1942	Cspg3	chondroitin sulfate proteoglycan 3	BM945195
1456616_a_at	0.1942	Bsg	AV035166 Mus musculus adult C57BL/6J placenta Mus musculus cDNA clone 1600013O06, mRNA sequence.	AV035166
1460424_at	0.1942	1810008O21Rik	RIKEN cDNA 1810008O21 gene	BI411309
1422186_s_at	0.1943	Dia1	diaphorase 1 (NADH)	NM_029787
1415974_at	0.1947	Map2k2	mitogen activated protein kinase kinase 2	AW553456
1416257_at	0.1950	Capn2	calpain 2	NM_009794
1426596_a_at	0.1950	Smn	survival motor neuron	BB821035
1429104_at	0.1950	0610025L06Rik	RIKEN cDNA 0610025L06 gene	AK012581
1435869_s_at	0.1950	Ap2a2	ES cells cDNA, RIKEN full-length enriched library, clone:2410074K14 product:expressed sequence AW146353, full insert sequence	BQ175609
1444952_a_at	0.1950	8430423A01Rik	RIKEN cDNA 8430423A01 gene	BB260383
1448344_at	0.1950	Rps12	ribosomal protein S12	NM_011295
1427295_at	0.1952	1810073N04Rik	RIKEN cDNA 1810073N04 gene	BB406585
1427119_at	0.1953	Spink4	serine protease inhibitor, Kazal type 4	AV066321
1423959_at	0.1957	AV047578	expressed sequence AV047578	AF305427
1437975_a_at	0.1957	BC029892	Similar to 60S ribosomal protein L23a (LOC268449), mRNA	C87154
1451895_a_at	0.1963		Mus musculus mRNA similar to dual specificity phosphatase 9 (cDNA clone MGC:6681 IMAGE:3501447), complete cds.	BC004738
1422525_at	0.1965	Atp5k	ATP synthase, H+ transporting, mitochondrial F1F0 complex, subunite	NM_007507
1435413_x_at	0.1965	2700060E02Rik	AV167958 Mus musculus head C57BL/6J 13-day embryo Mus musculus cDNA clone 3110059K19, mRNA sequence.	AV167958
1449482_at	0.1965	Hist3h2ba	histone 3, H2ba	NM_030082
1456036_x_at	0.1965	Gsto1	glutathione S-transferase omega 1	AV003026
1422593_at	0.1967	Ap3s1	adaptor-related protein complex 3, sigma 1 subunit	NM_009681
1426680_at	0.1973	Sepn1	RIKEN cDNA 1110019I12 gene	AK003819
1426245_s_at	0.1979	Mapre2	microtubule-associated protein, RP/EB family, member 2	BC027056
1455283_x_at	0.1994	Ndufs8	Transcribed sequence with moderate similarity to protein sp:O00217 (H.sapiens) NUIM_HUMAN NADH-ubiquinone oxidoreductase 23 kDa subunit, mitochondrial precursor	BB453395
1456226_x_at	0.1994	Ddr1	discoidin domain receptor family, member 1	BB234940
1415876_a_at	0.1997	Rps26	ribosomal protein S26	NM_013765
1416948_at	0.1997	Mrpl23	mitochondrial ribosomal protein L23	NM_011288
1419544_at	0.1997	Atp6v1c1	ATPase, H+ transporting, V1 subunit C, isoform 1	AA987147
1434230_at	0.1997	Polb	polymerase (DNA directed), beta	BG094331
1449003_a_at	0.1997	Vti1b	vesicle transport through interaction with t-SNAREs 1B homolog	NM_016800
1451998_at	0.1997	4930485D02Rik	RIKEN cDNA 4930485D02 gene	BC024597
1416764_at	0.2004	Ttc11	tetratricopeptide repeat domain 11	NM_025562
1418318_at	0.2004	Rnf128	ring finger protein 128	AK004847
1418704_at	0.2004	S100a13	S100 calcium binding protein A13	NM_009113
1418991_at	0.2004	Bak1	BCL2-antagonist/killer 1	NM_007523
1428257_s_at	0.2004	Dncl2a	dynein, cytoplasmic, light chain 2A	BG791323
1428608_at	0.2004	Mylc2b	RIKEN cDNA 1500001M02 gene	AW494458

Table 5-2. Genes identified by SAM[a] (continued)

1433520_at	0.2004	Scap	Sreb cleavage-activating protein	BI412871
1449299_at	0.2004	Lrp5	low density lipoprotein receptor-related protein 5	BC011374
1454807_a_at	0.2004	Snx12	sorting nexin 12	BB414983
1416842_at	0.2010	Gstm5	glutathione S-transferase, mu 5	NM_010360
1424490_at	0.2011	2410005H09Rik	RIKEN cDNA 2410005H09 gene	BC024802
1423231_at	0.2017	Nrgn	neurogranin	AK002933
1438647_x_at	0.2025	Cetn2	BB503830 RIKEN full-length enriched, 0 day neonate kidney Mus musculus cDNA clone D630045F01 3', mRNA sequence.	BB503830
1423897_at	0.2027	2410016F01Rik	RIKEN cDNA 2410016F01 gene	AW488376
1416567_s_at	0.2041	Atp5e	ATP synthase, H+ transporting, mitochondrial F1 complex, epsilon subunit	NM_025983
1416671_a_at	0.2041	Mcoln1	mucolipin 1	NM_053177
1416765_s_at	0.2041	Magmas	mitochondria-associated protein involved in granulocyte-macrophage colony-stimulating factor signal transduction	NM_025571
1418701_at	0.2041	Comt	catechol-O-methyltransferase	NM_007744
1423151_at	0.2041	Dnajb11	DnaJ (Hsp40) homolog, subfamily B, member 11	AK010861
1450560_a_at	0.2041	Ppp2r5d	protein phosphatase 2, regulatory subunit B (B56), delta isoform	NM_009358
1450640_x_at	0.2041	Atp5k	ATP synthase, H+ transporting mitochondrial F1F0 complex, subunit e	NM_007507
1450903_at	0.2041	Rad23b	RAD23b homolog (S. cerevisiae)	BF138887
1452490_a_at	0.2041	Ap2a2	adaptor protein complex AP-2, alpha 2 subunit	BC010597
1452585_at	0.2041	Mrps28	mitochondrial ribosomal protein S28	AK011036
1454860_x_at	0.2041	Dad1	defender against cell death 1	BI966630
1455749_x_at	0.2041	Ndufa7	NADH dehydrogenase (ubiquinone) 1 alpha subcomplex, 7 (B14.5a)	C88880
1460360_at	0.2041	Asrgl1	asparaginase like 1	AU040643
1419036_at	0.2042	Csnk2a1	casein kinase II, alpha 1 polypeptide	BB283759
1452579_at	0.2050	2310020H20Rik	RIKEN cDNA 2310020H20 gene	AK009021
1417976_at	0.2052	Ada	adenosine deaminase	NM_007398
1420513_at	0.2062	1700073K01Rik	RIKEN cDNA 1700073K01 gene	BC025062
1449194_at	0.2062	Mrps25	mitochondrial ribosomal protein S25	AK004037
1453564_a_at	0.2062	Vps24	RIKEN cDNA 4921505F14 gene	AK014818
1415671_at	0.2071	Atp6v0d1	ATPase, H+ transporting, V0 subunit D isoform 1	NM_013477
1416020_a_at	0.2071	Atp5g1	ATP synthase, H+ transporting, mitochondrial F0 complex, subunit c (subunit 9), isoform 1	NM_007506
1416243_a_at	0.2071	Rpl35	ribosomal protein L35	NM_025592
1416341_at	0.2071	Polr2c	polymerase (RNA) II (DNA directed) polypeptide C	NM_009090
1416412_at	0.2071	Nsmaf	neutral sphingomyelinase (N-SMase) activation associated factor	NM_010945
1416713_at	0.2071	2700055K07Rik	RIKEN cDNA 2700055K07 gene	NM_026481
1418010_a_at	0.2071	Sh3glb1	SH3-domain GRB2-like B1 (endophilin)	BB221842
1422506_a_at	0.2071	Cstb	cystatin B	NM_007793
1423680_at	0.2071	Fads1	RIKEN cDNA 0710001O03 gene	BC026831
1424095_at	0.2071	Rtcd1	RNA terminal phosphate cyclase domain 1	BC016519
1426964_at	0.2071	3110003A17Rik	RIKEN cDNA 3110003A17 gene	AK013984
1427481_a_at	0.2071	Atp1a3	ATPase, Na+/K+ transporting, alpha 3 polypeptide	BC027114
1427604_a_at	0.2071	Atp9a	ATPase, class II, type 9A	AF011336
1429723_at	0.2071	6330409N04Rik	RIKEN cDNA 6330409N04 gene	AK018153
1434637_x_at	0.2071	Sin3b	transcriptional regulator, SIN3B (yeast)	BF017589
1434883_at	0.2071	2610103J23Rik	RIKEN cDNA 2610103J23 gene	AV083741
1434924_at	0.2071	Phf2	PHD finger protein 2	BF468039
1435735_x_at	0.2071	H47	BB285733 RIKEN full-length enriched, 2 cells egg Mus musculus cDNA clone B020007I03 3', mRNA sequence.	BB285733

Table 5-2. Genes identified by SAM[a] (continued)

1435755_at	0.2071	1110001A16Rik	RIKEN cDNA 1110001A16 gene	BB609468
1437947_x_at	0.2071	Vdac1	AV036172 Mus musculus adult C57BL/6J placenta Mus musculus cDNA clone 1600017H06, mRNA sequence.	AV036172
1438948_x_at	0.2071	Bzrp	AV101079 Mus musculus C57BL/6J ES cell Mus musculus cDNA clone 2410071K12, mRNA sequence.	AV101079
1439444_x_at	0.2071	1110014C03Rik	AV213456 RIKEN full-length enriched, ES cells Mus musculus cDNA clone 2410127P20 3' similar to AJ004912 Rattus norvegicus mRNA for integral membrane protein Tmp21-I (p23), mRNA sequence.	AV213456
1448247_at	0.2071	Bcl7b	B-cell CLL/lymphoma 7B	NM_009745
1448699_at	0.2071	Mrpl54	mitochondrial ribosomal protein L54	NM_025317
1449429_at	0.2071	Fkbp1b	FK506 binding protein 1b	NM_016863
1450519_a_at	0.2071	Prkaca	protein kinase, cAMP dependent, catalytic, alpha	M12303
1450668_s_at	0.2071	Hspe1	heat shock protein 1 (chaperonin 10)	NM_008303
1450727_a_at	0.2071	Poldip2	polymerase (DNA-directed), delta interacting protein 2	NM_026389
1451229_at	0.2071	Hdac11	histone deacetylase 11	BC016208
1451745_a_at	0.2071	Znhit1	zinc finger, HIT domain containing 1	BC026751
1452048_at	0.2071	Mrpl12	mitochondrial ribosomal protein L12	AK002757
1456540_s_at	0.2071	Mtmr6	BB297632 RIKEN full-length enriched, 9.5 days embryo parthenogenote Mus musculus cDNA clone B130063F15 3' similar to AF072928 Homo sapiens myotubularin related protein 6 mRNA, mRNA sequence.	BB297632
1460581_a_at	0.2071	Rpl13	Transcribed sequence with strong similarity to protein ref:NP_150254.1 (H.sapiens) ribosomal protein L13; 60S ribosomal protein L13; breast basic conserved protein 1 [Homo sapiens]	AI506565
1420875_at	0.2079	Ptk9	protein tyrosine kinase 9	BI662615
1424013_at	0.2079	Etf1	eukaryotic translation termination factor 1	BC013717
1426661_at	0.2079	Rpl27a	ribosomal protein L27a	BG807647
1438166_x_at	0.2079	Ndufs4	NADH dehydrogenase (ubiquinone) Fe-S protein 4	AV219958
1448234_at	0.2079	Dnajb6	DnaJ (Hsp40) homolog, subfamily B, member 6	NM_011847
1448298_at	0.2079	Tnk2	tyrosine kinase, non-receptor, 2	NM_016788
1453256_at	0.2079	Polr3c	RIKEN cDNA 4933407E01 gene	BB772197
1455727_at	0.2079	U2af1-rs2	U2 small nuclear ribonucleoprotein auxiliary factor (U2AF) 1, related sequence 2	AW542140
1456495_s_at	0.2079	Osbpl6	oxysterol binding protein-like 6	BG070848
1418234_s_at	0.2080	Bcas2	breast carcinoma amplified sequence 2	NM_026602
1426811_at	0.2080	Ppp2r5b	glycoprotein hormone alpha 2	BB080065
1437043_a_at	0.2080	1110012M11Rik	RIKEN cDNA 1110012M11 gene	AV012400
1448295_at	0.2080	D13Wsu50e	DNA segment, Chr 13, Wayne State University 50, expressed	NM_138596
1448543_at	0.2080	2310042G06Rik	RIKEN cDNA 2310042G06 gene	NM_025531
1451217_a_at	0.2080	1500034J20Rik	RIKEN cDNA 1500034J20 gene	BC008259
1453569_s_at	0.2080	Mark4	MAP/microtubule affinity-regulating kinase 4	AK010751
1417295_at	0.2083	Mta1	metastasis associated 1	NM_054081
1415981_at	0.2087	5031400M07Rik	RIKEN cDNA 5031400M07 gene	AV258950
1418249_at	0.2087	Crcp	calcitonin gene-related peptide-receptor component protein	NM_007761
1423766_at	0.2087	Pak1ip1	PAK1 interacting protein 1 LocusID: 55003	AF386076
1417285_a_at	0.2088	Ndufa5	NADH dehydrogenase (ubiquinone) 1 alpha subcomplex, 5	NM_026614
1423746_at	0.2088	Txndc5	thioredoxin domain containing 5	BC016252
1433472_x_at	0.2088	Rpl38	RIKEN cDNA 0610025G13 gene	AA050777
1435734_x_at	0.2088	1110032N12Rik	BB396413 RIKEN full-length enriched, 0 day neonate cerebellum Mus musculus cDNA clone C230097H11 3', mRNA sequence.	BB396413

Table 5-2. Genes identified by SAM[a] (continued)

1426529_a_at	0.2090	Tagln2	transgelin 2	C76322
1460641_a_at	0.2090	3100004P22Rik	RIKEN cDNA 3100004P22 gene	NM_133693
1420776_a_at	0.2093	Auh	AU RNA binding protein/enoyl-coenzyme A hydratase	NM_016709
1416696_at	0.2113	D17Wsu104e	interleukin 25	NM_080837
1424628_a_at	0.2113	1500032D16Rik	RIKEN cDNA 1500032D16 gene	BC013640
1436783_x_at	0.2113	Ywhab	tyrosine 3-monooxygenase/tryptophan 5-monooxygenase activation protein, beta polypeptide	AV021552
1436542_at	0.2119	Ptger1	prostaglandin E receptor 1 (subtype EP1)	BE948730
1415948_at	0.2120	Creg	cellular repressor of E1A-stimulated genes	BC027426
1416605_at	0.2120	Nola2	nucleolar protein family A, member 2	BC024944
1417869_s_at	0.2120	Ctsz		NM_022325
1420833_at	0.2120	Vamp2	vesicle-associated membrane protein 2	BG871810
1427347_s_at	0.2120	Tubb2	tubulin, beta 2	BC003475
1439234_a_at	0.2120	2410018G23Rik	RIKEN cDNA 2410018G23 gene	BE200117
1448745_s_at	0.2120	Lor	loricrin	NM_008508
1448824_at	0.2120	Ube2j1	ubiquitin-conjugating enzyme E2, J1	NM_019586
1449964_a_at	0.2120	Mlycd	malonyl-CoA decarboxylase	NM_019966
1451386_at	0.2120	Blvrb	biliverdin reductase B (flavin reductase (NADPH))	BC027279
1418625_s_at	0.2124	LOC14433	glyceraldehyde-3-phosphate dehydrogenase	NM_008084
1448595_a_at	0.2124	Rex3	reduced expression 3	NM_009052
1424638_at	0.2130	Cdkn1a	cyclin-dependent kinase inhibitor 1A (P21)	AK007630
1426254_at	0.2130	Bbp	beta-amyloid binding protein precursor	AF353993
1452370_s_at	0.2130	B230208H17Rik	RIKEN cDNA B230208H17 gene	BB449608
1418430_at	0.2132	Kif5b	kinesin family member 5B	BI328541
1419419_at	0.2132	D0H6S2654E		NM_138746
1422451_at	0.2132	Mrps21	mitochondrial ribosomal protein S21	NM_078479
1426982_at	0.2132	E030034P13Rik	RIKEN cDNA E030034P13 gene	BB477613
1438776_x_at	0.2132	Rps17	AV046534 Mus musculus adult C57BL/6J testis Mus musculus cDNA clone 1700057O18, mRNA sequence.	AV046534
1438173_x_at	0.2136	Pmf1	AV307393 RIKEN full-length enriched, 8 days embryo Mus musculus cDNA clone 5730552G08 3', mRNA sequence.	AV307393
1423906_at	0.2137	Hsbp1	unnamed protein product; SIMILAR TO HEAT SHOCK FACTOR BINDING PROTEIN 1[Mus musculus] (SPTR|Q9CQZ1, evidence: FASTY, 100%ID, 100%length, match=228) putative; Mus musculus 13 days embryo liver cDNA, RIKEN full-length enriched library, clone:2510008P16 product:SIMILAR TO HEAT SHOCK FACTOR BINDING PROTEIN 1[Mus musculus], full insert sequence.	AK010939
1437767_s_at	0.2137	Fts	retinoblastoma-like 2	AA138720
1423448_at	0.2139	Rab11b	RAB11B, member RAS oncogene family	BE986863
1416337_at	0.2144	Uqcrb	ubiquinol-cytochrome c reductase binding protein	NM_026219
1418506_a_at	0.2146	Prdx2	peroxiredoxin 2	NM_011563
1420843_at	0.2146	Ptprf	protein tyrosine phosphatase, receptor type, F	BF235516
1452181_at	0.2146	Ckap4	BB312117 RIKEN full-length enriched, adult male corpora quadrigemina Mus musculus cDNA clone B230331K02 3' similar to X69910 H.sapiens p63 mRNA for transmembrane protein, mRNA sequence.	BB312117
1417507_at	0.2147	Cyb561	cytochrome b-561	BC006732
1415747_s_at	0.2151	Riok3	RIO kinase 3 (yeast)	C80812
1437423_a_at	0.2154	Sra1	steroid receptor RNA activator 1	BG074964
1434507_at	0.2156	Npepl1	aminopeptidase-like 1	BG076209
1416742_at	0.2157	Cfdp	craniofacial development protein 1	NM_011801

Table 5-2. Genes identified by SAM[a] (continued)

1417311_at	0.2157	Crip2	cysteine rich protein 2	NM_024223
1423105_a_at	0.2157	Gas41	glioma-amplified sequence-41	AK010522
1423364_a_at	0.2157	Fts	fused toes	AW490901
1423425_at	0.2157	1300012G16Rik	RIKEN cDNA 1300012G16 gene	BB018522
1426733_at	0.2157	Itpk1	inositol 1,3,4-triphosphate 5/6 kinase	AW552407
1426998_at	0.2157	Tex27	testis expressed gene 27	BG976649
1439235_x_at	0.2157	2410018G23Rik	RIKEN cDNA 2410018G23 gene	BE200117
1451712_at	0.2157	8030411F24Rik	RIKEN cDNA 8030411F24 gene	AF440735
1456241_a_at	0.2157	1810073N04Rik	BB315716 RIKEN full-length enriched, adult male corpora quadrigemina Mus musculus cDNA clone B230359J01 3', mRNA sequence.	BB315716
1456436_x_at	0.2157	Rps20	ribosomal protein S20	AV002845
1416606_s_at	0.2158	Nola2	nucleolar protein family A, member 2	BC024944
1450696_at	0.2161	Psmb9	proteosome (prosome, macropain) subunit, beta type 9 (large multifunctional protease 2)	NM_013585
1416810_at	0.2163	Mea1	male enhanced antigen 1	BC013344
1450916_at	0.2163	Stau2	staufen (RNA binding protein) homolog 2 (Drosophila)	AI843206
1416990_at	0.2164	Rxrb	retinoid X receptor beta	BC019432
1417978_at	0.2164	1300018P11Rik	RIKEN cDNA 1300018P11 gene	BC027014
1427180_at	0.2164	Slc27a3	solute carrier family 27 (fatty acid transporter), member 3	BB147793
1435395_s_at	0.2164	Atp5j2	ATP synthase, H+ transporting, mitochondrial F0 complex, subunit f, isoform 2	BG794445
1453199_at	0.2164	Acbd6	acyl-Coenzyme A binding domain containing 6	AK011781
1417102_a_at	0.2168	Ndufb5	NADH dehydrogenase (ubiquinone) 1 beta subcomplex, 5	BC025155
1417286_at	0.2168	Ndufa5	NADH dehydrogenase (ubiquinone) 1 alpha subcomplex, 5	NM_026614
1417460_at	0.2168	Ifitm2	interferon induced transmembrane protein 2	NM_030694
1418085_at	0.2168	Prkcz	protein kinase C, zeta	NM_008860
1420613_at	0.2168	Ptp4a2	protein tyrosine phosphatase 4a2	BE134116
1424037_at	0.2168	Itpka	inositol 1,4,5-trisphosphate 3-kinase A	BC027291
1424791_a_at	0.2168	Lu	Lutheran blood group (Auberger b antigen included)	BC004826
1426738_at	0.2168	Dgkz	diacylglycerol kinase zeta	BC014860
1427511_at	0.2168	B2m	beta-2 microglobulin	AA170322
1428331_at	0.2168	2210016F16Rik	RIKEN cDNA 2210016F16 gene	BB547211
1438317_a_at	0.2168	Endog	AV104666 Mus musculus liver C57BL/6J 13-day embryo Mus musculus cDNA clone 2510008K06, mRNA sequence.	AV104666
1438982_s_at	0.2168	2810417J12Rik	BB251185 RIKEN full-length enriched, 7 days neonate cerebellum Mus musculus cDNA clone A730045B05 3', mRNA sequence.	BB251185
1451379_at	0.2168	Rab22a	RAB22A, member RAS oncogene family	BC006596
1453412_a_at	0.2168	Sec14l1	SEC14-like 1 (S. cerevisiae)	BI652727
1455129_at	0.2169	2610103J23Rik	RIKEN cDNA 2610103J23 gene	AV083741
1422678_at	0.2170	Dgat2	diacylglycerol O-acyltransferase 2	AK002443
1432444_a_at	0.2170	1810011O16Rik	RIKEN cDNA 1810011O16 gene	AK012800
1417331_a_at	0.2172	Arl6	myc induced nuclear antigen	NM_019665
1435429_x_at	0.2172	Rps27l	ribosomal protein S27-like	AV111399
1448737_at	0.2172	Tm4sf2	transmembrane 4 superfamily member 2	AF052492
1459986_a_at	0.2172	Rps17	ribosomal protein S17	NM_009092
1418263_at	0.2174	Ddx25	DEAD (Asp-Glu-Ala-Asp) box polypeptide 25	BC024852
1423152_at	0.2174	Vapb	vesicle-associated membrane protein, associated protein B and C	BF303544
1423676_at	0.2174	Atp5h	ATP synthase, H+ transporting, mitochondrial F0 complex, subunit d	AF354051
1429708_at	0.2174	Ndufa11	NADH dehydrogenase (ubiquinone) 1 alpha subcomplex	AA596846

Table 5-2. Genes identified by SAM[a] (continued)

1435232_x_at	0.2174	Mrpl15	mitochondrial ribosomal protein L15	BI791064
1448353_x_at	0.2174	Rpn1	ribophorin I	NM_133933
1452506_a_at	0.2174	0710007A14Rik	RIKEN cDNA 0710007A14 gene	BC011427
1454716_x_at	0.2174	Cox5b	cytochrome c oxidase, subunit Vb	AA960638
1455106_a_at	0.2174	Ckb	creatine kinase, brain	BG967663
1456663_x_at	0.2174	2410018G23Rik	BB718785 RIKEN full-length enriched, adult male liver tumor Mus musculus cDNA clone C730019F01 3', mRNA sequence.	BB718785
1427029_at	0.2175	9530081K03Rik	RIKEN cDNA 9530081K03 gene	AK008764
1418089_at	0.2179	Stx8	syntaxin 8	NM_018768
1418202_a_at	0.2179	Wiz	widely-interspaced zinc finger motifs	NM_011717
1418936_at	0.2179	Maff	v-maf musculoaponeurotic fibrosarcoma oncogene family, protein F (avian)	BC022952
1420879_a_at	0.2179	Ywhab	tyrosine 3-monooxygenase/tryptophan 5-monooxygenase activation protein, beta polypeptide	NM_018753
1421817_at	0.2179	Gsr	glutathione reductase 1	AK019177
1423574_s_at	0.2179	Srd5a2l	steroid 5 alpha-reductase 2-like	BB206480
1423993_at	0.2179	Atp6v1f	ATPase, H+ transporting, V1 subunit F	BC016553
1424660_s_at	0.2179	4632407F12Rik	RIKEN cDNA 4632407F12 gene	BC023091
1424763_at	0.2179	1700027N10Rik	RIKEN cDNA 1700027N10 gene	BC019423
1425806_a_at	0.2179	Surb7	SRB7 (supressor of RNA polymerase B) homolog (S. cerevisiae)	BC012286
1426323_x_at	0.2179	Siva	Cd27 binding protein (Hindu God of destruction)	AF033112
1428745_a_at	0.2179	2310003L22Rik	RIKEN cDNA 2310003L22 gene	AK009123
1429558_a_at	0.2179	C330027G06Rik	RIKEN cDNA C330027G06 gene	BI104294
1434755_at	0.2179	E130012P22Rik	RIKEN cDNA E130012P22 gene	BB538661
1435863_at	0.2179	Commd6	Adult male corpora quadrigemina cDNA, RIKEN full-length enriched library, clone:B230114J18 product:unknown EST, full insert sequence	BE133720
1436567_a_at	0.2179	Ndufa7	NADH dehydrogenase (ubiquinone) 1 alpha subcomplex, 7 (B14.5a)	C88880
1448277_at	0.2179	Pold2	polymerase (DNA directed), delta 2, regulatory subunit	NM_008894
1448284_a_at	0.2179	Ndufc1	NADH dehydrogenase (ubiquinone) 1, subcomplex unknown, 1	NM_025523
1450106_a_at	0.2179	Evl	Ena-vasodilator stimulated phosphoprotein	NM_007965
1450894_a_at	0.2179	Ap2m1	adaptor protein complex AP-2, mu1	C76671
1451747_a_at	0.2179	Apg12l	autophagy 12-like (S. cerevisiae)	AK016474
1452026_a_at	0.2179	Pla2g12a	phospholipase A2, group XIIA	AY007382
1452619_a_at	0.2179	6530406M24Rik	RIKEN cDNA 6530406M24 gene	AI463408
1456315_a_at	0.2179	Ptpla	protein tyrosine phosphatase-like (proline instead of catalytic arginine), member a	BB014781
1457675_at	0.2179	AA409624	RIKEN cDNA 2510002D24 gene	BG063089
1418986_a_at	0.2183	Uxt	ubiquitously expressed transcript	NM_013840
1434642_at	0.2183	Dhrs8	dehydrogenase/reductase (SDR family) member 8	BB546344
1426480_at	0.2185	Sbds	Shwachman-Bodian-Diamond syndrome homolog (human)	BB773592
1419812_s_at	0.2190	D11Ertd99e	DNA segment, Chr 11, ERATO Doi 99, expressed	C77389
1416054_at	0.2191	Rps5	ribosomal protein S5	NM_009095
1422670_at	0.2192	Rohn	ras homolog N (RhoN)	NM_009708
1424018_at	0.2192	Hint1	histidine triad nucleotide binding protein 1	U60001
1416825_at	0.2195	Snta1	syntrophin, acidic 1	NM_009228
1418656_at	0.2195	Lsm5	LSM5 homolog, U6 small nuclear RNA associated (S. cerevisiae)	NM_025520
1448772_at	0.2195	Ube2a	ubiquitin-conjugating enzyme E2A, RAD6 homolog (S. cerevisiae)	BG868960
1415947_at	0.2199	Creg	cellular repressor of E1A-stimulated genes	BC027426
1416022_at	0.2199	Fabp5	fatty acid binding protein 5, epidermal	BC002008

Table 5-2. Genes identified by SAM[a] (continued)

1435364_at	0.2199		4 days neonate male adipose cDNA, RIKEN full-length enriched library, clone:B430101C18 product:HYPOTHETICAL 19.9 KDA PROTEIN homolog [Homo sapiens], full insert sequence	BB323901
1423365_at	0.2205	Cacna1g	calcium channel, voltage-dependent, T type, alpha 1G subunit	AW494038
1455364_a_at	0.2205	Rps7	Similar to Rpl7a protein (LOC245667), mRNA	AI414989
1418181_at	0.2213	Ptp4a3	protein tyrosine phosphatase 4a3	AK014601
1435509_x_at	0.2213	Cdk2ap1	BB145140 RIKEN full-length enriched, adult female vagina Mus musculus cDNA clone 9930028J15 3' similar to AF011644 Mus musculus oral tumor suppressor homolog (Doc-1) mRNA, mRNA sequence.	BB145140
1420731_a_at	0.2219	Csrp2	cysteine and glycine-rich protein 2	NM_007792
1415763_a_at	0.2221	2510006D16Rik	Transcribed sequence	BE853401
1434057_at	0.2231		Similar to NADH dehydrogenase (LOC230075), mRNA	C78790
1425801_x_at	0.2239	Cotl1	coactosin-like 1 (Dictyostelium)	BC011068
1437510_x_at	0.2239	Rps17	ribosomal protein S17	BB724547
1450891_at	0.2239	Srp19	signal recognition particle 19	W08076
1426783_at	0.2242	Gcn5l2	GCN5 general control of amino acid synthesis-like 2 (yeast)	AW212720
1416491_at	0.2243	Numbl	numb-like	NM_010950
1417183_at	0.2243	Dnaja2	DnaJ (Hsp40) homolog, subfamily A, member 2	C77509
1417481_at	0.2243	Ramp1	receptor (calcitonin) activity modifying protein 1	NM_016894
1418225_at	0.2243	Orc2l	origin recognition complex, subunit 2-like (S. cerevisiae)	BB830976
1419302_at	0.2243	Heyl	hairy/enhancer-of-split related with YRPW motif-like	BG695100
1423266_at	0.2243	2810405K02Rik	RIKEN cDNA 2810405K02 gene	AI836168
1423299_at	0.2243	Txnl1	thioredoxin-like	BI416051
1434930_at	0.2243	Tpcn1	two pore channel 1	BI904914
1448704_s_at	0.2243	H47	histocompatibility 47	NM_024439
1451714_a_at	0.2243	Map2k3	mitogen activated protein kinase kinase 3	AI481780
1455482_at	0.2243	Ap2a2	ES cells cDNA, RIKEN full-length enriched library, clone:2410074K14 product:expressed sequence AW146353, full insert sequence	BQ175609
1455531_at	0.2247	A930031D07Rik	RIKEN cDNA A930031D07 gene	AI426503
1416937_at	0.2249	Gabarap	gamma-aminobutyric acid receptor associated protein	BC024621
1416850_s_at	0.2251	D10Ertd214e	DNA segment, Chr 10, ERATO Doi 214, expressed	NM_134007
1425066_a_at	0.2251	1110061O04Rik	RIKEN cDNA 1110061O04 gene	BC018294
1452051_at	0.2261	Actr3	ARP3 actin-related protein 3 homolog (yeast)	BE372352
1428181_at	0.2263	Etfb	electron transferring flavoprotein, beta polypeptide	BI692487
1448203_at	0.2263	Atp5l	ATP synthase, H+ transporting, mitochondrial F0 complex, subunit g	NM_013795
1422650_a_at	0.2264	Riok3	RIO kinase 3 (yeast)	NM_024182
1429555_at	0.2264	1110019C08Rik	RIKEN cDNA 1110019C08 gene	AA408371
1434254_at	0.2264	Gna11	guanine nucleotide binding protein, alpha 11	BM235739
1435638_at	0.2264	9130221H12Rik	RIKEN cDNA 9130221H12 gene	BG808297
1415690_at	0.2265	Mrpl27	mitochondrial ribosomal protein L27	NM_053161
1417913_at	0.2267	2810037C03Rik	RIKEN cDNA 2810037C03 gene	NM_024240
1422830_s_at	0.2267	Drd4	dopamine receptor 4	NM_007878
1423625_a_at	0.2267	1810055D05Rik	RIKEN cDNA 1810055D05 gene	AV053772
1423716_s_at	0.2267	Atp5d	RIKEN cDNA 0610008F14 gene	BC008273
1449590_a_at	0.2267	Mras	muscle and microspikes RAS	AB004879
1422998_a_at	0.2271	Glrx2	glutaredoxin 2 (thioltransferase)	NM_023505
1423956_at	0.2271	Smap1	stromal membrane-associated protein 1	BC006946
1448238_at	0.2271	2700060E02Rik	RIKEN cDNA 2700060E02 gene	NM_026528

Table 5-2. Genes identified by SAM[a] (continued)

1451307_at	0.2271	1110006I11Rik	RIKEN cDNA 1110006I11 gene	BC027021
1451707_s_at	0.2271	1010001P06Rik	RIKEN cDNA 1010001P06 gene	BC011108
1452812_at	0.2271	Lphn1	latrophilin 1	AA987131
1417081_a_at	0.2272	Syngr2	synaptogyrin 2	BC004829
1423054_at	0.2272	Wdr1	WD repeat domain 1	AK004644
1415721_a_at	0.2278	1200013P24Rik	RIKEN cDNA 1200013P24 gene	AK004750
1428823_at	0.2278	2310057G13Rik	RIKEN cDNA 2310057G13 gene	AK009957
1438717_a_at	0.2282	Osbpl6	oxysterol binding protein-like 6	BG070848
1423240_at	0.2287	Src	Rous sarcoma oncogene	BG868120
1439410_x_at	0.2294	3010027G13Rik	RIKEN cDNA 3010027G13 gene	BI966363
1460698_a_at	0.2294	1810029G24Rik	RIKEN cDNA 1810029G24 gene	AK007641
1437908_a_at	0.2302	1200007D18Rik	RIKEN cDNA 1200007D18 gene	BB095626
1419484_a_at	0.2304	Gbas	glioblastoma amplified sequence	NM_008095
1426223_at	0.2304	2810439F02Rik	RIKEN cDNA 2810439F02 gene	BC020021
1428062_at	0.2306	Cpa1	carboxypeptidase A1	AK003088
1428189_at	0.2307	5730494M16Rik	RIKEN cDNA 5730494M16 gene	BQ174627
1416056_a_at	0.2310	Np15	nuclear protein 15.6	BC027265
1418274_at	0.2310	Nutf2	nuclear transport factor 2	AA920031
1419003_at	0.2310	Bves	blood vessel epicardial substance	NM_024285
1423548_s_at	0.2310	Sdbcag84	BB556862 RIKEN full-length enriched, 2 days pregnant adult female ovary Mus musculus cDNA clone E330025K14 3' similar to AL161963 Homo sapiens mRNA; cDNA DKFZp547A2190 (from clone DKFZp547A2190), mRNA sequence.	BB556862
1423978_at	0.2310	Sbk	SH3-binding kinase	BC025837
1424517_at	0.2310	2700094L05Rik	RIKEN cDNA 2700094L05 gene	BC026668
1427922_at	0.2310	1110046L09Rik	RIKEN cDNA 1110046L09 gene	AW045976
1428530_x_at	0.2310	Rps24	ribosomal protein S24	AV206764
1448893_at	0.2310	Ncor2	nuclear receptor co-repressor 2	NM_011424
1449024_a_at	0.2310	Hexa	hexosaminidase A	U07631
1455138_x_at	0.2310	Cfl1	AV148266 Mus musculus C57BL/6J 10-11 day embryo Mus musculus cDNA clone 2810474L04, mRNA sequence.	AV148266
1456582_x_at	0.2310	5230400G24Rik	BB024498 RIKEN full-length enriched, adult male pituitary gland Mus musculus cDNA clone 5330422C22 3', mRNA sequence.	BB024498
1428675_at	0.2311	1110049F12Rik	RIKEN cDNA 1110049F12 gene	AK004208
1448266_at	0.2311	Edf1	endothelial differentiation-related factor 1	AB030185
1417240_at	0.2312	Zyx	zyxin	NM_011777
1424133_at	0.2312	6530411B15Rik	RIKEN cDNA 6530411B15 gene	BC011208
1423181_s_at	0.2313	Clns1a	chloride channel, nucleotide-sensitive, 1A	AK011789
1438058_s_at	0.2315	Ptov1	prostate tumor over expressed gene 1	BG073526
1418743_a_at	0.2317	Tesc	tescalcin	NM_021344
1425758_a_at	0.2323	Impg1	interphotoreceptor matrix proteoglycan 1	AF266478
1428118_at	0.2323	Lrrn6a	RIKEN cDNA 4930471K13 gene	BB078751
1434646_s_at	0.2328	Sap18	Sin3-associated polypeptide 18	AV023865
1431744_a_at	0.2332	Smap1	Mus musculus adult male testis cDNA, RIKEN full-length enriched library, clone:4921514B13 product:STROMAL MEMBRANE-ASSOCIATED PROTEIN SMAP1B homolog [Homo sapiens], full insert sequence.	AK014888
1423221_at	0.2336	Tubb4	tubulin, beta 4	AK013717
1424212_at	0.2336	9430023L20Rik	RIKEN cDNA 9430023L20 gene	BC016463
1416104_at	0.2338	Mpdu1	mannose-P-dolichol utilization defect 1	NM_011900
1416566_at	0.2345	Strap	serine/threonine kinase receptor associated protein	NM_011499
1417192_at	0.2345	D16Wsu109e	DNA segment, Chr 16, Wayne State University 109, expressed	NM_138599

Table 5-2. Genes identified by SAM[a] (continued)

1417418_s_at	0.2345	Cox6a1	cytochrome c oxidase, subunit VI a, polypeptide 1	NM_007748
1420679_a_at	0.2345	Aig1	androgen-induced 1	NM_025446
1424300_at	0.2345	Gemin6	gem (nuclear organelle) associated protein 6	BC025157
1425780_a_at	0.2345	0610041E09Rik	RIKEN cDNA 0610041E09 gene	BC024352
1425891_a_at	0.2345	Grtp1	GH regulated TBC protein 1	AF329833
1428554_a_at	0.2345	1810035L17Rik	10 days neonate skin cDNA, RIKEN full-length enriched library, clone:4732452F11 product:weakly similar to DC50 (DC23) [Homo sapiens], full insert sequence	BQ126239
1428843_at	0.2345	1810015H18Rik	RIKEN cDNA 1810015H18 gene	AK009364
1429252_at	0.2345	0610010K14Rik	RIKEN cDNA 0610010K14 gene	AK002491
1431506_s_at	0.2345	Ppih	unnamed protein product; U-SNRNP-ASSOCIATED CYCLOPHILIN (EC 5.2.1.8) homolog [Homo sapiens] (SPTR|O43447, evidence: FASTY, 100%ID, 100%length, match=531) putative; Mus musculus adult male small intestine cDNA, RIKEN full-length enriched library, clone:2010111B15 product:U-SNRNP-ASSOCIATED CYCLOPHILIN (EC 5.2.1.8) homolog [Homo sapiens], full insert sequence.	AK008394
1431665_a_at	0.2345	Timm8b	unnamed protein product; putative translocase of inner mitochondrial membrane 8 homolog b (yeast) (MGD|MGI:1353424); Mus musculus 18-day embryo whole body cDNA, RIKEN full-length enriched library, clone:1110046L21 product:translocase of inner mitochondrial membrane 8 homolog b (yeast), full insert sequence.	AK004190
1434971_x_at	0.2345	Mrpl15	AV216669 RIKEN full-length enriched, ES cells Mus musculus cDNA clone 2410165L09 3', mRNA sequence.	AV216669
1448368_at	0.2345	Dctn6	dynactin 6	NM_011722
1451162_at	0.2345	Hsbp1	unnamed protein product; SIMILAR TO HEAT SHOCK FACTOR BINDING PROTEIN 1[Mus musculus] (SPTR|Q9CQZ1, evidence: FASTY, 100%ID, 100%length, match=228) putative; Mus musculus 13 days embryo liver cDNA, RIKEN full-length enriched library, clone:2510008P16 product:SIMILAR TO HEAT SHOCK FACTOR BINDING PROTEIN 1[Mus musculus], full insert sequence.	AK010939
1451731_at	0.2345	Abca3	ATP-binding cassette, sub-family A (ABC1), member 3	AK007703
1452721_a_at	0.2345	2900091E11Rik	RIKEN cDNA 2900091E11 gene	BM210204
1454688_x_at	0.2345	1110014C03Rik	RIKEN cDNA 1110014C03 gene	AV103299
1460308_a_at	0.2345	Ict1	immature colon carcinoma transcript 1	NM_026729
1418567_a_at	0.2347	Srp14	signal recognition particle 14	NM_009273
1449119_at	0.2347	Arih2	ariadne homolog 2 (Drosophila)	NM_011790
1451572_a_at	0.2349	5230400G24Rik	RIKEN cDNA 5230400G24 gene	BC016597
1434214_at	0.2351	0910001L09Rik	RIKEN cDNA 0910001L09 gene	BI525016
1415873_a_at	0.2363	Actr1a	ARP1 actin-related protein 1 homolog A (yeast)	NM_016860
1417502_at	0.2363	Tm4sf2	transmembrane 4 superfamily member 2	AF052492
1424122_s_at	0.2363	Commd1	COMM domain containing 1	AB076722
1424211_at	0.2363	5730438N18Rik	RIKEN cDNA 5730438N18 gene	BC011293
1452580_a_at	0.2363	BC028768	cDNA sequence BC028768	BI692686
1454921_at	0.2363		Hypothetical LOC228715 (LOC228715), mRNA	AV111575
1456373_x_at	0.2363		ribosomal protein S20	AV046829
1460008_x_at	0.2363	Rpl31	ribosomal protein L31	AV109882

[a] Six probes included by Affymetrix as controls were removed from this list

Table 5-3. Genes in common between bioweight (BW) and SAM[a]

Probe ID	BW	Gene	Description
1452790_x_at	4.068	Ndufa3	NADH dehydrogenase (ubiquinone) 1 alpha subcomplex, 3
1422586_at	3.041	Ecel1	endothelin converting enzyme-like 1
1448685_at	2.975	2900010M23Rik	RIKEN cDNA 2900010M23 gene
1418300_a_at	2.861	Mknk2	MAP kinase-interacting serine/threonine kinase 2
1456109_a_at	2.860	Mrps15	mitochondrial ribosomal protein S15
1450795_at	2.837	Lhb	luteinizing hormone beta
1416134_at	2.792	Aplp1	amyloid beta (A4) precursor-like protein 1
1418255_s_at	2.695	Srf	serum response factor
1437164_x_at	2.657	Atp5o	ATP synthase, H+ transporting, mitochondrial F1 complex, O subunit
1428464_at	2.585	Ndufa3	NADH dehydrogenase (ubiquinone) 1 alpha subcomplex, 3
1448830_at	2.578	Dusp1	dual specificity phosphatase 1
1427985_at	2.541	9630042H07Rik	RIKEN cDNA 9630042H07 gene
1436064_x_at	2.425	Rps24	ribosomal protein S24
1455950_x_at	2.404	Rpl35	RIKEN cDNA 1700123D08 gene
1422532_at	2.396	Xpc	xeroderma pigmentosum, complementation group C
1460711_at	2.388	9930116P15Rik	ES cells cDNA, RIKEN full-length enriched library, clone:C330022M23 product:unclassifiable, full insert sequence
1450008_a_at	2.365	Catnb	catenin beta
1451307_at	2.355	1110006I11Rik	RIKEN cDNA 1110006I11 gene
1437354_at	2.316		0 day neonate cerebellum cDNA, RIKEN full-length enriched library, clone:C230091D08 product:unclassifiable, full insert sequence
1437621_x_at	2.308		AV216768 RIKEN full-length enriched, ES cells Mus musculus cDNA clone 2410167D16 3' similar to L21027 Mus musculus A10 mRNA, mRNA sequence.
1423948_at	2.242	Bag2	Bcl2-associated athanogene 2
1433603_at	2.210	BC059730	CDNA clone IMAGE:6772417, with apparent retained intron
1422614_s_at	2.192	Bloc1s1	GCN5 general control of amino acid synthesis-like 1 (yeast)
1416367_at	2.175	1110001J03Rik	RIKEN cDNA 1110001J03 gene
1417657_s_at	2.121	Zrf2	zuotin related factor 2
1455106_a_at	2.120	Ckb	creatine kinase, brain
1416584_at	2.109	Man2b2	mannosidase 2, alpha B2
1416494_at	2.091	Ndufs5	NADH dehydrogenase (ubiquinone) Fe-S protein 5
1424766_at	2.044	BC004701	cDNA sequence BC004701
1418256_at	2.043	Srf	serum response factor
1427294_a_at	2.036	1810073N04Rik	RIKEN cDNA 1810073N04 gene
1417348_at	2.034	2310039H08Rik	male enhanced antigen 1
1418910_at	2.011	Bmp7	bone morphogenetic protein 7
1452367_at	2.008	Coro2a	tripartite motif-containing 14
1454674_at	1.994	Fez1	fasciculation and elongation protein zeta 1 (zygin I)
1429144_at	1.994	2310032D16Rik	RIKEN cDNA 2310032D16 gene
1428494_a_at	1.985	Polr2i	polymerase (RNA) II (DNA directed) polypeptide I
1419529_at	1.976	Il23a	interleukin 23, alpha subunit p19
1428869_at	1.961	Nolc1	nucleolar and coiled-body phosphoprotein 1
1420922_at	1.945	Usp9x	Similar to ubiquitin specific protease 9, X-linked isoform 2; Drosophila fat facets related, X-linked; ubiquitin specific protease 9, X chromosome (fat facets-like Drosophila) (LOC240170), mRNA
1419292_at	1.938	9530081K03Rik	RIKEN cDNA 9530081K03 gene
1434392_at	1.930	Usp34	U2af1-rs1 region 2
1424871_s_at	1.930	1500031H01Rik	cDNA sequence BC013706

Table 5-3. Genes in common between bioweight (BW) and SAM[a] (continued)

1429850_x_at	1.921	2010004B12Rik	RIKEN cDNA 2010004B12 gene
1416713_at	1.917	2700055K07Rik	RIKEN cDNA 2700055K07 gene
1434646_s_at	1.916	Sap18	Sin3-associated polypeptide 18
1423857_at	1.914	Mrpl30	mitochondrial ribosomal protein L30
1418448_at	1.914	Rras	Harvey rat sarcoma oncogene, subgroup R
1424018_at	1.910	Hint1	histidine triad nucleotide binding protein 1
1437450_x_at	1.877	2700060E02Rik	RIKEN cDNA 2700060E02 gene
1425248_a_at	1.875	Tyro3	TYRO3 protein tyrosine kinase 3
1424002_at	1.874	Pdcl3	phosducin-like 3
1450466_at	1.867		Adult male corpora quadrigemina cDNA, RIKEN full-length enriched library, clone:B230310J22 product:unclassifiable, full insert sequence
1448917_at	1.865	Thrap6	thyroid hormone receptor associated protein 6
1423676_at	1.861	Atp5h	ATP synthase, H+ transporting, mitochondrial F0 complex, subunit d
1416495_s_at	1.849	Ndufs5	NADH dehydrogenase (ubiquinone) Fe-S protein 5
1428076_s_at	1.843	Ndufb4	NADH dehydrogenase (ubiquinone) 1 beta subcomplex 4
1420368_at	1.830	Denr	Mus musculus ES cells cDNA, RIKEN full-length enriched library, clone:2410004J11 product:DENSITY-REGULATED PROTEIN (DRP), full insert sequence.
1418709_at	1.785	Cox7a1	cytochrome c oxidase, subunit VIIa 1
1418273_a_at	1.770	Rpl30	ribosomal protein L30
1416859_at	1.766	Fkbp3	FK506 binding protein 3
1424172_at	1.763	Hagh	hydroxyacyl glutathione hydrolase
1437133_x_at	1.751	Akr1b3	2 days pregnant adult female oviduct cDNA, RIKEN full-length enriched library, clone:E230024H01 product:unknown EST, full insert sequence
1424391_at	1.750	Nrd1	nardilysin, N-arginine dibasic convertase, NRD convertase 1
1434396_a_at	1.739	Myl6	myosin light chain, alkali, nonmuscle
1435755_at	1.734	1110001A16Rik	RIKEN cDNA 1110001A16 gene
1448794_s_at	1.730	Zrf2	zuotin related factor 2
1460724_at	1.729	Ap2a1	adaptor protein complex AP-2, alpha 1 subunit
1416337_at	1.719	Uqcrb	ubiquinol-cytochrome c reductase binding protein
1422480_at	1.710	Snx3	sorting nexin 3
1454686_at	1.703	6430706D22Rik	RIKEN cDNA 6430706D22 gene
1460581_a_at	1.701	Rpl13	Transcribed sequence with strong similarity to protein ref:NP_150254.1 (H.sapiens) ribosomal protein L13; 60S ribosomal protein L13; breast basic conserved protein 1 [Homo sapiens]
1423090_x_at	1.698	Sec61g	Transcribed sequence with strong similarity to protein sp:P38384 (H.sapiens) S61G_HUMAN Protein transport protein SEC61 gamma subunit
1421260_a_at	1.697	Srm	spermidine synthase
1417155_at	1.691	Nmyc1	neuroblastoma myc-related oncogene 1
1434053_x_at	1.681	Atp5k	ATP synthase, H+ transporting, mitochondrial F1F0 complex, subunit e
1427490_at	1.679	Abcb7	ATP-binding cassette, sub-family B (MDR/TAP), member 7
1425300_at	1.670	BC021917	cDNA sequence BC021917
1420811_a_at	1.664	Catnb	catenin beta
1439389_s_at	1.659	Myadm	BB500055 RIKEN full-length enriched, 0 day neonate kidney Mus musculus cDNA clone D630024J02 3' similar to AJ001616 Mus musculus mRNA for myeloid associated differentiation protein, mRNA sequence.
1417394_at	1.658	Klf4	Kruppel-like factor 4 (gut)
1438563_s_at	1.650	Mrps24	AV069725 Mus musculus small intestine C57BL/6J adult Mus musculus cDNA clone 2010312F15, mRNA sequence.

Table 5-3. Genes in common between bioweight (BW) and SAM[a] (continued)

1449029_at	1.648	Mknk2	MAP kinase-interacting serine/threonine kinase 2
1416098_at	1.648	Syngr3	synaptogyrin 3
1426653_at	1.645	Mcm3	minichromosome maintenance deficient 3 (S. cerevisiae)
1448440_x_at	1.631	D17Wsu104e	interleukin 25
1427943_at	1.629	Acyp2	acylphosphatase 2, muscle type
1448319_at	1.628	Akr1b3	aldo-keto reductase family 1, member B3 (aldose reductase)
1422608_at	1.625	Arpp19	cAMP-regulated phosphoprotein 19
1452519_a_at	1.621	Zfp36	unnamed protein product; TIS11 (AA 1 - 183); Mouse TPA-induced TIS11 mRNA.
1452184_at	1.620	Ndufb9	NADH dehydrogenase (ubiquinone) 1 beta subcomplex, 9
1451959_a_at	1.617	Vegfa	vascular endothelial growth factor A
1456128_at	1.616	Atp5g2	ATP synthase, H+ transporting, mitochondrial F0 complex, subunit c (subunit 9), isoform 2
1456691_s_at	1.614	Srd5a2l	BB825787 RIKEN full-length enriched, mammary gland RCB-0526 Jyg-MC(A) cDNA Mus musculus cDNA clone G830039K08 3', mRNA sequence.
1418226_at	1.607	Orc2l	origin recognition complex, subunit 2-like (S. cerevisiae)
1434442_at	1.607	D5Ertd593e	DNA segment, Chr 5, ERATO Doi 593, expressed
1449011_at	1.607	Slc12a7	solute carrier family 12, member 7
1423610_at	1.605	Metap2	Adult retina cDNA, RIKEN full-length enriched library, clone:A930035J23 product:unknown EST, full insert sequence
1416673_at	1.600	Bace2	beta-site APP-cleaving enzyme 2
1416765_s_at	1.598	Magmas	mitochondria-associated protein involved in granulocyte-macrophage colony-stimulating factor signal transduction
1417432_a_at	1.596	Gnb1	guanine nucleotide binding protein, beta 1
1433451_at	1.592	Cdk5r	cyclin-dependent kinase 5, regulatory subunit (p35)
1418942_at	1.591	Ccdc2	coiled-coil domain containing 2
1435041_at	1.582	Myl6	myosin light chain, alkali, nonmuscle
1426659_a_at	1.571	BC029892	Similar to 60S ribosomal protein L23a (LOC268449), mRNA
1452357_at	1.569	Sept5	septin 5
1456471_x_at	1.569	Phgdh	Transcribed sequence with strong similarity to protein sp:Q61753 (M.musculus) SERA_MOUSE D-3-phosphoglycerate dehydrogenase
1448483_a_at	1.569	Ndufb2	NADH dehydrogenase (ubiquinone) 1 beta subcomplex, 2
1453362_x_at	1.567	Rps24	ribosomal protein S24
1448050_s_at	1.566	Map4k4	mitogen-activated protein kinase kinase kinase kinase 4
1422967_a_at	1.564	Tfrc	transferrin receptor
1422507_at	1.552	Cstb	cystatin B
1427939_s_at	1.551	Mycbp	c-myc binding protein
1436510_a_at	1.547	Lrrfip2	leucine rich repeat (in FLII) interacting protein 2
1427913_at	1.546	Rwdd1	RWD domain containing 1
1417389_at	1.545	Gpc1	glypican 1
1448353_x_at	1.534	Rpn1	ribophorin I
1425231_a_at	1.526	Zfp46	zinc finger protein 46
1417380_at	1.526	Iqgap1	IQ motif containing GTPase activating protein 1
1452143_at	1.524	Spnb2	spectrin beta 2
1426657_s_at	1.522	Phgdh	3-phosphoglycerate dehydrogenase
1426964_at	1.521	3110003A17Rik	RIKEN cDNA 3110003A17 gene
1415761_at	1.521	Mrpl52	mitochondrial ribosomal protein L52
1435857_s_at	1.520	Aplp1	amyloid beta (A4) precursor-like protein 1
1416850_s_at	1.519	D10Ertd214e	DNA segment, Chr 10, ERATO Doi 214, expressed

Table 5-3. Genes in common between bioweight (BW) and SAM[a] (continued)

1448439_at	1.515	D17Wsu104e	interleukin 25
1438001_x_at	1.510	Dp1	deleted in polyposis 1
1428286_at	1.508	2900097C17Rik	13 days embryo forelimb cDNA, RIKEN full-length enriched library, clone:5930433F13 product:unknown EST, full insert sequence
1425384_a_at	1.507	Ube4a	ubiquitination factor E4A, UFD2 homolog (S. cerevisiae)
1428340_s_at	1.503	1110012E06Rik	RIKEN cDNA 1110012E06 gene
1449482_at	1.498	Hist3h2ba	histone 3, H2ba
1448784_at	1.496	Taf10	TAF10 RNA polymerase II, TATA box binding protein (TBP)-associated factor
1418327_at	1.495	1110058L19Rik	RIKEN cDNA 1110058L19 gene
1449324_at	1.489	Ero1l	Transcribed sequences
1424110_a_at	1.486	Nme1	expressed in non-metastatic cells 1, protein
1434561_at	1.484	Asxl1	additional sex combs like 1 (Drosophila)
1416834_x_at	1.469	Ndufb2	NADH dehydrogenase (ubiquinone) 1 beta subcomplex, 2
1428679_s_at	1.461	0610010K14Rik	RIKEN cDNA 0610010K14 gene
1420971_at	1.460	Ubr1	ubiquitin protein ligase E3 component n-recognin 1
1448623_at	1.456	2310075C12Rik	RIKEN cDNA 2310075C12 gene
1423804_a_at	1.455	Idi1	isopentenyl-diphosphate delta isomerase
1428848_a_at	1.450	Macf1	microtubule-actin crosslinking factor 1
1431771_a_at	1.446	Irak1bp1	interleukin-1 receptor-associated kinase 1 binding protein 1
1424121_at	1.444	Commd1	COMM domain containing 1
1421519_a_at	1.435	Zfp120	zinc finger protein 120
1437013_x_at	1.433	Atp6v0b	AV339131 RIKEN full-length enriched, adult male olfactory bulb Mus musculus cDNA clone 6430502C13 3', mRNA sequence.
1437908_a_at	1.432	1200007D18Rik	RIKEN cDNA 1200007D18 gene
1423916_s_at	1.429	Mlf2	myeloid leukemia factor 2
1422718_at	1.427	Ap3s2	adaptor-related protein complex 3, sigma 2 subunit
1451259_at	1.424	Smfn	small fragment nuclease
1448595_a_at	1.416	Rex3	reduced expression 3
1422432_at	1.412	Dbi	diazepam binding inhibitor
1448331_at	1.411	Ndufb7	calmegin
1424396_a_at	1.407	Asrgl1	asparaginase like 1
1427938_at	1.407	Mycbp	c-myc binding protein
1419398_a_at	1.406	Dp1	deleted in polyposis 1
1415899_at	1.405	Junb	Jun-B oncogene
1451109_a_at	1.404	Nedd4	neural precursor cell expressed, developmentally down-regulted gene 4
1419647_a_at	1.403	Ier3	immediate early response 3
1460670_at	1.399	Riok3	RIO kinase 3 (yeast)
1418577_at	1.396	Trim8	tripartite motif protein 8
1449080_at	1.394	Hdac2	histone deacetylase 2
1416129_at	1.391	1300002F13Rik	RIKEN cDNA 1300002F13 gene
1421333_a_at	1.390	Mynn	myoneurin
1425188_s_at	1.387	Sel1h	Sel1 (suppressor of lin-12) 1 homolog (C. elegans)
1428075_at	1.386	Ndufb4	NADH dehydrogenase (ubiquinone) 1 beta subcomplex 4
1451045_at	1.379	Syt13	synaptotagmin 13
1417652_a_at	1.376	Tbca	tubulin cofactor a
1460701_a_at	1.371	Mrpl52	mitochondrial ribosomal protein L52
1434872_x_at	1.369	Rpl37	AV170241 Mus musculus head C57BL/6J 13-day embryo Mus musculus cDNA clone 3110094P05, mRNA sequence.

Table 5-3. Genes in common between bioweight (BW) and SAM[a] (continued)

1456244_x_at	1.359	Txnl2	thioredoxin-like 2
1418896_a_at	1.359	Rpn2	ribophorin II
1455749_x_at	1.359	Ndufa7	NADH dehydrogenase (ubiquinone) 1 alpha subcomplex, 7 (B14.5a)
1437907_a_at	1.352	Tbca	tubulin cofactor a
1430533_a_at	1.351	Catnb	catenin beta
1449294_at	1.348	Mrps15	mitochondrial ribosomal protein S15
1452646_at	1.347	1110029F20Rik	RIKEN cDNA 1110029F20 gene
1426660_x_at	1.345	BC029892	Similar to 60S ribosomal protein L23a (LOC268449), mRNA
1439415_x_at	1.345	Rps21	ribosomal protein S21
1426297_at	1.344	Tcfe2a	transcription factor E2a
1450638_at	1.342	Pdcd5	programmed cell death 5
1426744_at	1.339	Srebf2	sterol regulatory element binding factor 2
1416057_at	1.335	Np15	nuclear protein 15.6
1422615_at	1.315	Map4k4	mitogen-activated protein kinase kinase kinase kinase 4
1449256_a_at	1.313	Rab11a	RAB11a, member RAS oncogene family
1422778_at	1.312	Taf9	TAF9 RNA polymerase II, TATA box binding protein (TBP)-associated factor
1424684_at	1.310	Rab5c	RAB5C, member RAS oncogene family
1428257_s_at	1.305	Dncl2a	dynein, cytoplasmic, light chain 2A
1456615_a_at	1.305	Falz	vx16a10.r1 Soares_thymus_2NbMT Mus musculus cDNA clone IMAGE:1264602 5', mRNA sequence.
1448127_at	1.304	Rrm1	ribonucleotide reductase M1
1417103_at	1.298	Ddt	D-dopachrome tautomerase
1416910_at	1.296	Dnajd1	DnaJ (Hsp40) homolog, subfamily D, member 1
1415919_at	1.295	Npdc1	neural proliferation, differentiation and control gene 1
1417510_at	1.293	Vps4a	vacuolar protein sorting 4a (yeast)
1426209_at	1.291	Strn4	striatin, calmodulin binding protein 4
1435431_at	1.289	2310047M15Rik	RIKEN cDNA 2310047M15 gene
1455372_at	1.288	Cpeb3	cytoplasmic polyadenylation element binding protein 3
1448427_at	1.283	Ndufa6	NADH dehydrogenase (ubiquinone) 1 alpha subcomplex, 6 (B14)
1425721_at	1.283	Phip	pleckstrin homology domain interacting protein
1419356_at	1.282	Klf7	Kruppel-like factor 7 (ubiquitous)
1425702_a_at	1.280	Enpp5	ectonucleotide pyrophosphatase/phosphodiesterase 5
1417399_at	1.280	Gas6	growth arrest specific 6
1423086_at	1.275	Npc1	RIKEN cDNA 2400010D15 gene
1456663_x_at	1.273	2410018G23Rik	BB718785 RIKEN full-length enriched, adult male liver tumor Mus musculus cDNA clone C730019F01 3', mRNA sequence.
1449429_at	1.273	Fkbp1b	FK506 binding protein 1b
1448566_at	1.273	Slc40a1	solute carrier family 40 (iron-regulated transporter), member 1
1429708_at	1.271	Ndufa11	NADH dehydrogenase (ubiquinone) 1 alpha subcomplex
1420842_at	1.269	Ptprf	protein tyrosine phosphatase, receptor type, F
1425206_a_at	1.269	0610009M14Rik	BB224620 RIKEN full-length enriched, adult male aorta and vein Mus musculus cDNA clone A530087G20 3', mRNA sequence.
1418019_at	1.267	Cpd	carboxypeptidase D
1435517_x_at	1.266	Ralb	BB465250 RIKEN full-length enriched, 12 days embryo spinal ganglion Mus musculus cDNA clone D130097N13 3' similar to L19699 Rat GTP-binding protein (ral B) mRNA, mRNA sequence.
1420878_a_at	1.264	Ywhab	tyrosine 3-monooxygenase/tryptophan 5-monooxygenase activation protein, beta polypeptide
1448320_at	1.256	Stim1	stromal interaction molecule 1

Table 5-3. Genes in common between bioweight (BW) and SAM[a] (continued)

1424285_s_at	1.254	Arl6ip4	ADP-ribosylation factor-like 6 interacting protein 4
1435873_a_at	1.253	Rpl13a	Transcribed sequence with strong similarity to protein pir:S29539 (H.sapiens) S29539 ribosomal protein L13a, cytosolic - human
1416816_at	1.253	Nek7	NIMA (never in mitosis gene a)-related expressed kinase 7
1416845_at	1.252	Hspa5bp1	heat shock 70kDa protein 5 binding protein 1
1452111_at	1.247	Mrps35	mitochondrial ribosomal protein S35
1426475_at	1.244	Hmbs	Similar to Hydroxymethylbilane synthase (LOC383565), mRNA
1427903_at	1.242	Phpt1	RIKEN cDNA 1700008C22 gene
1418888_a_at	1.239	Sepr	selenoprotein R
1418991_at	1.235	Bak1	BCL2-antagonist/killer 1
1416782_s_at	1.235	DXImx39e	DNA segment, Chr X, Immunex 39, expressed
1427119_at	1.230	Spink4	serine protease inhibitor, Kazal type 4
1417285_a_at	1.230	Ndufa5	NADH dehydrogenase (ubiquinone) 1 alpha subcomplex, 5
1417340_at	1.223	Txnl2	thioredoxin-like 2
1449138_at	1.222	Sf3b1	splicing factor 3b, subunit 1
1422527_at	1.221	H2-DMa	histocompatibility 2, class II, locus DMa
1450162_at	1.219	Dpf3	D4, zinc and double PHD fingers, family 3
1454870_x_at	1.218	D15Ertd747e	DNA segment, Chr 15, ERATO Doi 747, expressed
1451399_at	1.218	Brp17	brain protein 17
1460739_at	1.217	D11Bwg0280e	DNA segment, Chr 11, Brigham & Women's Genetics 0280e expressed
1460718_s_at	1.216	Mtch1	mitochondrial carrier homolog 1 (C. elegans)
1418225_at	1.215	Orc2l	origin recognition complex, subunit 2-like (S. cerevisiae)
1427173_a_at	1.213	Mrps33	mitochondrial ribosomal protein S33
1422430_at	1.212	Fignl1	fidgetin-like 1
1426940_at	1.209	BC023957	cDNA sequence BC023957
1418439_at	1.208	2900055D03Rik	RIKEN cDNA 2900055D03 gene
1449855_s_at	1.206	Uchl3	ubiquitin carboxyl-terminal esterase L3 (ubiquitin thiolesterase)
1416243_a_at	1.203	Rpl35	ribosomal protein L35
1418567_a_at	1.200	Srp14	signal recognition particle 14
1451385_at	1.199	2310056P07Rik	RIKEN cDNA 2310056P07 gene
1416062_at	1.196	Tbc1d15	TBC1 domain family, member 15
1415971_at	1.192	Marcks	myristoylated alanine rich protein kinase C substrate
1427764_a_at	1.189	Tcfe2a	transcription factor E2a
1424708_at	1.188	1110014C03Rik	RIKEN cDNA 1110014C03 gene
1424269_a_at	1.187	Myl6	myosin light chain, alkali, nonmuscle
1435067_at	1.187	B230208H17Rik	RIKEN cDNA B230208H17 gene
1448604_at	1.185	AA407809	expressed sequence AA407809
1424988_at	1.184	Mylip	myosin regulatory light chain interacting protein
1433472_x_at	1.182	Rpl38	RIKEN cDNA 0610025G13 gene
1421889_a_at	1.180	Aplp2	amyloid beta (A4) precursor-like protein 2
1435232_x_at	1.173	Mrpl15	mitochondrial ribosomal protein L15
1425194_a_at	1.173	6330577E15Rik	RIKEN cDNA 6330577E15 gene
1424204_at	1.173	Mrpl13	mitochondrial ribosomal protein L13
1415997_at	1.170	Txnip	thioredoxin interacting protein
1417379_at	1.168	Iqgap1	IQ motif containing GTPase activating protein 1
1415762_x_at	1.164	Mrpl52	mitochondrial ribosomal protein L52
1448543_at	1.163	2310042G06Rik	RIKEN cDNA 2310042G06 gene

Table 5-3. Genes in common between bioweight (BW) and SAM[a] (continued)

1424515_at	1.162		BB440272 RIKEN full-length enriched, 9 days embryo Mus musculus cDNA clone D030020O16 3', mRNA sequence.
1417320_at	1.161	Grpel1	GrpE-like 1, mitochondrial
1434120_a_at	1.159	Metap2	methionine aminopeptidase 2
1437679_a_at	1.159	Glrx2	BB172698 RIKEN full-length enriched, adult male hypothalamus Mus musculus cDNA clone A230040G05 3', mRNA sequence.
1423764_s_at	1.158	Mrpl37	mitochondrial ribosomal protein L37
1428842_a_at	1.155	Ngfrap1	nerve growth factor receptor (TNFRSF16) associated protein 1
1423680_at	1.155	Fads1	RIKEN cDNA 0710001O03 gene
1421861_at	1.155	Clstn1	calsyntenin 1
1434924_at	1.149	Phf2	PHD finger protein 2
1426480_at	1.148	Sbds	Shwachman-Bodian-Diamond syndrome homolog (human)
1417481_at	1.146	Ramp1	receptor (calcitonin) activity modifying protein 1
1420628_at	1.145	Pura	purine rich element binding protein A
1452272_a_at	1.144	Gfer	growth factor, erv1 (S. cerevisiae)-like (augmenter of liver regeneration)
1428310_at	1.142	D3Wsu161e	RIKEN cDNA C330027G06 gene
1428823_at	1.140	2310057G13Rik	RIKEN cDNA 2310057G13 gene
1424773_at	1.140	1110012M11Rik	RIKEN cDNA 1110012M11 gene
1418248_at	1.140	Gla	galactosidase, alpha
1418123_at	1.140	Unc119	unc-119 homolog (C. elegans)
1417773_at	1.139	Nans	602916387F1 NCI_CGAP_Lu29 Mus musculus cDNA clone IMAGE:5067068 5', mRNA sequence.
1423240_at	1.134	Src	Rous sarcoma oncogene
1423919_at	1.133	BC023882	cDNA sequence BC023882
1448292_at	1.129	Uqcr	ubiquinol-cytochrome c reductase (6.4kD) subunit
1455288_at	1.128	1110036O03Rik	RIKEN cDNA 1110036O03 gene
1450106_a_at	1.127	Evl	Ena-vasodilator stimulated phosphoprotein
1426895_at	1.124	Zfp191	BB579760 RIKEN full-length enriched, 1 day pregnant adult female ovary Mus musculus cDNA clone 7230402O10 5', mRNA sequence.
1418704_at	1.122	S100a13	S100 calcium binding protein A13
1426648_at	1.122	Mapkapk2	MAP kinase-activated protein kinase 2
1416519_at	1.120	Rpl36	ribosomal protein L36
1417368_s_at	1.116	Ndufa2	NADH dehydrogenase (ubiquinone) 1 alpha subcomplex, 2
1435413_x_at	1.115	2700060E02Rik	AV167958 Mus musculus head C57BL/6J 13-day embryo Mus musculus cDNA clone 3110059K19, mRNA sequence.
1418000_a_at	1.115	Itm2b	integral membrane protein 2B
1419550_a_at	1.113	Stk39	6 days neonate head cDNA, RIKEN full-length enriched library, clone:5430411A13 product:serine/threonine kinase 39, STE20/SPS1 homolog (yeast), full insert sequence
1450640_x_at	1.109	Atp5k	ATP synthase, H+ transporting, mitochondrial F1F0 complex, subunit e
1421395_at	1.108	Zik1	zinc finger protein interacting with K protein 1
1451602_at	1.105	Snx6	sorting nexin 6
1424073_at	1.100	5430437P03Rik	RIKEN cDNA 5430437P03 gene
1426811_at	1.099	Ppp2r5b	glycoprotein hormone alpha 2
1434019_at	1.099	Pdap1	PDGFA associated protein 1
1437976_x_at	1.097	BC029892	Similar to 60S ribosomal protein L23a (LOC268449), mRNA
1452099_at	1.097	AA408296	expressed sequence AA408296
1417026_at	1.096	Pfdn1	prefoldin 1
1448346_at	1.095	Cfl1	cofilin 1, non-muscle

Table 5-3. Genes in common between bioweight (BW) and SAM[a] (continued)

1450668_s_at	1.094	Hspe1	heat shock protein 1 (chaperonin 10)
1416636_at	1.093	Rheb	RAS-homolog enriched in brain
1416285_at	1.093	Ndufc1	NADH dehydrogenase (ubiquinone) 1, subcomplex unknown, 1
1418625_s_at	1.090	LOC14433	glyceraldehyde-3-phosphate dehydrogenase
1415879_a_at	1.088	Rplp2	ribosomal protein, large P2
1416074_a_at	1.088	Rpl28	ribosomal protein L28
1450700_at	1.088	Cdc42ep3	CDC42 effector protein (Rho GTPase binding) 3
1424488_a_at	1.087	1110013G13Rik	RIKEN cDNA 1110013G13 gene
1454760_at	1.086	2600017A12Rik	RIKEN cDNA 2600017A12 gene
1449108_at	1.086	Fdx1	ferredoxin 1
1417585_at	1.085	Nup210	nucleoporin 210
1423133_at	1.085	0610040D20Rik	RIKEN cDNA 0610040D20 gene
1435112_a_at	1.083	Atp5h	ATP synthase, H+ transporting, mitochondrial F0 complex, subunit d
1456373_x_at	1.079		ribosomal protein S20
1437767_s_at	1.079	Fts	retinoblastoma-like 2
1426244_at	1.079	Mapre2	microtubule-associated protein, RP/EB family, member 2
1418022_at	1.076	Narg1	NMDA receptor-regulated gene 1
1451747_a_at	1.075	Apg12l	autophagy 12-like (S. cerevisiae)
1451425_a_at	1.075	Mkrn1	makorin, ring finger protein, 1
1450878_at	1.074	Sri	RIKEN cDNA 2210417O06 gene
1436949_a_at	1.073	Tceb2	AV068352 Mus musculus small intestine C57BL/6J adult Mus musculus cDNA clone 2010303D07, mRNA sequence.
1415811_at	1.073	Uhrf1	ubiquitin-like, containing PHD and RING finger domains, 1
1451432_x_at	1.070	2010004B12Rik	RIKEN cDNA 2010004B12 gene
1448971_at	1.070	2410022L05Rik	RIKEN cDNA 2410022L05 gene
1416480_a_at	1.070	Hig1	hypoxia induced gene 1
1426323_x_at	1.064	Siva	Cd27 binding protein (Hindu God of destruction)
1417511_at	1.062	Lyar	Ly1 antibody reactive clone
1427143_at	1.060	Jarid1b	jumonji, AT rich interactive domain 1B (Rbp2 like)
1436859_at	1.060	2700007P21Rik	RIKEN cDNA 2700007P21 gene
1418901_at	1.058	Cebpb	CCAAT/enhancer binding protein (C/EBP), beta
1448656_at	1.057	Cacnb3	calcium channel, voltage-dependent, beta 3 subunit
1452585_at	1.057	Mrps28	mitochondrial ribosomal protein S28
1456243_x_at	1.056	Mcl1	BB374534 RIKEN full-length enriched, 16 days embryo head Mus musculus cDNA clone C130075I17 3' similar to U35623 Mus musculus EAT/MCL-1 mRNA, mRNA sequence.
1417792_at	1.054	Np220	nuclear protein 220
1426529_a_at	1.052	Tagln2	transgelin 2
1448284_a_at	1.051	Ndufc1	NADH dehydrogenase (ubiquinone) 1, subcomplex unknown, 1
1460354_a_at	1.050	Mrpl13	mitochondrial ribosomal protein L13
1415950_a_at	1.048	Pbp	phosphatidylethanolamine binding protein
1422134_at	1.047	Fosb	FBJ osteosarcoma oncogene B
1417774_at	1.045	Nans	602916387F1 NCI_CGAP_Lu29 Mus musculus cDNA clone IMAGE:5067068 5', mRNA sequence.
1424894_at	1.045	Rab13	RAB13, member RAS oncogene family
1437975_a_at	1.043	BC029892	Similar to 60S ribosomal protein L23a (LOC268449), mRNA
1439234_a_at	1.042	2410018G23Rik	RIKEN cDNA 2410018G23 gene
1438058_s_at	1.041	Ptov1	prostate tumor over expressed gene 1
1418714_at	1.041	Dusp8	dual specificity phosphatase 8

Table 5-3. Genes in common between bioweight (BW) and SAM[a] (continued)

1424456_at	1.037	Pvrl2	poliovirus receptor-related 2
1433549_x_at	1.036	Rps21	ribosomal protein S21
1435712_a_at	1.033	Rps18	Transcribed sequence with strong similarity to protein ref:NP_072045.1 (H.sapiens) ribosomal protein S18; 40S ribosomal protein S18 [Homo sapiens]
1451012_a_at	1.032	Csda	AV216648 RIKEN full-length enriched, ES cells Mus musculus cDNA clone 2410165I03 3' similar to D14485 Mouse mRNA for dbpA murine homologue, mRNA sequence.
1418656_at	1.032	Lsm5	LSM5 homolog, U6 small nuclear RNA associated (S. cerevisiae)
1448592_at	1.031	Crtap	cartilage associated protein
1455129_at	1.030	2610103J23Rik	RIKEN cDNA 2610103J23 gene
1433991_x_at	1.030	Dbi	diazepam binding inhibitor
1433946_at	1.028	Zik1	zinc finger protein interacting with K protein 1
1421131_a_at	1.028	Zfp111	zinc finger protein 111
1416250_at	1.027	Btg2	B-cell translocation gene 2, anti-proliferative
1438659_x_at	1.027	0710001P09Rik	BB458460 RIKEN full-length enriched, 12 days embryo spinal ganglion Mus musculus cDNA clone D130057E08 3', mRNA sequence.
1419351_a_at	1.025	0610007P06Rik	RIKEN cDNA 0610007P06 gene
1433721_x_at	1.024	Rps21	ribosomal protein S21
1416245_at	1.023	0610033H09Rik	RIKEN cDNA 0610033H09 gene
1421152_a_at	1.021	Gnao	guanine nucleotide binding protein, alpha o
1450981_at	1.020	Cnn2	calponin 2
1450925_a_at	1.019	Rps27l	ribosomal protein S27-like
1424771_at	1.019	E130307C13	hypothetical protein E130307C13
1449289_a_at	1.018	B2m	RIKEN cDNA E130113K22 gene
1452002_at	1.018	BC024969	cDNA sequence BC024969
1428189_at	1.018	5730494M16Rik	RIKEN cDNA 5730494M16 gene
1456745_x_at	1.018	Sdbcag84	serologically defined breast cancer antigen 84
1427511_at	1.014	B2m	beta-2 microglobulin
1455364_a_at	1.013	Rps7	Similar to Rpl7a protein (LOC245667), mRNA
1425196_a_at	1.011	Hint2	histidine triad nucleotide binding protein 2
1451211_a_at	1.009	Lgtn	ligatin
1424222_s_at	1.008	Rad23b	Mus musculus cDNA clone IMAGE:3256899, complete cds.
1421955_a_at	1.008	Nedd4	neural precursor cell expressed, developmentally down-regulted gene 4
1417102_a_at	1.007	Ndufb5	NADH dehydrogenase (ubiquinone) 1 beta subcomplex, 5
1417879_at	1.007	1110060M21Rik	RIKEN cDNA 1110060M21 gene
1448344_at	1.003	Rps12	ribosomal protein S12
1448699_at	1.002	Mrpl54	mitochondrial ribosomal protein L54
1448086_at	1.001	D1Ertd164e	Transcribed sequences
1426510_at	1.000	C330023F11Rik	RIKEN cDNA C330023F11 gene
1452679_at	1.000	2410129E14Rik	Transcribed sequence with strong similarity to protein ref:NP_001060.1 (H.sapiens) tubulin, beta polypeptide [Homo sapiens]
1416247_at	0.999	Dctn3	dynactin 3
1424738_at	0.999	4932432K03Rik	RIKEN cDNA 4932432K03 gene
1417183_at	0.996	Dnaja2	DnaJ (Hsp40) homolog, subfamily A, member 2
1452754_at	0.996	5730592L21Rik	RIKEN cDNA 5730592L21 gene
1460697_s_at	0.995	2610209M04Rik	RIKEN cDNA 2610209M04 gene
1417869_s_at	0.994	Ctsz	

Table 5-3. Genes in common between bioweight (BW) and SAM[a] (continued)

1433554_at	0.994	AU022870	hypothetical protein MGC56855
1438986_x_at	0.994	Rps17	ribosomal protein S17
1426680_at	0.993	Sepn1	RIKEN cDNA 1110019I12 gene
1452315_at	0.992	Kif11	kinesin family member 11
1444952_a_at	0.991	8430423A01Rik	RIKEN cDNA 8430423A01 gene
1452370_s_at	0.990	B230208H17Rik	RIKEN cDNA B230208H17 gene
1422720_at	0.989	Isl1	UI-M-DJ2-bwa-g-01-0-UI.s1 NIH_BMAP_DJ2 Mus musculus cDNA clone UI-M-DJ2-bwa-g-01-0-UI 3', mRNA sequence.
1451255_at	0.988	Lisch7	liver-specific bHLH-Zip transcription factor
1428214_at	0.988	Tomm7	translocase of outer mitochondrial membrane 7 homolog (yeast)
1423087_a_at	0.987	1110002E23Rik	RIKEN cDNA 1110002E23 gene
1423365_at	0.987	Cacna1g	calcium channel, voltage-dependent, T type, alpha 1G subunit
1434976_x_at	0.985	Eif4ebp1	AV216412 RIKEN full-length enriched, ES cells Mus musculus cDNA clone 2410160M04 3' similar to U28656 Mus musculus insulin-stimulated eIF-4E binding protein PHAS-I mRNA, mRNA sequence.
1456540_s_at	0.982	Mtmr6	BB297632 RIKEN full-length enriched, 9.5 days embryo parthenogenote Mus musculus cDNA clone B130063F15 3' similar to AF072928 Homo sapiens myotubularin related protein 6 mRNA, mRNA sequence.
1448498_at	0.981	Rps6ka4	ribosomal protein S6 kinase, polypeptide 4
1448876_at	0.978	Evc	Ellis van Creveld gene homolog (human)
1418545_at	0.978	Wasf1	WASP family 1
1437947_x_at	0.976	Vdac1	AV036172 Mus musculus adult C57BL/6J placenta Mus musculus cDNA clone 1600017H06, mRNA sequence.
1417131_at	0.973	Cdc25a	C76119 Mouse 3.5-dpc blastocyst cDNA Mus musculus cDNA clone J0003H02 3' similar to Rat mRNA for cdc25A, mRNA sequence.
1423294_at	0.972	Mest	Transcribed sequence with moderate similarity to protein sp:Q9UBF2 (H.sapiens) CPG2_HUMAN Coatomer gamma-2 subunit
1460424_at	0.971	1810008O21Rik	RIKEN cDNA 1810008O21 gene
1422451_at	0.967	Mrps21	mitochondrial ribosomal protein S21
1422524_at	0.967	Abcb6	ATP-binding cassette, sub-family B (MDR/TAP), member 6
1417357_at	0.966	Emd	emerin
1426606_at	0.965	Crtac1	cartilage acidic protein 1
1452181_at	0.965	Ckap4	BB312117 RIKEN full-length enriched, adult male corpora quadrigemina Mus musculus cDNA clone B230331K02 3' similar to X69910 H.sapiens p63 mRNA for transmembrane protein, mRNA sequence.
1418986_a_at	0.964	Uxt	ubiquitously expressed transcript
1451071_a_at	0.963	Atp1a1	ATPase, Na+/K+ transporting, alpha 1 polypeptide
1453550_a_at	0.961	3732409C05Rik	RIKEN cDNA 3732409C05 gene
1438776_x_at	0.961	Rps17	AV046534 Mus musculus adult C57BL/6J testis Mus musculus cDNA clone 1700057O18, mRNA sequence.
1424640_at	0.961	1110033P22Rik	RIKEN cDNA 1110033P22 gene
1449040_a_at	0.960	Sephs2	selenophosphate synthetase 2
1417722_at	0.960	Pgls	6-phosphogluconolactonase
1422683_at	0.955	Irak1bp1	interleukin-1 receptor-associated kinase 1 binding protein 1
1421881_a_at	0.954	Elavl2	ELAV (embryonic lethal, abnormal vision, Drosophila)-like 2 (Hu antigen B)
1423181_s_at	0.954	Clns1a	chloride channel, nucleotide-sensitive, 1A
1427282_a_at	0.952	Frda	Friedreich ataxia
1416054_at	0.951	Rps5	ribosomal protein S5
1448952_at	0.948	A030009H04Rik	RIKEN cDNA A030009H04 gene

Table 5-3. Genes in common between bioweight (BW) and SAM[a] (continued)

1428954_at	0.947	Slc9a3r2	solute carrier family 9 (sodium/hydrogen exchanger), isoform 3 regulator 2
1418744_s_at	0.946	Tesc	tescalcin
1421698_a_at	0.946	Col19a1	procollagen, type XIX, alpha 1
1451291_at	0.946	2610036N15Rik	RIKEN cDNA 2610036N15 gene
1416696_at	0.943	D17Wsu104e	interleukin 25
1451017_at	0.942	Sdbcag84	BB556862 RIKEN full-length enriched, 2 days pregnant adult female ovary Mus musculus cDNA clone E330025K14 3' similar to AL161963 Homo sapiens mRNA; cDNA DKFZp547A2190 (from clone DKFZp547A2190), mRNA sequence.
1420617_at	0.941	Cpeb4	cytoplasmic polyadenylation element binding protein 4
1434230_at	0.941	Polb	polymerase (DNA directed), beta
1449267_at	0.939	3110023E09Rik	RIKEN cDNA 3110023E09 gene
1424750_at	0.939	Zbtb1	zinc finger and BTB domain containing 1
1417886_at	0.939	1810009A15Rik	RIKEN cDNA 1110055N21 gene
1416412_at	0.937	Nsmaf	neutral sphingomyelinase (N-SMase) activation associated factor
1418443_at	0.937	Xpo1	exportin 1, CRM1 homolog (yeast)
1422520_at	0.936	Nef3	neurofilament 3, medium
1425617_at	0.935	Dhx9	DEAH (Asp-Glu-Ala-His) box polypeptide 9
1430692_a_at	0.934	Sel1h	Sel1 (suppressor of lin-12) 1 homolog (C. elegans)
1439466_s_at	0.933	Ptcd1	BB001490 RIKEN full-length enriched, 13 days embryo head Mus musculus cDNA clone 3110026K15 3' similar to AF058791 Rattus norvegicus G10 protein homolog (edg2) mRNA, mRNA sequence.
1434883_at	0.929	2610103J23Rik	RIKEN cDNA 2610103J23 gene
1435652_a_at	0.929	Gnai2	uz40a02.x1 NCI_CGAP_Mam5 Mus musculus cDNA clone IMAGE:3671498 3', mRNA sequence.
1452246_at	0.929	Ostf1	osteoclast stimulating factor 1
1420513_at	0.928	1700073K01Rik	RIKEN cDNA 1700073K01 gene
1416605_at	0.927	Nola2	nucleolar protein family A, member 2
1449194_at	0.926	Mrps25	mitochondrial ribosomal protein S25
1416349_at	0.926	Mrpl34	mitochondrial ribosomal protein L34
1424300_at	0.919	Gemin6	gem (nuclear organelle) associated protein 6
1417959_at	0.918	Pdlim7	PDZ and LIM domain 7
1418743_a_at	0.918	Tesc	tescalcin
1422525_at	0.918	Atp5k	ATP synthase, H+ transporting, mitochondrial F1F0 complex, subunit e
1421817_at	0.913	Gsr	glutathione reductase 1
1427876_at	0.912	2610312B22Rik	RIKEN cDNA 2610312B22 gene
1422977_at	0.912	Gp1bb	glycoprotein Ib, beta polypeptide
1423897_at	0.907	2410016F01Rik	RIKEN cDNA 2410016F01 gene
1439451_x_at	0.906	D15Ertd747e	BB487787 RIKEN full-length enriched, 13 days embryo lung Mus musculus cDNA clone D430044J16 3', mRNA sequence.
1430295_at	0.906	Gna13	guanine nucleotide binding protein, alpha 13
1423242_at	0.906	Mrps36	mitochondrial ribosomal protein S36
1436803_a_at	0.903	Ndufb9	NADH dehydrogenase (ubiquinone) 1 beta subcomplex, 9
1421266_s_at	0.902	Nfkbib	nuclear factor of kappa light chain gene enhancer in B-cells inhibitor, beta
1418588_at	0.902	Vmp	vesicular membrain protein p24
1448737_at	0.901	Tm4sf2	transmembrane 4 superfamily member 2
1416022_at	0.899	Fabp5	fatty acid binding protein 5, epidermal
1456584_x_at	0.898	Phgdh	BB495884 RIKEN full-length enriched, 13 days embryo stomach Mus musculus cDNA clone D530050H10 3' similar to L21027 Mus musculus A10 mRNA, mRNA sequence.

Table 5-3. Genes in common between bioweight (BW) and SAM[a] (continued)

1439410_x_at	0.897	3010027G13Rik	RIKEN cDNA 3010027G13 gene
1423321_at	0.896	Myadm	myeloid-associated differentiation marker
1416965_at	0.893	Pcsk1n	proprotein convertase subtilisin/kexin type 1 inhibitor
1423653_at	0.893	Atp1a1	ATPase, Na+/K+ transporting, alpha 1 polypeptide
1423993_at	0.890	Atp6v1f	ATPase, H+ transporting, V1 subunit F
1419456_at	0.890	Dcxr	dicarbonyl L-xylulose reductase
1451745_a_at	0.889	Znhit1	zinc finger, HIT domain containing 1
1423746_at	0.889	Txndc5	thioredoxin domain containing 5
1450389_s_at	0.889	Pip5k1a	phosphatidylinositol-4-phosphate 5-kinase, type 1 alpha
1433616_a_at	0.888	2310028O11Rik	Adult male xiphoid cartilage cDNA, RIKEN full-length enriched library, clone:5230400C04 product:unknown EST, full insert sequence
1426641_at	0.887	Trib2	expressed sequence AW319517
1430571_s_at	0.885	2410153K17Rik	unnamed protein product; hypothetical Armadillo repeat/Armadillo/plakoglobin ARM repeat profile containing protein (InterPro|IPR000225, PROSITE|PS50176, evidence: InterPro) putative; Mus musculus ES cells cDNA, RIKEN full-length enriched library, clone:2410153K17 product:hypothetical Armadillo repeat/Armadillo/plakoglobin ARM repeat profile containing protein, full insert sequence.
1435364_at	0.883		4 days neonate male adipose cDNA, RIKEN full-length enriched library, clone:B430101C18 product:HYPOTHETICAL 19.9 KDA PROTEIN homolog [Homo sapiens], full insert sequence
1421903_at	0.883	2810405O22Rik	RIKEN cDNA 2810405O22 gene
1456616_a_at	0.880	Bsg	AV035166 Mus musculus adult C57BL/6J placenta Mus musculus cDNA clone 1600013O06, mRNA sequence.
1424171_a_at	0.879	Hagh	hydroxyacyl glutathione hydrolase
1423507_a_at	0.879	Sirt2	Transcribed sequence with moderate similarity to protein ref:NP_036369.2 (H.sapiens) sirtuin 2, isoform 1; SIR2
1451386_at	0.879	Blvrb	biliverdin reductase B (flavin reductase (NADPH))
1448824_at	0.878	Ube2j1	ubiquitin-conjugating enzyme E2, J1
1435690_at	0.878	9030624J02Rik	RIKEN cDNA 9030624J02 gene
1434325_x_at	0.877	Prkar1b	BB274009 RIKEN full-length enriched, 10 days neonate cortex Mus musculus cDNA clone A830086C24 3', mRNA sequence.
1454807_a_at	0.877	Snx12	sorting nexin 12
1416528_at	0.875	Sh3bgrl3	SH3 domain binding glutamic acid-rich protein-like 3
1423959_at	0.874	AV047578	expressed sequence AV047578

[a] Five probes included by Affymetrix as controls were removed from this list

Table 5-4. KEGG pathways identified by bioweight

Category	Pathway(s)	Probe ID(s)	Gene	Description	R/P[a]
Carbohydrate Metabolism	Aminosugars metabolism; Fructose and mannose metabolism	1425485_at, 1456540_s_at	Mtmr6	myotubularin related protein 6	R
	Aminosugars metabolism	1417773_at, 1417774_at	Nans	N-acetylneuraminic acid synthase (sialic acid synthase)	R
	Aminosugars metabolism; Fructose and mannose metabolism	1427903_at	Phpt1	phosphohistidine phosphatase 1	R
	Galactose metabolism	1418248_at	Gla	galactosidase, alpha	R
	Glycolysis / Gluconeogenesis; Pyruvate metabolism	1427943_at	Acyp2	acylphosphatase 2, muscle type	R
	Glycolysis / Gluconeogenesis	1418625_s_at	LOC14433		R
	Inositol phosphate metabolism	1450389_s_at	Pip5k1a	phosphatidylinositol-4-phosphate 5-kinase, type 1 alpha	R
	Pentose and glucuronate interconversions; Fructose and mannose metabolism; Galactose metabolism; Pyruvate metabolism	1437133_x_a, 1448319_at	Akr1b3	aldo-keto reductase family 1, member B3 (aldose reductase)	R
	Pentose and glucuronate interconversions	1419456_at	Dcxr	dicarbonyl L-xylulose reductase	R
	Pentose phosphate pathway	1417722_at	Pgls	6-phosphogluconolactonase	R
	Pyruvate metabolism	1424171_a_at, 1424172_at	Hagh	hydroxyacyl glutathione hydrolase	R
	Citrate cycle (TCA cycle)	1425326_at	Acly	ATP citrate lyase	P
	Citrate cycle (TCA cycle)	1451274_at	Ogdh	oxoglutarate dehydrogenase (lipoamide)	P
	Starch and sucrose metabolism	1448497_at	Ercc3	excision repair cross-complementing rodent repair deficiency, complementation group3	P
Energy Metabolism	Oxidative phosphorylation	1424488_a_at	1110013G13Rik	RIKEN cDNA 1110013G13 gene	R
	Oxidative phosphorylation; ATP synthesis	1415980_at	Atp5g2	ATP synthase, H+ transporting, mitochondrial F0 complex, subunit c (subunit 9), isoform 2	R
	Oxidative phosphorylation; ATP synthesis	1423676_at, 1435112_a_at	Atp5h	ATP synthase, H+ transporting, mitochondrial F0 complex, subunit d	R
	Oxidative phosphorylation; ATP synthesis	1422525_at, 1434053_x_at, 1450640_x_at	Atp5k	ATP synthase, H+ transporting, mitochondrial F1F0 complex, subunit e	R
	Oxidative phosphorylation; ATP synthesis	1437164_x_at	Atp5o	ATP synthase, H+ transporting, mitochondrial F1 complex, O subunit	R

Table 5-4. KEGG pathways identified by bioweight (continued)

Energy Metabolism (continued)	Oxidative phosphorylation; ATP synthesis	1416769_s_at, 1437013_x_at	Atp6v0b	ATPase, H+ transporting, V0 subunit B	R
	Oxidative phosphorylation; ATP synthesis	1423993_at	Atp6v1f	ATPase, H+ transporting, V1 subunit F	R
	Oxidative phosphorylation	1418709_at	Cox7a1	cytochrome c oxidase, subunit VIIa 1	R
	Oxidative phosphorylation	1416971_at	Cox7a2	cytochrome c oxidase, subunit VIIa 2	R
	Oxidative phosphorylation	1429708_at	Ndufa11	NADH dehydrogenase (ubiquinone) 1 alpha subcomplex 11	R
	Oxidative phosphorylation	1417368_s_at	Ndufa2	NADH dehydrogenase (ubiquinone) 1 alpha subcomplex, 2	R
	Oxidative phosphorylation	1428464_at, 1452790_x_at	Ndufa3	NADH dehydrogenase (ubiquinone) 1 alpha subcomplex, 3	R
	Oxidative phosphorylation	1417285_a_at	Ndufa5	NADH dehydrogenase (ubiquinone) 1 alpha subcomplex, 5	R
	Oxidative phosphorylation	1448427_at	Ndufa6	NADH dehydrogenase (ubiquinone) 1 alpha subcomplex, 6 (B14)	R
	Oxidative phosphorylation	1428360_x_at 1455749_x_at	Ndufa7	NADH dehydrogenase (ubiquinone) 1 alpha subcomplex, 7 (B14.5a)	R
	Oxidative phosphorylation	1416057_at	Ndufb11	NADH dehydrogenase (ubiquinone) 1 beta subcomplex, 11	R
	Oxidative phosphorylation	1416834_x_at 1448483_a_at	Ndufb2	NADH dehydrogenase (ubiquinone) 1 beta subcomplex, 2	R
	Oxidative phosphorylation	1428075_at, 1428076_s_at	Ndufb4	NADH dehydrogenase (ubiquinone) 1 beta subcomplex 4	R
	Oxidative phosphorylation	1417102_a_at 1448589_at	Ndufb5	NADH dehydrogenase (ubiquinone) 1 beta subcomplex, 5	R
	Oxidative phosphorylation	1448331_at	Ndufb7	NADH dehydrogenase (ubiquinone) 1 beta subcomplex, 7	R
	Oxidative phosphorylation	1448198_a_at	Ndufb8	NADH dehydrogenase (ubiquinone) 1 beta subcomplex 8	R
	Oxidative phosphorylation	1436803_a_at 1452184_at	Ndufb9	NADH dehydrogenase (ubiquinone) 1 beta subcomplex, 9	R
	Oxidative phosphorylation	1416285_at, 1448284_a_at	Ndufc1	NADH dehydrogenase (ubiquinone) 1, subcomplex unknown, 1	R
	Oxidative phosphorylation	1416494_at, 1416495_s_at	Ndufs5	NADH dehydrogenase (ubiquinone) Fe-S protein 5	R
	Oxidative phosphorylation	1423907_a_at	Ndufs8	NADH dehydrogenase (ubiquinone) Fe-S protein 8	R
	Oxidative phosphorylation	1428179_at	Ndufv2	NADH dehydrogenase (ubiquinone) flavoprotein 2	R
	Oxidative phosphorylation	1448292_at	Uqcr	ubiquinol-cytochrome c reductase (6.4kD) subunit	R

Table 5-4. KEGG pathways identified by bioweight (continued)

Energy Metabolism (continued)	Oxidative phosphorylation	1416337_at	Uqcrb	ubiquinol-cytochrome c reductase binding protein	R
	Methane metabolism	1422198_a_at	Shmt1	serine hydroxymethyl transferase 1 (soluble)	P
	Oxidative phosphorylation; ATP synthesis	1438809_at	Atp5c1	ATP synthase, H+ transporting mitochondrial F1 complex, gamma polypeptide 1	P
	Oxidative phosphorylation; ATP synthesis	1456128_at	Atp5g2	ATP synthase, H+ transporting, mitochondrial F0 complex, subunit c (subunit 9), isoform 2	P
	Oxidative phosphorylation; ATP synthesis	1450634_at	Atp6v1a	ATPase, H+ transporting, V1 subunit A1	P
	Oxidative phosphorylation	1435934_at	Ndufab1	NADH dehydrogenase (ubiquinone) 1, alpha/beta subcomplex1	P
Lipid Metabolism	Androgen and estrogen metabolism	1454987_a_at	H2-Ke6	H2-K region expressed gene 6	R
	Biosynthesis of steroids	1423804_a_at	Idi1	isopentenyl-diphosphate delta isomerase	R
	Fatty acid biosynthesis	1423828_at	Fasn	fatty acid synthase	R
	Glycerolipid metabolism	1437133_x_a, 1448319_at	Akr1b3	aldo-keto reductase family 1, member B3 (aldose reductase)	R
	Glycerolipid metabolism; Sphingolipid metabolism	1418248_at	Gla	galactosidase, alpha	R
	Sphingolipid metabolism	1441866_s_at	Ptdss1	phosphatidylserine synthase 1	R
	Fatty acid metabolism	1451828_a_at	Acsl4	acyl-CoA synthetase long-chain family member 4	P
	Fatty acid metabolism	1460409_at	Cpt1a	carnitine palmitoyltransferase 1a, liver	P
	Glycerophospholipid metabolism	1454633_at	Etnk1	ethanolamine kinase 1	P
	Glycerophospholipid metabolism	1448086_at	Lypla1	lysophospholipase 1	P
	Glycerophospholipid metabolism; Arachidonic acid metabolism	1454157_a_at	Pla2g2d	phospholipase A2, group IID	P
Nucleotide Metabolism	Purine metabolism; Pyrimidine metabolism	1438177_x_at	Entpd4	ectonucleoside triphosphate diphosphohydrolase 4	R
	Purine metabolism; Pyrimidine metabolism	1424110_a_at 1435277_x_at	Nme1	expressed in non-metastatic cells 1, protein	R
	Pyrimidine metabolism	1423717_at	Ak3	adenylate kinase 3	R
	Pyrimidine metabolism	1448604_at	Uck2	uridine-cytidine kinase 2	R
	Purine metabolism; Pyrimidine metabolism	1419397_at	Pola1	polymerase (DNA directed), alpha 1	P
	Purine metabolism; Pyrimidine metabolism	1448650_a_at	Pole	polymerase (DNA directed), epsilon	P
	Purine metabolism; Pyrimidine metabolism	1433552_a_at	Polr2b	polymerase (RNA) II (DNA directed) polypeptide B	P
	Purine metabolism; Pyrimidine metabolism	1448127_at	Rrm1	ribonucleotide reductase M1	P
Amino Acid Metabolism	Arginine and proline metabolism; Urea cycle and metabolism of amino groups	1455106_a_at	Ckb	creatine kinase, brain	R

Table 5-4. KEGG pathways identified by bioweight (continued)

Amino Acid Metabolism (continued)	Arginine and proline metabolism; Urea cycle and metabolism of amino groups	1421260_a_at	Srm	spermidine synthase	R
	Glutamate metabolism	1421817_at	Gsr	glutathione reductase 1	R
	Glycine, serine and threonine metabolism	1426657_s_at 1456471_x_at	Phgdh	3-phosphoglycerate dehydrogenase	R
	Glycine, serine and threonine metabolism	1415673_at	Psph	phosphoserine phosphatase	R
	Glycine, serine and threonine metabolism; Lysine degradation	1422198_a_at	Shmt1	serine hydroxymethyl transferase 1 (soluble)	P
	Methionine metabolism	1435122_x_at	Dnmt1	DNA methyltransferase (cytosine-5) 1	P
	Tryptophan metabolism; Lysine degradation	1451274_at	Ogdh	oxoglutarate dehydrogenase (lipoamide)	P
	Tryptophan metabolism	1424988_at	Mylip	myosin regulatory light chain interacting protein	P
	Tryptophan metabolism	1437354_at	Ube3a	ubiquitin protein ligase E3A	P
	Tryptophan metabolism	1415811_at	Uhrf1	ubiquitin-like, containing PHD and RING finger domains, 1	P
	Valine, leucine and isoleucine biosynthesis	1452154_at	Iars	isoleucine-tRNA synthetase	P
Metabolism of Other Amino Acids	Aminophosphonate metabolism	1441866_s_at	Ptdss1	phosphatidylserine synthase 1	R
	beta-Alanine metabolism	1421260_a_at	Srm	spermidine synthase	R
	Glutathione metabolism	1421817_at	Gsr	glutathione reductase 1	R
	Selenoamino acid metabolism	1449040_a_at	Sephs2	selenophosphate synthetase 2	R
	Cyanoamino acid metabolism	1422198_a_at	Shmt1	serine hydroxymethyl transferase 1 (soluble)	P
Glycan Biosynthesis and Metabolism	Glycosphingolipid biosynthesis - globoseries	1418248_at	Gla	galactosidase, alpha	R
	N-Glycan biosynthesis	1416493_at	Ddost	dolichyl-di-phosphooligosaccharide-protein glycotransferase	R
	N-Glycan biosynthesis	1448353_x_at	Rpn1	ribophorin I	R
	N-Glycan biosynthesis	1418896_a_at	Rpn2	ribophorin II	R
	N-Glycan degradation	1416109_at	Fuca1	fucosidase, alpha-L- 1, tissue	R
	N-Glycan degradation	1416584_at	Man2b2	mannosidase 2, alpha B2	R
	Chondroitin / Heparan sulfate biosynthesis	1422539_at	Extl2	exotoses (multiple)-like 2	P
Metabolism of Cofactors and Vitamins	Nicotinate and nicotinamide metabolism; Riboflavin metabolism; Thiamine metabolism; Vitamin B6 metabolism	1425485_at, 1456540_s_at	Mtmr6	myotubularin related protein 6	R
	Nicotinate and nicotinamide metabolism; Riboflavin metabolism; Thiamine metabolism; Vitamin B6 metabolism	1427903_at	Phpt1	phosphohistidine phosphatase 1	R

Table 5-4. KEGG pathways identified by bioweight (continued)

Metabolism of Cofactors and Vitamins (continued)	Nicotinate and nicotinamide metabolism; Pantothenate and CoA biosynthesis	1423507_a_at	Sirt2	sirtuin 2 (silent mating type information regulation 2, homolog) 2 (S. cerevisiae)	R
	Porphyrin and chlorophyll metabolism	1426475_at	Hmbs	hydroxymethylbilane synthase	R
	Ubiquinone biosynthesis	1416057_at	Ndufb11	NADH dehydrogenase (ubiquinone) 1 beta subcomplex, 11	R
	Folate biosynthesis	1448497_at	Ercc3	excision repair cross-complementing rodent repair deficiency, complementation group3	P
	One carbon pool by folate	1422198_a_at	Shmt1	serine hydroxymethyl transferase 1 (soluble)	P
Biosynthesis of Secondary Metabolites	Terpenoid biosynthesis	1423804_a_at	Idi1	isopentenyl-diphosphate delta isomerase	R
Xenobiotics Biodegradation and Metabolism	Benzoate degradation via CoA ligation	1427943_at	Acyp2	acylphosphatase 2, muscle type	R
	Caprolactam degradation	1423507_a_at	Sirt2	sirtuin 2 (silent mating type information regulation 2, homolog) 2 (S. cerevisiae)	R
Transcription	Basal transcription factors	1422778_at	Taf9	TAF9 RNA polymerase II, TATA box binding protein (TBP)-associated factor	R
	Basal transcription factors	1448784_at	Taf10	TAF10 RNA polymerase II, TATA box binding protein (TBP)-associated factor	R
	RNA polymerase	1433552_a_at	Polr2b	polymerase (RNA) II (DNA directed) polypeptide B	P
Translation	Ribosome	1460581_a_at	Rpl13	ribosomal protein L13	R
	Ribosome	1433928_a_at 1435873_a_at	Rpl13a	ribosomal protein L13a	R
	Ribosome	1454859_a_at	Rpl23	ribosomal protein L23	R
	Ribosome	1426659_a_at 1426660_x_at 1437975_a_at 1437976_x_at	Rpl23a	ribosomal protein L23a	R
	Ribosome	1448217_a_at	Rpl27	ribosomal protein L27	R
	Ribosome	1416074_a_at	Rpl28	ribosomal protein L28	R
	Ribosome	1418273_a_at	Rpl30	ribosomal protein L30	R
	Ribosome	1416243_a_at 1436840_x_at 1454856_x_at 1455950_x_at	Rpl35	ribosomal protein L35	R
	Ribosome	1416519_at	Rpl36	ribosomal protein L36	R
	Ribosome	1416807_at	Rpl36a	ribosomal protein L36a	R
	Ribosome	1434872_x_at	Rpl37	ribosomal protein L37	R
	Ribosome	1433472_x_at	Rpl38	ribosomal protein L38	R
	Ribosome	1415879_a_at	Rplp2	ribosomal protein, large P2	R
	Ribosome	1415912_a_at	Rps13	ribosomal protein S13	R
	Ribosome	1438776_x_at 1438986_x_at	Rps17	ribosomal protein S17	R
	Ribosome	1435712_a_at	Rps18	ribosomal protein S18	R
	Ribosome	1456373_x_at	Rps20	ribosomal protein S20	R

Table 5-4. KEGG pathways identified by bioweight (continued)

Translation (continued)	Ribosome	1433549_x_at 1433721_x_at 1439415_x_at	Rps21	ribosomal protein S21	R
	Ribosome	1436064_x_at 1453362_x_at 1456628_x_at	Rps24	ribosomal protein S24	R
	Ribosome	1415716_a_at	Rps27	ribosomal protein S27	R
	Ribosome	1450925_a_at	Rps27l	ribosomal protein S27-like	R
	Ribosome	1416054_at	Rps5	ribosomal protein S5	R
	Ribosome	1455364_a_at	Rps7	ribosomal protein S7	R
	Aminoacyl-tRNA biosynthesis	1452154_at	Iars	isoleucine-tRNA synthetase	P
Folding, Sorting and Degradation	Protein export	1418567_a_at	Srp14	signal recognition particle 14	R
Replication and Repair	DNA polymerase	1434230_at	Polb	polymerase (DNA directed), beta	R
	DNA polymerase	1419397_at	Pola1	polymerase (DNA directed), alpha 1	P
	DNA polymerase	1448650_a_at	Pole	polymerase (DNA directed), epsilon	P
Membrane Transport	ABC transporters - General	1422524_at	Abcb6	ATP-binding cassette, sub-family B (MDR/TAP), member 6	R
	ABC transporters - General	1423030_at, 1427490_at	Abcb7	ATP-binding cassette, sub-family B (MDR/TAP), member 7	P
Signal Transduction	Calcium signaling	1423365_at	Cacna1g	calcium channel, voltage-dependent, T type, alpha 1G subunit	R
	Calcium signaling	1449245_at	Grin2c	glutamate receptor, ionotropic, NMDA2C (epsilon 3)	R
	Calcium signaling	1437947_x_at	Vdac1	voltage-dependent anion channel 1	R
	Jak-STAT signaling	1419455_at	Il10rb	interleukin 10 receptor, beta	R
	MAPK signaling	1418714_at	Dusp8	dual specificity phosphatase 8	R
	MAPK signaling	1422615_at	Map4k4	mitogen-activated protein kinase kinase kinase kinase 4	R
	MAPK signaling	1426648_at	Mapkapk 2	MAP kinase-activated protein kinase 2	R
	MAPK signaling	1418300_a_at 1449029_at	Mknk2	MAP kinase-interacting serine/threonine kinase 2	R
	MAPK signaling	1448498_at	Rps6ka4	ribosomal protein S6 kinase, polypeptide 4	R
	MAPK signaling	1418448_at	Rras	Harvey rat sarcoma oncogene, subgroup R	R
	MAPK signaling	1418255_s_at, 1418256_at	Srf	serum response factor	R
	Notch signaling	1449080_at	Hdac2	histone deacetylase 2	R
	Phosphatidylinositol signaling	1450389_s_at	Pip5k1a	phosphatidylinositol-4-phosphate 5-kinase, type 1 alpha	R

Table 5-4. KEGG pathways identified by bioweight (continued)

Signal Transduction (continued)	TGF-beta signaling; Hedgehog signaling	1418910_at	Bmp7	bone morphogenetic protein 7	R
	TGF-beta signaling	1437767_s_at	Rbl2	retinoblastoma-like 2	R
	Calcium signaling; Phosphatidylinositol signaling	1417279_at, 1460203_at	Itpr1	inositol 1,4,5-triphosphate receptor 1	P
	Jak-STAT signaling	1419529_at	Il23a	interleukin 23, alpha subunit p19	P
	Jak-STAT signaling	1452843_at	Il6st	interleukin 6 signal transducer	P
	Jak-STAT signaling	1433804_at	Jak1	Janus kinase 1	P
	Jak-STAT signaling	1422581_at	Pias1	protein inhibitor of activated STAT 1	P
	Jak-STAT signaling; Phosphatidylinositol signaling	1425514_at	Pik3r1	phosphatidylinositol 3-kinase, regulatory subunit, polypeptide 1 (p85 alpha)	P
	Jak-STAT signaling	1455899_x_at	Socs3	suppressor of cytokine signaling 3	P
	Jak-STAT signaling	1450034_at	Stat1	signal transducer and activator of transcription 1	P
	MAPK signaling	1448135_at	Atf4	activating transcription factor 4	P
	MAPK signaling	1448830_at	Dusp1	dual specificity phosphatase 1	P
	MAPK signaling	1426677_at	Flna	filamin, alpha	P
	MAPK signaling	1426750_at	Flnb	filamin, beta	P
	MAPK signaling	1454157_a_at	Pla2g2d	phospholipase A2, group IID	P
	MAPK signaling; Wnt signaling	1438808_at	Trp53	transformation related protein 53	P
	Wnt signaling	1420811_a_at 1430533_a_at 1450008_a_at	Ctnnb1	catenin (cadherin associated protein), beta 1, 88kDa	P
	Wnt signaling; Notch signaling	1448616_at	Dvl2	dishevelled 2, dsh homolog (Drosophila)	P
Signaling Molecules and Interaction	Cell adhesion molecules (CAMs)	1422527_at	H2-DMa	histocompatibility 2, class II, locus DMa	R
	Cell adhesion molecules (CAMs)	1420842_at	Ptprf	protein tyrosine phosphatase, receptor type, F	R
	Cell adhesion molecules (CAMs)	1424456_at	Pvrl2	poliovirus receptor-related 2	R
	Cytokine-cytokine receptor interaction	1418910_at	Bmp7	bone morphogenetic protein 7	R
	Cytokine-cytokine receptor interaction	1419455_at	Il10rb	interleukin 10 receptor, beta	R
	Cytokine-cytokine receptor interaction	1418572_x_at	Tnfrsf12a	tumor necrosis factor receptor superfamily, member 12a	R
	ECM-receptor interaction	1422977_at	Gp1bb	glycoprotein Ib, beta polypeptide	R
	Neuroactive ligand-receptor interaction	1449245_at	Grin2c	glutamate receptor, ionotropic, NMDA2C (epsilon 3)	R
	Neuroactive ligand-receptor interaction	1450795_at	Lhb	luteinizing hormone beta	R
	Cytokine-cytokine receptor interaction	1419529_at	Il23a	interleukin 23, alpha subunit p19	P
	Cytokine-cytokine receptor interaction	1452843_at	Il6st	interleukin 6 signal transducer	P
	Cytokine-cytokine receptor interaction	1451959_a_at	Vegfa	vascular endothelial growth factor A	P

Table 5-4. KEGG pathways identified by bioweight (continued)

Cell Motility	Regulation of actin cytoskeleton	1448346_at	Cfl1	cofilin 1, non-muscle	R
	Regulation of actin cytoskeleton	1430295_at	Gna13	guanine nucleotide binding protein, alpha 13	R
	Regulation of actin cytoskeleton	1450389_s_at	Pip5k1a	phosphatidylinositol-4-phosphate 5-kinase, type 1 alpha	R
	Regulation of actin cytoskeleton	1418448_at	Rras	Harvey rat sarcoma oncogene, subgroup R	R
	Regulation of actin cytoskeleton	1418545_at	Wasf1	WASP family 1	R
	Regulation of actin cytoskeleton	1417379_at, 1417380_at	Iqgap1	IQ motif containing GTPase activating protein 1	P
	Regulation of actin cytoskeleton	1425514_at	Pik3r1	phosphatidylinositol 3-kinase, regulatory subunit, polypeptide 1 (p85 alpha)	P
Cell Growth and Death	Apoptosis	1434325_x_at	Prkar1b	protein kinase, cAMP dependent regulatory, type I beta	R
	Cell cycle	1456293_s_at	Ccnh	cyclin H	R
	Cell cycle	1449080_at	Hdac2	histone deacetylase 2	R
	Cell cycle	1418225_at, 1418226_at	Orc2l	origin recognition complex, subunit 2-like (S. cerevisiae)	R
	Apoptosis	1421229_at	Dffb	DNA fragmentation factor, beta subunit	P
	Apoptosis	1425514_at	Pik3r1	phosphatidylinositol 3-kinase, regulatory subunit, polypeptide 1 (p85 alpha)	P
	Cell cycle; Apoptosis	1438808_at	Trp53	transformation related protein 53	P
	Cell cycle	1417131_at	Cdc25a	cell division cycle 25 homolog A (S. cerevisiae)	P
	Cell cycle	1417019_a_at	Cdc6	cell division cycle 6 homolog (S. cerevisiae)	P
	Cell cycle	1426002_a_at	Cdc7	cell division cycle 7 (S. cerevisiae)	P
	Cell cycle	1426653_at	Mcm3	minichromosome maintenance deficient 3 (S. cerevisiae)	P
	Cell cycle	1415945_at	Mcm5	minichromosome maintenance deficient 5, cell division cycle 46 (S. cerevisiae)	P
	Cell cycle	1422663_at	Orc1l	origin recognition complex, subunit 1-like (S.cereviaiae)	P
	Cell cycle	1449293_a_at	Skp2	S-phase kinase-associated protein 2 (p45)	P
Cell Communication	Adherens junction	1420842_at	Ptprf	protein tyrosine phosphatase, receptor type, F	R
	Adherens junction	1424456_at	Pvrl2	poliovirus receptor-related 2	R
	Adherens junction; Focal adhesion; Gap junction; Tight junction	1423240_at	Src	Rous sarcoma oncogene	R
	Adherens junction	1418545_at	Wasf1	WASP family 1	R
	Focal adhesion	1434396_a_at	LOC433297		R

Table 5-4. KEGG pathways identified by bioweight (continued)

Cell Communication (continued)	Focal adhesion; Tight junction	1424269_a_at 1435041_at	Myl6	myosin, light polypeptide 6, alkali, smooth muscle and non-muscle	R
	Focal adhesion; Gap junction; Tight junction	1418448_at	Rras	Harvey rat sarcoma oncogene, subgroup R	R
	Gap junction; Tight junction	1435652_a_at	Gnai2	guanine nucleotide binding protein, alpha inhibiting 2	R
	Tight junction	1451012_a_at	Csda	cold shock domain protein A	R
	Tight junction	1424894_at	Rab13	RAB13, member RAS oncogene family	R
	Adherens junction; Focal adhesion; Tight junction	1420811_a_at 1430533_a_at 1450008_a_at	Ctnnb1	catenin (cadherin associated protein), beta 1, 88kDa	P
	Adherens junction	1417379_at, 1417380_at	Iqgap1	IQ motif containing GTPase activating protein 1	P
	Focal adhesion	1426677_at	Flna	filamin, alpha	P
	Focal adhesion	1426750_at	Flnb	filamin, beta	P
	Focal adhesion	1425514_at	Pik3r1	phosphatidylinositol 3-kinase, regulatory subunit, polypeptide 1 (p85 alpha)	P
	Focal adhesion	1451959_a_at	Vegfa	vascular endothelial growth factor A	P
	Gap junction	1417279_at, 1460203_at	Itpr1	inositol 1,4,5-triphosphate receptor 1	P
	Tight junction	1421064_at	Mpp5	membrane protein, palmitoylated 5 (MAGUK p55 subfamily member 5)	P
	Tight junction	1422685_at	Sec8l1	SEC8-like 1 (S. cerevisiae)	P
	Tight junction	1427888_a_at	Spna2	spectrin alpha 2	P
	Tight junction	1452143_at	Spnb2	spectrin beta 2	P
Endocrine System	Adipocytokine signaling	1421266_s_at	Nfkbib	nuclear factor of kappa light chain gene enhancer in B-cells inhibitor, beta	R
	Insulin signaling	1434976_x_at	Eif4ebp1	eukaryotic translation initiation factor 4E binding protein 1	R
	Insulin signaling	1423828_at	Fasn	fatty acid synthase	R
	Insulin signaling	1418300_a_at 1449029_at	Mknk2	MAP kinase-interacting serine/threonine kinase2	R
	Insulin signaling	1434325_x_at	Prkar1b	protein kinase, cAMP dependent regulatory, type I beta	R
	Insulin signaling	1420842_at	Ptprf	protein tyrosine phosphatase, receptor type, F	R
	Insulin signaling	1416636_at	Rheb	RAS-homolog enriched in brain	R
	Insulin signaling	1418448_at	Rras	Harvey rat sarcoma oncogene, subgroup R	R
	Adipocytokine signaling	1451828_a_at	Acsl4	acyl-CoA synthetase long-chain family member 4	P
	Adipocytokine signaling	1460409_at	Cpt1a	carnitine palmitoyltransferase 1a, liver	P
	Adipocytokine signaling; Insulin signaling	1417592_at	Frap1	FK506 binding protein 12-rapamycin associated protein 1	P
	Adipocytokine signaling; Insulin signaling	1422248_at	Irs4	insulin receptor substrate 4	P
	Adipocytokine signaling	1433804_at	Jak1	Janus kinase 1	P

Table 5-4. KEGG pathways identified by bioweight (continued)

Endocrine System (continued)	Adipocytokine signaling; Insulin signaling	1455899_x_at	Socs3	suppressor of cytokine signaling 3	P
	Insulin signaling	1425514_at	Pik3r1	phosphatidylinositol 3-kinase, regulatory subunit, polypeptide 1 (p85 alpha)	P
Immune System	B cell receptor signaling; T cell receptor signaling	1421266_s_at	Nfkbib	nuclear factor of kappa light chain gene enhancer in B-cells inhibitor, beta	R
	B cell receptor signaling; T cell receptor signaling	1418448_at	Rras	Harvey rat sarcoma oncogene, subgroup R	R
	Hematopoietic cell lineage	1422977_at	Gp1bb	glycoprotein Ib, beta polypeptide	R
	B cell receptor signaling; T cell receptor signaling; Toll-like receptor signaling	1425514_at	Pik3r1	phosphatidylinositol 3-kinase, regulatory subunit, polypeptide 1 (p85 alpha)	P
	Hematopoietic cell lineage	1422967_a_at	Tfrc	transferrin receptor	P
	Toll-like receptor signaling	1450034_at	Stat1	signal transducer and activator of transcription 1	P
Development	Dorso-ventral axis formation	1418448_at	Rras	Harvey rat sarcoma oncogene, subgroup R	R
Behavior	Circadian rhythm	1418025_at	Bhlhb2	basic helix-loop-helix domain containing, class B2	P
Neurodegenerative Disorders	Alzheimer's disease	1416673_at	Bace2	beta-site APP-cleaving enzyme 2	R
	Alzheimer's disease; Dentatorubropallidoluysian atrophy (DRPLA); Huntington's disease; Neurodegenerative Disorders	1418625_s_at	LOC14433		R
	Amyotrophic lateral sclerosis (ALS)	1422520_at	Nef3	neurofilament 3, medium	R
	Neurodegenerative Disorders; Prion disease	1416134_at, 1435857_s_at	Aplp1	amyloid beta (A4) precursor-like protein 1	R
	Parkinson's disease	1452357_at	Sept5	septin 5	R
	Amyotrophic lateral sclerosis (ALS); Huntington's disease	1438808_at	Trp53	transformation related protein 53	P
	Huntington's disease	1454626_at	Cltc	clathrin, heavy polypeptide (Hc)	P
	Parkinson's disease	1448116_at	Ube1x	ubiquitin-activating enzyme E1, Chr X	P

REFERENCES

1. Jorgensen JS, Quirk CC, Nilson JH 2004 Multiple and overlapping combinatorial codes orchestrate hormonal responsiveness and dictate cell-specific expression of the genes encoding luteinizing hormone. Endocr Rev 25:521-42

2. Burger LL, Haisenleder DJ, Dalkin AC, Marshall JC 2004 Regulation of gonadotropin subunit gene transcription. J. Mol. Endocrinol. 33:559-584

3. Pawson AJ, McNeilly AS 2005 The pituitary effects of GnRH. Anim. Reprod. Sci. 88:75-94

4. Kraus S, Naor Z, Seger R 2001 Intracellular signaling pathways mediated by the gonadotropin-releasing hormone (GnRH) receptor. Arch. Med. Res. 32:499-509

5. Kaiser UB, Conn PM, Chin WW 1997 Studies of gonadotropin-releasing hormone (GnRH) action using GnRH receptor-expressing pituitary cell lines. Endocrine Rev. 18:46-70

6. Alarid ET, Windle JJ, Whyte DB, Mellon PL 1996 Immortalization of pituitary cells at discrete stages of development by directed oncogenesis in transgenic mice. Development 122:3319-3329

7. Thomas P, Mellon PL, Turgeon JL, Waring DW 1996 The LβT2 clonal gonadotrope: A model for single cell studies of endocrine cell secretion. Endocrinology 137:2979-2989

8. McArdle CA, Franklin J, Green L, Hislop JN 2002 Signalling, cycling and desensitisation of gonadotrophin-releasing hormone receptors. J. Endocrinol. 173:1-11

9. Liu F, Austin DA, DiPaolo D, Mellon PL, Olefsky JM, Webster NJG 2002 GnRH activates ERK1/2 leading to the induction of c-fos and LHβ protein expression in LβT2 cells. Mol. Endocrinol. 16:419-434

10. Naor Z, Benard O, Seger R 2000 Activation of MAPK cascades by G-protein-coupled receptors: the case of gonadotropin-releasing hormone receptor. Trends Endocrinol. Metab. 11:91-99

11. Mignone F, Gissi C, Liuni S, Pesole G 2002 Untranslated regions of mRNAs. Genome Biol. 3:REVIEWS0004

12. Merrick WC 2004 Cap-dependent and cap-independent translation in eukaryotic systems. Gene 332:1-11

13. Preiss T, M WH 2003 Starting the protein synthesis machine: eukaryotic translation initiation. Bioessays 25:1201-1211

14. Kapp LD, Lorsch JR 2004 The molecular mechanics of eukaryotic translation. Annu. Rev. Biochem. 73:657-704

15. Wickner W, Schekman R 2005 Protein translocation across biological membranes. Science 310:1452-1456

16. Gray NK, Wickens M 1998 Control of translation initiation in animals. Annu. Rev. Cell Dev. Biol. 14:399-458

17. Kleijn M, Scheper GC, Voorma HO, Thomas AA 1998 Regulation of translation initiation factors by signal transduction. Eur. J. Biochem. 253:531-544

18. Dennis PB, Fumagalli S, Thomas G 1999 Target of rapamycin (TOR): balancing the opposing forces of protein synthesis and degradation. Curr Opin Genet Dev 9:49-54

19. Proud CG 2006 Regulation of protein synthesis by insulin. Biochem. Soc. Trans. 34:213-216

20. Raught B, Gingras A-C, Sonenberg N 2000 Regulation of ribosomal recruitment in eucaryotes. In: Sonenberg N, Hershey JWB, Mathews M (eds) Translational control of gene expression, 2nd ed. ed. Cold Spring Harbor Laboratory Press, Cold Spring Harbor, NY; pp 245-294

21. Proud CG 2005 eIF2 and the control of cell physiology. Semin. Cell Dev. Biol. 16:3-12

22. Weiss J, Crowley WF, Jr., Jameson JL 1992 Pulsatile gonadotropin-releasing hormone modifies polyadenylation of gonadotropin subunit messenger ribonucleic acids. Endocrinology 130:415-420

23. Chedrese PJ, Kay TW, Jameson JL 1994 Gonadotropin-releasing hormone stimulates glycoprotein hormone alpha-subunit messenger ribonucleic acid (mRNA) levels in alpha T3 cells by increasing transcription and mRNA stability. Endocrinology 134:2475-2481

24. Tsutsumi M, Laws SC, Rodic V, Sealfon SC 1995 Translational regulation of the gonadotropin-releasing hormone receptor in alpha T3-1 cells. Endocrinology 136:1128-1136

25. Rolli-Derkinderen M, Machavoine F, Baraban JM, Grolleau A, Beretta L, Dy M 2003 ERK and p38 inhibit the expression of 4E-BP1 repressor of translation through induction of Egr-1. J. Biol. Chem. 278:18859-18867

26. Sosnowski R, Mellon PL, Lawson MA 2000 Activation of translation in pituitary gonadotrope cells by gonadotropin-releasing hormone. Mol. Endocrinol. 14:1811-1819

27. Nguyen KA, Santos SJ, Kreidel MK, Diaz AL, Rey R, Lawson MA 2004 Acute regulation of translation initiation by gonadotropin-releasing hormone in the gonadotrope cell line LbetaT2. Mol. Endocrinol. 18:1301-1312

28. Ron D, Walter P 2007 Signal integration in the endoplasmic reticulum unfolded protein response. Nat. Rev. Mol. Cell. Biol. 8:519-529

29. Schroder M, Kaufman RJ 2006 Divergent roles of IRE1alpha and PERK in the unfolded protein response. Curr. Mol. Med. 6:5-36

30. Kaufman RJ 2004 Regulation of mRNA translation by protein folding in the endoplasmic reticulum. Trends Biochem. Sci. 29:152-158

31. Rutkowski DT, Kaufman RJ 2004 A trip to the ER: coping with stress. Trends. Cell Biol. 14:20-28

32. Kang SW, Rane NS, Kim SJ, Garrison JL, Taunton J, Hegde RS 2006 Substrate-specific translocational attenuation during ER stress defines a pre-emptive quality control pathway. Cell 127:999-1013

33. Wu J, Kaufman RJ 2006 From acute ER stress to physiological roles of the Unfolded Protein Response. Cell Death Differ. 13:374-384

34. Reimold AM, Iwakoshi NN, Manis J, Vallabhajosyula P, Szomolanyi-Tsuda E, Gravallese EM, Friend D, Grusby MJ, Alt F, Glimcher LH 2001 Plasma cell differentiation requires the transcription factor XBP-1. Nature 412:300-307

35. Zhang K, Wong HN, Song B, Miller CN, Scheuner D, Kaufman RJ 2005 The unfolded protein response sensor IRE1alpha is required at 2 distinct steps in B cell lymphopoiesis. J. Clin. Invest. 115:268-281

36. Harding HP, Zeng H, Zhang Y, Jungries R, Chung P, Plesken H, Sabatini DD, Ron D 2001 Diabetes mellitus and exocrine pancreatic dysfunction in perk-/- mice reveals a role for translational control in secretory cell survival. Mol. Cell 7:1153-1163

37. Zhang P, McGrath B, Li S, Frank A, Zambito F, Reinert J, Gannon M, Ma K, McNaughton K, Cavener DR 2002 The PERK eukaryotic initiation factor 2 alpha kinase is required for the development of the skeletal system, postnatal growth, and the function and viability of the pancreas. Mol. Cell. Biol. 22:3864-3874

38. Scheuner D, Song B, McEwen E, Liu C, Laybutt R, Gillespie P, Saunders T, Bonner-Weir S, Kaufman RJ 2001 Translational control is required for the unfolded protein response and in vivo glucose homeostasis. Mol. Cell 7:1165-1176

39. Kakar SS, Winters SJ, Zacharias W, Miller DM, Flynn S 2003 Identification of distinct gene expression profiles associated with treatment of LbetaT2 cells with gonadotropin-releasing hormone agonist using microarray analysis. Gene 308:67-77

40. Zhang H, Bailey JS, Coss D, Lin B, Tsutsumi R, Lawson MA, Mellon PL, Webster NJ 2006 Activin modulates the transcriptional response of LβT2 cells to GnRH and alters cellular proliferation. Mol. Endocrinol. 20:2909-2930

41. Lawson MA, Tsutsumi R, Zhang H, Talukdar I, Butler BK, Santos SJ, Mellon PL, Webster NJ 2007 Pulse sensitivity of the luteinizing hormone beta promoter is determined by a negative feedback loop Involving early growth response-1 and Ngfi-A binding protein 1 and 2. Mol. Endocrinol. 21:1175-1191

42. Jiang HY, Wek SA, McGrath BC, Lu D, Hai T, Harding HP, Wang X, Ron D, Cavener DR, Wek RC 2004 Activating transcription factor 3 is integral to the eukaryotic initiation factor 2 kinase stress response. Mol. Cell. Biol. 24:1365-1377

43. Lee AH, Iwakoshi NN, Glimcher LH 2003 XBP-1 regulates a subset of endoplasmic reticulum resident chaperone genes in the unfolded protein response. Mol. Cell. Biol. 23:7448-7459

44. Bertolotti A, Zhang Y, Hendershot LM, Harding HP, Ron D 2000 Dynamic interaction of BiP and ER stress transducers in the unfolded-protein response. Nat. Cell Biol. 2:326-332

45. Ma Y, Lu Y, Zeng H, Ron D, Mo W, Neubert TA 2001 Characterization of phosphopeptides from protein digests using matrix-assisted laser desorption/ionization time-of-flight mass spectrometry and nanoelectrospray quadrupole time-of-flight mass spectrometry. Rapid Commun. Mass Spectrom. 15:1693-1700

46. Hollien J, Weissman JS 2006 Decay of endoplasmic reticulum-localized mRNAs during the unfolded protein response. Science 313:104-107

47. Liang SH, Zhang W, McGrath BC, Zhang P, Cavener DR 2006 PERK (eIF2alpha kinase) is required to activate the stress-activated MAPKs and induce the expression of immediate-early genes upon disruption of ER calcium homoeostasis. Biochem. J. 393:201-209

48. Yoshida H 2007 Unconventional splicing of XBP-1 mRNA in the unfolded protein response. Antioxid. Redox Signal. 9:232323-33

49. Hirota M, Kitagaki M, Itagaki H, Aiba S 2006 Quantitative measurement of spliced XBP1 mRNA as an indicator of endoplasmic reticulum stress. J. Toxicol. Sci. 31:149-156

50. Rispoli LA, Nett TM 2005 Pituitary gonadotropin-releasing hormone (GnRH) receptor: structure, distribution and regulation of expression. Anim. Reprod. Sci. 88:57-74

51. Keene JD 2001 Ribonucleoprotein infrastructure regulating the flow of genetic information between the genome and the proteome. Proc. Natl. Acad. Sci. USA 98:7018-7024

52. Hieronymus H, Silver PA 2004 A systems view of mRNP biology. Genes Dev. 18:2845-2860

53. Thomas G, Martin-Perez J, Siegmann M, Otto AM 1982 The effect of serum, EGF, PGF2 alpha and insulin on S6 phosphorylation and the initiation of protein and DNA synthesis. Cell 30:235-242

54. Rose A, Froment P, Perrot V, Quon MJ, LeRoith D, Dupont J 2004 The luteinizing hormone-releasing hormone inhibits the anti-apoptotic activity of insulin-like growth factor-1 in pituitary alphaT3 cells by protein kinase Calpha-mediated negative regulation of Akt. J. Biol. Chem. 279:52500-52516

55. Mutiara S, Kanasaki H, Harada T, Oride A, Miyazaki K 2007 The involvement of phosphatidylinositol 3-kinase in gonadotropin-releasing hormone-induced gonadotropin alpha- and FSHbeta-subunit genes expression in clonal gonadotroph LbetaT2 cells. Mol. Cell. Endocrinol. in press

56. Liu F, Ruiz MS, Austin DA, Webster NJ 2005 Constitutively active Gq impairs gonadotropin-releasing hormone-induced intracellular signaling and luteinizing hormone secretion in LbetaT2 cells. Mol. Endocrinol. 19:2074-2085

57. Hendershot LM 2004 The ER function BiP is a master regulator of ER function. Mt Sinai J Med 71:289-97

58. Yuen T, Wurmbach E, Ebersole BJ, Ruf F, Pfeffer RL, Sealfon SC 2002 Coupling of GnRH concentration and the GnRH receptor-activated gene program. Mol. Endocrinol. 16:1145-53

59. Wurmbach E, Yuen T, Ebersole BJ, Sealfon SC 2001 Gonadotropin-releasing hormone receptor-coupled gene network organization. J. Biol. Chem. 276:47195-201

60. Reimold AM, Etkin A, Clauss I, Perkins A, Friend DS, Zhang J, Horton HF, Scott A, Orkin SH, Byrne MC, Grusby MJ, Glimcher LH 2000 An essential role in liver development for transcription factor XBP-1. Genes Dev. 14:152-157

61. Brostrom MA, Brostrom CO 2003 Calcium dynamics and endoplasmic reticular function in the regulation of protein synthesis: implications for cell growth and adaptability. Cell Calcium 34:345-363

62. Yoshida H, Okada T, Haze K, Yanagi H, Yura T, Negishi M, Mori K 2000 ATF6 activated by proteolysis binds in the presence of NF-Y (CBF) directly to the cis-acting element responsible for the mammalian unfolded protein response. Mol. Cell. Biol. 20:6755-6767

63. Yoshida H, Haze K, Yanagi H, Yura T, Mori K 1998 Identification of the cis-acting endoplasmic reticulum stress response element responsible for transcriptional induction of mammalian glucose-regulated proteins. Involvement of basic leucine zipper transcription factors. J. Biol. Chem. 273:33741-33749

64. Yamamoto K, Yoshida H, Kokame K, Kaufman RJ, Mori K 2004 Differential contributions of ATF6 and XBP1 to the activation of endoplasmic reticulum stress-responsive cis-acting elements ERSE, UPRE and ERSE-II. J. Biochem. 136:343-350

65. Elzi DJ, Bjornsen AJ, MacKenzie T, Wyman TH, Silliman CC 2001 Ionomycin causes activation of p38 and p42/44 mitogen-activated protein kinases in human neutrophils. Am. J. Physiol. Cell Physiol. 281:C350-360

66. Brostrom CO, Chin KV, Wong WL, Cade C, Brostrom MA 1989 Inhibition of translational initiation in eukaryotic cells by calcium ionophore. J. Biol. Chem. 264:1644-1649

67. Rutkowski DT, Kaufman RJ 2003 All roads lead to ATF4. Dev. Cell 4:442-444

68. Tu BP, Weissman JS 2004 Oxidative protein folding in eukaryotes: mechanisms and consequences. J. Cell Biol. 164:341-346

69. Harding HP, Zhang Y, Zeng H, Novoa I, Lu PD, Calfon M, Sadri N, Yun C, Popko B, Paules R, Stojdl DF, Bell JC, Hettmann T, Leiden JM, Ron D 2003 An integrated stress response regulates amino acid metabolism and resistance to oxidative stress. Mol. Cell 11:619-633

70. Ozcan U, Ozcan L, Yilmaz E, Duvel K, Sahin M, Manning BD, Hotamisligil GS 2008 Loss of the tuberous sclerosis complex tumor suppressors triggers the unfolded protein response to regulate insulin signaling and apoptosis. Mol. Cell 29:541-551

71. Lievremont JP, Rizzuto R, Hendershot L, Meldolesi J 1997 BiP, a major chaperone protein of the endoplasmic reticulum lumen, plays a direct and important role in the storage of the rapidly exchanging pool of Ca2+. J. Biol. Chem. 272:30873-30879

72. Kawai T, Fan J, Mazan-Mamczarz K, Gorospe M 2004 Global mRNA stabilization preferentially linked to translational repression during the endoplasmic reticulum stress response. Mol. Cell. Biol. 24:6773-6787

73. Miles LE, Hanyaloglu AC, Dromey JR, Pfleger KD, Eidne KA 2004 Gonadotropin-releasing hormone receptor-mediated growth suppression of immortalized LbetaT2 gonadotrope and stable HEK293 cell lines. Endocrinology 145:194-204

74. Pfaffl MW 2001 A new mathematical model for relative quantification in real-time RT-PCR. Nucleic Acids Res. 29:e45

75. Waters C, Pyne S, Pyne NJ 2004 The role of G-protein coupled receptors and associated proteins in receptor tyrosine kinase signal transduction. Semin. Cell Dev. Biol. 15:309-323

76. Luttrell LM, Daaka Y, Lefkowitz RJ 1999 Regulation of tyrosine kinase cascades by G-protein-coupled receptors. Curr. Opin. Cell Biol. 11:177-183

77. Gavi S, Shumay E, Wang HY, Malbon CC 2006 G-protein-coupled receptors and tyrosine kinases: crossroads in cell signaling and regulation. Trends Endocrinol. Metab. 17:48-54

78. Mata J, Marguerat S, Bahler J 2005 Post-transcriptional control of gene expression: a genome-wide perspective. Trends Biochem. Sci. 30:506-514

79. Pradet-Balade B, Boulme F, Beug H, Mullner EW, Garcia-Sanz JA 2001 Translation control: bridging the gap between genomics and proteomics? Trends Biochem. Sci. 26:225-229

80. Stoneley M, Willis AE 2004 Cellular internal ribosome entry segments: structures, trans-acting factors and regulation of gene expression. Oncogene 23:3200-3207

81. Preiss T, Baron-Benhamou J, Ansorge W, Hentze MW 2003 Homodirectional changes in transcriptome composition and mRNA translation induced by rapamycin and heat shock. Nat. Struct. Biol. 10:1039-1047

82. Kumar TR, Matzuk MM 1995 Cloning of the mouse gonadotropin beta-subunit-encoding genes, II. Structure of the luteinizing hormone beta-subunit-encoding genes. Gene 166:335-336

83. Liu F, Austin DA, Webster NJ 2003 Gonadotropin-releasing hormone-desensitized LbetaT2 gonadotrope cells are refractory to acute protein kinase C, cyclic AMP, and calcium-dependent signaling. Endocrinology 144:4354-4365

84. Keyse SM 2000 Protein phosphatases and the regulation of mitogen-activated protein kinase signalling. Curr. Opin. Cell Biol. 12:186-192

85. Haneda M, Sugimoto T, Kikkawa R 1999 Mitogen-activated protein kinase phosphatase: a negative regulator of the mitogen-activated protein kinase cascade. Eur. J. Pharmacol. 365:1-7

86. Zhang T, Mulvaney JM, Roberson MS 2001 Activation of mitogen-activated protein kinase phosphatase 2 by gonadotropin-releasing hormone. Mol. Cell. Endocrinol. 172:79-89

87. Zhang T, Roberson MS 2006 Role of MAP kinase phosphatases in GnRH-dependent activation of MAP kinases. J. Mol. Endocrinol. 36:41-50

88. Zhang T, Wolfe MW, Roberson MS 2001 An early growth response protein (Egr) 1 cis-element is required for gonadotropin-releasing hormone-induced mitogen-activated protein kinase phosphatase 2 gene expression. J. Biol. Chem. 276:45604-45613

89. Windle JJ, Weiner RI, Mellon PL 1990 Cell lines of the pituitary gonadotrope lineage derived by targeted oncogenesis in transgenic mice. Mol. Endocrinol. 4:597-603

90. Schmidt EV 2004 The role of c-myc in regulation of translation initiation. Oncogene 23:3217-3221

91. Johannes G, Sarnow P 1998 Cap-independent polysomal association of natural mRNAs encoding c-myc, BiP, and eIF4G conferred by internal ribosome entry sites. RNA 4:1500-1513

92. Johannes G, Carter MS, Eisen MB, Brown PO, Sarnow P 1999 Identification of eukaryotic mRNAs that are translated at reduced cap binding complex eIF4F concentrations using a cDNA microarray. Proc. Natl. Acad. Sci. USA 96:13118-13123

93. Stoneley M, Paulin FE, Le Quesne JP, Chappell SA, Willis AE 1998 C-Myc 5' untranslated region contains an internal ribosome entry segment. Oncogene 16:423-8

94. Wek RC, Jiang HY, Anthony TG 2006 Coping with stress: eIF2 kinases and translational control. Biochem. Soc. Trans. 34:7-11

95. Dorn C, Ou Q, Svaren J, Crawford PA, Sadovsky Y 1999 Activation of luteinizing hormone beta gene by gonadotropin-releasing hormone requires the synergy of early growth response-1 and steroidogenic factor-1. J. Biol. Chem. 274:13870-13876

96. Kuhn KM, DeRisi JL, Brown PO, Sarnow P 2001 Global and specific translational regulation in the genomic response of Saccharomyces cerevisiae to a rapid transfer from a fermentable to a nonfermentable carbon source. Mol. Cell. Biol. 21:916-27

97. Smirnova JB, Selley JN, Sanchez-Cabo F, Carroll K, Eddy AA, McCarthy JE, Hubbard SJ, Pavitt GD, Grant CM, Ashe MP 2005 Global gene expression profiling reveals widespread yet distinctive translational responses to different eukaryotic translation initiation factor 2B-targeting stress pathways. Mol. Cell. Biol. 25:9340-9349

98. Irizarry RA, Bolstad BM, Collin F, Cope LM, Hobbs B, Speed TP 2003 Summaries of Affymetrix GeneChip probe level data. Nucleic Acids Res. 31:e15

99. Rosenfeld S, Wang T, Kim Y, Milner J 2004 Numerical deconvolution of cDNA microarray signal: simulation study. Ann. NY Acad. Sci. 1020:110-123

100. Tusher VG, Tibshirani R, Chu G 2001 Significance analysis of microarrays applied to the ionizing radiation response. Proc. Natl. Acad. Sci. USA 98:5116-5121

101. Storey JD 2002 A direct approach to false discovery rates. J Roy Stat Soc Ser B:479-498

102. Eisen MB, Spellman PT, Brown PO, Botstein D 1998 Cluster analysis and display of genome-wide expression patterns. Proc. Natl. Acad. Sci. USA 95:14863-14868

103. Gentleman R, Carey V, Huber W, Irizarry R, Dudoit S 2005 Bioinformatics and Computational Biology Solutions Using R and Bioconductor. Springer, New York

104. Mathews MB, Sonenberg N, Hershey JWB 2000 Origins and Principles of Translational Control. In: Sonenberg N, Hershey JWB, Mathews MB (eds) Translational Control of Gene Expression, 2nd ed. Cold Spring Harbor Laboratory Press, Cold Spring Harbor; pp 1-31

105. Gebauer F, Hentze MW 2004 Molecular mechanisms of translational control. Nat. Rev. Mol. Cell. Biol. 5:827-835

106. Dever TE 2002 Gene-specific regulation by general translation factors. Cell 108:545-556

107. Wickens M, Goodwin EB, Kimble J, Strickland S, Hentze MW 2000 Translational Control of Developmental Decisions. In: Sonenberg N, Hershey JWB, Mathews MB (eds) Translational Control of Gene Expression, 2nd ed. Cold Spring Harbor Laboratory Press, Cold Spring Harbor; pp 295-370

108. Mora GR, Mahesh VB 1999 Autoregulation of the androgen receptor at the translational level: testosterone induces accumulation of androgen receptor mRNA in the rat ventral prostate polyribosomes. Steroids 64:587-91

109. Yeap BB, Krueger RG, Leedman PJ 1999 Differential posttranscriptional regulation of androgen receptor gene expression by androgen in prostate and breast cancer cells. Endocrinology 140:3282-3291

110. Gonzalez-Herrera IG, Prado-Lourenco L, Pileur F, Conte C, Morin Section A, Cabon Section F, Prats H, Vagner S, Bayard F, Audigier S, Prats AC 2006 Testosterone regulates FGF-2 expression during testis maturation by an IRES-dependent translational mechanism. FASEB J. 20:476-478

111. Bouamoud N, Lerrant Y, Ribot G, Counis R 1992 Differential stability of mRNAs coding for alpha and gonadotropin beta subunits in cultured rat pituitary cells. Mol. Cell. Endocrinol. 88:143-451

112. Liu F, Usui I, Evans LG, Austin DA, Mellon PL, Olefsky JM, Webster NJ 2002 Involvement of both Gq/11 and Gs proteins in gonadotropin-releasing hormone receptor-mediated signaling in Lbeta T2 cells. J. Biol. Chem. 277:32099-32108

113. Burger LL, Dalkin AC, Aylor KW, Haisenleder DJ, Marshall JC 2002 GnRH pulse frequency modulation of gonadotropin subunit gene transcription in normal gonadotropes-assessment by primary transcript assay provides evidence for roles of GnRH and follistatin. Endocrinology 143:3243-9

114. Buggs C, Weinberg F, Kim E, Wolfe A, Radovick S, Wondisford F 2006 Insulin augments GnRH-stimulated LHbeta gene expression by Egr-1. Mol Cell Endocrinol. 249:99-106

115. Haisenleder DJ, Burger LL, Walsh HE, Stevens J, Aylor KW, Shupnik MA, Marshall JC 2008 Pulsatile gonadotropin-releasing hormone stimulation of gonadotropin subunit transcription in rat pituitaries: evidence for the involvement of Jun N-terminal kinase but not p38. Endocrinology 149:139-145

116. Topilko P, Schneider-Maunoury S, Levi G, Trembleau A, Gourdji D, Driancourt MA, Rao CV, Charnay P 1998 Multiple pituitary and ovarian defects in Krox-24 (NGFI-A, Egr-1)-targeted mice. Mol. Endocrinol. 12:107-122

117. Kanasaki H, Bedecarrats GY, Kam KY, Xu S, Kaiser UB 2005 Gonadotropin-releasing hormone pulse frequency-dependent activation of extracellular signal-regulated kinase pathways in perifused L{beta}T2 cells. Endocrinology 146:5503-5513

118. Holcik M, Sonenberg N 2005 Translational control in stress and apoptosis. Nat. Rev. Mol. Cell Biol. 6:318-327

119. Qin X, Sarnow P 2004 Preferential translation of internal ribosome entry site-containing mRNAs during the mitotic cycle in mammalian cells. J. Biol. Chem. 279:13721-13728

120. Pyronnet S, Sonenberg N 2001 Cell-cycle-dependent translational control. Curr. Opin. Genet. Dev. 11:13-18

121. Mignone F, Grillo G, Licciulli F, Iacono M, Liuni S, Kersey PJ, Duarte J, Saccone C, Pesole G 2005 UTRdb and UTRsite: a collection of sequences and regulatory motifs of the untranslated regions of eukaryotic mRNAs. Nucleic Acids Res. 33:D141-146

122. Lerner RS, Seiser RM, Zheng T, Lager PJ, Reedy MC, Keene JD, Nicchitta CV 2003 Partitioning and translation of mRNAs encoding soluble proteins on membrane-bound ribosomes. RNA 9:1123-1137

123. Lerner RS, Nicchitta CV 2006 mRNA translation is compartmentalized to the endoplasmic reticulum following physiological inhibition of cap-dependent translation. RNA 12:775-789

124. Stephens SB, Dodd RD, Brewer JW, Lager PJ, Keene JD, Nicchitta CV 2005 Stable ribosome binding to the endoplasmic reticulum enables compartment-specific regulation of mRNA translation. Mol. Biol. Cell. 16:5819-5831

125. Scheper GC, Proud CG 2002 Does phosphorylation of the cap-binding protein eIF4E play a role in translation initiation? Eur. J. Biochem. 269:5350-5359

126. Gingras AC, Raught B, Sonenberg N 1999 eIF4 initiation factors: effectors of mRNA recruitment to ribosomes and regulators of translation. Annu. Rev. Biochem. 68:913-963

127. Gross JD, Moerke NJ, von der Haar T, Lugovskoy AA, Sachs AB, McCarthy JE, Wagner G 2003 Ribosome loading onto the mRNA cap is driven by conformational coupling between eIF4G and eIF4E. Cell 115:739-750

128. Pyronnet S, Imataka H, Gingras AC, Fukunaga R, Hunter T, Sonenberg N 1999 Human eukaryotic translation initiation factor 4G (eIF4G) recruits mnk1 to phosphorylate eIF4E. EMBO J. 18:270-279

129. Hennecke M, Kwissa M, Metzger K, Oumard A, Kroger A, Schirmbeck R, Reimann J, Hauser H 2001 Composition and arrangement of genes define the strength of IRES-driven translation in bicistronic mRNAs. Nucleic Acids Res. 29:3327-3334

130. Wang X, Campbell LE, Miller CM, Proud CG 1998 Amino acid availability regulates p70 S6 kinase and multiple translation factors. Biochem. J. 334 (Pt 1):261-7

131. Zhang W, Feng D, Li Y, Iida K, McGrath B, Cavener DR 2006 PERK EIF2AK3 control of pancreatic beta cell differentiation and proliferation is required for postnatal glucose homeostasis. Cell Metab. 4:491-497

132. Harding HP, Zhang Y, Bertolotti A, Zeng H, Ron D 2000 Perk is essential for translational regulation and cell survival during the unfolded protein response. Mol. Cell 5:897-904

133. Hung CC, Ichimura T, Stevens JL, Bonventre JV 2003 Protection of renal epithelial cells against oxidative injury by endoplasmic reticulum stress preconditioning is mediated by ERK1/2 activation. J. Biol. Chem. 278:29317-29326

134. Lu PD, Jousse C, Marciniak SJ, Zhang Y, Novoa I, Scheuner D, Kaufman RJ, Ron D, Harding HP 2004 Cytoprotection by pre-emptive conditional phosphorylation of translation initiation factor 2. EMBO J. 23:169-179

135. Sisk CL, Richardson HN, Chappell PE, Levine JE 2001 In vivo gonadotropin-releasing hormone secretion in female rats during peripubertal development and on proestrus. Endocrinology 142:2929-2936

136. Moenter SM, Brand RM, Midgley AR, Karsch FJ 1992 Dynamics of gonadotropin-releasing hormone release during a pulse. Endocrinology 130:503-510

137. Xu C, Bailly-Maitre B, Reed JC 2005 Endoplasmic reticulum stress: cell life and death decisions. J. Clin. Invest. 115:2656-2664

138. Mulvaney JM, Roberson MS 2000 Divergent signaling pathways requiring discrete calcium signals mediate concurrent activation of two mitogen-activated protein kinases by gonadotropin-releasing hormone. J. Biol. Chem. 275:14182-14189

139. Wolfgang CD, Chen BP, Martindale JL, Holbrook NJ, Hai T 1997 gadd153/Chop10, a potential target gene of the transcriptional repressor ATF3. Mol. Cell. Biol. 17:6700-6707

140. Yin P, Arita J 2002 Proestrous surge of gonadotropin-releasing hormone secretion inhibits apoptosis of anterior pituitary cells in cycling female rats. Neuroendocrinology 76:272-282

141. Rutkowski DT, Kaufman RJ 2007 That which does not kill me makes me stronger: adapting to chronic ER stress. Trends Biochem. Sci. 32:469-476

142. Jousse C, Oyadomari S, Novoa I, Lu P, Zhang Y, Harding HP, Ron D 2003 Inhibition of a constitutive translation initiation factor 2alpha phosphatase, CReP, promotes survival of stressed cells. J. Cell Biol. 163:767-775

143. Rutkowski DT, Arnold SM, Miller CN, Wu J, Li J, Gunnison KM, Mori K, Sadighi Akha AA, Raden D, Kaufman RJ 2006 Adaptation to ER stress is mediated by differential stabilities of pro-survival and pro-apoptotic mRNAs and proteins. PLoS Biol. 4:e374

144. Levine JE, Duffy MT 1988 Simultaneous measurement of luteinizing hormone (LH)-releasing hormone, LH, and follicle-stimulating hormone release in intact and short-term castrate rats. Endocrinology 122:2211-2221

145. Weiss J, Cote CR, Jameson JL, Crowley WF, Jr. 1995 Homologous desensitization of gonadotropin-releasing hormone (GnRH)-stimulated luteinizing hormone secretion in vitro occurs within the duration of an endogenous GnRH pulse. Endocrinology 136:138-143

146. Turgeon JL, Kimura Y, Waring DW, Mellon PL 1996 Steroid and pulsatile gonadotropin-releasing hormone (GnRH) regulation of luteinizing hormone and GnRH receptor in a novel gonadotrope cell line. Mol. Endocrinol. 10:439-450

147. Nicol L, McNeilly JR, Stridsberg M, Crawford JL, McNeilly AS 2002 Influence of steroids and GnRH on biosynthesis and secretion of secretogranin II and chromogranin A in relation to LH release in LbetaT2 gonadotroph cells. J. Endocrinol. 174:473-483